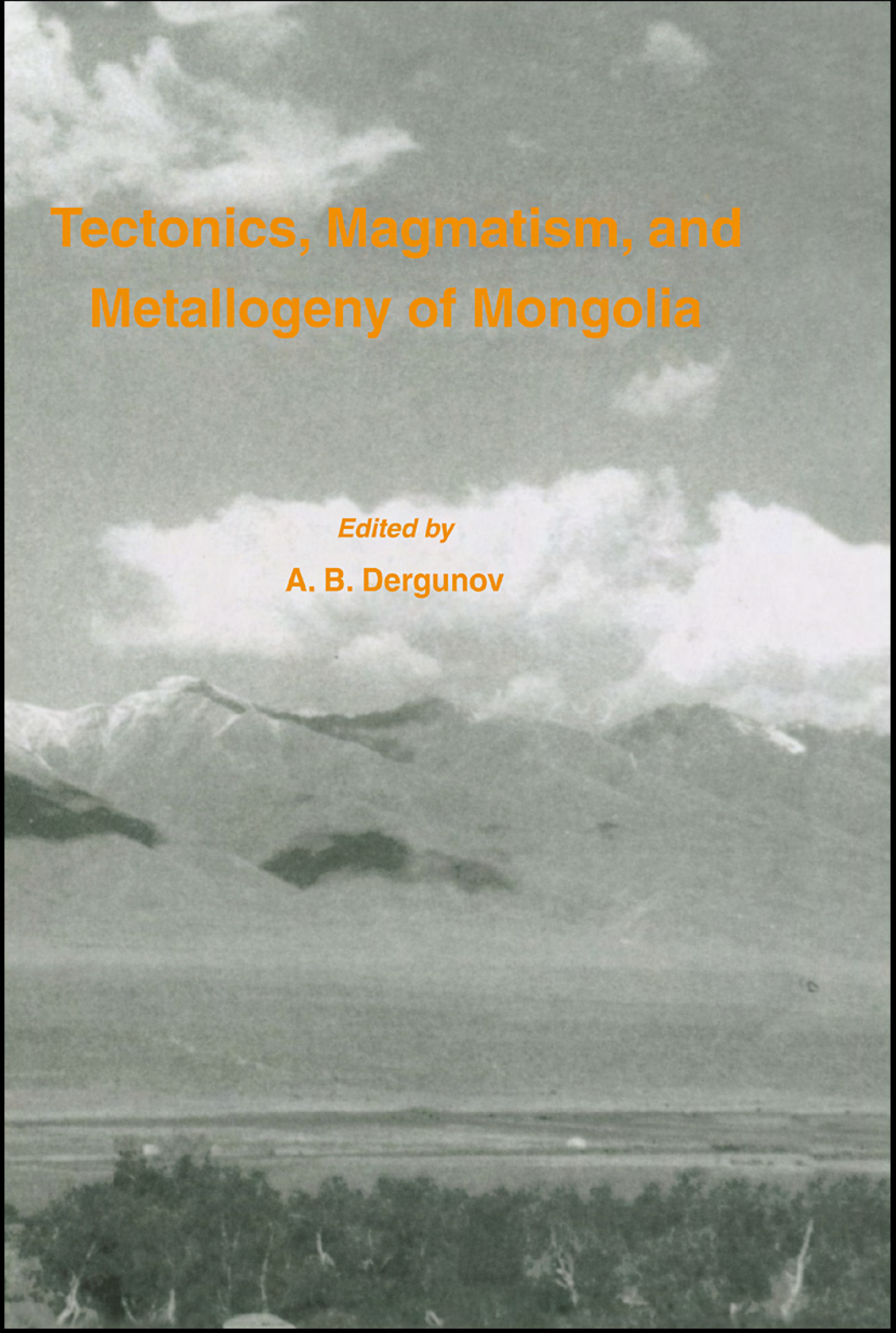

TECTONICS, MAGMATISM, AND METALLOGENY OF MONGOLIA

TECTONICS, MAGMATISM, AND METALLOGENY OF MONGOLIA

Edited by

A.B.Dergunov
Geological Institute
Russian Academy of Sciences, Moscow

Translated from the Russian by

R.E.Sorkina, R.V.Fursenko and
E.A.Miloradovskaya

London and New York

First published 2001 by Routledge 11 New Fetter Lane, London EC4P 4EE

Simultaneously published in the USA and Canada by Routledge 29 West 35th Street, New York, NY 10001

Routledge is an imprint of the Taylor & Francis Group
This edition published in the Taylor & Francis e-Library, 2005.
"To purchase your own copy of this or any of Taylor & Francis or Routledge's collection of thousands of eBooks please go to http://www.ebookstore.tandf.co.uk/.

British Library Cataloguing in Publication Data A catalogue record for this book is available from the British Library.

ISBN 0-203-01797-8 Master e-book ISBN

ISBN - (Adobe e-Reader Format)
ISBN: 0-415-26727-7 (Print Edition)

Dedicated to the respectful memory of the invariable scientific leader of geological investigations in Mongolia—academician and Professor Alexander Leonidovich Yanshin

CONTENTS

PREFACE

Geologically, Mongolia is made up of a number of tectonic zones that form part of the extensive Central Asiatic orogenic belt. The latter is located between the Siberian platform in the north and Katasia (Tarim and the Sino-Korean platform) in the south. Mongolia itself occupies a key position, linking the orogenic structures of Central Asia and Kazakhstan in the west, and Transbaikalia and the Khingan in the east. In general it is a structurally complex area comprising different Palaeozoic zones: Caledonian, Variscan, and Indo-Sinian. The Precambrian microcontinents form an important structural element of Mongolia. Orogenic formations (volcano-terrigenous molasse) are widespread infilling superimposed basins, and are associated with large granitoid bodies. They form extensive volcanic belts, with the Upper Palaeozoic Central Asiatic belt being the largest.

At the end of the last century, V.A.Obruchev studied the geology of Mongolia, and showed that Precambrian and Palaeozoic rocks are widely exposed there. Based on these data, S.Suess put forward a hypothesis regarding 'the ancient 'sinciput' of Asia'. These ideas were further developed by V.A.Obruchev, who assigned the Sayan-Baikal area, North and West Mongolia to the Archaean continental massif. He considered South Mongolia and the adjacent areas of China as Palaeozoic and assigned them to a limited zone of the Precambrian continental massif. Later hypotheses regarding the structural-spatial relationship between the Precambrian and Palaeozoic formations have been revised. For example, in the 1950s, V.M.Sinitsin suggested that most of Mongolia is composed of Caledonian rocks, while A.Kh.Ivanov assigned these rocks to the Hercynian. It was only in 1961 that V.A.Amantov and P.S.Matrosov proposed a more-or-less acceptable zonation for Mongolia. On this tectonic map, most of Central and North Mongolia consists of Precambrian massifs. West Mongolia and South Mongolia are assigned to the Caledonides and the Variscides, respectively.

In 1963, V.V.Bezzubtsev was the first to give a well-substantiated description of the metamorphic basement and cover of the Precambrian massifs. In the same year, V.A.Amantov published a description of the Cambrian sections of West Mongolia and showed that there was a drastic difference between the Caledonides of the Ozernaya (Lake) Zone and the Precambrian Dzabkhan Massif, and separated the latter (a microcontinent) from the terrain of eugeosynclinal (palaeooceanic) sections. L.P.Zonenshain (1970, Zonenshain *et al.*, 1978 etc.) formulated the modern principles of a pre-Mesozoic zonation for Mongolia. These have been used to compile *The Tectonic Map of Mongolia People's Republic* 1978 ed. Yanshin A.L. (1:1, 500000) and within the monograph *Tectonics of MPR* (ed. Yanshin A.L., 1974). The post-orogenic structures of Mongolia are discussed in *The Mesozoic and Cainozoic Tectonics and Magmatism of Mongolia* (ed. Yanshin A.L., 1975).

The Central Asiatic belt is now considered as a composite orogenic structure, comprising Riphean, early Caledonian (Salair), Caledonian, Variscan, and Indo-Sinian zones. As regards plate tectonics, accretionary (Kazakhstan, Altai, Sayan, North and Central Mongolia) and collisional (Inner and South Mongolia, Dzungaria, and Tien Shan)

structures can be distinguished, whose formation is closely connected with the numerous Precambrian microcontinents, mainly of the Gondwana series (Dzabkhan, Tuva-Mongolian, Central Mongolian, South Gobi, Ilian, and North Tien Shan, etc.). The emplacement of the belt resulted from the tectonic development of several palaeo-oceans: the palaeo-Asiatic (southern palaeo-Pacific), the proto-Tethys and the palaeo-Tethys 1 and 2. A combination of their structures mainly determined the type of tectonic development in Central Asia in the Late Precambrian and Palaeozoic (Mossakovsky *et al.*, 1993; Ruzhentrev *et al.*, 1995).

The Central Asiatic belt was found to include two types of tectonic structures, i.e. mosaic and linear. The mosaic structures (the Ripheides and Caledonides of Altai, Sayan, Central and North Mongolia, and Central Kazakhstan) are characterized by impersistent, transverse faults and fold systems, and by the angular folding and distinct boundaries of the systems. They formed mainly at the site of the palaeo-Asiatic ocean. The development of the latter took place from the Riphean to the Silurian (800–820 Ma), and, beginning in the Vendian, it consisted of a combination of diachronous volcanic arcs and conjugate basins. The accretionary tectonic style was marked by the successive attachment of accretionary complexes to the Siberian continent. The formation of this type of complex was accompanied by the intrusion of granitoids, from plagiogranites to granite batholiths, whose age can be correlated with that of the associated accretionary zones.

The linear fold structures of southern Mongolia, Dzungaria, and Turkestan-Alai (the Variscides), and Inner Mongolia (the Indo-Sinides) make up the southern Central Asiatic belt. These narrow zones, which stretch for thousands of kilometres, in their geometry commonly resemble the ophiolite sutures that separate fairly large continental plates. The sutures were apparently formed at the site of new oceanic basins. The latter resulted from the rifting of the ancient accretionary complexes of Siberia and Gondwanaland. The process occurred in pulses, which began in the Ordovician (Turkestan-Alai, Gobi-Altai) and which were very evident at the Silurian-Devonian boundary (southern Mongolia and Dzungaria) and in the Carboniferous (Inner Mongolia). The tectonic development of the structures listed above correlates with complete Wilson cycles, which are characterized by their short duration (30–80 Ma). A destructive emplacement pattern, with continental collision being dominated by the allochtonous mechanism of accretion of granite-metamorphic layers make it possible to assign these basins to the structures of the Tethyan series (palaeo-Tethys 1—Variscan, palaeo-Tethys 2—Indo-Sinian).

The book can be divided into three parts. Chapters 1, 2, 3, and 5 outline the stratigraphy and tectonics of precambrian massifs; Caledonian, Variscan and Indo-Sinian zones.

Chapters 4, 6 and 7 detail the composition, structure and evolution of magmatic bodies. The main specific features of ore deposits and metallogeny of Mongolia are charcterized in Chapter 8.

Figure 1 shows a map of the pre-orogenic tectonic zonation of Mongolia. This shows the position of major structures whose tectonic interpretation will be discussed in detail later in the book. The palaeo-oceanic zones of the Caledonides of the Lake region and the Mongolian Altai are located around the periphery of a system of microcontinents (Tuva-Mongolian, Dzabkhan, and Central Mongolian). The Lake region includes the early Caledonian (Salair) structures of the Dagandel, Lake, Khan Khukhei, Khairkhan, and

Khantaishir zones, with the Caledonides of the Mongolian Altai being located farther west. The Caledonian Bayankhonggor, North Khentei, Kerulen, and Dzidin zones extend north and north-east of the above microcontinental chain. The Variscan structures of Eastern Dzungaria and South Mongolia are markedly discordant with respect to the Caledonian structures. To the west, the former structures pass into those of Chinese Dzungaria and eastern Kazakhstan (Ob-Zaisan Zone), in the east the latter opens towards the Khingan. Two zones are recognized there: a palaeo-oceanic zone (Transaltai) with an axial ophiolite suture bounded to the north by the Gobi-Altai-Sukhebator Zone (the southern shelf of the Caledonian Siberian continent) and by the South Gobi Zone in the south (a Precambrian microcontinent where the shelf and slope parts can be distinguished).

The Indo-Sinides of Inner Mongolia (the Lugingol and Solonker zones), which are represented more fully in China, form the most southerly tectonic element.

Based on the theory of New Global Tectonics a substantiated interpretation of tectonic processes from the Riphean and up to the Cenozoic is given. These processes have generated the present geological structures of Mongolia.

1
PRECAMBRIAN MICROCONTINENTS

A.B.Dergunov

1.1 Introduction

Outcrops of highly metamorphosed rocks are widespread within the Mongolian Palaeozoic structures, particularly in the Caledonian northern megablock. There they form a pre-Riphean basement of three large massifs, which probably correspond with the Tuvin-Mongolian, Dzabkhan, and Central Mongolian microcontinents (Fig. 1: (I), (II), and (III)). Beyond the bounds of these massifs, similar metamorphic rocks are also encountered frequently, but their Precambrian age seems to be rather questionable, as they are nowhere overlapped by Palaeozoic cover and often have graduational contacts with surrounding Palaeozoic rocks. Moreover, recent U-Pb and Sm-Nd isotope studies have shown that many of these metamorphic rocks were formed in the middle and late Palaeozoic (Boishenko, 1987; Bibikova *et al.*, 1992; Neimark, 1993; Baikova and Amelin, 1994). Similar studies of the metamorphic basement rocks of the Tuvin-Mongolian and Dzabkhan massifs, which represent microcontinental fragments tend to confirm their pre-Riphean age (Ilyin, 1973; Kozakov, 1986; Bibikova *et al.*, 1990; Makarychev, 1993). It has been established that much of the structure of these three massifs is very similar: i.e. the Riphean protocover, the Upper Riphean-Vendian rift formations and the Lower-Middle Cambrian subplatform cover.

1.2 The Dzabkhan Massif

The massif occupies the western border of Central Mongolia (Fig. 1 (II)). The present-day structure is bounded tectonically by the Caledonian Ozernaya zone to the west, the Caledonian Bayan-Khongor zone to the east, the Tuvin-Mongolian Massif to the north, and the Hercynides of Southern Mongolia to the south. The formations of the initial lateral transition from the cover rocks of the massif to the Caledonian structures have been preserved on the western and eastern margins of the massif.

The basement of the Dzabkhan massif is best studied in its south-eastern part—the Baydarag inlier (Fig. 1-II- and Fig. 2). Three metamorphic rock complexes, corresponding with three tectonomagmatic cycles (TMC) have been distinguished there (Kozakov, 1986; Bibikova *et al.*, 1992). The oldest Early Archaean, TMC-I, is represented by a migmatizated tonalite (‘grey’) gneiss complex, amphibolites, plagiogneisses, and schists. They are encountered only as relics *(boudins)* within the Late Archaean metamorphic complex.

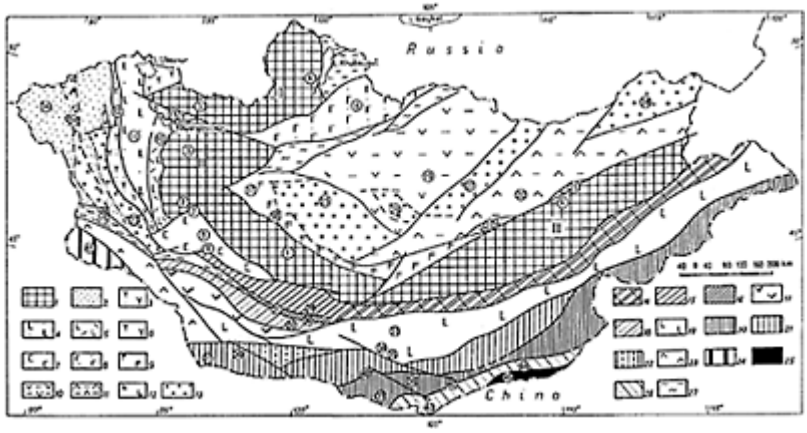

Key: I—Precambrian microcontinents: I—Tuva-Mongolian (TM), II—Ozakhan (O), III—Central Mongolian (CM); 2–12—Caledonian zones: 2—Mongol-Altai, 3—Kharkhirin, 4—Lake (Ozernaya), 5—Dagandel, 6—Khan-Khukhsi, 7—Khantaishir, 8—Dzhidin, 9—Bayan-Khongor, 10—North Khentei, 11—Kerulen, 12—South Kerulen; 13—Superimposed Palaeozoic troughs; 14–24—Variscan zones: 14–16—Gobi-Altai—Sukhe Bator (14—undifferentiated, 15—Bayan-Tsagan and 16—Dzhinset subzones); 17–18—Edrengin Zone: 17—Khuvnikhurin and 18—Edrengin-Nurin subzone; 19—Transaltai Zone; 20–22—South Gobi Zone: 20—Tsagan-Nuln, 21—Tumurta, 22—Ekhin-Gol subzones; 23—North Barunkhurai; 24—Olonbulak, Ulanus, and South Barunkhurai; 25–26—Indo-Sinian zones: 25—Solonker, 26—Lugin-Gol; 27—metamorphic belts.

Circled figures show location of key areas discussed in the text:

①—46°N, 100°E. The Baydarag inlier (see Fig. 2). ②—47°N, 95°E. The Gobi-Altai inlier (see p. 6 and Fig. 4). ③—48°N, 95°E. The South Songin inlier (see p. 9 and Fig. 5). ④—50°N, 100°E. The Western Prihubsugulye (see pp. 9–10 and Fig. 6) ⑤—49°30'N, 95°E. The northern slope of the Khan-Khuhei ridge inlier (see p. 10). ⑥—47°N, 110°E. The South-Kerulen zone of the Central Mongolian massif (see p. 12). ⑦—46°30'N, 95°30'E. The Nomangon subzone (see Fig. 7). ⑧—46°N, 96°E. The Khantaishir subzone (see Fig. 8) ⑨—45°30'N, 96°30'E (see Fig. 9). ⑩—48°30'N, 94°E. Position of the main section of the Dagandel Zone (see the text pp. 16, 23–24). ⑪—48°30'N, 92°30'E. Position of the main section of the Ozernaya Zone (see pp. 24–28 and Fig. 10). ⑫—49°00'N, 92°E. Position of the main section of the Kharkhirin Zone (see the text p. 28). ⑬—49°30'N, 94°E. Khan-Khukhei zone (see pp. 29–33 and Fig. 11, 12). ⑭—49°N, 84°E. Position of the main section of the Mongol-Altay Zone (see pp. 32–35 and Fig. 13). ⑮—46°N, 92°E. Position of the highly metamorphosed rocks in the basin of the Bodonchin river (see text pp. 35–36).

⑯—49°N, 102°E. Position of the central part of the Dzhidin Zone (see pp. 37–38 and Fig. 6). ⑰—47°N, 97°30'E. Position of the main section of the Sharaugol suite in the Baydaragin Gol river (see p. 39 and Fig. 2). ⑱—46°N, 99°E. Position of the main section of the Bayan-Khongor Zone (see pp. 39–40 and Fig. 2). ⑲—47°N, 101°E. Position of the main section of the Northern-Khentei Zone (see text pp. 45–46). ⑳—47°N, 109°E. Position of the main section of the Kerulen Rise (see pp. 46–47). ㉑—47°N, 111°E. Position of the main section of the Pre-Kerulen Zone (see pp. 47–48). ㉒—46°N, 108°E. Position of the Adachag ophiolitic zone (see p. 47). ㉓—46°30'N, 93°E. Position of the main section of the Kobdin trough (see text pp. 55–56 and Fig. 17). ㉔—48°30'N, 90°E. Position of the main section of the Deluno-Tustyd trough (see text p. 56 and Fig. 17). ㉕—47°N, 101°E. Position of the main section of the Khangay trough (see p. 57–58). ㉖—47°N, 104°E. Position of the West-Khentei trough (see pp. 57–58). ㉗—48°N, 107°E. Position of the main section of the Khentei trough (see pp. 57–58). ㉘—49°30'N, 114°30'E. Position of the main section of the Agin trough (see pp. 48, 58). ㉙—44°40'N, 100°30'E (see Fig. 14). ㉚—44°30'N, 100°30'E (see Fig. 17).

㉛—44° 40'N, 99°00'E. (see Fig. 18). ㉜—44°00'N, 100°00'E (see Fig. 19). ㉝—43°30'N, 104°00'E (see Fig. 20). ㉞—43°00'N, 103°00'E. (see Fig. 21). ㉟—42°40'N, 103°30'E (see Fig 22). ㊱—43°00'N, 98°00'E (see Fig. 24). ㊲—42°30'N, 96°40'E. (see Fig. 24). ㊳—43°00'N, 104°30'E (see Fig. 25). ㊴—42°00'N, 103°30'E (see Fig. 26). ㊵—42°40'N, 103°00'E (see Fig. 27) ㊶—45°30'N, 91°30'E (see Fig. 30). ㊷—43°00'N, 106°00'E. (see Fig. 47, 48). ㊸—41°30'N, 105°20'E. (see Fig. 49, 50). ㊹—42°40'N, 108°30'E. (see Fig. 50). ㊺—43°00'N, 107°00'E. (see Fig. 51, 52).

Figure 1 Pre-Mesozoic tectonic zonation of Mongolia.

TMC-I metamorphism occurred under conditions of low-moderate-pressure granulite facies, which is characterized by the following parageneses: monoclinic pyroxene + hypersthene+plagioclase Ab_{28-36} +quartz; monoclinic pyroxene +brown hornblende+plagioclase Ab_{32-42} +quartz; hypersthene+plagioclase Ab_{30-36} +quartz. Petrochemically, these rocks correspond with volcanics of the basalt-andesitedacite-rhyolite series. The U-Pb isotope analysis of zircons from the tonalitic ‘grey’ gneisses has yielded a minimum age of 2,646±45 Ma. When studying the Sm–Nd system in these rocks the ε_{Nd} was found to range from −3.3 to −0.5, indicating that their protolith was even more ancient: from 2.92 to 3.27 Ga.

The Late Archaean TMC-II complex is composed of leucocratic plagiogneisses, plagiomicroclinic gneisses, alternating marbles, quartzites and amphibolites. These metamorphic rocks occupy most of the area of the Baydarag inlier, forming very complex folded structures at the micro-, meso- and macro-scales and largely striking N–W.

Among these, the intrusive hypersthene and two-pyroxene quartz diorites and granodiorites (enderbites), which form elongated bodies, also striking NW-SE, are of considerable importance. Their contacts cut across the small-scale structures of the granulites but the schistosity, expressed by the hypersthenes, is superimposed on these enderbites. It follows that they were intruded between two stages of deformation, at the culmination of the TMC-II granulite metamorphism. Their characteristic mineral parageneses suggest amphibolite and possibly granulite-facies conditions (T=800°C and P=9 kbar), i.e. garnet +monoclinic pyroxene+plagioclase Ab_{32-40} +quartz, and garnet+green hornblende +plagioclase Ab_{30-38} +quartz.

The U-Pb isotope-geochemical studies of zircons from the enderbites of two massifs yielded ages of 2,374 and 2,367 Ma. The morphological and geochemical characteristics of the zircons confirm that TMC-II metamorphism occurred under granulite-facies conditions.

The present-day structure of the pre-Riphean formations of the Baydarag inlier is believed to be determined by the processes of the third tectonomagmatic cycle—TMC-III—which was preceded by the intrusion of metabasite dykes, which were in turn metamorphosed under amphibolite-facies conditions. This metamorphism was accompanied by the intrusion of garnet granodiorites (with the 42% garnet containing pyrope), forming elongated intrusive bodies aligned in a NW–SE direction, like the enderbites of the previous cycle. The TMC-III stage was completed by the intrusion of small bodies and veins of amphibole granosyenites, granodiorites and peralkaline granites. They occupy a transitional position relative to all the north-western formations of the previous TMC.

Uranium-lead isotope analysis of the zircons from the garnet granodiorites gave their age as 1854±5 Ma. The same analysis of the zircons from the amphibole granitoids gives an age of 1,825±5 Ma. It appears to mark the completion of TMC-III processes on the Baydarag inlier of the basement of the Dzabkhan Massif. The regional greenschist metamorphism, (TMC-IV), is of post-Riphean age and occurs mainly in the Riphean cover. In the basement rocks it is rarely encountered in some zones of schistosity.

The marginal eastern part of the Baydarag inlier is overlain by the Riphean protocover, which occupies a considerable area in the lower part of the basin of the

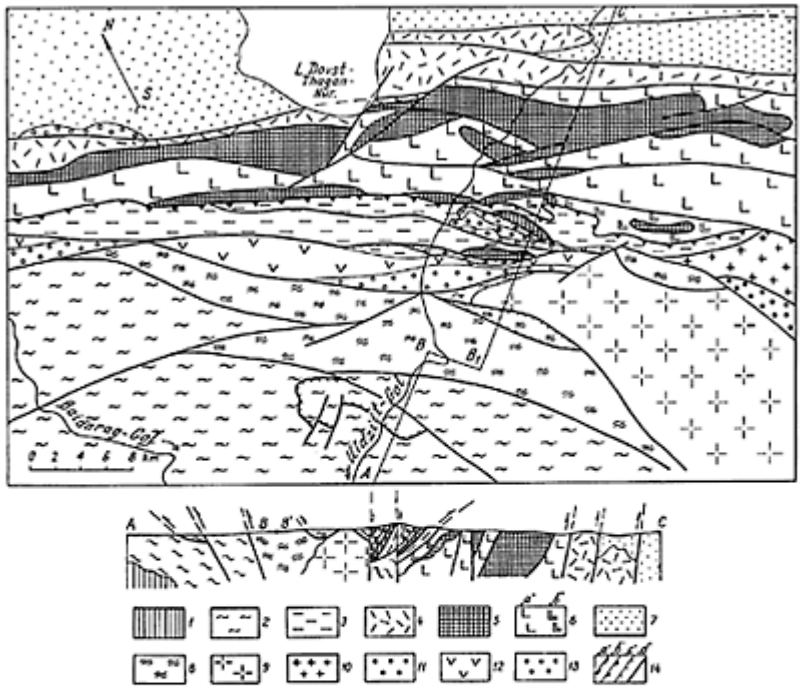

Key: 1–4—formations of the margin of Baydarag Inlier and the Dzabkhan Massif: 1—metamorphic basement (A—PR_1 on the profile); 2 and 3—protocover: 2—carbonaceous shale, terrigenous and carbonate turbidites, and dolomite (R_{1-2}), 3—sandstone, siltstone, carbonaceous shale, dolomite (R_3), calcarenite, sandstone, and conglomerates ($Є_2$); 4—riftogenic acid and basic volcanics, tuffite, sandstone, limestone, and jasper ($V–Є_1$); 5–7—palaeo-oceanic formations: 5—ophiolite, 6—basaltoids and greywacke of the north-eastern (a) and south-western (b) associations ($V–Є_1$), 7—terrigenous turbidites of the continental slope and rise ($Є_2–Є_3$); 8–10—formations of the ancient massif–palaeo-oceanic basin transitional zone: 8—metamorphic rocks, 9—palingenetic granitoids ($Є_3$), 10—granite ($Є_3$); 11–13—formations of the neoautochthon: 11—arkose conglomerates, sandstone, siltstone, and limestone (O_3), 12—sandstone, conglomerates, and trachyandesite (D), 13—conglomerates, sandstone, siltstone, limestone, and carbonaceous shale (C), 14—fault: overthrust (a), retrooverthrust (b), thrust (c), and the remainder (d).

Figure 2 Geological and structural map of the Bayan-Khongor Zone (see Fig.1-

River Uldziyt-Gol (Fig. 2). Eighteen kilometers east of Bumbuger village, immediately overlying the Lower Archaean tonalite gneisses, is a basal conglomerate, which up the section is overlain by a dolomitic siltstone containing Early-Middle Riphean stromatolites (collections and determinations were made by V.A. Komar) (Boishenko, 1978; Kozakov *et al.*, 1993). The basal bed dips to the NNE at an angle of 60–70° and has an apparent thickness of up to 250 m. The original stratigraphic relationships have only been retained in small areas, most commonly where steeply dipping faults cut across metasomatic quartzite bodies and quartz veins. The Lower-Middle Riphean sedimentary cover consists

of three units (Dergunov *et al.*, 1997): in addition to dolomites the lowermost unit is composed of black, carbonaceous pyrite-bearing schists (300 m thick), the middle unit—by dark carbonaceous schists and terrigenous turbidites (400–600 m thick), and the uppermost unit—by carbonate turbidites. The terrigenous rocks are represented by polymictic, rarely quartzose, often calcareous sandstones and aleurolites (sedimentary rock of cement aleurite), and the carbonate ones comprise sandy calacarenites and calcilutites. These rock units are folded into asymmetrical folds at several scales, with steep western limbs and gently dipping north-eastern limbs, often accompanied by upthrows and thrusts along the axial planes of the folds (Fig. 3).

The Lower-Middle Riphean cover also consists of rhythmically alternating aleurolites and sandstones and also layers of carbonaceous schists (this part of the sequence is 1,000 m thick), and is completed by quartzose sandstones (60 m) and dolomites (500 m thick), the latter containing with abundant Upper Riphean stromatolites (collected and identified by V.A.Komar). The Lower-Middle Cambrian unit (600 m thick) which unconformably overlaps Upper-Riphean rocks consists of a basal conglomerate, calcareous calcarenites, aleurolites, and greywacke sandstones, the latter containing clasts of volcanic rocks and granitoids. This unit shows typical features of shallow-marine sedimentation. Remnants of (akrotretidae) hyolithids, trilobites, and inarticulate brachiopods testify the Early-Middle Cambrian age of this unit (identifications were made by G.T.Ushatinskaya) (Dergunov *et al.*, 1997).

Isolated outcrops of ancient basement rocks, Upper Riphean-Vendian rift formations and Lower-Middle Cambrian formation are known in the other parts of the Dzabkhan Massif. On the south-western margin of the Dzabkhan Massif near the city of Gobi-Altai, there occurs the Gobi-Altai inlier (Fig. 1-II-) where two complexes of metamorphic rocks can be distinguished (Mitrofanov *et al.*, 1985). The older complex is composed of migmatized garnet amphibolites, biotiteamphibole, garnet-biotite, biotite and two-mica gneisses. The remains of a garnet paragenesis also containing monoclinic pyroxene have been recorded. The mineral parageneses and structural features allow us to attribute the metamorphic rocks of this complex to high-pressure amphibolite-facies metamorphism, which is characteristic of the TMC-II phase.

The complex containing quartzites, graphitic marbles, gneisses and amphibolites is considered to be the younger formation on the Gobi-Altai inlier. From its paragenesis and structural features, it was probably formed by low-pressure amphibolite-facies metamorphism, and it is probably associated with the TMC-III formations. In the same part of the Dzabkhan Massif, outcrops of Upper Riphean-Vendian rift volcanics, unconformably overlapped by terrigenous-carbonate deposits of the Vendian-Lower Cambrian subplatform cover, have been identified (Fig. 4) (Dergunov *et al.*, 1980). The volcanics are represented by lithic-crystal tuffs and andesite and rhyolite lavas with an apparent thickness of 100 m. They are overlapped by polymictic detrital conglomerates, which lie at the base of a thick unit of carbonates (600 m) and by alternating sandstones and shales

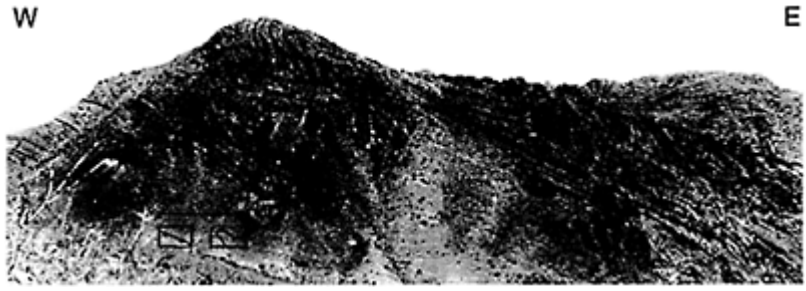

Figure 3 Thrusts accompanied by westerly recumbent drag-folds. Riphean sandstone sequence. Right bank of the River Uldziit-Gol (see Fig. 1- and Fig. 2).

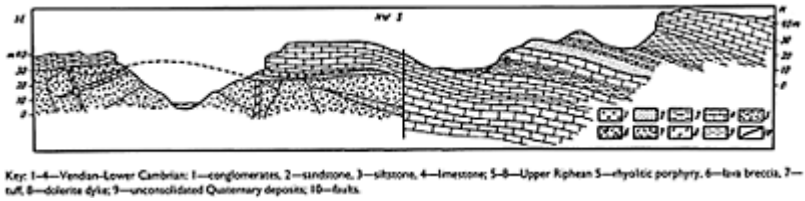

Key: 1–4—Vendian-Lower Cambrian: 1—conglomerates, 2—sandstone, 3—siltstone, 4—limestone; 5–8—Upper Riphean 5—rhyolitic porphyry, 6—lava breccia, 7—tuff, 8—dolerite dyke; 9—unconsolidated Quaternary deposits; 10—faults.

Figure 4 Vendian-Cambrian terrigenous-carbonate rocks unconformably overlapping the Upper Riphean subaerial volcanics of the Dzabkhan Zone (upper reaches of River Dzabkhan, Taishir village area (see Fig. 1–II)).

(totalling 500 m thick) containing the remains of Early Cambrian trilobites and archaeocyathids.

The South Songin Inlier Fig. 1-II- composed of metamorphic rocks, including chlorite-, actinolite-, and biotite-chlorite schists, with interlayers of marbles and quartzites (Fig. 5), can be distinguished in the central part of the northern Dzabkhan Massif between the Dzabkhan and Khungui rivers (Fig. 1-II -). Their mineral parageneses indicate that these rocks were formed under epidote-greenschist-facies conditions and that they are comparable with Riphean TMC-IV metamorphics from other regions. Moreover, the presence of relict mineral parageneses suggests that greenschist-facies metamorphism was preceded by granulite- or high-temperature amphibolite-facies, similar to that which occurred during the metamorphism of the ancient complexes of the Baydarag inlier basement (Kozakov, 1993).

Isolated outcrops of amphibole and sillimanite gneisses, found scattered within large Palaeozoic granitoid massifs, are related to ancient basement metamorphics in the core of the Dzabkhan Massif, in the Ider river basin. The specific relict mineral parageneses of these metamorphics also suggest that they resemble metamorphic formations associated with TMC-II within the Baydarag inlier.

Thus, the Dzabkhan Massif is the most representative and best studied ancient massif of Mongolia. Three pre-Riphean metamorphic complexes, corresponding with Early Archaean, Late Archaean, and Early Proterozoic TMC (TMC-I, TMC-II, TMC-III), have been reliably distinguished within its basement (the Baydarag inlier). Only in the south-eastern part of the Dzabkhan Massif are Riphean protocover rocks, metamorphosed during the course of TMC-IV, fully represented. The other parts of the Dzabkhan Massif contain only fragments of the basement and the cover, but they are probably comparable with appropriate elements of the Baydarag inlier.

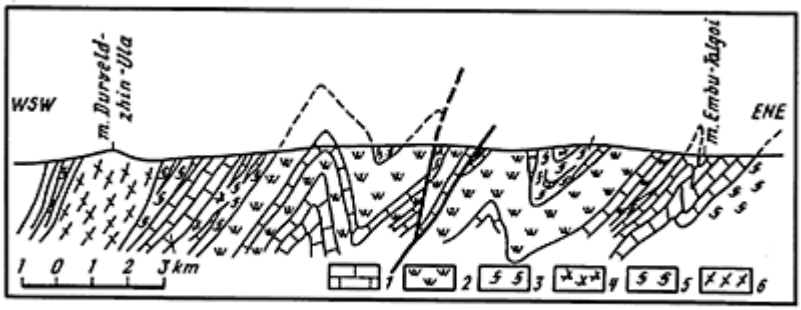

Key: 1—metamorphosed dolomite, 2—quartzite, 3—quartz-biotite schist, 4—quartz-amphibole schist, 5—biotite gneiss, 6—plagiogneiss (see Fig. 1-①).

Figure 5 Structural section of ancient metamorphic rocks in the Dzabkhan-Khungui watershed (Dzabkhan Zone).

1.3 The Tuvin-Mongolian Massif

The massif is (Fig. 1-I- ,). is located just north of the Dzabkhan Massif and, in Mongolia, occupies the area of the western Prikhubsugulye and the northern slope of the Khan-Khuhei Ridge (Fig. 1-I- ,). Furthermore, the larger and better studied north-western part of the massif is located outside Mongolia, in Tuva, within the Sangilen Plateau. All of the boundaries of the massif are of a tectonic nature: with the Dzabkhan Massif to the south, with the Caledonian structures of the Ilchir and Dzhidin zones to the east and with the Eastern Tuva Zone to the north-west, where elements of lateral transition to the Caledonides remained in the cover of the massif (Ilyin, 1973; Mitrofanov *et al.*, 1981; Gonikberg, 1995).

The basement of the Tuvin-Mongolian and Dzabkhan Massifs has almost the same structure (Mitrofanov *et al.*, 1985). Ancient metamorphic complexes corresponding with

the same four tectonometamorphic cycles as occurred in the Baydarag inlier have been recognized within the Sangilen Plateau and on the northern slope of the Khan-Khuhei Ridge (Fig 1-I-). Gneisses, igneous rocks, schists, quartzites, and marbles, with mineral parageneses that indicate low-pressure granulite-facies metamorphic conditions (800°C, 6–7 kbar) correspond with the Early Archaean TMC. These formations occur only as relics within the metamorphic rocks of the younger complexes. Zircons from granulite boulders are 3,100± 200 Ma old (Using the U–Th–Pb method) (Kozakov *et al.*, 1993).

Gneisses containing quartzite, amphibolite and marble layers can be correlated with the Late Archaean cycle. The mineral parageneses of these rocks are characteristic of high-pressure granulite- and amphibolite-facies conditions (sillimanitebiotite-garnet-orthoclase subfacies).

A complex of rocks corresponding with the Early Proterozoic cycle has been preserved in the Tuvin-Mongolian Massif, in contrast to the Dzabkhan Massif. This complex comprises marbles, quartzites, and gneisses, the mineral parageneses of which indicate formation under amphibolite-facies conditions (andalusitesillimanite facies series). Zircons and monazites from the migmatites, granites and pegmatites of the Sangilen have ages ranging from 2,100 to 1,710 Ma. As in the Dzabkhan Massif, Riphean metamorphism occurred here under greenschist-facies conditions and was only localized in its effects. A close analogy for both massifs is shown in the occurrences of igneous processes characteristic of each of the listed TMC (see pp. 1–4).

The Tuvin-Mongolian Massif is noted for its widespread development of early Riphean rift structures, especially in the Vendian-Precambrian terrigenous-carbonate cover. These formations are most completely represented in the north of Mongolia, in western Prikhubsugulye. (Fig. 1-I-) It is most likely here that the present Khubsugul and Darhat depressions, together with a ridge separating them, correspond with a Lower Riphean rift. Both depressions are referred to the Khubsugul phosphorite-bearing basin (Figs. 1- , Fig. 6)

The Darhat Depression extends from south to north for about 300 km, with a width of up to 100 km, and runs along the bank of Lake Khubsugul to the west. In

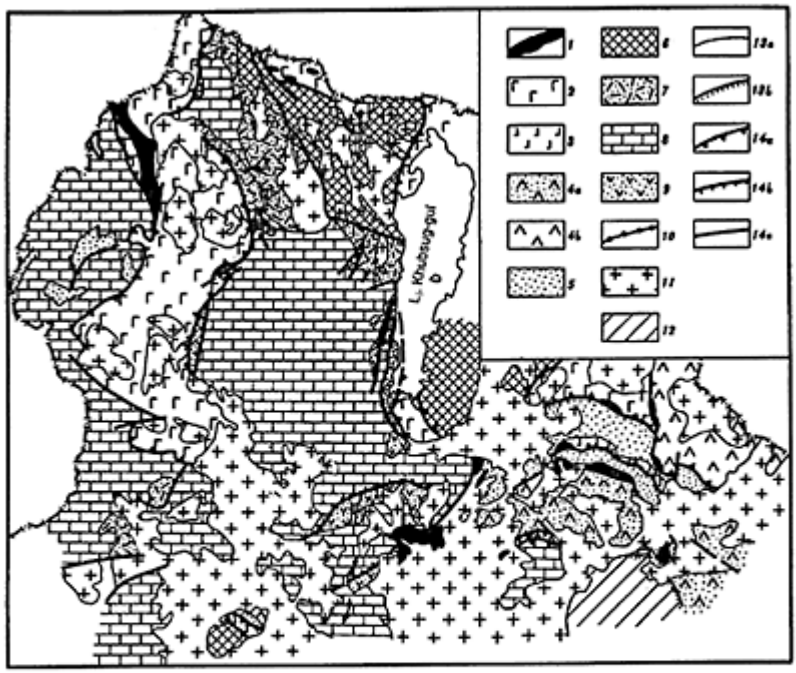

Key: 1—ultrabasic rocks and serpentinized *mélange*: 2–4—formational subzones of the Dzhidin Zone: 2—Alagtsarigol, 3—Urgol, 4a—Egingol, 4b—Buryatskaya; 5—terrigenous flyschoid and olistostrome assemblages; 6—metamorphic rocks: 7–9—formations of the Tuva–Mongolian Massif: 7—porphyry (R_3), 8—terrigenous arkose and siliceous–carbonate phosphorite-bearing ($V–C_1$) formations, 9—andesite and tuffite flyschoid (C_{1-2}) formations; 10—phosphorite; 11—granitoids; 12—Upper Palaeozoic volcanic belt; 13—geological boundaries (a—conformable, b—unconformable); 14—fault (a—base of tectonic nappe, b—thrust, c—overthrusts and faults).

Figure 6 Structural map of the Tuva-Mongolian Massif and the Dzhidin Zone. Compiled on the basis of data from A.V.Ilyin (Kheraskova *et al.*, 1987, see Fig. 1-1-).

the present-day structure the boundaries of the depression are apparently tectonic although outcrops of polymictic boulder-pebble conglomerates with granitoid boulders 823 Ma old (from K-Ar data) can be found along its western slope. A schematic section of the early Riphean deposits infilling the depression can be represented from base to top by: basal conglomerates, sandstones, and gravelstones of arkosic and quartzose composition, occasional acid and basic volcanics, aleurolites, shales, and dolomites. The thickness of these sediments is sometimes 3,000 m, with the clastic part of the section appreciably increasing in thickness near the flanks of the depression. Furthermore, the amount of volcanic rocks increases northwards, along strike, and in the northern areas of the depression they become dominant. In these particular areas their absolute age has

been determined as 718 Ma (using the whole-rock K-Ar method). As a whole, the Darhat series is a typical arkose formation, and the degree of maturity of the arkoses and the fineness of their grain size increase up the section. This indicates a gradual peneplanation of the erosional surface that was formed at the beginning of 'Darhat times' (Late Riphean) (Illyin, 1990).

The cover of the Tuvin-Mongolian Massif is the thick, almost wholly carbonate, Khubsugul Series, which is widely known due to the occurrence of phosphate (Ilyin, 1990). It overlaps the rocks of the underlying Darhat Series with an erosional unconformity but not a structural unconformity, and commonly extends far beyond the limits of the Darhat Series. Only in the lower part of the Khubsugul suite are cherts, phosphorites, black carbonaceous shales, fissile siliceous shales, and aleurolites present, in addition to carbonates. The remains of trilobites, archaeocyathids, brachiopods, and hyolithids of early Cambrian age have been found only in the limestones of the sequence above the phosphorite, which is upto 3,000 m thick. The Khubsugul series section is considered to be Vendian-Middle Cambrian in age.

A phosphate-bearing rock unit, which contains several economic phosphate deposits, is located in the middle carbonate part of the section and is distinguished by its variety of rock compositions. Besides phosphorites it includes dolomites, limestones, cherts, black carbonaceous shales, and fissile siliceous shales. The main bed of massive fine-grained phosphorite occurs at the base of the phosphate-bearing unit and reaches 10 m in thickness. The upper layer, which is usually thinner, is composed of granular phosphorites. The overall thickness of the phosphate-bearing unit reaches 100 m; its structure and the location of phosphorites within it change appreciably in the different parts of the Khubsugul Basin. The P_2O_5 content also varies significantly, from 40–45 tons to 5–8 tons in the column of phosphate-bearing rocks with a section of 1 m and length equal to the thickness of the entire phosphate-bearing unit.

1.4 The Central Mongolian Massif

This appears to occupy a similar proportion of the northern megablock as the other ancient massifs (Fig. 1-III). It appears to extend along the boundary with the south Mongolian Hercynides, from the eastern termination of the Baydarag inlier, for about 500 km. The position and dimensions of the Central Mongolian Massif can be only speculated upon, as it is almost completely hidden under the younger Mesozoic-Cainozoic deposits.

The exposed northern part of the massif is known as the South Kerulen Zone (Fig. 1-III-) (Blagonravov *et al.*, 1990). It is separated from the Caledonides of the Kerulen Rise by a major fault, coinciding with the Kerulen River valley and located on its right bank. The South Kerulen Zone has an ancient metamorphic basement composed of paraschists and amphibolite-facies gneisses, referred to the pre-Riphean by correlation with similar rocks from other regions. Above this section, there is a thick unit (up to 2,000 m thick) of green, sometimes carbonaceous shales (containing quartz+sericite+chlorite); quartzites, metavolcanics and limestones also occur, although more rarely. This zone is suggested to be of early-middle Riphean age.

The greenschist unit is unconformably overlapped by a gravelstoneconglomerate unit, followed by sandstone-aleurolite-shale, and, finally, by limestone units with the remains

of archaeocyathids of early Cambrian age. These deposits are 1,200 m thick and are also considered to represent the sedimentary cover of the microcontinent.

Some general considerations about the palaeotectonic position of the TuvinoMongolian Massif and other massifs have allowed us to make a detailed study of the carbonate rocks of the Khubsugul phosphate-bearing basin. They show a distinct predominance of dolomites over limestones and rapidly decrease in thickness westwards. Any indications of their deposition under shallow-water conditions tend to disappear in the same direction. The base of the carbonate unit, which is bounded to the east by the base of the Lower Cambrian and to the west occurs within the Lower Vendian, therefore occurs on progressively older rocks, towards the west. This evidence indicates that in the Vendian-Cambrian the Tuvin-Mongolian Massif was covered by a shelf sea, which opened westward into a deep-sea Caledonian oceanic basin. It is possible that at the same time, the massif 'represented a single whole with the Siberian continent' (Ilyin, 1990).

However, some of the results of recent study cast doubt on this conclusion. Primarily, the tectonometamorphic cycles established for the basements of the Dzabkhan and Tuvin-Mongolian massifs do not entirely coincide with the Siberian continental basement cycles, where the second Late Archaean metamorphic cycle, which occurred at 2,370 Ma, is expressed only weakly (Bibikova *et al.*, 1990). At that time in the north-east, the Tuvin-Mongolian Massif appears to have been separated from the Siberian continent and then metamorphosed Caledonian formations occurred there (Belichenko and Boos, 1990). And, finally, recent world-wide generalizations concerning stratigraphy, volcanism, palaeomagnetism, and tectonics suggest that the Dzabkhan, Tuvin-Mongolian, and Central Mongolian microcontinents may have separated from Eastern Gondwana in the late Riphean, and may have collided with the Siberian continent as late as the beginning of the Ordovician (Mossakovsky *et al.*, 1993; Kheraskova *et al.*, 1995).

2
THE CALEDONIDES

A.B.Dergunov

Structurally, most of North Mongolia consists of Caledonian features, which extend northwards into southern Siberia and westwards and eastwards into China. To the south the Caledonides are bounded by the Variscides of south Mongolia (Fig. 1).

The ancient Tuvin-Mongolian, Dzabkhan, and Central Mongolian massifs (microcontinents), described in Chapter 1, consist of ancient pre-Riphean metamorphic basement overlain by a Riphean and Cambrian sedimentary cover, which in several places grades laterally into Caledonian deposits. It should be emphasized that beyond the limits of the microcontinents the ancient pre-Riphean age of any sialic metamorphic rocks there has not been proven and therefore there is no reason to attribute them to the basement of the Caledonides (Dergunov and Kheraskov, 1985).

2.1 Melanocratic Basement Complex

Extensive ophiolitic belts, consisting mostly of basic-ultrabasic rocks, pyroxenites, complexes of parallel dykes and serpentinite *mélanges,* are widespread in all of the Caledonian zones. Moreover, they are encountered in the remains of nappes and numerous horsts at the boundaries and margins of the Caledonian zones and adjacent structures. The widespread exposure of these rocks (more than 100 exposures are known from just the western Mongolian Caledonides) suggests that the rocks of the ophiolitic association occur at the base of the Caledonian zone. From this it can be inferred that the Caledonides were predominantly developed on oceanic crust (Dergunov, 1989).

The largest, Shishkid, basic-ultrabasic massif (Fig. 6) extends from the northermost part of Mongolia for more than 50 km N–S, with a width of up to 10 km. The massif remains poorly studied. From the work of A.Savelyev it is known that the eastern part of the massif is composed of dunites, within which large isolated Iherzolite and harzburgite masses are encountered. Dunites, wehrlites, and clinopyroxenites are best preserved in the western part of the massif, which is characterized by the irregular alternation of these rocks. Massive gabbroic rocks are exposed along the western border of the Shishkid Massif. The contacts between the dunite, dunite-wehrlite-clinopyroxenite and gabbroic parts of the massif are tectonic in character. To the west the ultra basic rocks occur adjacent to the basaltoids, which in turn give way to metamorphosed volcanogenic-schist and calcareous deposits.

The structural position of the melanocratic rocks at the base of the ophiolite has been established with greater certainty on the Khan-Khuhei Ridge (Fig. 1- and), where a band of outcrops of polymictic serpentinite *mélange* extends for more than 100 km (Dergunov, 1989). The *mélange* occurs at the base of a pile of tectonic sheets composed

of Vendian-Early Precambrian ophiolitic rocks (Figs. 11, 12). Thick bodies of crushed serpentinite, which form the matrix of the *mélange* occur on the borders of the Ichutuin-Gol river valley and its tributaries. This matrix contains rounded pebbles and boulders, as well as non-rounded blocks, sometimes very large (up to several metres in diameter) of massive serpentinites formed by the alteration of dunites and pyroxenites, more rarely of harzburgites. Individual large blocks consist of amphibolites and micaceous marbles, probably representing detached fragments of the ancient metamorphic basement. Sometimes individual large boulders of gabbro dolerites, other volcanics, cherts and (metamorphosed limestones) are encountered. To the east, in the Dzun-Khangai village area, in the Khan-Khuhey Zone, a continuation of small remnant of serpentinite *mélange* (approximately 1×2 km) with blocks of the same metamorphics is found within the Pre-Caledonian metamorphics (Palei, 1979).

The relatively large Khutul ultrabasic Massif (Fig. 1-) is oriented N–S and has a complex boundary and dimensions of 20×10 km. It occurs in the north-east part of the Dzabkhan microcontinent, 30 km east of its tectonic boundary. It is composed of serpentinite dunites and harzburgites, sometimes with a banded structure. The polymictic serpentinite *mélange* overlies the ancient metamorphics at the base of the massif. To the south-west the *mélange* occurs adjacent to highly epidotized and schistose basic volcanics, which have been subject to only greenschist metamorphism, in contrast to the surrounding ancient metamorphic rocks. These ultrabasic rocks and greenschist volcanics appear to be fragments of the tectonic cover, thrust over on the Dzabkhan Massif metamorphics from the west.

The southern margin of the same Dzabkhan microcontinent is marked by exposures of Caledonian ophiolites. It is associated with the Khantaishir, Khasagtin, and Darbin gabbro-ultrabasic massifs, each of which is located at the base of the ophiolitic association. The Khantaishir Massif, which is the best studied (Zonenshain and Kuzmin, 1978), adjoins the ancient metamorphics in its lower, dunite-harzburgite sequence. Later faults have subdivided it into large individual bodies and have also affected the overlying pyroxenite and gabbroid formations. However, they are found to be located regularly, according to this sequence, from north to south, moving away from the ancient metamorphic rocks. The gabbrodolerites are gradually replaced by a sheeted dyke complex, which in turn is replaced by basaltoid pillow lavas and occurs immediately south of the gabbroids. Further to the south, the basaltoid pillow lavas are overlapped by the terrigenous-carbonate-siliceous rocks of the Lower Cambrian. The sequence listed is entirely consistent with the sequence of the ophiolitic association, and therefore it can be considered as a large layered body of Caledonian ophiolites thrust over the metamorphic rocks of the Dzabkhan Massif from the south.

The Khasagtin dunite-harzburgite massif, located north-west of the Khantayshir Massif, is also believed to be a fragment of the Caledonian ophiolitic cover, but occurs under more complex structural conditions (Ruzhentsev and Burashnikov, 1995).

This tectonic style is maintained in the extreme south-western part of the ancient Dzabkhan Massif, within the structures of the Darbi Ridge. The southern slope and the south-western base of the massif are composed of rocks of the gabbro-ultrabasic complex, while the northern slope of this ridge consists of predominantly ancient metamorphic rocks. The relatively large Alagul Massif, composed of serpentinized dunites and harzburgites, is also located here.

Rare gabbro-ultrabasic bodies, which are similar in their composition and structural position, are known in other Caledonian zones of Central and West Mongolia (the Dzhidin, Bayan-Khongor, and Prikerulen Zones, etc.). They are everywhere characterized by their allochthonous position, together with other members of the ophiolitic association, and are most likely to be located near to the base of the ophiolitic cover. Even rare horst highs among the huge outcrops of terrigenous turbidites within the Mongol-Altai Zone, as a rule, contain serpentized ultrabasic bodies that indicate the presence of ophiolites and, consequently, of primary oceanic-type crust even, beneath these huge terrigenous rock masses.

In West Mongolia, sills and dolerite dyke complexes are known from nearly all of the exposures of melanocratic ophiolite basement: Khantaishir, Darbin, Khan-Khuhei, Erdeni-Ulin, Ih-Bogdin, and Bayan-Khongor. They occur at the base of the large tectonic nappes overthrust on the margin of the ancient Dzabkhan Zone and subdivided into tectonic slices (Dergunov *et al.*, 1980; Dergunov and Luvsandanzan, 1984).

On the SE margin of the Ozyernaya Zone, the dolerite dykes of the Khantaishir Massif are located above the transitional gabbro-pyroxenite complex and form an individual layer up to 1,000 m thick. In the upper part of the complex they permeate the entire area, forming a layer of unusual dolerite breccias, which in turn give way to pillow lavas. A direct transition from dolerite dykes to pillow lavas has been established here, and both are believed to have formed after the magma chamber opened (the transitional gabbro-pyroxenite complex was formed during this earlier opening phase (Zonenshain and Kuzmin, 1978)).

As has been elucidated (Perfiliev and Kheraskov, 1980), the rock complexes that make up the ophiolitic association form individual tectonic sheets, which consist of intensively feldspathized rocks, plagioclase pyroxenites, and quartz gabbrodiorites. These rocks are broken by dolerite dykes and zigzagging dolerite veins, which have distinct quenched contacts.

The overlying sheet consists of parallel dolerite dykes, dipping steeply eastwards, i.e. perpendicular to the sheet, which subsided south-westwards. The country rock between the dykes at the base of the sheet make up only $\leq$50% of its volume and are composed of fine-grained and medium-grained gabbro and quartz diorites. These were originally dykes, not subjected to metasomatism, which cut through the dolerite breccias to the pillow lavas of the Vendian-Lower Cambrian. Thus, two generations of dolerites, separated by periods of feldspathization, have been established in the Khantaishir ophiolitic complex. The change from dykes to dolerite breccias and then to pillow lavas is referred to as the second generation of dyke injection.

The Erdeni-Ula ophiolitic massif is located approximately 200 km SE of the Khantaishir Massif. It also has a complex imbricate structure, with its two lower slices being composed of sedimentary-volcanogenic rocks the green tuff formation and three formations of basic melanocratic igneous rocks (Perfiliev and Kheraskov, 1980). In the lower sheet, basal conglomerates containing ultrabasic and gabbroid pebbles occur overlying the ultrabasic rock, and some of the inter-layers are composed of serpentinite aleurolites and sandstones. In the upper slices, serpentinites, Iherzolites, dunites and wehrlites occur, overlain by melanocratic gabbro, grading into leucocratic gabbro intruded by dolerite dykes. A complex of branching and nearly parallel dolerite dykes of two generations occurs above these, with the earlier dykes showing a higher degree of

greenstone alteration. Screens of ultrabasic rocks and gabbro also occur between these dykes. Second-generation dolerite dykes predominantly permeate the lower part of the dolerite layer. They are compositionally similar to oceanic tholeiites and possibly served as feeder channels for the basalts.

The above descriptions reflect the complex and long-term history of metamorphism of the basal melanocratic rocks, and confirm that there was a time gap between the formation of the basal melanocratic rocks and the sedimentary-volcanogenic sections of the ophiolites. However, dolerite complexes occur world-wide and are associated with melanocratic basement rocks, and are spatially and structurally connected with them, i.e. together they form a consistent paragenetic association. Recently, dolerite dyke complexes have been discovered within the outcrops of the melanocratic basement rocks of the Darby Ridge (Kheraskova *et al.*, 1985); in the ophiolitic complexes of the Ih-Bogdo Ridge and in the Bayan-Khongor zone (Kopteva *et al.*, 1984); and among the exposures of serpentinite *mélange* on the southern slope of the Khan-Khuhey Ridge (Dergunov and Luvsandanzan, 1984).

Thus, dolerite complexes of sills, breccias, and dykes are widespread in the Mongolian Caledonides and everywhere occupy a definite position in the upper section of the melanocratic basement. It is most likely that the dyke complex formed at a high-level (near the surface) within the melanocratic basement, during extension and horizontal sliding of tectonic sheets, made up of rocks of the upper gabbro-amphibolite and transitional dunite-pyroxenite-gabbroic complexes of the melanocratic basement (Kolman, 1979; Perfiliev and Kheraskov, 1980).

The dolerite complexes are of several generations, separated by major breaks, with even the earlier stage being formed essentially later than the gabbro-ultrabasic basement and intruded into already solidified rocks. The direct transitions between the late-generation dolerite dykes and the basalt lavas indicate that the dolerite complexes formed intermittently over a long time interval, following the formation of the ancient gabbro-ultrabasic basement and before the formation of the upper siliceous-volcanogenic sections of the ophiolite. Summarizing these data, it can be inferred that the dolerite complexes have no direct genetic link with the melanocratic basement. The gabbro-ultrabasic basement was the protolith, which under conditions of near-surface extension generated dolerite dykes, sills and basalt volcanics. Processes of dyke formation reflect the tectonic layering of the oceanic lithosphere, and the relative horizontal motions of these layers (Peive, 1980).

2.2 Caledonian Zones of West Mongolia

The ancient Tuvin-Mongolian and Dzabkhan massifs (microcontinents) separate the Caledonides of West Mongolia from those of Central and East Mongolia: the Caledonian structures of West and Central Mongolia being thrusted over the western and eastern margins of these massifs (Zonenshain and Tomurtogoo, 1979; Dergunov and Luvsandanzan, 1984; Dergunov, 1988; Ruzhentsev and Burashnikov, 1995).

In West Mongolia, the early Caledonian (salairian) Khantaishir, Dagandel, Ozernaya, Kharkhirin, and Caledonian Altai zones are located south-west and west of the ancient massifs. All of them have a NNW strike and are bounded by major faults trending in the

same direction. To the north of these zones is the Khan-Khuhei Zone, which occupyies the southern slope of the Khan-Khuhei Ridge. As in the case of three previous Early Caledonian zones, its structure had already formed by the Middle Cambrian, but due to Cainozoic E–W thrusting the Khan-Khuhei Zone bounds the Dagandel and Ozernaya zones to the north. In the south of western Mongolia, all of these zones, as well as the ancient massifs, are cut across by the Variscides of South Mongolia. To the north, Caledonian structures extend into southern Siberia and—to the north-east—into China (Fig. 1).

The Khantaishir Zone

This is an early Caledonian folded zone, formed from Vendian-Cambrian volcanogenic and sedimentary deposits thrust over the southern tip of the Dzabkhan microcontinent (Fig. 1- , , and). Within the southern margin of the latter, the shelf zone (Tsaganolom Zone—arkose sandstones, dolomites, limestones, V_2– $Є_1b$) and the slope zone (Khasagtin Zone—arkose sandstones, dolomites, chert, carbonate turbidites, V–$Є_1a$; terrigenous flysch, $Є_1b$) are distinguished (Fig. 1- , Fig. 7) (Ruzhentsev and Burashnikov, 1995). A characteristic element of the section at the southern tip of the microcontinent is the Shargyn-Gol Complex (R_3–V_1), containing volcanogenic-terrigeneous deposits associated with extensive dolerite dyke swarms. From their chemistry, the volcanics and dolerites can be classified as subalkaline and alkali-olivine basalts and are considered to be intraplate formations. Based on this evidence and on the structure of the terrigeneous units (which show wide variations in thickness over a small area: from 0 to 3 km thick) and their composition (the widespread development of conglomerates and the arkosic composition of the material), it is believed that the complex was formed within an intracontinental rift which marked the beginning of continental breakup and the formation of the Khantaishir palaeo-ocean (Burashnikov and Ruzhentsev, 1993).

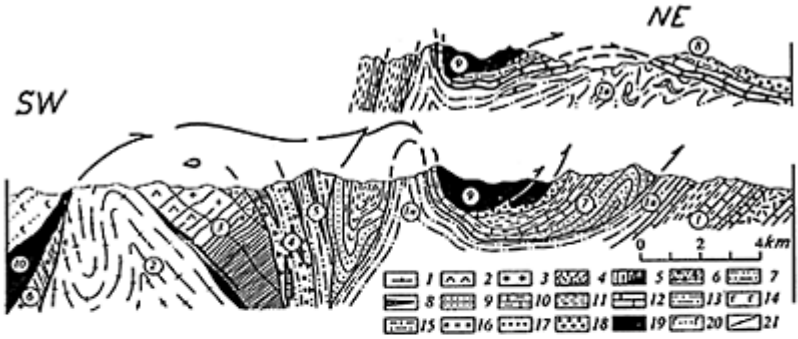

Key: 1—schist, granite gneiss, amphibolite, marble, quartzite (A–PR); 2—gabbro diorite, tonalite, and quartz diorite (P–C); 3—granodiorite (P€); 4—rhyolite, dacite, and their tuffs, in the Dzabkhan Formation (R_3); 5–8—Shargyn-Gol complex (R_3–V_1): 5—dyke, 6—coarse epiclastics, tephroids, 7—turbidites, 8—basalt lava flows and sills; 9—sandstone of the Khasagtin Formation (V); 10—dolomite and limestone of the Tsaganolom Formation (V); 11—carbonate–terrigenous Bayangol Formation ($€_1$tm–at); 12—limestone of the Salanygol formation ($€_1$at–bt); 13—flysch of the Khairkhan Formation ($€_1$bt–$€_2$?); 14–15—Uet Formation (V_2–$€_1$?): 14—basalt, 15—jasper and limestone; 16—limestone of the Khamardaba Formation (C_1bt); 17 and 18—conglomerates: 17—C_{2-3}, 18—0?; 19—ophiolite; 20—basalt, epiclastics, greywacke, and limestone of the Khantaishir Formation ($€_1$tm–at); 21—faults; Circled numbers: ①–⑦ Dzabkhan Massif: ①—Tsaganolom shelf zone (*Io*—Khairkhan flysch), ②–⑦—Khasagtin Zone: ②—inlier of crystalline basement, ③—Dund orthocomplex, ④—marginal and ⑤—axial sections of the Shargyngol riftogenic complex, ⑥—Urd riftogenic complex, ⑦—slope complex of the massif; ⑧–⑩—zones of a palaeo-ocean: ⑧—Nomongon, ⑨—Khasagtin, and ⑩—Khantaishir ophiolite massifs.

Figure 7 Geological sections across the Khasagtin—Ula Ridge (see Fig. 1-).

In the Khantaishir Zone, the following subzones are distinguished (from north to south): the Nomongon, the Khantaishir itself, the Noran, the Satyrbulak, the Ulanshandin and the Khurai subzones.

The Nomongon subzone is the remnant of ophiolitic cover in the Khasagtin-Ula Ridge (Fig. 7). The serpentinite *mélange* layer is exposed at its base, with sills and pillow lavas (300–600 m thick) occurring above this; these are similar to MORB in their chemical composition. The unit (200–250 m thick) is composed of jaspers and a Vendian-Lower Cambrian (pre-Botomian layer of) micritic limestones occurs above this.

The Khantaishir subzone (the northern slope of the Khantayshir-Ula Ridge) is characterized by the widespread development of ophiolites, forming a series of tectonic slices (Fig. 8). The summary ophiolitic section here is as follows (from bottom to top):

1) Harzburgites and dunites (up to 1500 m);
2) Wehrlite-clinopyroxenite cumulates (200–250 m);
3) Banded gabbros (100–150 m);
4) Massive gabbros (250–300 m);

Key: 1—dunite and harzburgite; 2—banded assemblage, gabbroids; 3—dyke series; 4—basalt, jasper, epiclastics of the Khantaishir Formation ($Є_1$tm); 5—limestone of the Khamardaba Formation ($Є_1$bt); 6—coarse epiclastics of the Arainbulak Formation ($Є_1$tm–at); 7—tuffite, fine epiclastics of the Arainbulak Formation (V_2–$Є_1$tm); 8—greywacke of the Noran Formation ($Є_1$at); 9—Satirbulak flysch ($Є_1$bt); 10—epiclastics, tuff, and tephroids of the Ulanshandin Formation (V_2–$Є_1$at); 11—faults; Circled numbers—zones: ①—Khantaishir, ②—Noran, ③—Satirbulak; ④, ⑤—Ulanshandin (④—lower, ⑤—middle sheets).

Figure 8 Geological section across the Khantaishir-Ula and Ula-Shandy-Ula Mountains (see Fig. 1- and)

5) Dyke series;

6) Pillow lavas (V_1–$Є_1$t, 500–600 m);

7) Alternating of basalts, jaspers, epiclastites (volcanoclastites), archaeocyathid limestones (the Khantaishir suite, $Є_1$a; 400–800 m);

8) Archaeocyathid limestones (Khamardabas suite, $Є_1$b; 200–250 m), with a basal conglomerate unconformably overlying the underlying deposits.

The Petrochemical data (Kepezhinskas *et al.*, 1987; Izoch *et al.*, 1990; Kepezhinskas *et al.*, 1991) indicate different differentia tion trends for the gabbropyroxenites (tholeiitic type) and the basaltoids (calcalkaline island-arc type). Among the latter, low-Ti calcalkaline and boninite-series rocks can be distinguished. The composition and structure of the Khantaishir suite deposits indicate that the latter were formed above a subduction zone, generated within the limits of a primitive island-arc rise (Ruzhentsev and Burashnikov, 1995).

The Noran Subzone

This zone is situated on the southern slope of the Khantaishiryn-Ula Ridge. Here the ophiolites are also exposed at the base of the section (harzburgites, ultrabasic and basic cumulates, massive gabbronorites, dyke series, and basalts). The ophio-lites are usually highly tectonized (often to form thick *mélange* layers).

The ophiolites are overlapped by a tephra-greywacke series. Its lower unit (the Arainobulak suite, V_2–$Є_1$t; up to 1,500 m thick) is represented by epiclastic rock, greywackes, and various tuffs containing rare limestone interlayers. The upper unit (the Noran suite, $Є_1$t-a, which is up to 2,000 m thick) is made up of grey-wacke turbidites passing up section into relatively coarse terrigenous deposits containing polymictic conglomerate members. Taking into account the composition of the sediments, the Noran subzone is considered by us to be a Vendian-Cambrian interarc trough.

The Satirbylak Subzone

This is situated in northern part of the Ulan-Shandy-Ula Mountains and is a zone of flysch development (up to 1,700 m thick), with a basal conglomerate overlying the Noran greywackes. In the middle part of the flysch section, archaeocyathid limestone interlayers are present ($Є_1$–b). The upper part of the section contains (up to 200 m thick) lenses of blocks of quartz porphyries, felsites, pyroxene and plagioclase porphyries, dolerites, various granitoids, and stromatolitic and oncolitic limestones.

Ulanshandin Subzone

This zone is situated in the Ulan-Shandy-Ula Mountains and is a belt of predominantly varied volcanic and volcanic-terrigenous rocks making up three layers. The lower (northern) layer is composed of basalts alternating with tephroturbidites. The section of the middle layer is as follows (from bottom to top):

1) Basalts with marble interlayers (700–800 m).

2) Epiclastites (volcanoclastites) of basic and intermediate composition, with stromatolitic and oncolitic limestone interlayers (V, 150–170 m).

3) Volcanomictic conglomerates, gravelstones, coarse-grained tuffs and plagioporphyry (1,500–1,800 m).

4) Volcanomictic and tuffs of intermediate composition alternating with quartz-porphyry tuffs (1,200–1,300 m); numerous layered and cross-cutting bodies of quartz porphyry and felsite.

The upper layer consists of conglomerates and conglobreccias (dolerite pebbles and boulders, pyroxene and plagioclase porphyries, quartz-porphyries, felsites, and granite-porphyries). Numerous dolerite sills and bomb-tuff layers are present, as well as numerous brecciated bodies of quartz-porphyry volcanics.

All of the formations listed were generated within a large island-arc rise. The deposits of the lower layer correspond to the fore-arc, the middle layer—to the slope, and the upper layer—to the apical part.

The Khuroi Subzone

This is the southernmost subzone—see Fig. 1- and is represented by Vendian-Cambrian terrigenous-siliceous shales, including dolerite sills and flows. Sometimes serpentinite *mélange* bodies are exposed beneath these shales. In the Cambrian this zone represented a back-arc basin, located between the Ulashandin Rise and the South Gobi microcontinent, which separated from the Dzabkhan microcontinent in the Vendian.

The palaeotectonic profile of the Khantaishir Zone in the Vendian-Atdabanian is considered to be as follows (Fig. 9): the Tsaganolom subzone—the inner shelf of the Dzabkhan microcontinent, Khasagtin subzone—its outer shelf and slope, the Nomangan subzone—a fragment of the Khantaishir oceanic basin

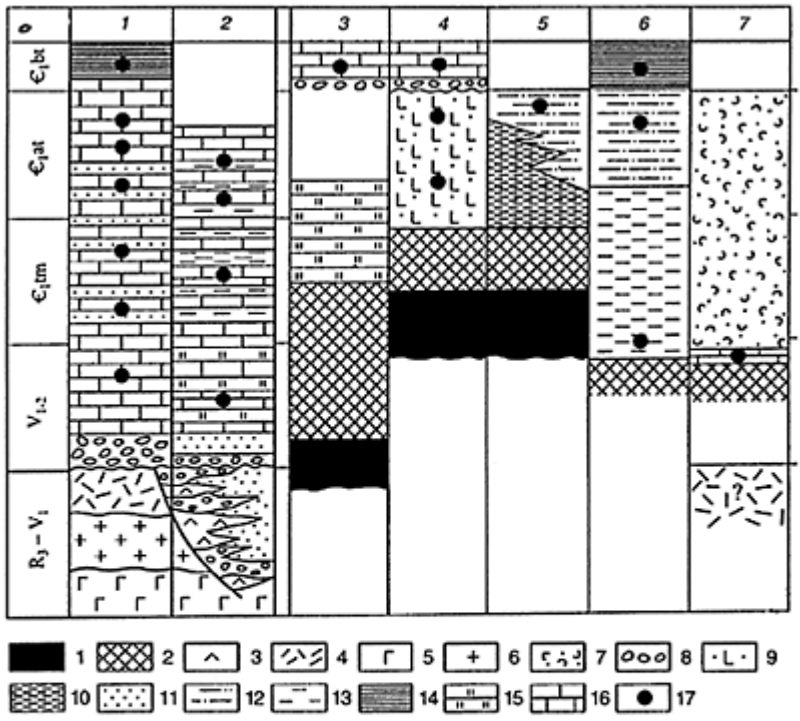

Key: 1—ophiolite; 2 and 3—basaltoids: 2—of ophiolite assemblages—alkaline; 4—rhyolite of the Dzabkhan Formation; 5—gabbro-diorite and tonalite; 6—granodiorite; 7—epiclastics, tephroids, and tuff of the Ulanshandin Formation; 8—conglomerates; 9—epiclastics, basaltoids, and limestone of the Khantaishir Formation; 10—tuffite, shale, and fine epiclastics of the Arainbulak Formation; 11—sandstone; 12—greywacke; 13—clay-carbonate turbidites; 14—flysch; 15—siliceous deposits; 16—limestone; 17—fossil sampling sites (Levels); Numbers on the chart: *1*—Zaganolom Zone, *2*—Khasagtin Zone; *3–6*—Khantaishir Zone (subzones: *3*—Nomgon, *4*—Khantaishir, *5*—northern and *6*—southern parts of the Noran subzone), *7*—Ulanshandin Zone.

Figure 9 Comparison of standard sections of the Dzabkhan Massif and the Lake Zone.

lithophere obducted on to the continent in Botomian times, the Khantaishir subzone—the primitive ensimatic island arc, the Noran subzone—the interarc trough, the Ulashandin subzone—the mature island arc with the fore-arc Satyrbylak flysch trough formed in Botomian times, the Khuroi subzone—the backarc trough adjacent to the South Gobi microcontinent to the north (in current co-ordinates).

The Dagandel Zone

This adjoins the western margin of the Dzabkhan Massif and extends for about 250 km in a N–S direction with a width of up to 40 km (Fig. 1-). It occupies much of the lower

part of the basin of the river Dzabkhan and its right tributary: the River Khungui. Within this zone, incomplete folds with steeply dipping limbs, bounded by faults of mainly NNW strike, are predominant. The layers and sheets are overturned eastwards relative to the Dzabkhan Massif, where the constituent volcanogenic and carbonate rocks and ophiolites are encountered as fragments of nappes. The most complete section of the Dagandel Zone (2,600 m thick) has been described in the area of Mt Dagandel (Kheraskova, 1986) (from the bottom upwards):

1) Spilites and dolerites—more than 1,000 m thick;
2) Keratophyres with layers and lenses of acidic tuffs—400 m;
3) Spilites—100 m;
4) Basic tuffs with keratophyre lenses—150 m;
5) Siliceous rocks with interlayers of cherts, aleurolites, and dolomites;
6) Dolomites with aleurolite interlayers with siliceous rocks lenses—350 m;
7) Massive, thick-layered dolomites and limestones, containing archaeocyathid remains and siliceous tuffite interlayers—700 m.

Spilite pillow lavas occur at the base of the section (Dergunov and Kheraskova, 1981), they sometimes alternate with massive dolerites and lava breccias. The central parts of the pillows contain more phenocrysts, and these are composed of albitized and saussuritizated plagioclase and, very occasionally, chlorite pseudomorphing pyroxenes. The groundmass contains microliths of plagioclase, or, more rarely, plagioclase and pyroxene. The spilites are often amygaloidal, with the amygdales containing calcite, quartz, epidote, and albite.

The keratophyres are altered to porphyries and are heavily veined with quartz, albitized K-feldspar and albite. The micropoikilitic groundmass is composed of a quartz-albitic aggregate with disseminated epidote. The tuffs and tuffites are usually altered to quartz-albite-chlorite schists (epidotic or actinolitic). They are often banded, due to the enrichment of some layers in highly coloured components. Angular grains of quartz and feldspar are disseminated in this groundmass. Spilites and keratophyres, which predominate in the Dagendel Zone are classified as bimodal series, with modes plotting in the field of basalts (50–60%) and rhyolites (20–30%). In this case, almost all of the basalts belong to the alkaline-olivine basalt group, with up to half of them containing more than 0.9% K_2O. An increase in TiO_2 occurs in parallel with an increase in alkalinity, which indicates the original composition of these rocks. Acidic volcanic—keratophyres—can also be attributed to the differentiates of the alkali-olivine-basalt series. Hence, the spilite-keratophyre series can be considered as a typical bimodal series, with high alkalinity.

The carbonate portion of the section (Dergunov and Kovalenko, 1995) is dominated by detrital limestones: i.e. calcarenites, calcilutites, and, rarely, calcirudites size. Sometimes they contain detrital quartzites, quartz and feldspars (from 0 to 50%), and sometimes the limestones grade into calcareous sandstones. Dark-

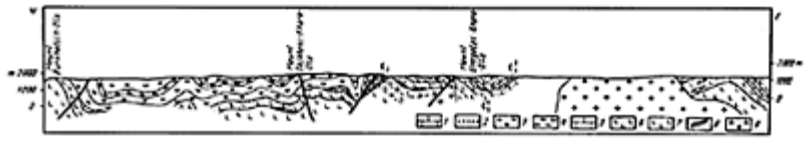

Key: 1 and 2—Middle Cambrian calcareous sandstone (1) and basal conglobreccia (olistostrome) (2); 3–8—Vendian–Cambrian formations: 3—Upper part of siliceous terrigenous tuffaceous assemblage; 4—olistostrome horizon; 5—reef limestone; 6—lower part of the siliceous tuffaceous–terrigenous assemblage; 7—spilite–dolerite assemblage; 8—jasperoids; 9—granitoids.

Figure 10 Structural section in the middle Lake Zone. Eastern Ser Ridge (see Fig. 1-).

coloured siliceous rocks form individual interlayers. The detritus is characterized by the graded bedding typical of turbidite flows. Interlayers of micro-laminated calcareous shales, containing sole marks also occur. The Vendian-Lower Cambrian carbonate units of the cover of the adjacent Dzabkhan and Tuvin-Mongolian massifs may have provided the provenance for the carbonate calcarenites. The thick dolerite members probably resulted from post-sedimentary processes.

The Ozernaya Zone

This occupies the central part of West Mongolia, west from the Dagandel Zone (Fig. 1-). It is the most prominent part of the early Caledonide of Mongolia, and contains the most typical formations of the Vendian-early Cambrian basin (Dergunov and Kheraskova, 1981; Dergunov, 1989). The Ozernaya Zone is separated from the adjacent Dagandel and Kharkhirin tectonic zones, to the east and west respectively, by high-angle faults. Between these it forms a rather wide (up to 100 km) band, tapering markedly to the south and bounded by Cainozoic E-W thrusts to the north, as mentioned above. This zone almost completely coincides with the so-called Basin of Large Lakes, of West Mongolia, which is cross-cut by the E-W Ser and Khan-Khuhei ridges, and, to the south, by an E–W branch of the Mongolian Altai Ridge. These are ridges where the most representative sections of the Ozernaya Zone are exposed, and the type and degree of dislocations can be observed in the constituent units. The different tensions of the structures are noticeable. In the middle part (Ser Ridge) the structures are represented by open folds with limbs dipping at angles of 30–50° (Fig. 10). On the western and eastern margins, the layers are much more steeply dipping, and the southern and northern terminations are characterized by imbricate thrusts and nappe systems forming zones of crustal thickening as, for example, in the Khan-Khuhei Zone, on the southern slope of the ridge of the same name.

The key section of the Vendian-Lower Cambrian formations of the Ozernaya Zone is exposed in the middle part of the Ser Ridge, which bounds some large lakes to the north: Lakes Khara-Us-Nur, Dayan-Nur and Khara-Nur. In the Tsom-Ula mountain area the deepest parts of the section are exposed. Here they are tilted steeply eastwards and young in the same direction.

It is typical that here the lowest part of the Vendian-Lower Cambrian section is unconformable, with conglomerates at the base, overlapped by shallow-water calcareous sandstones and silts, containing the abundant remains of Middle Cambrian trilobites. These layers are usually tilted to the opposite side, to the west, at 30–40°. Hence, this is precisely the place where the early Caledonian age of the West Mongolian tectonic zones is most reliably defined.

The visible lower section of Vendian-Lower Cambrian deposits is exposed in the Tsom-Ula Mountains where layered bodies dip steeply to the east (from the bottom upwards):

1) Spilites with interlayers of tuffs of basic composition, tuffites and silicified tuffs—more than 800 m;

2) Andesite-basalts—100 m;

3) Alternation of large spilite members with lava breccias and tuffites—350 m;

4) Alternation of the large sandstone layers with tuffites and silicified tuffs—200 m;

5) Sandstones with rare tuff and silicified tuffs interlayers—400 m;

6) Olistrostrome—100 m;

7) Limestone with remnants of archaeocyathids and algae, with gravelstone and conglomerate interlayers—400 m;

8) Olistostromes with olistoliths of limestones, siliceous tuffites, and basaltoids—100 m;

9) Alternation of sandy limestone layers with siliceous tuffites. The limestones contain the remains of Cambrian algae (identified by N.A.Drozdova)—300 m.

Laterally this calcareous rock unit probably passes in a westerly direction into a layer of massive limestones. These limestones form large, lenticular bodies containing numerous remains of Lower Cambrian archaeocyathids, trilobites, brachio-pods, and algae (Voronin and Drozdova, 1976). In the section described, the calcareous unit is overlain by:

10) Alternating layers of fine-grained sandstones, siliceous silts, and tuff-silicilith—300 m;

11) Well-sorted, medium-grained massive sandstones, sometimes with coarse cross-bedding—500 m. The total thickness of the section 7 is more than 3,000 m.

This section typifies the main features of the Vendian-Lower Cambrian dolerite-spilite formation and thus the whole of the Ozernaya Zone. The lower part of the formation is dominated by spilite pillow lavas cut by dolerite sills. The proportion of lava breccias of lithic tuffs, hyaloclastites, and then tuff-silicilith and tuffites, increases upwards. The proportion of carbonate material also increases up the section: first in the intra-pillow zones of the volcanics, and then as calcareous tuff-silicilith and, finally, in the middle part of the section as large reef-like bodies. Large lenticular bodies of reefal archaeocyathid-algal limestones occur in the median zone of the Ser Ridge, crossing it from north to south. The limestones are grey and white, and more often massive, and are rarely brecciated. On the western and eastern side of the reef they contain chert interlayers. They probably mark the outer end of the reef island-chain, as from the opposite, north-eastern, side the reef massifs occur adjacent to rocks characteristic of back-reef lagoon deposits—thin alternations of fine-grained limestones, spongolites, and silicified tuffs containing the remains of fossil sponges.

Basalts make up ≤80% of the total volume of the volcanics. The spilites, variolites, dolerites, and their lava breccias show distinctive structural features. Aphyric spilites are the most widespread rock types, with plagioclase impregnations and rare chlorite pseudomorphs usually occurring only in the cores of the pillows.

The groundmass of the basalts consists of microliths of plagioclase, or more rarely, pyroxene. Amygdales of calcite, quartz, albite and epidote are not very common, but sometimes make up ≤50% of the rock's volume.

The tuffites are usually thin layered, the layers being due to variations in the size and colour of the clasts (which are bright red to grey in colour) which often consist of altered spilites, or, more rarely, of keratophyres, or, rarer still, by albite and limestone clasts.

The upper part of the section is dominated by detrital rocks, beginning with an alternation of fine-grained siliceous tuffites and tephrogenic sandstones, grading into more medium-grained varieties. The tephrogenic sandstones consist of basaltoid clasts, with rare andesite porphyries and acid volcanics, plagioclase, and quartz. Some typical lateral variations can be seen in the composition of the sandstones: in the western part of the Ser Ridge they are dominated by eroded basaltoid material; in the median part of the ridge a significant proportion of the eroded material is made up of andesites, possibly derived from eroded andesitebasalt units to the north (Khan-Khuhei Ridge). And, finally, spilite and keratophyre material possibly derived from the adjacent Dagandel Zone, predominates in the eastern, beyond the calcareous reef zone.

A characteristic thick olistostrome layer (60–80 m thick) occurs approximately in the middle of the exposed part of the section. It is made up of unsorted detritus, from 1–2 cm to 2–3 m in diameter, showing varying degrees of roundness. Poorly sorted polymictic sandstone forms the matrix, and contains 'floating' pebbles and blocks. The olistostrome material is composed of predominantly spilites, dolerites, plagioporphyries hyaloclastites, and plagioclases. Serpentinized dunites, pyroxenites and gabbro-dolerites are encountered more rarely. Andesitic pophyries, liparite porphyries, and quartz occur rarely as small grains. The largest angular blocks are generally of limestone and sometimes siliceous tuffite. The gradual transitions between the olistostromes and the underlying and overlying units suggest that they accumulated in the same basins, probably due to rapid submarine erosion of the frontal part of the nappe.

Their petrochemical characteristics enable more than 80% of the volcanics to be attributed to poorly differentiated basalts. Only single samples correspond with andesite-basalts. In addition to their generally low alkalinity, these rocks are characterized by their low K_2O (0.2%), TiO_2 (0.76%), and P_2O_5 (0.08%) contents, which are typical of oceanic tholeiite-series rocks, but, in contrast to the latter, their Ti and Mg contents are low.

The Vendian-early Cambrian deposits of the Osyernaya Zone are overlapped by a heterogeneous unit of calcareous polymictic sandstone (Fig. 10). It crosses the median part of the Ser Ridge, east of the reef limestone band. Here, near the eastern foot of Mt Chiheny-Khara-Ula, the following rocks dip steeply westwards and overlaing the Vendian-Lower Cambrian basalts, with a conglomerate at the base. The sequence is as follows:

1) Polymictic fine-grained sandstones with gravelstone lenses—70 m;

2) Conglomerates with sandy cement, pebbles and boulders composed of archaeocyathid limestones, basalts, dolerites gabbroids, and siliceous tuffites—40 m;

3) Polymictic medium-grained sandstones, alternating with calcareous aleurolites—75 m;

4) The same rocks with gravelstone and conglomerate interlayers—80 m;

5) Calcareous aleurolites, sandstones, and sandy limestones—180 m;

6) Massive sandstones with aleurolite interlayers—60 m;

7) Sandy limestones, calcareous sandstones and aleurolites with numerous remains of paradoxid trilobites from the early (Amgin) stage of the Middle Cambrian (collected and identified by N.V.Pokrovskaya)—40 m.

A unit of the same age, composition, and structural position occurs at the western boundary of the Ozyernaya Zone, near the Shara-Khutul Pass. It is characterized by its greater thickness (up to 1 km) compared with the thick siliceous-carbonate aleurolite member (0.4–0.5 km) containing abundant paroxidid trilobite remains.

The Kharkhirin Zone

This separates the Ozernaya Zone from the Mongolian Altai Caledonides (Fig. 1-). It is bounded on two sides by high-angle faults, and occupies the eastern part of the Kharkhirin uplands to the north and south, and outcrops sporadically along the slope and rise of the Mongolian Altai Ridge for approximately 350 km, as far as the Daribi Ridge. The Kharkhirin Zone is represented by narrow tectonic blocks, where volcanogenic rocks, striking roughly N–S and containing lenticular limestone bodies, dip very steeply. There has been no detailed study of the whole of the Kharkhirin Zone, but its key sections have been known for many years, and up to now have been considered similar to Vendian-Lower Cambrian sections from the central Ozernaya Zpne. A key section of the Kharkhirin Zone has been studied, near the Burgasutiin River. From bottom upwards the sequence is as follows:

1) Spilites with layers basic tuffs >500 m;

2) Alternation of layered spilite bodies, their tuffs, and lava breccias—150 m;

3) Alternation of layered spilites containing carbonate between the pillows, with oncolite limestones, tuffs of basic and intermediate composition, lava breccias, tuffites, and limestones—300 m;

In the same area, and probably at the same level of this carbonate member, archaeocyathid remains allowed the rocks to be assigned to the Lower Cambrian (Volochkovich and Leontiev, 1964).

The second part of the section of the same unit differs noticeably from lower part, due to the predominance of greenschists, which, according to the latest studies (N.A.Berzin pers. comm.) are actually altered andesite porphyries.

4) Greenschists overlying andesite porphyries—150 m;

5) Tuffs of basic and intermediate composition and tephrogenic sandstones—100 m;

6) Alternating thick layers of green andesite schists, tuffs, sandstones, and lava breccias—400 m.

At present this section does not allow the volcanogenic unit to be classified either as one entity, or as being made up of two tectonically combined portions. However, it should be noted that the upper part, which contains a high proportion of andesite porphyries, has also been observed far to the south, up to the Daribi Ridge and can be used to distinguish the Kharkhirin Zone as a large island-arc volcanic zone.

The Khan-Khuhei Zone

This occupies an unusual position in the West Mongolian Caledonides (Fig. 1-). It can be traced in an E–W direction along the southern slope of the Khan-Khuhei Ridge for 150 km, and has a width of 20–25 km. Its tectonic contacts are young E-W-trending thrusts to the south and faults and shears to the north. These contacts are still experiencing present-day tectonic movements (Fig. 11).

The second distinctive feature of the Khan-Khuhei Zone is its nappe structure, which can be easily observed in the Ichutuin-Gol River valley. The two nappes each from different units, of differing rock composition although they are similar in age. According to the available data, they can both be assigned to the Lower Cambrian, although their basal layers possibly belong to the Vendian (Dergunov, 1989).

The most convincing section of the lower part of the Khan-Khuhei Zone, which probably occupies an autochthonous or para-autochthonous position beneath the intermediate and upper nappes, is exposed within the upper part of the valley of the Ichituin-Gol River. Here the sheet-like sedimentary-volcanic bodies dip steeply northwards and are folded into steep, often isoclinal folds, sometimes with overturned southern limbs (Fig. 12).

A schematic section of the Khan-Khuhei Zone para-autochthon consists of two formations, one of which conformably overlies the other. The lower andesite formation is dominated by porphyries of andesite and andesite-basalt composition, with subordinate basalts and dolerites. Irregular layers of lava breccias, tuffs, tuff-conglomerates, and limestone lenses, with thicknesses varying from fractions of a metre to several metres have been observed. Overlying these are tuffs

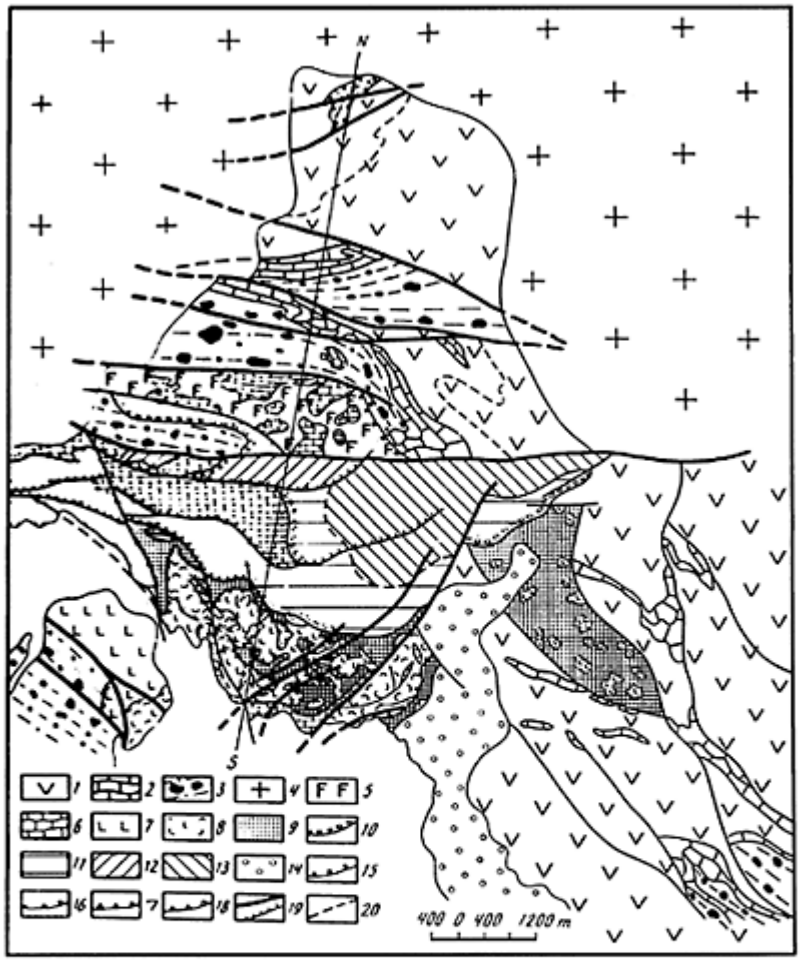

Key: 1–4 —autochthonous or para-autochthonous sedimentary–Volcanic (C_1) and intrusive (C_{2-3}) formations: 1—andesite–basalt porphyries and tuff, 2—limestone containing archaeocyathids, 3—*mélange* olistostromes, conglomerates, gravelstone, and sandstone; 4—granitoids; 5 and 6—lower nappe (V–C_1): 5—spilite–Keratophyre lava and tuff, 6—massive limestone containing archaeocyathids and interbedded with siliceous rocks; 7–9—upper nappe (V–C): 7—*melange*, spilite lava, and tuff, 8—siliceous rocks, 9—polymictic serpentinite *mélange*; 10–14—neo-autochthon (D_1): 10—basal conglomerates, 11—red and variegated polymictic sandstone and siltstone, 12—basaltoids, 13—liparite porphyries, 14—Jurassic conglomerates; 15–19—fault: 15—tectonic base of the lower nappe, 16—tectonic base of the upper slice of the lower nappe, 17—tectonic base of the upper nappe, 18—tectonic base of the upper slice of the upper nappe, 19—steeply dipping fault (a), thrust (b), 20—boundaries of units and beds.

Figure 11 Structural—geological map of the basin of the River Ichtuin-Gol on the southern slope of the Khan—

Khukhei Ridge (West Mongolia, see Fig. 1-).

Key: 1–5—autochthonous sedimentary–volcanic (ϵ_1) and intrusive (ϵ_{2-3})formations: 1—andesite porphyries and tuff, 2—tuffaceous sandstone, 3—limestone containing archaeocyathids, 4—*mélange* olistostromes, conglomerates, and gravelstone; 5—granitoids; 6 and 7—lower nappe (V–C_1): 6—spilitic and keratophyre lava and tuff, 7—archaeocyathid limestone interbedded with siliceous rocks; 8–10—upper nappe (V–C_1): 8—spilitic lava and tuff forming a *mélange*, 9—siliceous rocks, 10—serpentinite *mélange*; 11–13—neoautochthon (D_1): 11—conglomerates, 12—red sandstone and siltstone, 13—basaltoids; 14 and 15—fault: 14—Cambrian nappe 15—Post-Devonian thrust and slip fault (see Fig. 1-⑪).

Figure 12 Geological section along the right bank of the River Ichtuin-Gol, along the southern slope of the Khan-Khuhei Ridge (see Fig. 1-).

and tephrogenic sediments, which show a characteristic alternation of lithiccrystal stal tuffs of andesite and rhyolite composition. The upper part of the section contains beds and lenses of archaeocyathid limestone, which reach 50–70 m in thickness, and which sometimes grade into detrital cross-bedded limestones and limestone conglomerates. The identification of the numerous archaeocyathid remains, carried out by A.Zhuravlyev, shows that they can be assigned to the Atdabanianlower Botomian stage of the Lower Cambrian. The visible thickness of the andesite formation is ≤1,500 m. The petrochemical features of the volcanics suggest that they can be classified as a typical continuous igneous series, with the mode within the andesite-basalt field. They are characterized by their high alumina content and low titanium and magnesium contents, which enable them to be classified as island-arc volcanics (Kheraskova *et al.*, 1983).

Olistostromes are very characteristic of the upper sections of the Khan-Khuhei Zone, where they sometimes underlie allochthonous, often calcareous tectonic sheets. The olistostrome matrix consists of poorly sorted clayey or coarse-grained sandstone. It shows indistinct lenticular or graded bedding, with the thickness of the graded units being from 20 to 50 cm in thickness. Sometimes sandy and archaeocyathid limestones with Botomian archaeocyathid remains (identified by A.Zhuravlev) are also present. They form discontinuous layers, rarely reaching 20–50 m in thickness. Unsorted pebbles, boulders and blocks from 2 cm to over 15 m in size (usually up to 2.5 m) of archaeocyathid, limestones oncolitic and sandy limestones, dolomites, cherts, siliceous-clay shales, siliceous tuffites, spilites, plagioporphyries, and, very rarely, granitoids and keratophyres. The thickness of the olistostrome unit varies from 100 to 250 m, sometimes reaching 600 m.

Both the andesite and olistostrome formations are deformed by narrow linear folds of predominantly north-east strike, with noticeably undulating hinges. Two nappes are thrust

over on to these structures, from the south-west (Figs. 11–12). The lower nappe includes lower, spilite-keratophyric and upper, siliceous-carbonate sheets, usually overlapping the olistostrome, in which the size and amount of the olistoliths decreases downwards. The Archaeocyathid remains from the olistolith limestones and the tectonic sheet indicate an Atdabanian age (Lower Cambrian)—somewhat older than the Botomian limestones which occur in the olistostrome matrix.

The upper nappe consists of tectonic sheets, made up of serpentinite *mélange,* spilites, and siliceous rocks, thrust over the lower nappe and/or the only paraautochthonous unit. It is significant that the whole upper nappe has a sub-horizontal dip, in spite of obvious mylonitization and *mélange* formation. Comparing these structures with the steep, narrow folds of the para-autochthon, we can suggest that the compression in the para-autochthon gave rise to compressional folding, and that compression in the allochthon led to horizontal transportation of the tectonic sheets and nappes. All of the units of the autochthon and the allochthon are affected by the Middle-Upper Cambrian plagiogranite-granodiorite intrusion of the Tannuol Complex, and, together with this intrusion, are stratigraphically overlapped by the neo-autochthon, which consists of Silurian-Devonian molasse. Later, the entire Khan-Khuhei Zone was cut by E–W high-angle step faults into tectonic slices, which were then thrust over on to each other in a southerly direction (Fig. 12). The Khan-Khuhei Zone is believed to have served as a tectonic accumulation model, formed by the overthrusting of Vendian-Lower Precambrian ophiolite nappes on to an island-arc complex of similar age (Dergunov and Luvsandanzan, 1984).

The island-arc complexes of the Khan-Khuhei and Kharkhirin zones were possibly formed on melanocratic basement, which is represented by large blocks of amphibolites within the serpentinite *mélange,* together with other fragments of these complexes.

The Mongol-Altai Zone

This forms the westernmost part of Mongolia (Fig. 1- ,) i.e. the whole of the Mongolian Altai Ridge, whose watershed coincides with the Chinese border. Its western slope, is known as the Chinese Altai (Volchkovich and Leontiev, 1964; Kazmin and Kudanov, 1966, Windley *et al.,* 1994). In contrast to other West Mongolian Caledonide zones, the outcrops of Vendian-Early Cambrian ophiolitic and carbonate-volcanogenic units in the Mongol-Altai Zone occur as rare, small horsts. They occur among compositionally homogeneous oligomictic sandstonealeurolite-shale units, occupying the whole of this zone. It is this thick (≤5 km) and homogeneous unit that affects the tectonic nature of the Mongol-Altai Zone (of probable Middle-Upper Cambrian age) and enables us to consider it as middle Caledonian or simply Caledonian rather than early Caledonian, as its formation appears to have mainly ceased by the end of the Ordovician-earliest Silurian (Dergunov *et al.,* 1980).

The homogeneous composition and structure of the Middle-Upper Cambrian unit within the whole of the zone means that it is impossible to subdivide it stratigraphically or structurally. Only small horsts are encountered in this zone, and these occur along its eastern tectonic boundary, which is marked by the Tsagin-Shibetin and Kobdin faults. The south-western boundary of the Mongol-Altai Zone is the continuation of the Irtysh slump zone in China and the Bulgan Fault in Mongolia.

The rocks forming the summit of the horst to the north of the Kobdin Fault zone provide an example of probable older units underlying the Middle-Upper Cambrian deposits of the Mongol-Altai Zone. Here, in the Kholoin-Khobtsal Valley, the following rocks are exposed (from the bottom upwards):

1) Siliceous tuffites—20 m;
2) Mylonites overlying basic volcanices—20 m;
3) Siliceous tuffites and tuffs—100 m;
4) Basaltoids (variolites)—100 m;
5) Tuffs of basic lavas—50 m;
6) Tuffs and greenstone lavas—200 m;
7) The same rocks, but containing limestone lenses—200 m;
8) Andesite-basalt porphyrites—500 m.

The compositions and structures of these rocks are similar to those described in the Burgasutiin-Gol valley, in the Kharkhirin Zone and it is most probable that they can also be assigned to the Vendian-early Cambrian. Minor outcrops of similar rocks are known from the more southern parts of the eastern margin of the Mongol-Altai Zone. Sometimes they occur as small horsts in the middle parts of this zone (e.g. near the village of Ulan-Khus) and in adjacent areas of Gorny Altai and China (Kazmin and Kudanov, 1966; Dergunov, 1967). Therefore it is probable that the Vendian-Lower Cambrian deposits, characteristic of the neighbouring Kharkhirin and Ozernaya zones of West Mongolia, occur at the base of the terrigenous units of the Mongol-Altai Zone. This is all the more probable as, together with these rocks, serpentinized ultrabasic and other rocks of the melanocratic ophiolitic basement are sometimes exposed within the horsts. In spite of this, nothing is known about the other rocks underlying the Middle-Upper Cambrian terrigenous units within the boundaries of the Mongol-Altai Zone.

The homogeneous composition of the Middle Cambrian-Lower Ordovician unit makes it difficult to subdivide its section, even when it is subjected to detailed study. In the north-western Mongol-Altai Zone, in the area between the Kobdo, Khargantu and Sagsay rivers, three major divisions have been found in the continuous section (from the bottom upwards) (Fig. 1-):

1) Shale: quartz-sericite-chlorite shales overlying argillites and aleurolites, and chloritized sandstone layers. Visible thickness 1,000 m.

2) Sandstone-aleurolitic: a flyschoid alternation of plagioclase-quartz sandstones, aleurolites, and, more rarely, phyllitized clay shales—1500 m.

3) Coarse-grained aleurolite-sandstone: feldspar-quartz and polymictic sandstones (sometimes cross-bedded), gravelstones, pebble conglomerates (containing siliceous clasts) and acid volcanics. Lilac and red-brown aleurolites and sandstones also occur. The thickness of the upper part is up to 2,000 m.

The section described is typical of a huge area extending east-west for about 1,000 km and for a similar distance north-south, containing the same assemblage of terrigenous rocks: plagioclase-quartz or quartz-plagioclase sandstones, aleurolites, and clay shales. They are usually phyllitized and are sometimes altered to greenschists. The almost total absence of carbonates and volcanogenic deposits is highly significant.

The terrigenous rocks of the lower part of the section are characterized by flysch-type graded bedding, with the thickness of the layers varying from a few centimetres to 40–50 cm, and sometimes up to 0.8–1.2 m, with two-member rhythms: fine sandstone-siltstone.

Submarine slump structures are not uncommon, as well as series of layers (3–5 cm thick) showing thin horizontal bedding, unidirectional or multidirectional cross-bedding and other turbiditity-current structures.

Poorly sorted polymictic sediments, with clast sizes ranging from clay to gravel become widespread only in the upper part of the terrigenous complex. Fragments of siliceous shales, quartzites, micaceous shales, volcanics, and sometimes granitoids, are found here, together with quartz and feldspars. These rocks often form thick (0.5–5 m) layers separated by aleurolite interlayers, which are often red or reddish-brown in colour. In contrast to the lower units, the upper units apparently accumulated under shallower water due to the infilling of the basin by sediments derived from the erosion of local source areas.

The age of the terrigenous complex can be inferred from its stratigraphic position above the Lower-Middle Cambrian and Lower Ordovician deposits. Moreover, Palaeozoic trace fossils were recently discovered on the surface of some beds in the Mongolian Altai (Voznesenskaya, and Dergunov, 1982).

Features such as poor rounding and sorting of the clasts, the presence of different elements of the Bouma turbidite sequence and the above-mentioned graded and cross-bedding and submarine slump structures imply that turbidity-current deposition was predominant. The material was deposited in a large canyon-fan system, under conditions of relatively deep-water avalanche sedimentation (Lisitsyn, 1983). Other indicators of this type of deposition are: the non-calcareous composition, which cannot be explained by cold climatic conditions as limestones of similar age are known from adjacent areas; a lack of benthonic fauna; and a lack of structures characteristic of shallow-marine deposition.

The huge volume ($\leq 3\times10^6$ km^3) of these homogeneous quartzofeldspathic deposits excludes an origin by erosion of local source areas. The large continental massifs, such as the Siberian (Dergunov, 1989) or eastern Gondwana continents (Mossakovsky *et al.*, 1993) were the most likely source areas. However, confirmation of the first theory is prevented by the widespread development of accretion zones, possibly separating the Mongol-Altai Basin from the Siberian continent, and the second theory cannot be confirmed either, because of a lack of any objective data on the timing and direction of migration of the Mongol-Altai oceanic terrane.

The Middle-Upper Cambrian complex of the Mongol-Altai Zone is characterized not only by its homogenous composition and the structural features of its terrigenous rocks but also by its surprisingly homogeneous fold structures. Narrow

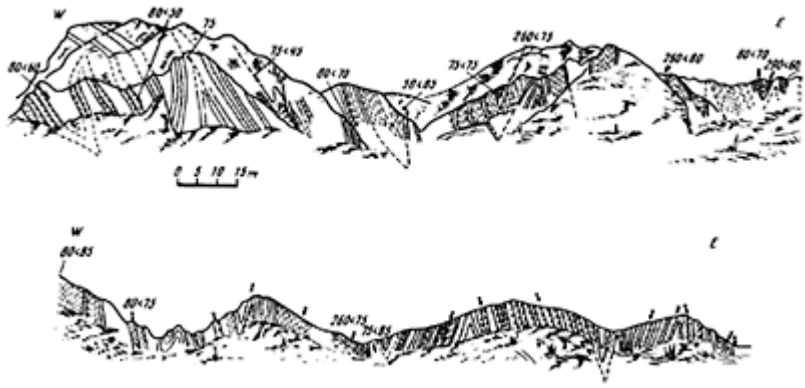

Figure 13 Structural section of the Middle Cambrian-Lower Ordovician sequence, composed of sandstone and siltstone, within the northern Kobdin subzone (on the northern slope of the Achit-Nur Lake and the northern slope of the Khuv-Us-Gol river valley. Narrow, linear, often isoclinal folds are easily discernible (see Fig. 1-)).

linear folds, sometimes isoclinal, striking NW–SE are predominant. The largest folds, with wavelengths of up to several kilometres, smaller folds with wave-lengths of tens of metres, and the smallest folds with wavelengths of tens of centimetres and less, all show the same morphology (Fig. 13).

However, in some areas, particularly those showing obvious evidence of greenschist metamorphism, the original concentric anticlinal structures can be observed. Within these areas these layers are gently dipping, in contrast with the steeply dipping beds separating them from the synclines, where the layers typically form narrow isoclinal folds (Volochkovich and Leontiev, 1964). This indicates that the lower layers of the terrigenous complex, which are exposed in the cores of these domes are less deformed than the upper ones. The upper units are isoclinally folded but are less altered than the lower, gentlly folded units which often show evidence of greenschist metamorphism. Thus it is likely that the terrigenous rocks of these lower layers were subjected to higher lithostatic pressures and temperatures than those located nearer the surface. This resulted in the alteration of the lower rocks to high-pressure greenschists, with compression leading to flow deformation. In this manner, relatively gently dipping major structures, with very complex, minor plication-type folds could have formed at that depth. In this case the less-altered upper units were deformed by linear folds of different orders with high-angle limbs, under the influence of horizontal compressional stress.

It is probable that the upper zone of steep, linear folds and the lower zone of gently dipping structures complicated by plication were separated by an unusual structural-

metamorphic surface that emphasized the tectonic disharmony between these zones. This postulated surface would have been highly significant, as below it, the units were probably formed and metamorphosed under conditions of high lithostatic pressure and relatively high temperatures. Therefore the area of the structural-metamorphic surface separating the upper and lower sections could have been essentially decreased, thus contributing to the regular transfer of horizontal compressional stresses to the upper layers, which were probably deformed without lateral compression by any massifs. This could explain the fact that near the flanks and within the middle parts of the depressions, the upper units are equally folded into the linear folds with high-angle limbs.

There is a high probability that the above-described tectonic disharmony represents a more-common phenomenon—the tectonic stratification of the upper layers of some parts of the Earth's crust.

Over almost the whole of the Mongol-Altai Zone, the terrigenous rocks of the Middle-Upper Cambrian are phyllitized or altered to greenschists. However, in some fairly major parts of the zone, they are more highly metamorphosed, up to amphibolite facies. These rocks can be found on the southern slope of the Mongolian Altai Ridge in particular in the basin of the Bodonchin River (Fig. 1-), as well as in its watershed in the Lake Khotton-Nur area. The Southern flank of the ridge has been particularly well studied. There, in the Bodonchin River basin, highly metamorphosed rocks of the amphibolite facies—biotite plagiogneisses, amphibolites, garnet-Kyanite-staurolite schists and synmetamorphic granitoids are widely developed. Uranium-lead isotopic dating indicates concordant age values of 370±5 Ma and 385±5 Ma for tectonic-metamorphic cycles (Bibikova *et al.*, 1992). It should be noted that earlier field observations reliably established a gradation from these metamorphics to weakly altered Palaeozoic rocks. Similar transitions were also observed in other regions as well. Therefore, these metamorphices may have been formed during local metamorphism of the Palaeozoic rocks, both within Mongolia and in adjacent areas of southern Siberia (Dergunov, 1967; Dergunov, 1989).

By this means, the Caledonian zones of West Mongolia are characterized by Vendian-Lower Cambrian and Middle-Upper Cambrian formations formed in different parts of the palaeo-oceanic basin and under different geodynamic conditions.

By contrast, the spilite-keratophyre formation of the Dagandel Zone was apparently formed in Vendian-Lower Cambrian times, under ensialic island-arc conditions. The island arc was probably laterally connected to the slope and shelf of the Dzabkhan microcontinent. Later, probably at the end of the early-middle Cambrian, this formation and some rock complexes of the melanocratic ophiolite basement were obducted to the border of Dzabkhan microcontinent.

The formations of the Ozernaya Zone were generated at the same time, probably under oceanic, or maybe intra-arc basin, conditions. The predominant tholeiitic basalt pillow lavas and—to a lesser extent—the alkali-olivine basalts associated with tuffs, siliceous tuffites, tephrogenic sandstones, and reef limestones in the upper parts of the formation, are particularly characteristic. Unique interformational olistostromes, which were probably formed by submarine movements of tectonic sheets of ocean-floor rocks, are also present here.

The andesite and andesite-basalt formations of the Khantaishir, Khan-Khuhei and Kharkhirin zones, which occur associated with tuffs, volcanomictic rocks, olistostromes

and reef archaeocyathid limestones, can be considered as typical assemblages of mature and primitive island arcs. It is significant that during obduction these island-arc complexes in the Khan-Khuhei Zone were located in the island-arc position and were overlapped first by the Dangel and then by Ozernaya Zone formations. It is significant that the obduction and transportation of the nappes also occurred in the early Cambrian (Botomian), only slightly later than the formation of the reef limestones (Atdabanian).

The problem of Middle-Upper Cambrian basin development is less well-defined; however, the structural-lithological features of the oligomictic turbidites that infill it point unambiguously to their accumulation in a pelagic basin in fans within a submarine canyon system. It is also probable that the palaeobasin of the Mongol-Altai Zone corresponded with the avalanche sedimentation zone of the current oceans. The problem of locating the source area of this vast volume of terrigenous turbidites is made even more complicated by the fact that reliable data on the direction of transportation of these terrigeneous rocks or the direction of motion of the Mongol-Altai Zone.

2.3 The Caledonian Zones of North, Central, and East Mongolia

East of the Tuvin-Mongolian and Dzabkhan massifs, the Caledonian structures do not occupy such vast areas as in West Mongolia. They are exposed as large but separate zones, of independent tectonic importance, or as small fragments of Vendian-Cambrian ophiolitic associations (Fig. 1). The trends of these large Caledonian structures are markedly different: they have a north-western trend in the ‘Khangai’ part of Central Mongolia and a north-eastern trend in East Mongolia. It is possible that these trends were affected by post-Caledonian motions.

The largest Caledonian zone in North Mongolia is the Dzhidin Zone, the largest Caledonian Zone in Central Mongolia is the Bayan-Khongor Zone, and the largest Caledonian Zones in East Mongolia are the North Khentei, and Kerulen zones. The latter two zones bound the middle-late Palaeozoic Khentei Trough, which is superimposed on Caledonian basement.

The structure and the tectonic nature of most of eastern Mongolia remain largely unknown. Two theories have been put forward regarding their structure, namely:

1) east of the Tuvin-Mongolian and Dzabkhan massifs and north of the southern Mongolian Variscides, Caledonian structures dominate, possibly containing insignificant fragments of the older Precambrian massifs (Zonenshain and Filippova, 1974; Tomurtogoo, 1989; Belichenko *et al.*, 1994; Dergunov *et al.*, 1980);

2) the area is dominated by ancient Precambrian microcontinental structures, in places reworked by later movements and overlapped by Caledonian allochthons (Kepezhinskas *et al.*, 1987; Blagonravov *et al.*, 1990; Shcherbak, 1986).

Here we consider that the first theory is correct, as many metamorphic rocks appear to be Palaeozoic in age, according to radiometric dating and other features (Boishenko, 1987; Belichenko and Boos, 1990). Only in a few cases are sufficiently reliable Precambrian datings available (Makarychev, 1993; Belichenko *et al.*, 1994).

The Dzhidin Zone

This (Fig. 1-) occupies the eastern part of Prikhubsugulye, in North Mongolia. Its western boundary with the Tuvin-Mongolian Massif has been reliably established. It runs along the eastern bank of Lake Khubsugul. The northern continuation of the Dzhidin Zone is inferred from the Palaeozoic age of the Khamar-Daban Ridge metamorphic rocks (Belichenko and Boos, 1990). The vast fields of Palaeozoic granitoids and Upper Palaeozoic volcanics form the southern boundary of the Dzhidin Zone. The imbricated nappe structure, composition, and origin of the geological formations are revealed in the Dzhidin Zone (Ilyin, 1982; Kheraskova *et al.*, 1987).

In Mongolia the Dzhidin Zone can be traced for 150–200 km, from south to north, and for 100 km from west to east, from Lake Khubsugul (Fig. 6).

The main structural elements of the Dzhidin Zone are nappes. They were limited primarily by subhorizontal surfaces, which were later inclined and deformed. Currently they have an E–W trend, with a predominantly northern dip. The initial movement of the nappes probably occurred to the north-west, i.e. on to the Tuvin-Mongolian microcontinent, and later retro-thrusts moved in opposite directions, which is evident from the presence of blocks and sheets of metamorphic rocks of characteristically microcontinental composition. Within the northern nappe, rocks of the carbonate-spilite formation, altered to greenschists, over lie serpentinized ultrabasic rocks. To the south, the middle nappe is composed predominantly of rocks of the tuffite flyschoid formation, which contains large olistoliths and small tectonic sheets, consisting of carbonate-spilite and basalt-andesite-rhyolite formations. In the southernmost nappe the oligomictic flyschoid formation rocks are overlain by serpentinite *mélange*, which underlies the basalt-andesite-rhyolite formations, which, in turn, are covered by calcarenite and/or tuffite flyschoid formations containing olistostromes.

The above-mentioned rocks are unconformably overlapped by a conglomerate molasse of presumed Ordovician-Silurian age. The age of the other formations is conventionally determined using Lower-Middle Cambrian inarticulate brachiopods, which can be found at the base of the flyschoid formation (identified by G. Ushatinskaya) and Lower Cambrian archaeocyathids from olistoliths in the olistostrome of the upper part of the same formation. These data suggest that the age of above-mentioned formations of the Dzhidin Zone is early-middle Cambrian, and the latest age of nappe movement was Ordovician. The similarity between the petrographic and petrochemical features of the rocks from the Dzhidin and West Mongolian zones suggests that they were formed in similar geodynamic environments. The carbonate-spilite formation of the Dzhidin and Ozernaya zones, particularly its volcanogenic part, was most probably formed in the central parts of the palaeo-oceanic basins. The bimodal composition of the other volcanic units, indicates that the basalt-andesite-rhyolite formation of the Dzhidin Zone is similar to the spilite-keratophyre formations of the Dagandel Zone of West Mongolia, which was formed at the junction of the Dzabkhan microcontinent with the palaeo-oceanic Ozernaya Zone. The Calcarenite-flyschoid formation also overlies the bimodal basalt-andesite-rhyolite formation in the Dagandel Zone, but it does not contain erosion products and is composed almost entirely of clastic material supplied from the Tuvin-Mongolian and/or Dzabkhan microcontinent. And, finally, the tuffite-flyschoid formation of the Dzhidin

Zone has a very similar composition to the terrigenous olistostrome unit (Kheraskova, 1986) that terminates the andesite section of West Mongolia and corresponds with an ensimatic island-arc formation. It is obvious that the timing, type of tectonic movement and geodynamic movement during the formation of all of the nappe-folded structures of the Dzidin Zone and almost all of the West Mongolian Caledonian zones have a lot in common, except for the Mongol-Altai Zone.

The Bayan-Khongor Zone

This occupies the watershed area and the south-western slope of the Khangai Ridge in Central Mongolia (Tomurtogoo, 1989) (Fig. 1- ,). It encompasses the eastern margin of the Dzabkhan microcontinent and the western part of the Central Mongolian Caledonides (Fig. 2). The narrow, usually linear structures of the Bayan-Khongor Zone are bounded by high-angle faults trending NW–SE and extend in this direction for at least 300 km. To the north-east, the Bayan-Khongor Zone is overlapped by the Devonian-Upper Palaeozoic rocks of the Khangai Depression. The South-western boundary of the Bayan-Khongor Zone is less marked, as it depends on what part of the Dzabkhan microcontinent is included in the Bayan-Khongor Zone. Probably only that part of the Dzabkhan microcontinent where its interaction with the Caledonides is noticeable can be referred to the Bayan-Khongor Zone. In this case the width of the Bayan-Khongor Zone does not exceed 30–50 km. In spite of its apparent uniformity, the structure of the Bayan Khongor zone is very complex, as, in addition to the margin of the Dzabkhan microcontinent, it contains all of the formations and structures of the Vendianearly Palaeozoic oceanic basin, including ophiolites. The separate exposures of these formations can be traced from the Bayan-Khongor zone a long way northeastward along the flanks of the Khangai-Khentei depression. This is why the Bayan-Khongor Zone can be considered as the western margin of the Central and East Mongolian Caledonides. It should be also noted that the Caledonian formations of the Bayan-Khongor Zone and West Mongolia are very similar in their ages and compositions.

As mentioned above, the margin of the Dzabkhan microcontinent, which is adjacent to the Bayan-Khongor Zone, from west to east is composed of an ancient basement uplift, two zones representing the lower and upper parts of the nappe and a third zone—the Dzabkhan microcontinent passive margin, whose structure is complicated by rifting. Acid and intermediate volcanic units, carbonates and terrigenous rocks were formed within this margin. The major field of their distribution is located in the basin of the River Sharausgol (Fig. 1-), where the Bayan-Khongor Series can be distinguished by its contained Vendian-Lower Cambrian oncolites (Voznesenskaya, 1993, 1995). Within this region the outcrop of the Sharausgol suite is separated from the Dzabkhan microcontinent by a band of ophiolite exposures of the Bayan-Khongor Zone which have tectonic boundaries (Fig. 2). In the area of the River Baydaragin-Gol the section of the suite, from south to north (from the bottom upwards) contains:

1) Alternating red and green basalts, calcilutites, rhyolite tuffites, gravelstones, and conglomerates with quartz-rhyolite pebbles—200 m;

2) Dense dolomitized limestones with a clastic structure—150 m;

3) Massive limestones with interlayers (2–10 cm thick) of black aleurolite, amygdaloidal basalts and siliceous aleurolites—250 m;

It is probable that in the valley of the River Uldzyitgol the section is made up of a thick unit of metatuffite (?) schists (1,000 m thick), containing basalt members (150 m) consisting of lenses of ribbon jasper and siliceous aleurolites. The total visible thickness reaches 1,750 m. Sponge spicules found in jaspers from the Lake Dovstcagangur area do not contradict the Vendian-Early Cambrian age. Taking into account the abundance of picrite basalts within the volcanics the rock association in the section can be compared with continental-rift formations. The Sharausgol Zone is characteristic of the continental margin of the palaeo-oceanic basin during its opening stage. A zone of thick and homogeneous terrigenous turbidites (the Dzagin Suite), which also occurs in the Mongolian Altai (Voznesenskaya and Dergunov, 1982) (Fig. 2), occurs to the east of the latter (Voznesenskaya *et al.*, 1992). However, their structural and stratigraphic position here is more definite, as, in some places (e.g. the basin of the River Sharausgol) they overlap Vendian-Lower Cambrian reef deposits of the passive margin of the Dzabkhan microcontinent, with an erosion and boulder-block conglomerate at the base, but without a structural unconformity. The upper age limit for these turbidites is determined from early Palaeozoic trace fossils (identified by M.A. Fedonkin), as in the Mongolian Altai. It is significant that these terrigenous units can be traced without significant changes in their composition and structure far to the north-east of the Bayan-Khongor Zone. It is universally dominated by terrigenous turbidites, which were supplied from the ancient continent and accumulated in the avalanche sedimentation zone of a pelagic oceanic basin (Lisitsyn, 1983; Voznesenskaya et al., 1992).

The ophiolitic part of the Bayan-Khongor Zone forms an independent structural unit and extends along the entire zone as a narrow band up to 10–20 km wide. It is the most obvious example of a palaeo-oceanic basin in Central Mongolia. High-angle faults trending NW–SE currently bound the ophiolitic band to the north-east. To the north of the Bayan-Khongor Zone they separate the ophiolitic zone from the rift zone of the Dzabkhan microcontinental margin and, to the south—from the Caledonian turbidite zone. In the same way, the north-eastern boundary of the ophiolites cuts the structural-formational zonation of the Bayan-Khongor Zone at a low angle. The south-western boundary of the ophiolites is represented by the Dzabkhan microcontinental margin, which was thrust over them (Dergunov *et al.*, 1997). The ophiolites are closely associated and overlapped by greywackes, forming a complex system of folds and nappes. From their lithology and petrochemical features, the ophiolites can be subdivided into two associations, separated by a high-angle NW–SE fault, along which the serpentinite lenses extend (Fig. 2). The rocks of the ‘north-eastern’ association mainly make up the central and northern part of the ophiolite band, which has an antiformal structure. The rocks of the ‘south-western’ association form folds and nappes along their south-western border of the ophiolite band. The section of the ‘northeastern’ association reveals the following complexes in the core and limbs of the antiform (from the bottom upwards): layered gabbroids, parallel dykes, serpentinized dunites and harzburgites, and pillow basalts. Layered gabbroids form elongated massifs 8–10 km in length and up to 2 km in width. Cumulate structures also occur, with the regular alternation of melanocratic (up to pyroxenites) and more leucocratic varieties. Some structural elements are made up of massive gabbros. The sheeted dyke complex can be observed for 30–35 km. The individual dykes are 250–300 m wide and are represented by aphyric and plagio-clase-phyric dolerites (Kopteva *et al.*, 1984). The orientation of the dykes is conformable with

the overall stratification; their thickness is 0.2–2 m. The dyke complex proper, where the 'dyke within dyke' relationship is observed has distinct upper and lower boundaries, which are the *décollement* surfaces and tectonic sliding. The gabbroids occur as screens in the lower part of the section, and ultrabasic rocks occur in the upper part. In the overlying ultrabasic rocks the dykes are crushed and represented by lenticular blocks of rödingitized rocks orientated parallel to the general strike. The penetration of the dykes into the basalt unit and indications of their role as feeder channels have been noted. On the left bank of the River Uldzyit-Gol the strike of the dyke swarms within the gabbroids conforms to the gabbro banding, but is 15–20° steeper. However, the dykes occurring individually have sharply discordant boundaries. A dunite-harzburgite complex occurs as a 50–100 m thick layer between the sheeted dyke complex and the basalts. Serpentinized harzburgites predominate in this section. *Mélange* is universally developed. On the right bank of the River Baydaragin-Gol, where the thickness increases up to 250 m, this level is represented by a serpentinite *mélange* with fragments of dykes and blocks of gabbros and pyroxenites. Pillow basalts with their contacts fragmented along the bedding, overlie the ultrabasic rocks. Aphyric and porphyric varieties of predominantly grey-green basalt occur here. In the middle part of the section, layers and units of hyaloclastites appear. Lenticular chert interlayers occur locally. The partial thickness (the lower part has been removed by thrusting) is 50–200 m. Sponge spicules can be found in the intra-pillow limestones, on the right bank of the River Uldzyitgol.

In the 'south-western' association the sheeted-dyke complex is not present in the sequence. The layered gabbroid complex contains differentiates up to gabbrodiorites. The banded series within these gabbro-diorites were interrupted by the injection of pegmatoid pyroxenites and gabbros. In places the serpentinites wedge out and the basalts directly overlie the gabbroids. The volcanics are intruded by swarms of plagiogranophyre veins, 2–5 m thick. In addition to the basalts, the andesite-basalts, dacites, and single interlayers of siliceous tuffites occur in lower volumes in the volcanic unit. An abundance of reddened olivine basalts in this part of the section is characteristic.

A linear fold system can be observed in the structure of the ophiolitic bands. It is especially well displayed in the 'north-eastern' association, where the section is consequently thicker at the limbs and in the cores of the folds. This structure is confirmed by the presence of conglomerates at the base of the greywacke complex. The elements of the folds are confirmed by the occurrence of banding in the gabbroids but at the expense of localized crushing large areas are made up of breccias containing blocks up to several metres in diameter, with randomly oriented gabbro banding and fragments of dykes. On the right bank of the River Uldsyitgol, inverted sequences can be observed within the northern limb of the antiform, and the fault bounding the antiform is also apparently inclined towards the northeast.

Petrochemically, the basalts of the 'north-eastern' association are similar to MOR tholeiites in their contents of Cr, Ni, Co, and REE (Lutz, 1980; Bogatikov *et al.*, 1987). However, in contrast to the latter, they are enriched in lithophile elements (Kopteva *et al.*, 1984). The gabbros and dykes also belong to the tholeiite series. Among the rocks of the south-western association, subalkaline-series rocks are also important, in addition to the tholeiites. Reddened oxidized basalts with a composition corresponding with subalkaline olivine basalts (ocean-island basalts) have distinctively high Ti and K contents. Generally, because of the presence of differentiates of acid and intermediate composition,

as well as from their petrogeochemical features, these volcanics are comparable with the Na and Na-K series of the islands on mid-oceanic ridges (Bogatikov *et al.,* 1987). This comparison is not contradicted by the fact that the gabbroids of both associations can be assigned to the high-Ti type, which, according to G.Serri (Serri, 1981) are usually formed in oceanic basins which originated by spreading of continental crust.

The uppermost part of the ophiolitic section comprises a greywacke complex, which conformably (sometimes with basal conglomerates) overlies the lavas. The lower part of the units (250 m) is represented by gray, well-bedded, polymictic sandstones, aleurolites, and occasional cherts containing rare layers and lenses of calcarenites, which alternate with the sandstones in the upper part of the section (300 m thick). Clasts of volcanogenic quartz, feldspars, carbonates, lavas and tuffs of different compositions are present within the sandstones and aleurolites. The greywackes could mark a short stage of cessation of spreading and basin infilling at the beginning of a period of tectonic nappe-thrusting.

Little is known regarding the age of ophiolites. Values of 596±21 Ma are obtained on the gabbros, which correspond with the early Cambrian (Kepezhinskas *et al.,* 1991). Judging from the sponge spicules in the intra-pillow limestones, the pillow basalts are no older than Cambrian. The greywackes are apparently no older than the Vendian-Lower Cambrian Sharausgol Suite, whose erosion produced the volcanogenic quartz found within the greywackes. It is probable that the greywacke complex represents a stratigraphic analogue of a Lower-Middle Cambrian unit of sedimentary cover of the Baidarag inlier. This is suggested by the similarity of their facies in some parts of their sections. The age of the ophiolite is therefore taken as early-middle Cambrian for the gabbroids, dykes, lavas and greywackes.

The preashgill structures are ‘sealed’ (overlapped) by a neoautochthon formed by Upper Ordovician and Middle Palaeozoic formations (Fig. 2). Outcrops of Upper Ordovician deposits occur as narrow bands in the area between the Uldzyit-Gol and Buriduin-Gol rivers, towards the margin of the Baydarag inlier. The stratigraphic contact of the Upper Ordovician deposits with an Upper Cambrian granitoid tectonic sheet can be observed on the left bank of the River Uldzyit-Gol, 2.5 km south-east of Mt Delhairhanula. Here the weathered surface of brownish-red microcline granosyenites grades into saprolite and, subsequently into an arkosic gravel sandstone, which shows faint parallel and cross-bedding and irregular rhythmicity, becoming more obvious upwards with the appearance of conglomerate lenses. The clast size generally decreases up section, giving way to alternating red beds and chocolate-brown aleurolites with rare intercalations of olive-grey fine-grained sandstones. The thickness of the basal arkose deposits is 150 m. A coarse-grained unit of predominantly calcarenites, shelly limestones and biogenic grey limestones overlies the arkoses. This contains abundant fossils of bryozoans, corals, trilobites, and the brachiopods *Hesperorthis acuticostata* Rozman, H.aff.*laticostata* Rozman, *Strophomena* aff.*boishenko* Rozman, and *Wysogarskiella mongoliensis* Rozman, etc., which belong to the Ashgillian stage, according to D.A.Andreev. Grains and pebbles of quartz, chert, jaspers, schists and sandstones occur in the calcarenites. The thickness of the limestone unit is no more than 200 m. The entire unit, as well as the eroded granite surface, dips southwards at an angle of 60°. Lateral changes in the composition of the basal unit are shown in the appearance of coarse-boulder conglomerates with predominantly Upper Cambrian granitoid boulders, or, if they overlie ancient terrigenous carbonate rocks, in the replacement of the arkoses by red

marls. Formationally, these deposits are comparable with the terrigenous-carbonate cover formed at passive continental margins.

Narrow, often one-sided grabens are often associated with Middle Palaeozoic formations. These grabens, as a rule, extend along the faults at the boundaries of particular structure-formational zones. Grabens infilled with Silurian terrigenous deposits, dated using zone fossils, are mapped along the contact between the pre-Riphean and Riphean deposits. The Devonian section is divided into two members. The lower part (200 m) is dominated by red beds and variegated terrigenous deposits, often conglomerates containing pebbles of predominantly carbonate rocks, interlayered with acid tuffites. The upper part (500–600 m) consists of a differentiated series of volcanics, with predominant trachyandesites, rarer basalts and minor amounts of quartz trachyrhyolites. Fossiliferous Devonian deposits infill the graben up to 3 km in width at the boundary of the Lower-Middle Riphean and Upper Riphean zones of the Baydarag inlier and also infill narrow grabens within the boundaries of the Baydarag (Boishenko, 1977). Formationally, the Devonian deposits can be Inlier interpreted as a molasse and an orogenic volcanic complex characteristic of Andean-type active continental margins.

Carboniferous deposits occur transgressively overlapping Devonian and older formations. The section is represented by alternating boulder and pebble conglomerates grading upwards into grey sandstones, aleurolites and argillites with layers and lenses of limestones. The remains of crinoids, bryozoans, and the brachiopods *Torynifer*, *Neospirifer*, and *Dengalosis gobica* Manankov *et* Pavlova, 1981 of the upper substage of the Viséan stage (identifications by S.S.Lazarev) are found in this section. The topmost part of the section comprises carbonaceous shales, aleurolites, and sandstones. Wide grabens infilled by Carboniferous deposits extend within the Baydarag Inlier along the boundary between Riphean and preRiphean formations, as well as along the faults in the Bayan-Khongor Zone. This complex apparently reflects a new, passive stage of continental-margin evolution.

The most complex tectonic relationships of sets of tectonic sheets can be observed on the right bank of the River Uldzyit-Gol, north and south of Mt Delhairhanula (Fig. 2). Owing to a N–S upfault, with an amplitude of approximately 3 km the sequence of allochthonous sheets is repeated here in two blocks. All of the units and sheets are downfaulted southwestward and located in the same structural order. The ophiolites and greywackes of the major ophiolitic band, which show deformation at the tectonic contact are overlain by Upper Riphean terrigenous and carbonate deposits, further overlain by a thinner (100–200 m) sheet with a complete set of ophiolitic association rocks, which is followed, in turn, by an Upper Cambrian granitoid sheet. In the north-eastern block, the set of sheets is ‘sealed’ (overlapped) by the Upper Ordovician and Carboniferous autochthon. The conformity of the sheets with the neo-autochthon probably indicates the near-horizontal primary occurrence of the nappes. In the south-western block, a set of similar sheets is overlain by Devonian and Carboniferous rocks. The granitoids are intensely tectonized and altered to augen mylonites with lenses of metamorphosed rocks from the sedimentary cover.

Developmental Stages and Interaction of Structures of the Bayan-Khongor Zone with the Eastern Margin of the Dzabkhan Microcontinent

In the Riphean, the Dzabkhan microcontinent was apparently an element of the Gondwanan passive margin (Mossakovsky *et al.*, 1993). Terrigenous and carbonate deposits accumulated on its Archaean and Lower Proterozoic basement. Their high carbon content and the presence of pyrite are indicative of an anoxic environment in the sedimentary basin. A noticeable decrease in the circulation and the basin subsidence probably occurred only in the late Riphean, when thick units of stromatolitic dolomites were deposited.

In the Vendian and early Cambrian this microcontinental margin was characterized by active rifting, with continental volcanism that reflected the separation of the Dzabkhan microcontinent from the main continent. The interaction between the Dzabkhan microcontinent and the palaeo-Asian ocean is noted both for the western (Dergunov, 1989) and eastern margins of the Dzabkhan microcontinent (Dergunov *et al.*, 1997). The passive regime of the eastern margin is reflected in the formations of the Bayan-Khongor Zone. At the end of the early and middle Cambrian, the geodynamic environment changed drastically, which led to the accretion of island arcs to the west and two-sided (from the west and the east) obduction on to the Dzabkhan microcontinent. In the middle-late Cambrian the remnant basin was infilled with laterally extensive terrigenous turbidites (Dzagin and Gorno-Altai suites), which were carried in from the ancient continents of Gondwana and Siberia. Obduction of the sheets and nappes was spread over the cover of the Dzabkhan microcontinental margin, where asymmetric macro-drag-folds, accompanied by upfaulting and overthrusting of predominantly southwestern vergence, occurred (Fig. 3). Obduction resulted in crustal thickening and subsidence of the Earth's crust into a zone of high pressure and temperature. Terrigenous shale units of Riphean cover were intensively metamorphosed, and palingenetic granitoid partial melting probably took place within the crystalline schists of the basement. Large-scale granite formation within the Caledonides of Central Asia occurred from the end of the Cambrian to the beginning of the Ordovician (Tannuol and other complexes). It is most probable that it was completed by significant uplift and, as a consequence, in retro-overthrust sliding towards the palaeo-oceanic basins (Dergunov, 1988). Hence, the folded-nappe structures at the site of the paleo-oceanic basin were formed on both sides of the Dzabkhan microcontinent as early as the late Ordovician when a relatively thin Upper Ordovician cover (neoautochthon) was formed. The transition to a convergent plate boundary is reflected in the sections of Devonian formations dominated by molasse and differentiated-series trachybasalts and trachyrhyolites, comparable with formations from the active Andean-type continental margins. Subsidence and infilling of the Khangai-Khentei Basin occurred at this time, probably as a back-arc depression. The destruction of the basin in the Zaaltai Zone (Ruzhentsev *et al.*, 1989), in the Viséan, led to the appearance of formations typical of passive margins, i.e. terrigenous-carbonate and coal-bearing sequences. In Middle Carboniferous times, plate collision in the western part of the Hercynian Basin (Barunhuray Zone) was reflected in the Caledonides by tectonic compression, with the formation of high-angle linear structures complicated by high-

angle upfaults (or faults), shears, and conjugate grabens. Synchronously with the late Permian plate collision in South Mongolia, injection of granitoid plutons, uplift, and deep erosion occurred in the Bayan-Khongor Zone.

The North Khentei zone

The North Khentei and Kerulen uplifted zones surround the Middle-Upper Palaeozoic Khangai-Khentei Depression from the north-west and south-east, respectively. The basal sequence of this depression overlaps the terrigenous turbidites ($Є_{2–3}$) with a major angular unconformity, i.e. the sediments directly over-lie the Caledonian folded basement. Apart from this, these uplifted zones are laterally connected with the Caledonides of the Bayan-Khongor Zone by sporadic exposures of Caledonian formations (Fig. 1): within the the Northern Khentei Rise these are mainly exposures of Lower Palaeozoic oligomictic turbidites (the Dzagin and Kharin Suites) (Voznesenskaya, 1993), and for the Kerulen Rise they are Vendian-Lower Cambrian ophiolites (Tomurtogoo, 1989). Therefore it can be postulated that the Central Mongolian Caledonides continue from the BayanKhongor Zone to East Mongolia and beyond (Belichenko *et al.*, 1994).

The northern Khentei Zone (Fig. 1–10,) occupies the north-western slope and foot of the Khentei Ridge (the right bank of the River Tola and the basins of the Khara-Gol and Ero-Gol rivers). It bounds the Khentei depression to the west, extending north-eastward for more than 400 km, with a width of up to 150 km. The Eravnin Zone in Zabaikalie serves as its continuation beyond the Mongolian boundary (Yanshin, 1989; Belichenko *et al.*, 1994). The northern Khentei Zone is made up of Upper Riphean-Lower Cambrian (?) greenschists, overlying volcanogenicterrigenous rocks and Lower Palaeozoic terrigenous turbidites, in places partially replaced by intermediate and acidic volcanics. The main sections of the Northern Khentei Zone and their relationships are described by I.Phillipova (Kassin *et al.*, 1980). The section begins with greenschists of the Mandal Series (upwards):

—metaterrigenous schists (quartz-chlorite-biotite, chlorite-sericite-muscovite)—up to 1,800 m thick;
—metavolcanogenic schists (actinolite-chlorite, actinolite-epidote-chlorite), basic lavas altered to greenschists; quartzites, and tuffogenic—sometimes calcareous sandstones—(up to 2,000 m thick;)
—gravelstones, sandstones, aleurolites—up to 2,000 m thick.

The thick, predominantly terrigenous (Kharin) Series occurs with angular and stratigraphic unconformity up the section (from the bottom upwards):

—conglomerates containing pebbles from the underlying sandstones and siliceous tuffites—200 m;
—gravel saprolite conglomerates with clasts of feldspar; fine-grained granites; fine-coarse-grained sandstones; and siliceous tuffites—400 m;
—sandstones of various grain sizes, gravelstones, aleurolites, and tuffites—400 m.

Sometimes the terrigenous rocks of these three units are replaced laterally by dacite tuffites and tuff-breccias, andesite porphyries, and sometimes amygdaloidal basalts. Their total thickness is 1,000 m.

Higher up, the section contains terrigenous turbidites:

—oligomictic sandstones, aleurolites, and shales, often rhythmically bedded—2,000 m;
—rhythmically bedded, variegated sandstones, aleurolites, and shales, sometimes containing Lower Palaeozoic algae (?)—100 m.

Based on the identification of oncolite remains from the lower (Mandal) series, it can be assigned to the Upper Riphean-Lower Cambrian, and, taking account of the distinct erosional unconformity, the upper (Kharin) unit is considered to be Lower Palaeozoic in age (Yanshin, 1989). The northern continuation of the northern Khentei Rise, the Eravnin Zone in the Zabaikalie of Russia is fairly similar in its lithology and structure, and is believed to have formed under island-arc conditions (Belichenko *et al.,* 1994). However, within the North Khentei Rise, the island-arc formations were dislocated, metamorphosed, and granitized, and then deeply eroded, prior to the accumulation of this thick turbidite unit. These features, which are common in the Caledonides of the north Khentei and BayanKhongor zones, indicate that their structures are similar and that they possibly developed at the site of a single palaeo-oceanic basin. Moreover, regarding the paragenetic link between metamorphism and granite formation and tectonic thickening (Dergunov, 1988), as well as the widespread presence of major early Palaeozoic granitoid massifs on the NW margin of the Northern Khentei Rise and Lower Mesozoic granitoids on its SE margin, it is possible that the predominant tectonic movements resulted in tectonic thickening towards the north-west in the early Palaeozoic and towards the south-east in the early Mesozoic. These latter movements are distinguished by the vertical vergence of the folds and overthrusting of the south-eastern termination of the North Khentei Rise on to the Khentey Depression (Khassin *et al.,* 1980).

The Kerulen Zone

This (Fig. 1–11,), the largest Caledonian Zone of East Mongolia, is restricted by NE-SW-trending faults. It is traced as a rise along the entire south-eastern flank of the Khentei depression, for more than 400 km, with a width from 100 km in the south-west and up to 200 km in the north-east, where it is split by the termination of the Ogin Depression in Zabaikalie (Fig. 1-㉘) (Belichenko *et al.,* 1994). The Kerulen Rise occupies the entire left bank of the River Kerulen and probably extends south-westwards, under the Mesozoic deposits, at least up to the Adatsag ophiolitic zone (Fig. 1-㉒) The structure of the Kerulen Rise is extremely complex and varied. It contains outcrops of metamorphic rocks. These rocks, which are sometimes assigned to Precambrian (Blagonravov *et al.,* 1990), are closely associated with Lower Palaeozoic granitoids and are possibly similar in age (Belichenko *et al.,* 1994). Moreover, the Kerulen Rise is saturated by outcrops of Middle and Upper Palaeozoic granitoids and partially overlapped by Mesozoic deposits. Therefore the Caledonian structures, outcrops, and deposits occupy the smallest part of the rise area.

The most characteristic sequence within the rise is a 1600-m thick terrigenousvolcanogenic sequence of andesite-dacite-rhyolite composition, represented by marine and subaerial tuffs lavas, and ignimbrites, as well as associated conglomerates, sandstones, and limestones. From their chemistry, the volcanics can be referred to the calcalkaline K–Na series. They are conventionally assigned to the Cambrian, from their

location between units of Vendian and Silurian age, and also on the basis of a comparison with Cambrian units from other regions (Blagonravov *et al.*, 1990). The general characteristics of these Cambrian rocks enable them to be classified as an ensialic island-arc series, folded into NE–SW-trending high-angle linear folds.

A major compressional and deformational stage for both the Kerulen and the North Khentei zones is supposed to occur at the end of the Cambrian. It resulted in tectonic thickening, accompanied by metamorphism and large-scale granite formation, which indicates the growth of a new layer of granite-metamorphic crust within the limits of the rise.

Silurian sedimentary rocks infill scarce, isolated depressions within the limits of the Kerulen Rise. They are represented by a conglomerate-sandstone-aleurolite unit in the east, and a sandstone-aleurolite-limestone one in the west, there containing the remains of Wenlock-Lower Ludlow brachiopods. The thickness of each unit reaches 1,800 m.

Lower Devonian deposits of marine origin, reaching 4,000 m in thickness, are more widespread within the rise. They unconformably overlap the older units and are composed of regularly alternating clayey shales, aleurolites, and sandstones, with interlayers of gravelstones, conglomerates, intermediate volcanics, siliceous rocks, and limestones. Remains of Lower Devonian bryozoans, brachiopods, and crinoids have been found in the lower layers of these deposits. It is suggested that there was a connection between the Early Devonian depression and the Mongol-Okhotsk Basin (Blagonravov *et al.*, 1990).

The Pre-Kerulen Zone

The south-eastern margin of the Kerulen rise—the pre-Kerulen zone—is not wide (≤30 km) and differs markedly from the main part of the Kerulen Rise (Fig. 1-㉑). It runs along the left bank of the River Kerulen, south-west of Idermeg village, for about 150 km, but possibly extends farther, under younger deposits, as far as the Adatsag ophiolitic zone (Tomurtogoo, 1989). The pre-Kerulen Zone is bounded by two branches of the Kerulen Fault and has a complex folded-nappe structure (Palei and Zhuravleva, 1978). According to these data the predominantly volcanogenic unit, which is located within the nappe, and contains layered bodies of ultrabasic rocks and serpentenite *mélange* at the base, should be considered as the most ancient unit within the pre-Kerulen Zone. This nappe is thrust over a unit of terrigenous sedimentary cover which contains thin lenses of archaeocyathid limestones. Hence, the pre-Kerulen Zone is characterized by an inverted age sequence. It is most probable that the unit that overlies the ultrabasic rocks is actually stratigraphically lower. Its most complete section is described near Mt Undur-Khan by M.V.Durante (Palei and Zhuravleva, 1978) (from the bottom upwards):

—siliceous tuffites, basalt porphyries—120 m;
—limestones with oncolites—20 m;
—basalt, sometimes with amygdaloidal plagioporphyries—420 m;
—siliceous tuffites, plagioporphyries—200 m;
—tuffogenic aleurolites, plagioporphyries, jaspers—140 m;

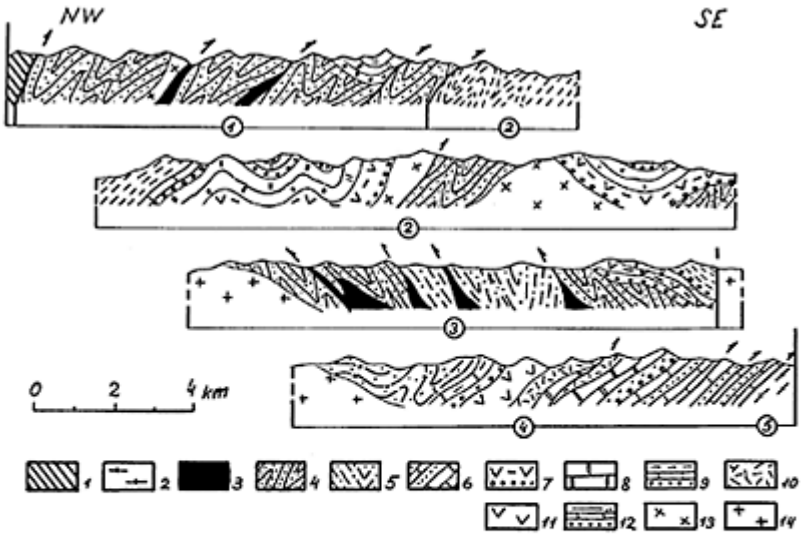

Key: 1—Salairides of the Khantaishir Zone; 2—Tselsky metamorphic assemblage; 3—ultrabasic rocks and gabbroids; 4—quartz–feldspar sandstone, locally interbedded with basalt, tuff and limestone (O–S); 5—greywacke, tuff, limestone (O–S); 6– biohermal limestone and sandstone (O–S)); 7—basaltic andesite, andesite, epiclastics, greywacke (D_{1-2}); 8—biohermal limestone (D_{1-2}); 9—greywacke and limestone (D_{2-3}); 10—rhyolite, dacite and andesite tuff, and epiclastics (D_{2-3}); 11—andesite and basaltic andesite (D_3); 12—conglomerates, sandstone, and limestone (C_1); 13—plagiogranite (S); 14—granite and granodiorite (PZ_3); Numbers on profiles: *1–3* Bayan–Tsagan subzone (*2*—Bayan–Gobi, *3*—Bayan–leg and Bayan–Tsagan blocks); *4*—Dzhinset subzone; *5*—Tselsky metamorphic assemblage. For location see Fig. 1-㉒ (E 101°–N 45°, and 30, E 101°–N 44° 40′).

Figure 14 Geological sections across the Gobi-Altai.

—andesite-basalt and basalt plagioporphyries—60 m;
—tuffs, tuffites, lenses of limestones and tuff-conglomerates—200 m;
—andesite, andesite-basalt and basalt porphyries—300 m;
—limestones with poorly preserved archaeocyathids—50 m;
—tuff-breccias and massive plagioporphyries—200 m;
—andesite, andesite-basalt, basalt porphyries—200 m.

According to Palei's data, this unit tectonically overlaps a thick (2,000 m) terrigenous unit, consisting of clayey shales, sandstones, gravelstones, conglomerates, and fairly thin limestone lenses with poorly preserved archaeocyathids. It is younger than the ophiolites as it contains rounded fragments of rocks from the ophiolites. Hence, the pre-Kerulen Zone is represented by tectonic remnants of island-arc sequences and their ophiolitic basement.

These remnants of the pre-Kerulen Zone, together with similar formations of the Adatsag Zone, located to the west (Fig. 1-㉒) (Tomurtogoo, 1989), apparently mark a major suture between the pre-Kerulen Zone to the north and the central Mongolian Massif to the south.

2.3 Late Caledonides of South Mongolia

S.V.Ruzhentsev

Gobi-Altai—Sukhebator Zone

The late Caledonides of this zone can be traced from the southern branches of the Mongolian and Gobi-Altai in the west up to the Khalhin-Gol River basin in the east (Fig. 1). Here the Caledonian structural sequence includes both Ordovician and Silurian deposits. They form the basement, on which the Devonian cover of the southern (according to present-day co-ordinates) shelf of the Siberian Caledonian continent was deposited.

We have studied the geological structure of the zone in the Gobi-Altai (the areas Bayan-Gobi, Bayan-Leg, Bayan-Tsagan, and Dzhinset). Structurally, they represent narrow E–W-trending blocks, within the limits of which Ordovician and Silurian deposits are folded into compressive folds complicated by longitudinal upfaults (Fig. 14). Two subzones have been distinguished in the Gobi-Altai zone: the northern (Bayantsagan) and the southern (Dzhinset).

The Bayantsgan subzone

This includes the Kharyn-Shandy-Nuru, Naryin-Tsahir, Bayan-Tsagan, and Khuh-Tologoy mountains. Serpentinized harzburgites and serpentinite *mélange* bodies occur at the base of the exposed section within this subzone. The *mélanges* include clinopyroxenite and gabbro-norite blocks. Ultrabasites form a chain of relatively small bodies with a total length of 100 km. A volcanogenic-sedimentary series occurs structurally above the ultrabasite-basite basement, sometimes with transgressive contact, but more often with a tectonic contact. This series consists of two units:

1) Phyllitized quartz-plagioclase sandstones, micaceous aleurolites (≤1,500 m) alternating with basalt flows and epiclastic layers. In the northern part of the zone (the Bayan-Gobi Village) numerous conglomerate lenses (pebbles and boulders of granitoids, quartz porphyries, acid epiclastites, quartzites, and mica schists) are present in the section.

2) Quartz-plagioclase sandstone, grey shales (900–1,000 m) alternating with white, recrystallized limestones. The latter form relatively persistent interlayers (1–5 m) and thick (up to 150m) bioherm bodies. Llandovererian tabulate coral remains *(Karagemia gobialtaica* Minzh. and *Khangaites* sp.) and bryozoans *(Hallopora* sp. and *Homotrypa* sp.) have been collected from limestones near the Ulan-Shand well. Five kilometres east of this, the limestones of the upper part of the section contain brachiopod remains *(Pentameris longiseptatus* Boris, $S_1L–W_1$).

In the Khuh-Tologoy Mountains (south of the Bayan-Leg village) remains of the tabulate corals *Palaeofavosites forbesiformis* Sok., *P. schmidt* Sok *et al.* (S_1L) have been collected from the limestones.

The Dzhinset subzone

This is located in the Dzhinset Mountains and represents a series of tectonic slices formed by carbonate and carbonate-terrigenous deposits of Upper Ordovician-Silurian age (Fig. 15).

In the west of the zone the section is represented by:

1) Grey or pink, massive biohermal limestones (up to 200 m thick); coral remains: *Halysites praecedens* W. *et* Sem., *Transitonolites* sp., *Mongoliolites* sp., and *Khagailites* sp. (O_3a).

2) Calcareous conglomerates (1–15 m).

3) Red, quartzose sandstones (150–160 m).

4) Grey, layered, detrital limestones with abundant brachiopods *Hesperorthis laticostata* Rozm., *Triplasia mongolica* Tschern., etc. (O_3a).

Eastwards, 4 km south of the Tsahirin Khunduk Well, the section is different. Upper Ordovician deposits are represented here by sandstones of various colours, aleurolites, and limestones (Rozman and Minzhin, 1981).

The most complete Lower Silurian section is located in the source area of the Tsagan-Bular:

1) Quartz sandstones (30 m), alternating with detrital limestones.

2) Clayey limestones (9 m), containing the tabulate corals: *Palaeofavosites porosus* Sok., *Mesofavosites akchokkensis* Sok.; the brachiopods *Dalerorthis llandoverensis* Lop. and *Isorthis angaciensis* Rozm., etc. (S_1L_{1-2}).

3) Aleurolites and clay limestones (35 m), containing the brachiopods: *Cardatomionia disjuncta* Vlad., *Sowerbyella millinensis* Jones, and *Glassia minu*ta Rybn. (S_1L_2).

Upper Llandovery-Wenlock beds are exposed near the Shara-Chulgun Well:

1) Alternating quartz aleurolites and brown organic limestones (60 m), containing the brachiopods: *Stegerhynchus angaciensis* Tschern., *S.coccinnus* Savage, *Spirigirina* cf.*marginalis* (Dalm.), *and Alispira gracilis* Nikif *et al.* (S_1L_2).

2) Grey massive limestones (30 m).

3) Alternating quartz sandstones and limestones (40–50 m); *Sowerbyella millinensis* Jones, *Eopholidostropha* sp., *Glassia minuta* Rybn., and *Leptaena aequalis* Amsd. (S_1L_3).

4) Unit (350–400 m) of alternating variegated oligomictic sandstones, aleurolites, clayey shales, and sandy limestones.

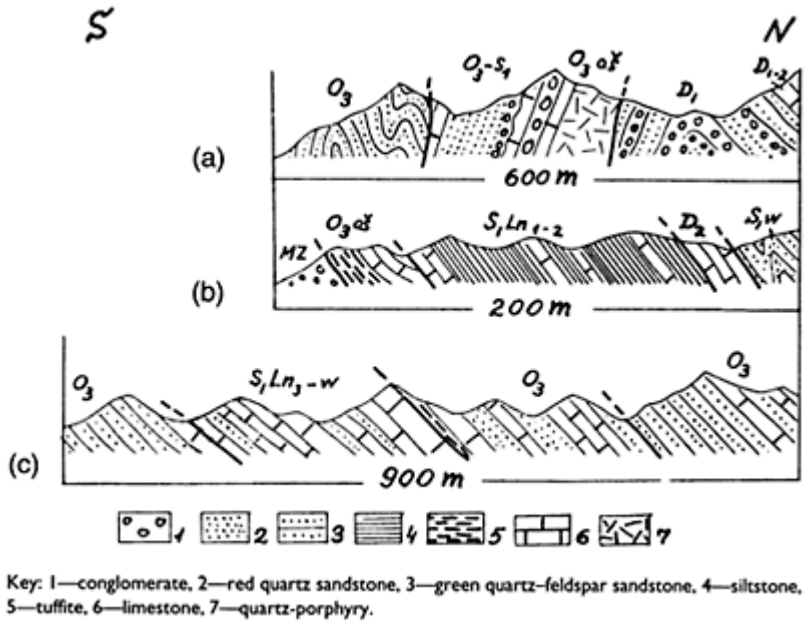

Figure 15 Geological sections across the southern spurs of the Dzhinset Massif (A—Baishintin—Dzagdai area, B—Tsakhirin—Khuduk Well, C—Shara-Chulutun Well; for the location see Fig. 1-㉚) (E 101°–N44° 40′).

5) Black bituminous limestones (25–30 m) containing the remains of the tabulate corals *Halysites junior* Klaam., *Favosites exilis* Sok., *Barrandeolites bowerbanki* (E. *et* H.), *Subalveolites lunatus* Lel., *Syringopora khalaganensis* Tschern. *et al.;* and the brachiopods: *Isorthis sagsaensis* Rozm., *Leptaena depressa* (Sow.), and *Tataria gobica* Rozm. *et al.* (S_1W_2).

Wenlock-Ludlow transitional beds are located 2 km south of the TsahirinKhuduk Well:

6) Coarse-layered dark-grey, bituminous limestones (60–70 m) containing the remains of the tabulate corals: *Favosites kennichoensis* Ozaki and *Syringopora gorski* Tschern; and the brachiopod: *Tuvaella gigantea* Tschern.

7) Grey, layered biogenic-detrital limestones (90–95 m) with polymictic sandstone interlayers. In places they are replaced by massive, light-grey recrystallized coral limestones.

8) Clayey shales and marls (20–23 m), containing thin interlayers of limestones. The limestones contain the remains of the brachiopods: *Tuvaella gigantea* Tschern., *Leptaena* ex gr. *rhomboidalis* Wilch., *Tannuspirifer padaschenkoi* (Tschern.), *Isorthis* sp., and *Meristina narkolensis* Zhang (S_2L_2).

9) Layered grey limestones (28 m) *(Axuolites* sp., *Favosites* sp., *Schizophoria* sp.,; $S_2p–D_1L$). They are transgressive, with a basal conglomerate (up to 1 m) overlying the Ludlow deposits.

Two types of Caledonian structures can be distinguished within the limits of the Gobi-Altai: the northern (Bayan-Sagan subzone) and southern (Dzhinset subzone) types. The first represents the depression, with the melanocratic basement infilled by a volcanic-sedimentary series. From the time of its development and its structural features it apparently corresponds with the Kobdin Depression of the Mongolian Altai. In our opinion, it originated in the late Ordovician, as a result of the destruction of the Salair-Caledonian accretionary system of Central Mongolia. The main background of the section is composed of quartz-feldspar and quartz sandstones and aleurolites. In the Bayan-Gobi Zone they are associated with conglomerates, which mark the northern flank of the Gobi-Altai Caledonian depression. Basaltoids are widely developed in its axial and southern parts ($O_3– S_1L$).

Dzinset Zone

This forms the southern continental margin of the Gobi Depression. It is a relatively uplifted block, within which a fairly thin sequence of predominantly carbonate rocks was deposited. It was probably initiated on sialic (Precambrian or Caledonian) basement, under shallow-water conditions, as evidenced from the widespread development of biohermal and biogenic-clastic deposits and the abundance of non-sequences (Ruzhentsev *et al.*, 1987).

2.4 Superimposed Palaeozoic Troughs and Depressions within the Caledonides

The completion of the formation of the most important Caledonian zone is traditionally determined from the time of emergence of the first superimposed troughs and depressions infilled with terrigenous and/or volcanic molasse-like sequences. The timing of their development as a rule closely coincides with the time of large-scale granite formation, which also marks the end of the formation of Caledonian zones. Taken together, these features enable the Caledonides to be subdivided into Early ($Є_2–Є_3$), Middle ($O–S_1$) and Late ($S_2–D$) Zones. The younger superimposed structures and granitoids do appear later in the Caledonian zone, but they are not used to determine the age of these zones.

Superimposed Troughs of the Early Caledonian Ozyernaya Zone ($Є_2–Є_3$) (Fig. 1 -)

The molasses that infilled this trough unconformably overlie various beds of Lower Cambrian age. As noted above, in the middle and westernmost part of the Ser Ridge they also include a layered unit of calcareous, often volcanomictic sandstones, aleurolites, and sandy limestones (Fig. 10 and pp. 27–28). In the middle part of the Ser Ridge they have a thickness of 500 m and dip westwards at angles of 30–50°. Abundant paroxidid trilobite remains have been collected and identified by N.Pokrovskaya, from the upper layers of

the unit, within the sandy limestones (the Amgin stage is the lower stage of the Middle Cambrian in Siberia). The unit has a N–S strike and a narrow (up to 1 km) width of exposure between the eastern (stratigraphic) and the western (tectonic) contact, the latter being represented by overthrusting of Lower Cambrian deposits from the west. The similar rock composition and the same assemblage of trilobite remains are characteristic of the unit located on the western margin of the Ozernaya Zone, in the area of the Shara-Hutul Pass. However, here its thickness increases to 1 km, due to a major (0.5 km) upper unit of siliceous aleurolites containing the remains of the same trilobites (from the collection of O.I.Arkhipova).

Among the other superimposed troughs, the most representative are the Chigirtay troughs which are located within the western part of the Ser Ridge (Fig. 1- , Fig. 16). They have a very complex structure: almost a concentric structure with younger troughs occurring nested within the older ones, despite the sharply unconformable structural and stratigraphic relationships between them. The general geometry of these troughs is oval, extending for 25 km N–S and 10 km E–W. Ordovician, Silurian, Lower-Middle Devonian, and Carboniferous molassoid deposits have been distinguished. These infill the troughs. A volcanogenic unit of basalt-andesite-dacite composition, with thickness of ≤900 m is assigned to the ordovician. It is unconformably overlain by Silurian conglomerates, gravelstones, and sandstones, with lenses of sandy limestones that contain the remains of brachiopods and corals. The visible thickness is ≤800 m. Lower Devonian acid lavas and tuffs (≤500 m thick) also occur with an unconformity; these are overlain by Middle Devonian calcareous-terrigenous deposits with lenses and layers of limestones (500 m) and, finally, Lower Carboniferous red conglomerates, sandstones, and aleurolites (400 m). In the other parts of the Ozernaya Zone these molassoids of various ages infill small, isolated troughs but, as has been mentioned, the age of formation of the Ozernaya Zone is determined by the Middle Cambrian molassoids.

Superimposed Troughs and Depressions which define the Middle Caledonian Age of the Mongolian Altai Zones

No Late-Caledonian zones have been established in Mongolia, although some have been identified in the Devonian of adjacent areas of the Altai-Sayan of Russia (Dergunov, 1967). Therefore, in contrast to the early Caledonides of West Mongolia, the remaining zones of the North Mongolian megablock should be classified as Middle Caledonides or as Caledonides that had formed by latest Ordovician-earliest Silurian times.

The largest superimposed structures in these Caledonian zones are large troughs, elongated in a NW–SE direction in West Mongolia, in an E–W direction in Central Mongolia, and in a NE–SW direction in East Mongolia. These troughs

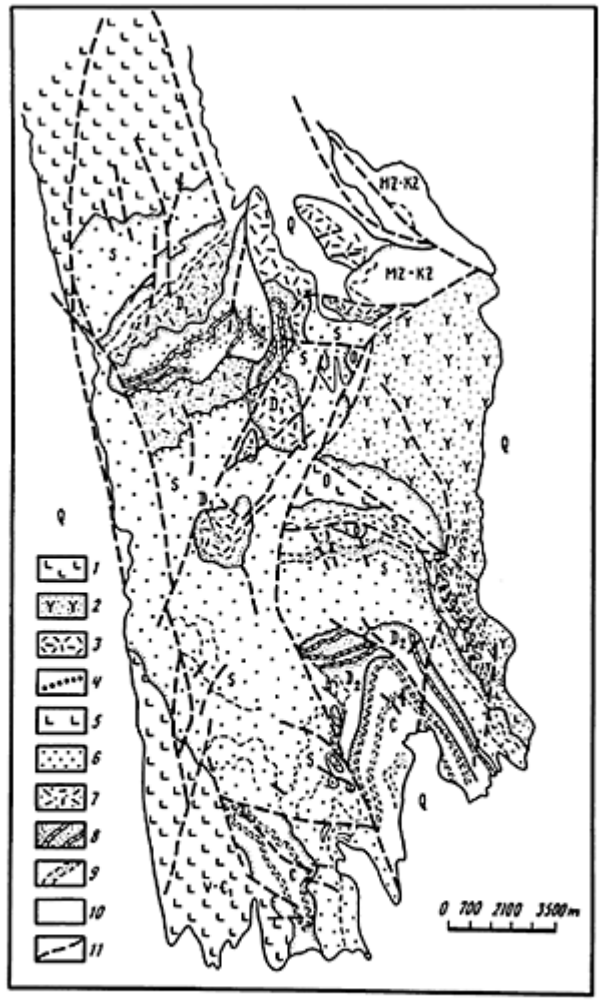

Key: 1—volcanic and carbonate rocks of the Vendian–Lower Cambrain complex. 2–5—Lower–Middle Ordovician rocks: 2—mixed lava and tuff, 3—acid lava, 4—agglomerate, 5—basic lava and tuff; 6—Silurian red conglomerates and sandstone, 7—Lower Devonian lava and tuff; 8—Middle Devonian limestone–terrigenous deposits; 9—Lower Carboniferous red siltstone and sandstone; 10—unconsolidated Quaternary deposits; 11—fault.

Figure 16 Schematic geological map of the area around Mt Sharagat and Mt Urgat, on the northern slope of the Khara-Us-Nur Lake: Chigirtai troughs (see Fig. 1-).

are, as a rule, associated with small circular isolated troughs infilled with rocks from any part of the section.

The Kobdin Trough

This is located in West Mongolia (Fig. 1-㉓, Fig. 17(1)) extends in a NW–SE direction along the eastern foot of the Mongolian Altai Ridge, between the Ozernaya Caledonian zone to the east and the Mongol-Altai one to the west. Its length is 400 km and its width is up to 50–60 km. To the east the trough is limited by upfaults and thrusts, along which the units of the Ozernaya Zone are thrusted over it. Basal conglomerates of the trough rocks overlap unconformably on to Mongolian-Altai Zone units in some places along the western border of the trough. The trough is infilled by a lower tuffogenic-terrigenous unit, an intermediate siliceous terrigenous unit containing graptolites, and an upper basalt-andesite unit containing some reef limestones. The total thickness of these units is more than 2 km. The fossils limit the age of all of the trough deposits to late Ordovician-

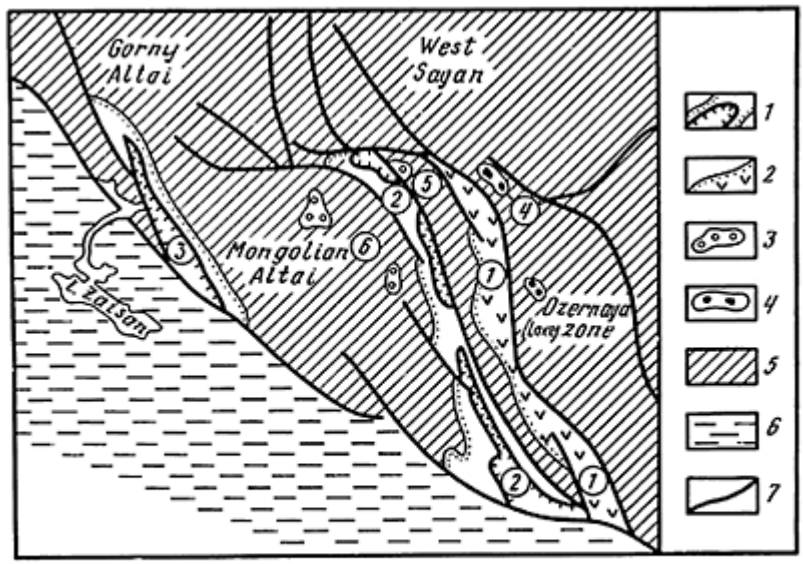

Fault troughs: 1—Middle–Upper Devonian and 2—Upper Ordovician–Silurian. Superimposed depressions: 3—Middle–Upper Devonian and 4—Upper Ordovician–Silurian, 5—Caledonides, 6—Hercynides, 7—fault; Circled numbers on the map: *1*—Kobdin, 2—Delyuno–Yustyd, *3*—South Altai troughs; 4—Uregnur, *5*—Sharogobi and 6—Baintuin depressions.

Figure 17 Location of fault troughs, and coeval superimposed depressions in West Mongolia (see Fig. 1-㉓and㉔).

Silurian. Characteristic changes in the facies of the rocks occur along the strike, from north to the south. The coarse-clastic molassoid rocks become more important northwards. They infill the minor Ureg-Nur Trough, which is located within the northern continuation of the Kobdin Trough. The same, but more rapid, changes in rock composition occur across the trough strike, with the Silurian deposits continuing beyond its boundaries as individual superimposed troughs (Dergunov, 1989). The composition and assemblage of the rocks that infill the Kobdin Trough and which are usually folded into high-angle linear folds, correspond with island-arc formations, which show more resemblance to similar Hercynian formations in the southern part of the trough. The markedly elongated, straight geometry of the trough indicates that it formed by rifting, initiated as a result of extension within the large north-western branches of the main shear, which probably coincide with the E–W South Mongolian lineament.

The Delyuno-Yustyd Trough

This (Fig.1-㉔, Fig. 17–2 (2)) extends almost parallel to the Kobdin Trough, but is located to the west within the same Mongol-Altai zone, along the entire slope of the Mongol-Altai Ridge. It has a length of about 500 km and a width of up to 50 km and an asymmetrical structure similar to the Kobdin Trough, i.e. it is restricted by upfaults and thrusts to the east and often stratigraphically overlaps the Middle-Upper Cambrian units of this zone to the west. Basal conglomerates, gravelstones, and calcareous sandstones (containing the remains of brachiopods of Lower-Middle Devonian age), which underlie a volcanogenic unit of intermediate and acid composition (1–1.5 km thick) are exposed at the base of the Delyuno-Yustyd Trough. The layers transitional to the upper parts of the section are represented by alternating volcanics and sandstone-aleurolitic, sometimes siliceous rocks. In the central part of the trough the sandstone-aleurolite-shale units reach 4,000 m in thickness and contain the remains of bryozoans, brachiopods, and flora from the Givetian and Frasnian stages of the Middle-Upper Devonian (identified by R.Alekseeva, I.Morozova, and Yu.Dubatolova) in the upper part of the section.

The deposits of the Delyuno-Yustyd Trough are characterized by very gradual facies changes, from fine-grained siliceous deposits in the south, up to coarseclastic molasse in the north. Isolated exposures of lower volcanic and upper terrigenous units are often found beyond the boundaries of the trough, across its strike, where they give way to molassoids and infill separated superimposed troughs.

The overall similarity between the structures of the Kobdin and Delyuno-Yustyd troughs allows us to suggest that their geodynamic conditions of formation were for a long time similar. The Delyuno-Yustyd Trough appears to have formed as the result of extension and rifting, which, in turn, were caused by oblique motions in the subduction zone coinciding with the South Mongolian lineament. It is significant that these structural features and their orientation are also characteristic of the Devonian Jamatau-Gol Trough, located to the east in an adjacent area of Mongolia, and also of the Carboniferous southern Altai Trough, located far to the west, in Russia (Fig. 17(1), (2), (3)).

The Khangai-Khentei Zone

This is located in the Caledonides of Central and East Mongolia. The largest superimposed troughs, infilled with huge thicknesses of Middle and Upper Palaeozoic deposits (≥10 km) are represented in central Mongolia by the almost circular Khangai Trough (Fig. 1- ,⑬) and, to the east, by the angular West Khentei Trough (Fig. 1- ,㉖), and, in East Mongolia, by the elongated Khentei Trough (Fig. 1- ,㉗). Initially, these troughs were probably incorporated in one huge depression but in the current structure they are separated by transverse rises and are limited by N–S faults: north-western in Central, and north-eastern in East Mongolia. According to their names, the troughs occupy the eastern part of Khangai and the entire Khentei Ridge, extending from the west to the north-east for a total of more than 700 km (Zonenshain and Philippova, 1974) and continuing into the eastern Zabaikalie of Russia (Belichenko *et al.*, 1994).

The Khangai and Khentei troughs are infilled by a thick Devonian-Carboniferous unit, containing irregularly or regularly alternating sandstones, aleurolites, argillites, and rare conglomerates. The troughs retain their original syndepositional structure and can be described as synclinoria (Philippova, 1976; Zonenshain and Philippova, 1974). However, the initial stratigraphic unconformity, with its basal conglomerates, is preserved only in now isolated parts of the western closure of the Khangai Trough, where Middle Devonian (Eifelian?) deposits directly overlap Middle-Upper Cambrian terrigenous turbidites. It should be noted that Ordovician-Silurian deposits are supposed to occur at the base of the section, at the eastern termination of the Khentei Trough. At the same time, in the adjacent Agin Trough, the section continues up to the Triassic. These data indicate that the Khangai-Khentei Trough system penetrated into East Mongolia from the north-east and retreated in the opposite direction. This suggests that its origin can be associated with the development of the Mongol-Okhotsk palaeooceanic basin (Tomurtogoo, 1989). The composition and structural-textural features of the terrigenous units of the Khangai-Khentei system, i.e. the abundance of jasper interlayers, localized acid and intermediate volcanics, as well as the volcanomictic and greywacke composition of the psammites, the slide structures, the rhythmic nature, and the graded bedding, and other indications characterize the predominantly turbidite regime of these rocks. The type of dislocations within the Khangai part of the trough allows it to be considered as a synclinorium with a concentric structure, which has a possibly syndepositional origin. Complex folding is also observed, including ‘amoeboid’ folds with two intersecting axial trends.

The deformations within the narrow Khentei Trough are completely different. The trough is bordered on both sides by faults: high-angle ones to the south-east and low-angle thrusts to the north-west. Accordingly, within the Khentei Trough, the folds are narrow, linear and usually asymmetric, with high-angle, often overturned south-eastern and more gently dipping north-western limbs.

To the north-west and the south-east the Khangai-Khentei Trough system is accompanied by typical superimposed troughs infilled by Middle-Upper Palaeozoic shallow-water molasse-type deposits. To the north-west it is adjacent to the Orkon-Selengin Trough, containing Carboniferous deposits, which are laterally connected with the Khangai-Khentei system, and Upper Palaeozoic-Triassic terrigenous and

volcanogenic rocks which characterize the new stage of its development (Tomurtogoo, 1972).

To the east, the Khangai-Khentei system occurs adjacent to the Agin Trough (Fig. 1-㉘) (Zonenshain and Philippova, 1974); its southern termination, 60–70 km wide, extends into Mongolia. The trough is infilled by a Middle Devonian terrigenous unit containing basaltoids, and, in the axial part of the trough, by a Triassic-Lower Jurassic flysch-like, but often coarse-clastic, sedimentary rock unit. The compressive imbricated dislocations, containing lenses of glaucophane schists and ophiolites, which are related to collisional processes in the Mongol-Okhotsk Belt (Belichenko *et al.*, 1994) are especially characteristic. Upper Palaeozoic-Triassic granitoids complete the development of the Khangai-Khentei system and its accompanying troughs (Zonenshain and Philippova, 1974).

3
THE VARISCAN BELT OF SOUTH MONGOLIA AND DZUNGARIA

S.V.Ruzhentsev

3.1 The Variscides of South Mongolia (Gobiides)

The Variscides of South Mongolia include five zones: the Gobi-Altai-Sukhe Bator Zone, Tsei Zone (Tsei metamorphic belt), the Edrengin Zone, the Transaltai Zone, and the South Gobi Zone.

The Gobi-Altai-Sukhe Bator Zone

This zone represents the northern (according to present-day co-ordinates) continental margin of the South Mongolian Variscan palaeo-ocean. The geological structure of the zone has been studied in detail in the Gobi-Altai (Borzakovsky and Suetenko, 1970; Ruzhentsev *et al.*, 1987, 1992a), where the zone is divided into the northern (Bayantsagan) and southern (Dzinset) subzones. The Variscan complex of the Gobi-Altai includes both Devonian and Lower Carboniferous deposits and consists of three sequences, separated by angular unconformities: Lower-Middle Devonian (Eifelian), Middle (givetian)-Upper Devonian, and Carboniferous sequences (Fig. 18).

The lower sequence in the Bayan-Tsagan subzone is composed of:

1) Conglomerate (10–80 m), variegated, made up of pebbles of quartz-diorite, granodiorite, quartz-porphyry, gabbro and gabbro-amphibolites, dolerites, ultra basic rocks, various terrigenous rocks, and Ordovician and Silurian limestones.

2) Sandstone and siltstone (100–120 m), variegated, containing thin layers of arenaceous limestone.

3) A sequence (30–500 m) of variegated rhyolitic tuff, tuffite, and epiclastic (volcanoclastic) rocks, also containing basalt flows that increase in number up section, and thin layers of limestone.

4) Limestone (90–100 m), pink and laminated, containing the tabulate corals: *Pachyfavosites preplacenta* (Dubat.), *P.gicingeri* Mir., *Thamnopora diserta* Mir., *Coenites dungenensis* Schark., and *Plicatomorus giganteus* Schark *et al.* (D_1p).

5) Limestone (200–600 m), light-grey, massive, biogenic, crinoid-algal-coral, containing the tabulate corals: *Placocoenites medium* (Lec.), *Gephuropora maculata* Schark., *Pachypora* cf.*tortuosa* Schark., *Squameofavosites delicatus* Dubat., and *Alveolites levis grandic* Schark. *et al.* (D_1e–D_2e). The limestone contains separate basalt flows and numerous bodies of dolerite and quartz-porphyry.

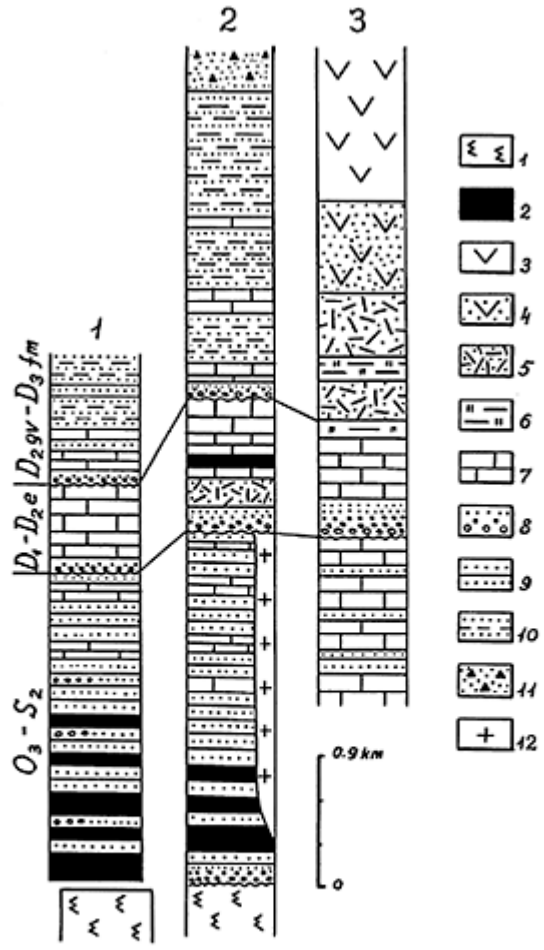

Key: 1—ultrabasic rocks, *mélange*: 2—basalt; 3—basaltic andesite andesite; 4—tuff and andesite epiclastics; 5—tuff and rhyolite and dacite epiclastics; 6—tuffite and siliceous sinter; 7—limestone; 8—polymictic conglomerate and sandstone; 9—oligomictic (quartz–feldspar) sandstone; 10—greywacke; 11—mixtite; 12—plagiogranite; Numbers on Figure: *1*—northern and 2—southern Bayan–Tsagan subzones, 3—Dzhinset subzone.

Figure 18 Lower and Middle Palaeozoic type sections of the Gobi-Altai.

Deposits from this level are widely developed in the Dzinset subzone. Their section is as follows:

1) Conglomerate (10–200 m), variegated, thick-bedded; consists of pebbles of Ordovician and Silurian limestone; contains thin layers of oligomictic sandstone.

2) Sandstone (150–160 m), polymictic, variegated; contains lenses of calcareous conglomerate, rhyolitic tuff, and epiclastics.

3) Limestone (300–500 m), biogenic, detrital, muddy, in places siliceous; contains thin (up to 2 m) layers of polymictic sandstone, rhyolitic tuff, and tuffite. The bed yields abundant fauna and includes Lokhkovian, Pragian, Emsian, and Eifelian deposits (Ulitina *et al.*, 1976; Sharkova, 1981; Alekseeva, 1993).

The Lower Devonian and Eifelian deposits of the Gobi-Altai are mainly represented by various biogenic limestones, such as algal, coral, and bryozoan limestones. They are unevenly intercalated with detrital and muddy varieties and form complex constructed bioherms and biostromes, up to 200–300 m thick. The largest accumulations reach up to a few tens of kilometres in area.

The detrital limestone shows uneven bedding; it commonly contains flint nodules. Marlstone occurs along the bedding planes. Units and lenses of siltstone, sandstone, calcareous conglomerate, and karstic breccia are also present. It is evident that the above sediments were deposited in an extremely shallow basin. Individual fragments of the bioherms were transported to the zone of erosion (i.e. conglomerate, karst, and laterite). The deposits, which as a whole are rather thin, probably complete the period of emplacement of the southern shelf of the Siberian Caledonian continent. Volcanic and subvolcanic rocks are locally associated with the limestones. They are mainly rhyolites and dacites and their tuffs (including ignimbrites).

The Gobi Altai-Sukhe Bator shelf can be traced for a distance of 1,500km, from the Tsogt area in the west through the Mandalobo area to Bayan-Urt and Khalkhin-Gol in the east. The shelf was a zone where exclusively carbonates were deposited—mainly biostrome and detrital types (Alekseeva, 1993).

The Givetian-Upper Devonian sequence of the Dzinset subzone (Gobi-Altai Formation) shows the following stratigraphic section:

1) Alternating layers (300–350 m) of tuffite, tuff siltstone, rhyolitic tuff, and marlstone, containing the conodonts: *Polygnathus ensensis Z. et.* Kl., *P.* cf. *anguicostatus* Witt., and *Icriodus obliquimarginatus* Brisch. et. Z., *Dvorakia* sp. (D_2gv).

2) Alternating layers (900–1,000 m thick) of rhyolitic tuff, acid epiclastic rocks, tuffite, tuff siltstone, polymictic sandstone, tuff silicite, and flint, containing the conodonts: *Ancyrodella gigas* and *Palmatolepis* af. *punctata* Mull (D_3f).

3) Tuff, epiclastics, and flint (200–220 m), containing the conodonts: *Palmotolepis perlobata schindewolfi* Mull., *P.ex gr.delicatula* Br. *ed.* Mehl., and *Polygnathus* sp. (D_3fm).

4) Basalt and andesite tuff, water-lain breccia, and coarse epiclastics (1,200–1,300 m), containing horizons of basaltic pillow lavas.

In their silica content, the Upper Devonian volcanics of the Dzinset zone show continuous differentiation, with an antidromous sequence; they belong to the alkali-olivine basalt and high-Al series. They show high TiO_2 contents, locally high contents of P_2O_5 and total iron, and wide variations in their Mg, Ca, Na, and K contents(Table 1).

The stratigraphic section of the Middle and Upper Devonian deposits of the Baya-Tsagan subzone is as follows:

1) Conglomerates and polymictic sandstones (90–100 m), containing pebbles of the underlying limestone.

2) Limestone (150 m): grey, laminated, detrital-muddy; contains Middle Devonian tabulate corals and bryozoans.

3) Turbidites: greenish-grey, oligomictic, sandy-silty.

4) Calcarenite (100–120 m), rhythmically bedded, containing coarse organic debris at the base of each cycle.

5) Greywacke turbidite sequence (900–1,000 m).

6) Mixtite (300–350 m): alternating layers of conglomerate, breccia-conglomerate, and sandstone, containing blocks of granitoid, dolerite, gabbro, quartz-porphyry, and limestone; the sandstone contains abundant plant debris.

The Upper Devonian deposits from a thick suite, resting unconformably on the underlying rocks. The suite is made up of oligomictic and greywacke turbidite, conglomerate and mixtite, tuff and tuffite, calcarenite, and limestone. Coarse clastics occur higher up the section. The suite shows rhythmic stratification and has a flyschoid appearance. Oligomictic and greywacke material are mixed. The abovementioned rocks were formed within a trough, which, from its structural position and sedimentary infill, is considered to be the equivalent of a marginal basin, developed on a complex ensialic basement. To the south, the basin is bounded by the Gobi-Altai border volcanic belt, marking the boundary of an Andean-type active continental margin (Dzinset subzone).

The Tsei Metamorphic Belt

The Tsei belt of metamorphic rocks is located south of the above-mentioned zones at the boundary of the Mongolian and the Gobi-Altai on one side, and the Trans Altai Gobi on the other side. The belt stretches for 500 km and represents a chain of blocks (from west to east): the Bodonchin, Bulgan, Tsei, and Tsogt blocks. For the most part they are made up of rocks that have been metamorphosed to the greenschist or amphibolite facies, or locally to the granulite facies (Mitrofanov et al., 1981; Kozakov, 1986; Bibikova et al., 1992). It has been found that the crystalline rocks of the Tsei Belt are polymetamorphic.

The oldest, granulite-facies, metamorphic rocks occur within the Tsogt block (Gegetin River), where they form *boudins* in amphibolite-facies rocks. The granulite-facies rocks are represented by the association: hypersthene brown hornblende+plagioclase+orthoclase+quartz (Kozakov, 1986). The younger amphibolite-facies rocks include two complexes. The first complex (andalusitesillimanite series, T=600–700°C, P=4–6 kbar) is characterized by the following

Table 1 Composition of the Middle-Upper Devonian volcanics of the Dzhinset subzone.

Rock/ component	Picritie basalt	Basalt		Andesite basalt tuff	Andesite-basalt	Andesite	Andesite-dacite	Dacite	Rhyolite
	400	465/82	414	474/82	108/84	412	94/84	517/82	513/82
SiO_2	45.38	49.02	51.86	54.19	56.08	57.90	62.24	63.10	77.02
TiO_2	1.41	0.59	0.86	1.15	0.92	0.99	0.72	0.62	0.19
Al_2O_3	16.10	18.37	15.18	13.88	14.87	16.40	16.06	16.76	10.17
Fe_2O_3	4.69	5.63	3.19	4.09	7.13	3.71	0.94	2.31	2.38

FeO	6.68	6.51	6.21	8.71	4.72	3.40	13.18	2.35	1.66
MgO	8.06	4.84	5.55	5.99	4.05	3.88	2.00	2.30	0.93
CaO	10.80	7.67	8.72	4.52	2.14	6.94	1.90	4.96	0.74
MnO	0.17	0.10	0.17	0.21	0.13	0.10	0.02	0.06	0.08
Na_2O	1.96	4.48	4.00	1.80	5.92	3.54	8.36	3.18	3.30
K_2O	0.92	0.32	1.63	1.02	0.33	0.92	0.11	2.44	2.44
$H_2O^{\dagger}$	3.42†	2.20	2.57†	3.67	2.49	2.08†	1.70	1.35	0.93
P_2O_5	0.17	0.05	0.05	0.18	0.10	0.20	0.10	0.16	0.01
Cr	—	11	—	28	27	—	26	29	10
Ni	—	15	—	26	25	—	28	18	15
V	—	215	—	315	227	—	125	92	5
Cu	—	33	—	135	74	—	77	36	15
Co	—	28	—	30	26	—	16	12	10
Pb	—	5	—	5	5	—	5	5	5
Ga	—	10	—	12	10	—	16	15	10
Ge	—	1.7	—	1.5	1.5	2.5	2.5	1.5	1.5
Mo	—	1.5	—	1.5	1.5	1.5	1.5	1.5	1.5

* In samples 400, 412, and 414 the trace elements have not been determined.
† Ignition loss.

associations: sillimanite+cordierite+biotite±garnet+plagioclase+orthoclase +quartz, and andalusite+biotite+plagioclase+quartz. The above-mentioned rocks include bodies of amphibolitized gabbroids, and various granitoid bodies now metamorphosed into fine-grained gneiss. The U-Pb age of the latter is 385± 5 Ma (Bibikova *et al.*, 1992). The second complex (kyanite-sillimanite series, T= 600–650°C, P=5.5–7 kbar) is represented by the following associations: kyanite +garnet+biotite+muscovite+staurolite+plagioclase+quartz, and garnet+ zoisite+quartz+plagioclase+hornblende in essentially calcic rocks. In more high-temperature zones, metamorphism reached the sillimanite-biotite-garnetorthoclase subfacies. This metamorphism is ubiquitous and is superimposed on the rocks of the first complex.

Dolerite metaporphyry dyke swarms (the Gashunnur dyke series) are the oldest igneous bodies of the second complex. They were found in all blocks of the belt, where they locally make up about 50% of the exposed area and form narrow (3 km wide) zones up to 20 km in extent. The dykes are usually associated with bodies of ultrabasic rocks and metagabbroids. Intrusions of the latter, up to a few square kilometres in area, are represented by metadolerites, including lenticular bodies of amphibole-chlorite-, tremolite-carbonate-serpentinite schists, serpentinite and tremolite with fuchsite and asbestos veinlets. The Gashunnur dykes cross-cut the rocks of the first complex; Sm–Nd dating yielded a Devonian age (320±39 and 321±79 Ma) for their metamorphism (Baikova and Amelin, 1994). Positive εNd(T) values, (+6.1–7.6) indicate that the rocks, which show isotopic characteristics close to those in the depleted mantle, served as a source for the Gashunnur basic rocks. Synmetamorphic granitoids of the second complex (plagio-granites and quartz-diorites associated with gabbroids and anorthosites) are regarded as earlier folded mantle rocks (Kozakov, 1986). Their U-Pb age is late Devonian, 371±2 Ma (Bibikova *et al.*, 1992). There is limited evidence of autochthonous

crust formation, represented by concordant and cross-cutting veins of aplite, pegmatite, and garnet-bearing granite.

The youngest rocks of the belt are probably those of the greenschist series. Greenschists replace the above-mentioned metamorphic rocks and the Lower to Middle Palaeozoic deposits of the Mongolian and the Gobi-Altai. The metamorphic processes of these conditions were not accompanied by the formation of autochthonous granites. Large bodies of Upper Palaeozoic granitoids are typical allochthons.

Thus, the Tsei metamorphic belt experienced a complex polycyclic development, over a relatively short time span (25 Ma). The belt is believed to be spatially located in the zone of the Andean-type Variscan active continental margin (Kovalenko and Yarmolyuk, 1990), situated along the southern (according to present-day co-ordinates) border of the Siberian Caledonian continent. The constructive process of growth of the granite-metamorphic layer in Devonian times was sometimes interrupted by its destruction and the formation of dyke swarms and local exposure of the melanocratic basement. In this respect, the structure (i.e. Gashunnur Complex) that formed there in middle Devonian times is comparable with the somewhat older Ordovician-Silurian destructive troughs of the Gobi-Altai.

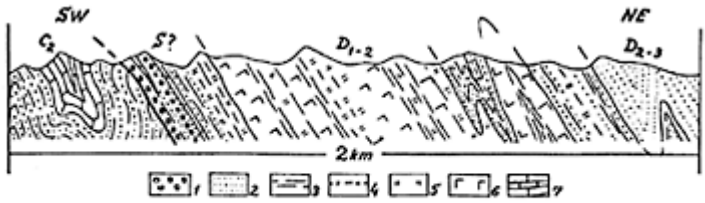

Key: 1—conglomerate, 2—sandstone, 3—shale, 4—tuffite, siliceous sinter, and chert; 5—jasper, 6—basalt, 7—limestone.

Figure 19 Geological section across the Khuvinkharin subzone (for location see Fig. 1-㉜, E 98° 30′–N 45°

The Edrengin Zone

This zone includes the northern, (Khuvinkharin) and the southern (Edrengin-Nuru) subzones.

The Khuvinkharin (Bayanbulak) subzone

This is located south of the Gobi-Altai, occupying the area of its southern offshoots and the Somon-Khairkhan Mountains. Structurally, it is a system of narrow tectonic blocks, within which the layers are strongly folded (Fig. 19). Small bodies of serpentinite *mélange* are exposed locally. The subzone sequence consists of the lower ($D–C_1t_1$) and the upper, orogenic ($C_{1–2}$) portions.

In the area of the Ulan-Chuluny Well the lower section consists of the following horizons, in ascending order:

1) Arkose sandstone, conglomerate (pebbles and boulders of granite, granitegneiss, quartz-porphyry, biotite schists, micaceous quartzite, marble, and various terrigenous rocks), rhyolitic tuff, and bodies of quartz-porphyry (up to 150m thick).

2) Clayey-flinty slates, chert, and jasper (700–900 m), with individual basalt flows occurring at the top of the sequence. They contain the conodonts: *Pandorinellina steinhornensis* (Ziegl.), *Polygnathus inversus* Klap. *et* Johns, and *'Hindeodella' sp.* (D_1e.)

3) Greywacke flysch (2,000–2,500 m), containing lenses of small-pebble conglomerate (pebbles of flint and basalt); abundant plant debris is present.

In their geochemistry, the volcanics of the second sequence represent a weakly differentiated (basalt, andesite-basalt) low-Ti series. The above-mentioned deposits are transgressively overlapped by a volcanic-terrigenous molasse, with conglomerate occurring at the base (C_{1-2}).

The Edrengin-Nuru subzone

This includes the Edrengin-Nuru Ridge and part of the Transaltai Gobi which is contiguous with to ridge in the south. An orogenic complex (volcanic-terrigenous molasse, C_{1-2}) with a Devonian volcanic sequence exposed beneath it, is widely developed within this subzone. Various tuffite, and epiclastics of rhyolite and dacite with rare thin layers of limestone (containing the brachiopods *Brachyspirifer* sp., and *Multispirifer* sp., D_2e) are exposed at the base of the Devonian sequence. Above these is a sequence of pyroxene-porphyry spilite, and epiclastic rocks with an aggregate thickness of up to 3–3.5 km (Table 2).

Table 2 Composition of the Devonian Volcanic rocks of the Edringin Zone.

Rock/ component	Basalt			Andesite-basalt		Trachy-andesite	Trachy-dacite
	23/82	246/82	241/82	104/85	105/85	108/85	112/85
SiO_2	48.79	49.03	49.59	53.05	55.34	63.40	67.80
TiO_2	0.85	0.83	1.29	1.62	1.57	0.58	0.56
Al_2O_3	15.13	16.31	15.66	16.57	16.62	17.20	15.70
Fe_2O_3	4.22	3.58	5.64	8.03	6.83	1.73	2.17
FeO	7.28	7.28	6.70	2.93	2.93	0.69	0.84
MnO	0.18	0.21	0.21	0.19	0.22	0.06	0.05
MgO	6.03	5.00	3.97	3.74	3.63	0.74	0.60
CaO	7.73	6.22	6.50	3.53	2.90	3.65	2.30
Na_2O	4.26	3.52	5.55	6.83	6.76	7.12*	6.44
K_2O	1.96	3.29	1.64	0.25	0.20	1.80	1.46
H_2O	2.62	2.60	2.38	1.86	1.74	1.52	1.12
H_2O^-	0.52	0.38	0.43	0.30	0.32	—	—
P_2O_5	0.29	0.69	0.46	0.94	0.71	0.11	0.16
Cr	12	18	24	12	13	38	30
Ni	60	20	26	20	27	10	8
V	162	160	175	290	342	22	18

Cu	117	147	108	236	285	16	12
Co	29	22	23	20	20	7	6
Pb	5	5	5	1.7	2	—	—
Ga	1.5	1.5	1.5	2	2.1	1.5	—
Ge	1.5	1.5	1.5	—	—	—	—
Mo	12	14	—	—	—	—	—
Sc	49	52		60	57	10	8
Zr	48	44	—	—	—	95	75
Y	—	—	—	—	—	14	14
Ba	—	—	—	—	—	50	45
Nb	—	—	—	15	17	5	5

* 0.60%—content of CO_2 in sample 446/82.

Thus, the zone consists of two heterogeneous subzones. The Edrengin-Nuru subzone is regarded as an ensialic island-arc dome. In its structure and development, it is similar to the volcanic belt of the Dzinset subzone. The Khuvinkharin Trough began to be formed in the Early Devonian (or possibly even in the late Silurian) due to rifting of the southern boundary of the Siberian Caledonian continent. The basal horizon of the Khuvinkharin section is considered to be a 'graben facies', marking the commencement of trough opening. The presence of *mélange* bodies suggests the participation of the melanocratic basement in the process of trough opening. The greywacke series corresponds with a regression cycle, the growth of the rises flanking the trough, and the progressive closure of the basin, caused by the collision of the Siberian continent with the Edrengin-Nuru island arc.

The Transaltai Zone

This zone includes the Nomin-Gobi Mountains, the Gurvansaikhan and Dzolen ridges, and the Manlai area. It extends E–W, throughout southern Mongolia and is characterized by the development of volcanic and volcano-sedimentary deposits; ophiolites are common there. The zone is described according to evidence obtained from the Gurvansaikhan and Dzolen ridges (Suetenko, 1973; Zonenshain *et al.*, 1975; Luvsandanzan and Tomurtogoo, 1982; Ruzhentsev *et al.*, 1985, 1987, 1992a). Four complexes of deposits, namely, the Dzolen, Khairkhan, Berkhe-Ula, and Gurvansaikhan deposits were recognized in the area. Each sequence consists of four parts (from the base up-wards): ultrabasic rocks and *mélange, jasper* ($S–D_1$?), volcanic rocks ($D_{1–2}$), and a terrigenous or tuff-terrigenous suite ($D_3–C_1$). Each of the above-mentioned complexes forms thick tectonic sheets, whose superposition and secondary deformation led to the development of complex, morphologically diverse anti-forms and synforms (Fig. 20). The succession of tectonic sheets can be most easily determined within the eastern part of the Dzolen Ridge (Khadat-Ula Mountains, Fig. 21). There it has

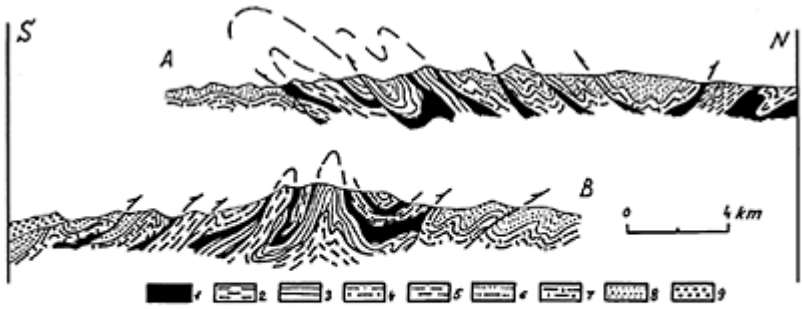

Key: 1—serpentinite *mélange*; 2—Dzolen Complex (S_2–D_3); 3 and 4—Khairkhan Complex (3—jasper and basalt, S?–D_2; 4—epiclastics, greywacke, D_2–C_1t); 5 and 6—Berkhe-Ula Complex, 5—jasper, basalt, D_{1-2}, 6—epiclastics and greywacke, D_2–C_1; 7 and 8—Gurvansaikhan Complex; (7—basaltic andesite, andesite, tuff, epiclastics, jasper, and D_{1-2}), 8—greywacke and tuffite (D_2–C_1); 9—volcano-terrigenous nolasse (PZ_3).

Figure 20 Geological sections across the Gurvansaikhan (A) and Dzolen (B) Ridges (for location see Fig. 1-㉝, E 103°–N43° 40′, and ㉞, E 103°–N43° 20′).

1—serpentinite *mélange*; 2—Dzolen Complex (S_2–D_3); 3–5—Khairkhan Complex: 3—jasper (S_2^2–D_1), 4—basalt and rhyolite (D_{1-2}), 5—greywacke (D_{2-3}); 6 and 7—Berkhe-Ula Complex: 6—variegated epiclastics, tuff, and tuffite (D_{2-3}), 7—greywacke (D_3–C_1); 8–10—Gurvansaikhan Complex: 8—basaltic andesite, andesite, dacite, tuff, epiclastics, and jasper (D_{1-2}); 9—tuff and greywacke (D_{2-3}), 10—greywacke (D_3–C_1).

Figure 21 Geological map of the Khadat-Ula Massif and the Dzolen Ridge (for location see Fig. 1-㉟), (E 103° 10′–N 43°).

been discovered that the Dzolen Complex is a lower structure feature (relative to autochthon), and the Gurvansaikhan Complex is the highest feature. The Gurvansaikhan Ridge has a more complicated structure, having mostly a complex imbricate, emphasized by numerous bodies of serpentinite *mélange* (Fig. 22).

The Dzolen Complex

This complex is made up of three rock types: greenschist, replacing basic lavas, flint, and schistose acid tuff and epiclastics. In the Khadat-Ula Mountains (Dzolen Ridge), the section is as follows (from the base upwards):

1) Serpentinite *mélange*.
2) Jasper (50–60 m thick), laminated; contains thin layers of volcanic sandstone.
3) Basaltic pillow lavas (150–200 m).
4) Rhyolitic tuff (400–450 m), variegated tuffite, epiclastics, rare basalt flows.

5) Greywacke (≤1,500 m), rhythmically bedded; contains beds of rhyolitic tuff and volcanics, as well as multiple bodies of quartz-porphyry.

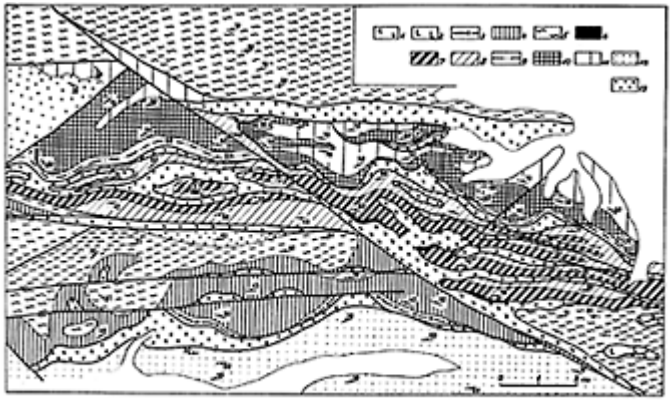

1—serpentinite mélange; 2—gabbro; 3-5—Dzolen Complex: 3—jasper (S_2!-D_1), 4—basalt (D_{1-2}), 5—tuff and greywacke (D_{1-2}); 6-8-Khairkhan Complex: 6-jasper (S_2!-D_1), 7—basalt and epiclastics (D_{1-2}), 8—epiclastics and greywacke (D_2-C_1); 9-11—Berkhe-Uls Complex: 9—jasper (S_2!-D_1), 10—basalt (D_{1-2}); 11—epiclastics, greywacke (S_{2-3}); 12—Gurvansaikhan Complex (S_2-D_2); 13—volcano-terrigenous molasse (PZ_3). Circled figures on the map: the Berkhe-Uls (1) and Khairkhan (2) massifs.

Figure 22 Geological map of the central Gurvansaikhan Ridge (for location see Fig. 1-㉝), E 103°–43° 10′)

Table 3 Average chemical composition of the major volcanic rock types of the Transaltai Zone.

Component	1	2	3	4	5	6	7
SiO_2	47.20	48.80	50.60	56.01	49.60	47.80	46.55
TiO_2	1.50	1.11	0.90	0.99	1.23	2.62	3.10
Al_2O_3	13.90	14.95	17.25	15.60	16.15	14.30	12.84
Fe_2O_3	5.79	4.45	4.34	6.78	4.07	9.24	4.00
FeO	7.30	7.42	6.13	2.90	7.32	4.82	7.54
MnO	0.30	0.19	0.16	0.12	0.21	0.46	0.08
MgO	6.84	5.60	5.35	4.15	5.15	5.46	5.10
CaO	9.65	9.17	6.83	2.30	7.44	9.40	6.18
Na_2O	2.90	3.88	5.16	4.70	4.10	3.22	5.24
K_2O	0.56	0.65	0.83	2.33	1.11	0.66	0.59
P_2O_5	0.14	0.32	0.15	0.19	0.14	0.37	0.32
H_2O^+	—	—	—	—	—	—	2.98
H_2O^-	2.92	3.76	2.72	2.88	3.38	1.38	0.43
CO_2	—	0.23	0.12	1.08	0.11	0.29	2.00
Cr	130	39	27	35	41	125	112
Ni	91	21	19	11	12	37	32
Co	40	21	20	12	19	33	92

V	160	65	88	55	92	105	85
Sc	32	18	23	14	19	30	21
Cu	34	36	80	65	82	33	32
Zr	80	43	93	62	70	230	110
Y	30	20	24	15	18	40	36
Ba	22	—	—	110	48	40	36
Ga	4	1	—	—	2	1	1
Nb	9	5	5	8	10	14	16
Zn	65	80	232	115	104	260	215
n	6	12	8	18	11	17	16

Note: Complexes of the Transaltai Zone: 1–2 Dzolen (basalts), 3 Khairkhan (plagiobasalt), 4–5 Berkhe-Ula (4 andesite, 5 basalt), 6–7 Gurvansaikhan (6 basalt, 7 subalkaline basalt).

The basaltoids of the complex are represented by pyroxene- and pyroxeneplagioclase porphyry, with the groundmass showing a doleritic texture. They have low contents of Al_2O_3 (13.51–15.63), TiO_2 (0.64–1.1.), K_2O (0.63–1.46), P_2O_5 (0.06–0.31) and relatively high MgO (4.78–8.89) (Table 3). The subalkaline character of the volcanic rocks is determined by their high Na_2O content and is caused by superimposed sodium metasomatism. For the most part, the Dzolen basalt belongs to the tholeiitic series. The bimodal (basalt-rhyolite) series (Layer 3) probably marks the initiation of the island-arc process.

The Khairkhan Complex

The most complete section of this complex was reconstructed in the central part of the Gurvansaikhan Ridge (7 km east of Mt Khairkhan):

1) Serpentinite *mélange* including blocks of harzburgite, dunite, wehrlite, and gabbro, cut by swarms of dolerite dykes, in places with chilled contacts with serpentinite.

2) Clayey-flinty slate and jasper (6 m), violet; cut by dolerite dykes.

3) Sandstone (60–70 m), volcanic; locally contains pebbles and boulders of ultrabasic rocks, porphyry, spilite, acid tuff, and epiclastics.

4) Pillow lavas of aphyric basalt (25 m).

5) Clayey-flinty slate, and flint (3–4 m); yielding the remains of the conodonts: *Ozarkodina remscheidensis remscheidensis(Ziegl.)*—D_1l

6) Tuff and epiclastic rocks of andesite-porphyry (170–190 m).

7) Basalt (60 m), forming a series of massive flows up to 2–3 m thick.

8) Epiclastic rocks (280 m), containing reworked basic and acid volcanics.

9) Silicified tuffite (3 m).

10) Dolerite (8 m).

11) Sandstone (380–400 m) polymictic; contains pebbles and boulders of tuff and epiclastic rocks, jasper, granitoid, gabbro, and ultrabasic rocks.

12) Sequence (1,000–1,200 m) of polymictic (essentially volcanic) sandstone with numerous thin layers of variegated tuffite, clayey-flinty slates, and ash tuff.

The Lower to Middle Devonian deposits of the complex (Layers 3–10) are composed of mixed-facies coarse (including boulder conglomerate and mixtite) epiclastic rocks, various tuffs, and tephroids. The epiclastics are the products of the reworking of basic and intermediate volcanics. Acid volcanics are subordinate. Aphyric tholeiitic basalt is a common component of the sequence. The tuff is the result of explosive volcanic activity within a volcanic dome. The source lavas belonged to the differentiated basalt-andesite-dacite-rhyolite series.

The Berkhe-Ula Complex

This complex is widely developed within both ridges; the bulk of the exposures of serpentinite *mélange* occur within this terrain. The most complete section can be observed in the Berkhe-Ula Mountains (Gurvansaikhan Ridge, Fig. 22); the following rocks are exposed there:

1) Harzburgite

2) Ophicalcite breccia (1–25 m).

3) Jasper-quartzite (0.2–1.5 m), infilling pockets at the top of the ophicalcite.

4) Gravelstone and sandstone (2–2.5 m), containing clasts of serpentinite and ophicalcite, without breccia also containing isolated boulders of harzburgite.

5) Jasper (7–10 m), containing radiolaria, less-common spongolite, laminated, with thin layers of polymictic sandstone.

6) Sandstone (3–4 m), coarse-grained, polymictic (including fragments of basalt, andesite, terrigenous rocks, clasts of pyroxene, plagioclase, quartz, serpentine, chromite, and magnetite).

7) Clayey-flinty slate, and jasper, intercalated with polymictic sandstone (35–40 m).

8) Gabbro-dolerite (1.5 m).

9) Clayey-flinty slate, and jasper (4 m).

10) Basaltic pillow lavas (200–800 m), containing thin (0.25–0.5 m) layers of jasper and silicified tuffite.

11) Sequence (400–450 m) of variegated tuffite, ash tuff, and epiclastics.

12) Greywacke (900–1,000 m); the upper section contains horizons of mixtite, made up of blocks of Ordovician, Silurian, and Lower to Middle Devonian limestone, plagiogranite, gabbro, basalt, ultrabasic rocks, flint, and epiclastic rocks; the rocks yield abundant plant debris (*Heleniella theodori Zal.*, D_3fm–C_1t).

The Berkhe-Ula basaltoids form multiple sills, sills/flows, and flows (2–5 m) with a pillowed structure at the top; ferricrusts are common on their exposed surfaces. Single interbeds of basic tuff, tephroids, epiclastics, jasper and flinty slates are present. They are essentially dolerites; plagioclase- and plagioclase-pyroxene porphyries are uncommon. The rocks contain clinopyroxene diopside-series, saussuritized plagioclase, magnetite, and chloritized glass. The volcanics are weakly differentiated; basalt is predominant; andesite-basalt is rare. In their basic petrology (see Table 3), they are comparable with volcanics from the base of island arcs and intra-arc rifts.

The Gurvansaikhan Complex

This complex is the most widely developed unit in the area under study. To a first approximation, its section consists of two parts: a lower, jasper-volcanic sequence, and an upper tuff-terrigenous sequence.

The lower sequence is best exposed on the southern slope of the Dzolen Ridge, where it is represented by deposits of various facies types, 0.5–2 km thick. They are for the most part complexly lensing flows and pillow lavas of violet and black basalt, andesite-basalt, and andesite, and a wide variety of corresponding tuffs—including very coarse volcanic rocks, tuffite, and tuff-mudstone. Radiolarian jasper, spongolite, and quartz-haematite rocks are common components of the section. The jasper is bedded; it forms units 0.5–10 m thick. In places (western Dzolen) it completely replaces the volcanic rocks. The above-mentioned deposits rest on the serpentinized peridotite with transgressive contacts. Radiolarian fossils give a Silurian-Lower Devonian age for the lower sequence (Zonenshain *et al.,* 1975; Ruzhentsev *et al.,* 1985).

Coeval deposits are exposed on the northern slope of the Dzolen Ridge, where they are mostly represented by jasper, which contains separate interbeds of acid and intermediate tuff, and volcanic sandstone. Within the Gurvansaikhan Ridge, the deposits are almost entirely jasper, reaching 200–300 m thick.

The upper sequence of the complex (Gurvansaikhan Formation, up to 3,000 m thick), has a rhythmically repeated structure. Sandy-silty, rhythmically bedded units, containing a more or less substantial admixture of tephra, occur at the base. Gravel horizons are common. Polymictic varieties are markedly predominant and are composed of grains of quartz, plagioclase, pyroxene, amphibole, and mica.

The lithic component is made up of basic, intermediate, and acid lavas, tuff, epiclastics, sandstone, and siltstone, with diverse compositions and structures. The section contains thin layers of silicified tuffite, ash tuff, jasper, and clayey-flinty slates. On the Gurvansaikhan Ridge (near the Khud-Bulak Well), the flints yielded the remains of the conodonts *Palmatolepis gracilis sigmoidalis Ziegl., P. gracilis gracilis* Br. *et* Mehl., and *Spathognathodus.* sp.(D_3fm_2). The upper parts of the section contain thick (up to 200 m) horizons and lenses of mixtites, composed of olistoliths of limestone, yielding Emsian and Eifelian corals and brachiopods.

Palinspastic reconstructions have enabled the relative positions of the above complexes to be established. From south to north (according to present-day co-ordinates) the Dzolen, Khairkhan, Berkhe-Ula, and Gurvansaikhan complexes were located there (Fig. 23). All of them were deposited on melanocratic basement, overlain by jasper or clayey-flinty slate. The Berkhe-Ula Complex has a transgressive contact. The products of the reworking of ultrabasic rocks have been found in the Khairkhan and Gurvansaikhan complexes. A sequence of lavas, usually regarded as a feature of ophiolitic association (Zonenshain *et al.,* 1975; Zonenshain and Tomurtogoo, 1979), overlies the jasper horizon. Its age and structure differ markedly from the rock of the ophiolitic suite. This is because the period of lava accumulation was preceded by regional structural reworking *(mélanging)* of the ophiolites.

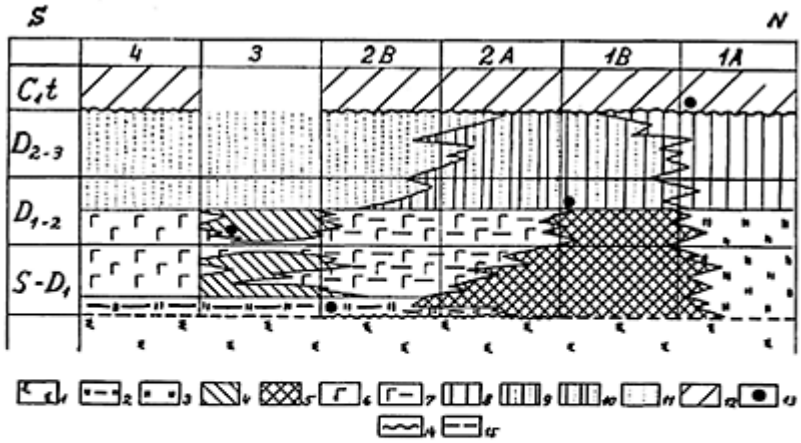

Key: 1—*mélange*; 2—jasper, sandstone, and tuffite; 3—jasper; 4—basalt, epiclastics, and tuff; 5—basaltic andesite, andesite dacite, tuff, epiclastics, jasper; 6—tholeiitic basalt, tuffite, and epiclastics; 8—greywacke and mixtite; 9 and 10—epiclastics, tuff, greywacke, and mixtite; 11—greywacke, tuffite, and ash tuff; 12—polymictic sandstone, containing abundant granitic material, and conglomerate; 13—stratigraphic levels where ultrabasic rocks and gabbro have been reworked 14—transgressive contacts; 15—tectonic contacts; 1A—northern and 1B southern parts of the Gurvansaikhan complex, 2A—southern and 2B—northern parts of the Berkheulin Complex, 3—Khairkhan and 4—Dzolen complexes.

Figure 23 Comparison of the Transaltai Zone complexes.

Starting in the Middle Devonian, a complex tuff-terrigenous suite was deposited in the Transaltai Zone. In spite of differences in their structure, the deposits of the suite form a single lateral series. To a first approximation, the suite consists of lower (tuff-terrigenous) and upper (greywacke) sequences. The tuff-terrigenous sequence (D_{2-3}) is made up of alternating basic tuffs and tephroids, acid tuffs and tephroids, epiclastic rocks, polymictic clastics, tuffite, ash tuff, tuff-siltstone, and clayey-flinty shales. Fine-grained rocks predominate to the south (the Dzolen Complex), and coarse rocks predominate to the north (the Khairkhan and Berkhe-Ula complexes). The former accumulated in the vast Dzolen Basin, corresponding with a major part of the South Mongolian Variscan ocean, while the latter mark the southern slope of the complex Khairkhan island-arc dome. The Middle to upper Devonian deposits of the most northerly Gurvansaikhan Complex show an unusual, very intricate vertical and lateral alternation of fine and coarse tuffaceous and terrigenous rocks. They accumulated in a basin situated between the Khairkhan and the Edrengin-Nuru island arcs. There, sedimentation was controlled by two processes: the accumulation of fine-grained pyroclastic rocks, argillaceous, and siliceous material, and the supply of clastic (essentially volcanic) material by turbidity flows *(sensu Lata).*

The greywacke sequence (D_2-C_1) is typical of the upper sections of the suites of the Transaltai Zone. Sandstone predominates, and contains clasts of quartz, plagioclase, pyroxene, amphibole, and biotite. The lithic clasts consist of basic, intermediate, and acid volcanics, flint, quartzite, siltstone, sandstone, and limestone; shelly fossils and plant

debris are common. The sandstone is rhythmically intercalated with siltstone and clay shale. Horizons of conglomerate and mixtite occur locally. The above deposits accumulated in a single extensive basin, which appeared at the site of an island-arc system. The conditions of sedimentation became fairly predictable. Volcanic activity died out, and at the same time erosional processes intensified in the marginal parts of the structure.

The South Gobi Zone

This zone is a terrain of Lower to Middle Devonian terrigenous and carbonate rocks, cross-cut by Devonian, Carboniferous, and Permian granitoids. The orogenic complex there (terrigenous and terrigenous-volcanic molasse) is Carboniferous to Permian in age. This region is one of the most inaccessible and poorly studied areas of Mongolia. Its description is based on the studies of Sinitsin, 1956; Markova, 1975; Ruzhentsev, 1985; and Ruzhentsev *et al.,* 1987.

From north to south the zone is divided into the Ekhingol, Tumurtia and Tsaganulin subzones (Ruzhentsev *et al.,* 1992a). Each subzone is made up of an unusual complex of deposits, which form a series of tectonic sheets, overthrust from south to north. The Ekhingol deposits are overlain by the Tumurtia rocks, which are in turn overlain by the Tsaganulin deposits. The internal structure of the sheets is intricate: the layers are deformed to form isoclinal folds, complicated by longitudinal folds and faults (Fig. 24). These dislocations are pre-Viséan in age. However, the Variscan structure was substantially complicated in Triassic times by superimposed Indo-Sinian (Triassic) deformations.

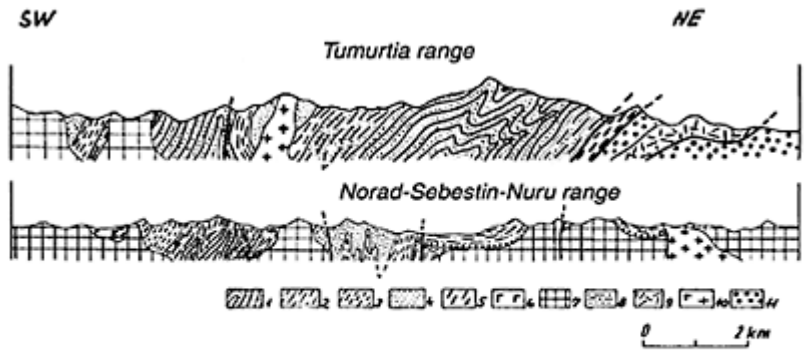

Key: 1 and 2—Tumurtia Formation: 1—oligomictic sandstone (O–S), 2—siltstone and limestone (S?–D_1); 3–6—Ekhingol Formation: 3—tuffite and limestone (D_1), 4—epiclastics (D_1), 5—rhyolite, dacite, tuff, and epiclastics (D_{1-2}); 6—andesite and basaltic andesite (D_{1-2}); 7—granite (D_2); 8—sandstone and limestone (D_2); 9—rhyolite and dacite (PZ_3); 10—granite (P); 11—conglomerate (MZ).

Figure 24 Geological sections across the Tumurtia subzone (for the location see Fig. 1-㊱) E98°–N43° 15′, and ㊲E 96° 20′–N 43°).

The Ekhinqol subzone

This subzone occupies the area of the Ekhinkhoity Khara-Nuru, Ikhe-Khabtsagain-Nuru and other mountains (which are the northern offshoots of the Gobi Tien Shan). Rocks of the Precambrian basement are not exposed there. The exposed section has the following structure, in ascending order:

1) A succession (≤600 m thick) of fine-grained sandstone and siltstone, greenish-grey quartz and quartz-plagioclase, calcareous, rhythmically bedded.

2) A succession (≤700 m thick) of variegated, thin-bedded (contourites) tuffite, and tuff-siltstone, with lenses of fine-grained rhyolitic tephroids.

The deposits are unfossiliferous. By analogy with the Tumurtia subzone, they are tentatively assigned to the Devonian. They are unconformably overlain by Viséan-Namurian molasse with a thick basal conglomerate horizon.

The Tumurtia subzone

This subzone is most completely represented in the west, in the Gobi Tien Shan (including the Tsagan-Bogdo, Alas-Bogdo, Tumurtin, Norad-Sebestin-Nuru, and other mountains). In Central and East Mongolia, it is present as separate tectonic blocks along the southern boundary of the Transaltai Zone.

In the Gobi Tien Shan, the section of the subzone is as follows;

1) Dolomitic marble (200–230 m), light-grey, thickly bedded, with thin lenses of quartzite.

2) Dolomitic limestone (80–100 m), black, laminated, and stromatolitic (R_3).

3) Conglomerate (10–50 m), consisting of well-rounded pebbles of marble and quartzite.

4) Rhyolitic tuff (including ignimbrite) and epiclastic rocks (300–350 m), buff, orange, and grey.

5) Conglomerate (2–15 m), chiefly made up of pebbles of rhyolitic tuff, less commonly containing marble and quartzite.

6) A sequence (700–800 m) of thin-bedded, grey arenaceous limestone, siltstone, quartz and quartz-plagioclase sandstone.

7) Sandstone (up to 1,000 m) greenish-grey, quartz-plagioclase, and micaceous, rhythmically intercalated with siltstone and clay shale.

8) Siltstone (300–400 m), quartzose, with thin layers of argillaceous limestone, containing the remains of poorly preserved tabulate corals of probable Silurian-Devonian age *(Alveotella?* sp.).

9) Tuffite, tuff-silicilyt, ash tuff, flint (70–80 m), lenses of biogenic limestone; tabulate corals: *Favosites archaensis* Sok.; brachiopods: *Aulacella* sp. *Gladiostrophia* sp., *Leptagonia* sp., *Delthyris* sp. ($D_{1–2}$).

10) Sandstone (450–500 m) polymictic, with thin layers and lenses of acid and intermediate tuff, epiclastic rocks (including conglomerate).

11) Pillow lavas and andesite and andesite-basalt (500–600 m).

In the section described above, horizons 1 and 2 are Riphean in age, and 3 and 4 are probably Vendian. The carbonate-terrigenous sequence (horizons 5–6) is tentatively assigned to the Lower Palaeozoic; horizons 7 and 8 are probably SilurianLower Devonia; horizon 9 is Lower and Middle Devonian, and 10–11 is Middle to Upper Devonian. In

the Elgenii-Kher Mountains (the eastern continuation of the Gobi Tien Shan), a Lower Carboniferous fossiliferous terrigenous sequence overlaps the volcanics and epiclastic rocks.

The Tsaqanulin subzone

This subzone is a terrain of carbonate and carbonate-terrigenous rocks. Riphean marmorized limestones and dolomites, quartzites (including ferruginous rocks), and flint are common there. In south-east Mongolia (Dzerem-Ula Mountains), the above mentioned deposits lie unconformably on Early Proterozic retrogrademetamorphosed gneisses and granite-gneisses, with a basal conglomerate at the unconformity a Riphean carbonate sequence with a basal conglomerate is overlain by rhyolitic tuffs and epiclastics which are similar in composition and stratigraphic position to the deposits from the Dzabkhan Formation of West Mongolia, whose Late Riphean to Early Vendian age is proven.

The lowermost fossiliferous horizons of the Palaeozoic section were found in the Tsakhirin-Kher Mountains (Fig. 25). The following deposits are exposed, in ascending order:

1) Limestone (1,000–1,200 m thick), grey, bedded, commonly bituminous; the upper section contains bands of pink and red sandstone, and pink algal limestone.

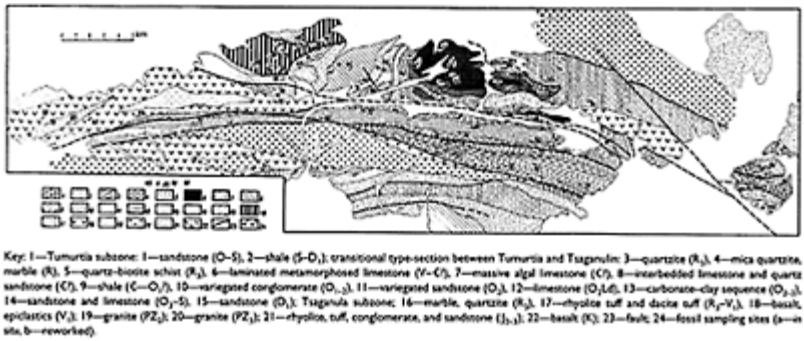

Key: 1—Tumurtia subzone: 1—sandstone (O–S); 2—shale (S–O_1); transitional type-section between Tumurtia and Tsaganulin: 3—quartzite (R_3); 4—mica quartzite, marble (R); 5—quartz-biotite schist (R_3); 6—laminated metamorphosed limestone (V–C?); 7—massive algal limestone (C?); 8—interbedded limestone and quartz sandstone (C?); 9—shale (C—O_1?); 10—variegated conglomerate (O_{1-2}); 11—variegated sandstone (O_2); 12—limestone (O_2Ld); 13—carbonate-clay sequence (O_{2-3}); 14—sandstone and limestone (O_3–S); 15—sandstone (O_3); Tsaganula subzone; 16—marble, quartzite (R_3); 17—rhyolite tuff and dacite tuff (R_3–V); 18—basalt, epiclastics (V); 19—granite (PZ_2); 20—granite (PZ_3); 21—rhyolite, tuff, conglomerate, and sandstone (J_{2-3}); 22—basalt (K); 23—fault; 24—fossil sampling sites (a—in situ, b—reworked).

Figure 25 Geological map of the Tsakhirin-Kher and Barun-Tsokhio Mountains (for location see Fig. 1-㊳) E107°–N 43°).

2) Conglomerate (20–180 m), variegated, consisting of large, well-rounded pebbles of limestone and quartz sandstone; pebbles of diverse tuffs and epiclastics, quartz-porphyries, and granitoids are less common.

3) Sandstone (300–350 m), variegated, polymictic, and thick bedded.

4) Limestone (250–300 m), grey, bituminous, laminated, includes lenses of brachiopod shells *(Onniella chancharica* Severg., *Cyclomionia* sp., *Fascifera* sp., *Atelelasma ex gr. elegantis* Sever., *and Eoanastrophia lebediensis* Severg., O_2Ld).

5) A sequence (400 m) of intercalated detrital and muddy limestone and silty-clayey beds.

6) Sandstone (1,400–1,500 m) greenish-grey, quartz-plagioclase, includes beds (up to 10 m thick) of buff, arenaceous limestone; the upper section contains numerous lenses of lamellibranch and brachiopod shells (*Leplaena depressa* Sow., *Testaria gobica* Rozm., *and Tuvaella gigantea* Tschern; S_1w_2-S_2l).

The limestone of horizon 1 is tentatively assigned to the Cambrian-early Ordovician, horizons 2–4 to the middle Ordovician, 5 to the late Ordovician, and 6 to the early Silurian. The section under consideration is intermediate between the typical Tsaganulia and Tumurtia sections. It resembles the Tsaganulia section in its abundance of limestone, and the Tumurtia section in its great thickness and the presence of Silurian-Lower Devonian oligomictic turbidites.

A rather different section was described from the more southerly areas of the zone. For example, the following section is found in the Tsagan-Sume Mountains (Fig. 26). Above the Riphean marble and quartzite lie:

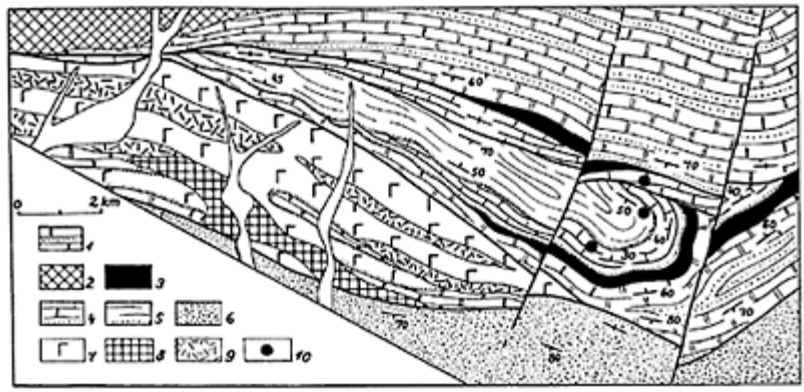

Key: 1—marble and quartzite (R_3), 2—granite (R_3), 3—limestone, and chert (R_3–V), 4—conglomerate and limestone (S_1L–W), 5—conglomerate, sandstone, siltstone, and limestone (S_1W_2–S_2), 6—sandy-shale sequence (PZ_3), 7—basalt and andesite (PZ_3), 8—granite (PZ_3), 9—quartz-porphyry (J), 10—fossil sampling sites.

Figure 26 Geological map of the Tsagan-Sume area (for location see Fig. 1-㊴), E 103° 20′–N 42°).

1) Conglomerate (1–50 m thick), composed of pebbles of Riphean marble and quartzite.

2) Limestone (180–200 m), grey, black, bituminous, and massive; the top yielded abundant remains of tabulate corals: *Favosites forbesi* M.E. *et* H., *Palaeofavosites raikulaensis* Sok., *P. balticus* Sok., *Multisolenia tortuosa* Fr., and the brachiopods: *Pentamerus longiseptatus* Boris. (S_1l–W_1).

3) Limestone (80–90 m), with thin layers of andesitic tuff.

4) Conglomerate (1–25 m): cobble and limestone, type lies on both the Riphean and the Lower Silurian deposits.

5) Sandstone-siltstone flyschoid (≤400 m) with beds (2–3 m) of biogenic limestone; corals: *Halysites sandpilensis* Nord. and *Favosites niagarensis* Hall. ($S_2$1).

The Devonian part of the section is better represented 40 km to the north, in the Elgenulin-Kher and Tsagan-Del mountains. In the Elgeaulin-Kher Mountains (Fig. 27), the top of carbonate-terrigenous sequence 5 yielded the remains of the brachiopods *Dalejina* sp. (D_1). Above them lie:

1) Variegated siliceous tuffite (50–60 m thick).

2) Limestone (120- 130 m) grey, laminated, yielding the remains of the brachio-pods: *Gladiostrophia kondoi* (Hamada), *Trilobostrophia bobilevi* Schischk., *Maoristrophia kailensis* Schischk., and *Strophonella* sp. (D_1p).

3) Variegated mudstone and siltstone (150–160 m) containing the remains of brachiopods of the family Chonetidae and *Coelospira burubaensis* Kaplan (D_1e).

In the Tsagan-Del Mountains, the section is more complete:

1) Sandstone-siltstone sequence (≤200 m).

2) Limestone (30–80 m) grey and massive, containing *Thamnopora* sp.

3) Tuffite, flint and siliceous limestone (90–100 m) variegated lenses of biogenic limestone *(Plicostropheodonta* sp., *Leptagonia orientalis* Aleks., *Spinatrypa bochatica* Aleks., *Delthyris* sp., and others, D_1e).

4) Sandstone-siltstone sequence, with numerous interbeds of limestone (up to 300 m thick).

5) Conglomerate and gravelstone (30–40 m), consisting of fragments of underlying limestone, sandstone, tuffite and flint.

6) Plagioporphyry, tuff and epiclastics (150 m).

7) Biogenic-detrital limestone (70 m), with intercalations (up to 0.5 m) of volcanic sandstone (contains the brachiopod *Spinatrypa aspera* Schloth; D_2e–gV_1).

8) Volcanic sandstone, andesitic tuff and rare flows of andesite lava (100–400 m).

9) A sequence (500–600 m thick) of intercalated limestone, oligomictic and polymictic sandstone, epiclastics and tuff; the top contains interbeds (up to 7–10 m) of polymictic conglomerate; contains the brachiopods: *Stropheodonta asella* Vern., *Atrypa* sp., *Productella* sp., *Cyrtospirifer shelonicus* Nal. (D_3).

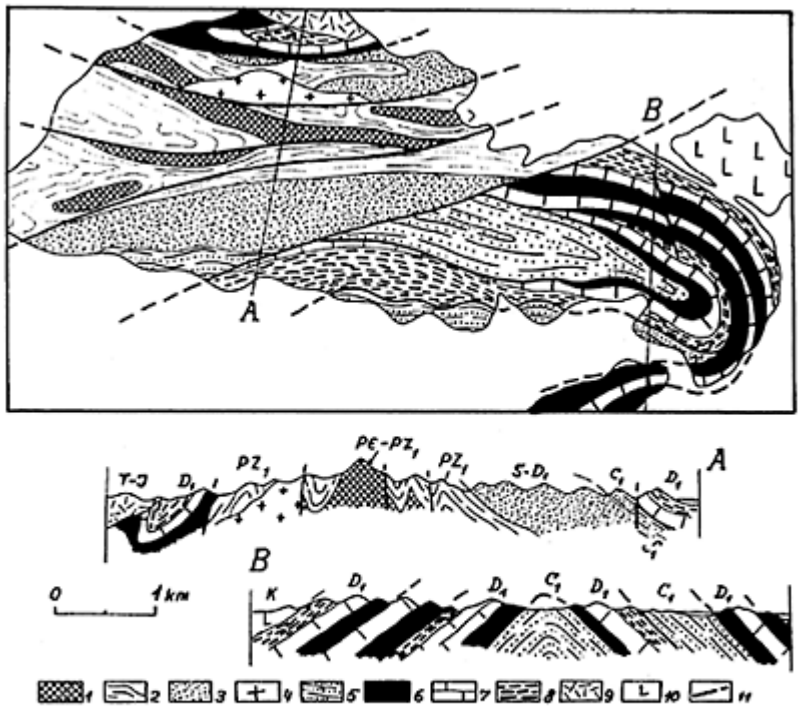

Key: Tumurtia subzone: 1—marble (R_3), 2—sandstone and limestone (PZ_1), 3—sandy-shale sequence ($S–D_1$), 4—granite (D), 5—flysch ($C_1t–v$); Tsaganula subzone: 6—sandstone and limestone (D_1p), 7—limestone (D_1p), 8—limestone and tuffite, siltstone (D_1e); 9—rhyolite and sandstone (J); 10—basalt (K); 11—fault.

Figure 27 Geological map and sections of Elgenula antiform (for location see Fig. 1-㊵), E 103°–N 42° 40′).

The most complete Devonian section is that of the Tsagal-Del Mountains. The lower terrigenous-carbonate sequence (horizons 1–4) is equivalent to the Lower Devonian deposits of the Elgenula-Kher Mountains; the upper volcanic sequence (horizons 5–9) is middle to late Devonian in age. The relative proportion of volcanics varies through the section. Some 20 km north of the Tsagan-Del Mountains, in the Barun-Tsokhio Mountains, a thick basalt complex, in which sediments are of minor importance, is equivalent to the upper sequence.

Thus, the deposits of the South Gobi Zone contain a characteristic lateral series (Fig 28). An overall increase in the volume of terrigenous rocks, dominated by oligomictic sandstone, is observed from south to north. This change marks the transition from an epicontinental shelf to proximal turbidites of the continental slope, and, farther north, to the distal turbidites and contourites of the continental rise. An increase up section in proportion of terrigenous deposits is associated

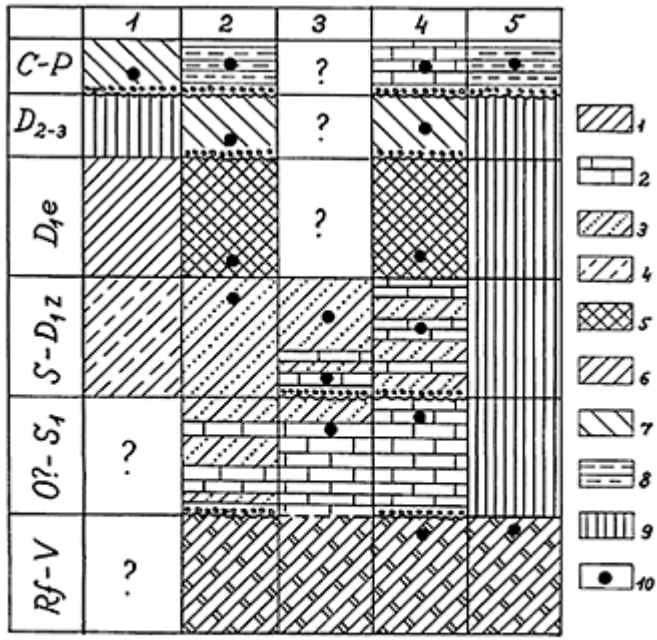

Key: 1—marble and quartzite (R–V); 2—limestone, 3—proximal oligomictic turbidites; 4—distal oligomictic turbidites; 5—terrigenous–volcanic deposits; 6—tephroid–epiclastic turbidites; 7—volcanic–terrigenous molasse; 8—flysh; 9—hiatus; 10—fossil sampling sites; Numbers on the map: 1—Ekhingol, 2—Tumurtia subzones; 3—Barun–Tsochio Massif; 4—Tsaganula subzone; 5—northern margin of the Lugingol Zone of the Indo-Sinides.

Figure 28 Correlation of type sections of the South Gobi Zone.

with tectonic activation, beginning in the Silurian; an increase in the topographic relief of the regions supplying the sediment provinces; the growth of intrabasin rises and their erosion. The Emsian was the time of formation of a volcanic belt (including Tumurtia and Tsaganulia subzones) within an Andean-type, active continental margin. An area of subsidence (the Ekhingol subzone), where siliceoustuffite contourties were accumulated, was located north of the continental margin.

3.2 Palaeotectonic Reconstructions of the Variscides of South Mongolia

The Transaltai zone is an axial element of the Variscan fold belt of South Mongolia. It was formed at the site of a palaeo-oceanic basin, which underwent complex tectonic evolution in the Palaeozoic. The Gobi-Altai and the Edrengin zones, located to the north (in present-day co-ordinates), and the Tsaganulia Zone, located to the south, are ancient continental blocks, reworked by Variscan movements (Ruzhentsev *et al.,* 1987). The

Gobi-Altai forms the border of the Siberian Caledonian continent, and the South Gobi is a Precambrian microcontinent.

Mélanged ophiolites are common in the Transaltai Zone. Serpentinized peridotites make up most of the *mélange*, while rocks of the banded complex and gabbro are less common. The *mélange* is overlapped by a terrigenous-jasper horizon above which the overwhelming proportion of the basaltoids were accumulated. The jasper is probably Silurian in age. Direct overlapping of the serpentinite by jasper is more common. This evidence suggests the existence of a Lower Palaeozoic ophiolitic association within the Transaltai zone. *Mélanging* took place in Silurian times.

The terrigenous-jasper horizon is regarded here as an unusual type of oceanic cover, overlying the *mélanged* basement during a period of relative tectonic quiescence. A rearrangement of the structural trend of the zone was related to a new phase of extension; as a result, the Silurian/Devonian boundary witnessed the appearance of a system of dyke swarms, which were dispersed over the area and served as feeders for the basaltoids. The extension in the southern part of the zone was compensated to the north, which was the site of formation of a complex accretionary system (Fig. 29), which includes the follwing structural features (from south to north):

1) an ‘island-arc dome’ with a well-marked slope (reconstructed from detailed study of the developed coarse clastics of the Khairkhan Complex) and also containing an intra-arc trough (Berkhe-Ula complex);

2) a back-arc trough (Gurvanasikhan Complex).

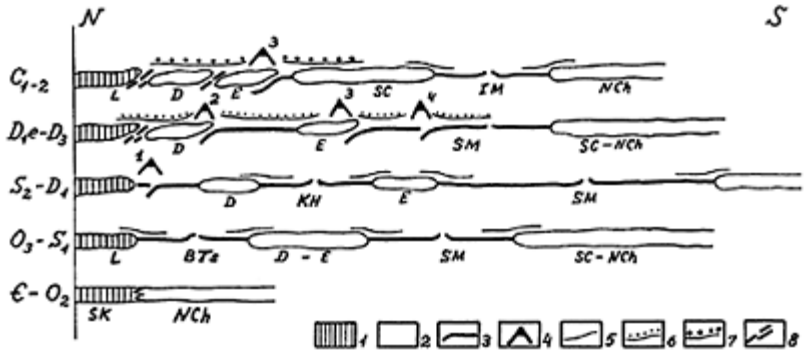

Key: 1—Salairides of the Lake Zone of Mongolia; 2—microcontinents of Gondwana type; 3—oceanic basins; 4—suprasubduction structures; 5—passive-margin formations (oligomictic turbidites; 6—greywacke; 7—molasse; 8—ophiolite sutures; Symbols on the map: SC—Siberian Caledonian continent; SK—Siberian continent; L—Salairides of the Lake Zone; microcontinents: D—Dzhinset microcontinent, E—Edrenginnurin, SG—South Gobi, NCh—North chinese; ocean basins: BTs—Bayan–Tsagan, KH—Khuvinkharin, SM—South Mongolian, IM—inter-Mongolian; supra-subduction structures: 1—Bayan–Leg. 2—Dzhinset, 3—Edenginnurin, 4—Khairkhan.

Figure 29 Tectonic development of South Mongolia.

As stated above, the South Gobi Zone is a continental block (the South Gobi microcontinent). Precambrian rocks are fairly widely developed within it.

The northern flanking region of the Transaltai Zone (Gobi-Altai and Edrengin zones) is much more complex in structure; during the Ordovician, Silurian, and the early half of the Devonian, the region represented a system of sialic blocks separated by troughs. The latter were formed on a melanocratic (ultrabasic) basement. We agree with the suggestion made by Pinus *et al.* (1981) that typical ophiolites are absent there. The basement is made up almost totally of serpentinite, which is locally overlapped by Lower Palaeozoic oligomictic sandstone and limestone; however, in most cases tectonic contacts were observed between the serpentinites and the surrounding deposits.

Beginning in the Lokhkovian (possibly Pridoli), a passive continental margin, marking the emplacement of the South Mongolian palaeo-ocean, was formed in the Gobi-Altai (Ruzhentsev *et al.,* 1992a). The Devonian shelf cover unconformably rests on the Caledonian folded basement.

Thus, in S–D_2 times the following tectonic features can be recognized from south to north:

1) the South Gobi Precambrian microcontinent with a well-marked passive margin (the Tsaganulin, Tumurtia, and Ekhingol subzones, representing shelf, continental slope, and continental rise, respectively);

2) the South Mongolian palaeo-ocean (Dzolen, Khairkhan, Gurvansaikhan complexes, representing the palaeo-ocean proper, ensimatic island arc containing the Berkhe-Ula intra-arc rift, and a back-arc trough, respectively);

3) the Edrengin-Nuru ensialic (?) island arc;

4) the Khuvinkharin back-arc trough; and

5) the southern passive margin of the Siberian Caledonian continent (Gobi-Altai Zone).

$D_{2–3}$ was the time of existence of:

1) the border volcanic belt along the northern boundary of the South Gobi microcontinent;

2) the Transaltai accretionary system, bounded by large greywacke basins to the north and south;

3) the Dzinset volcanic belt along the southern border of the Siberian continent.

3.3 The Variscides of East Dzungaria

The Variscan complexes of East Dzungaria occur within south-western Mongolia in (the Barunkhurai Depression and its surrounding mountains). As stated above, to the east the Dzungar orogenic belt is separated from the South Mongolian fold belt by the Gobi-Altai fault system (Ruzhentsev *et al.,* 1990). To the west, the structures extend into Xinjiang, as far as eastern. Kazakhstan and western Dzungaria. Devonian and Lower Carboniferous volcanic and volcano-sedimentary deposits, which form tectonic sheets, thrust over each other, are the predominant rocks there (Figs. 30 and 31). The overall structural trend is northerly; the northern and the southern complexes form an autochthon and an allochthon, respectively (Ruzhentsev *et al.,* 1992b). In this respect, the Dzungar structural grain differs from that in southern Mongolia, which is mostly southerly. The sheets are deformed to form a system of morphologically diverse antiforms and synforms,

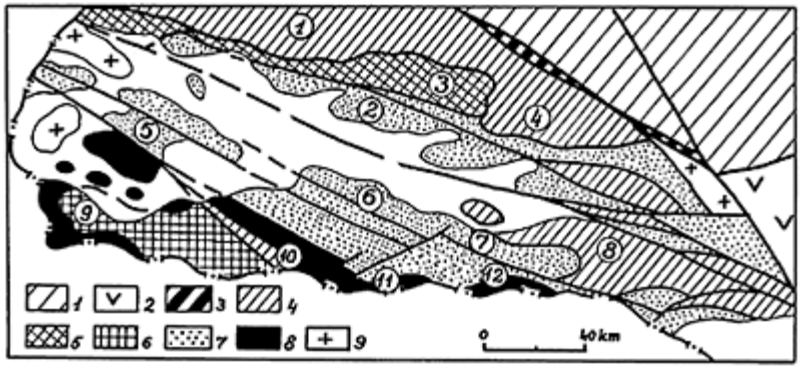

Key: 1—Caledonides of Mongolian Altai; 2—Variscides of South Mongolia; 3–9—Variscides of East Dzungaria: 3—Bidzha zone, 4 and 5—North Barunkhurai Zone (4—Argalantain and 5 5—Khaistyn subzones), 6—Olonbulak Zone, 7—Ulanus Zone, 8—South Barunkhurai (Baitak) Zone; 9—granitoids (PZ_3); Numbers on the Map—mountains: 1—Seriin-Nuru, 2—Sertengiin-Nuru, 3—Khaistyn-Ula, 4—Algalantain-Ula, 5—Maikham-Khara, 6—Idreigiin-Nuru, 7—Ulan-Us, 8—Khairkhan-Ula, 9—Baitak, 10—Sukhaityn-Ovgor-Nuru, 11—Ikh-Khavtag, 12—Khundryn-Nuru.

Figure 30 Tectonic zonation of East Dzungaria (for location see Fig. 1-41), E 92°– N 45° 30′).

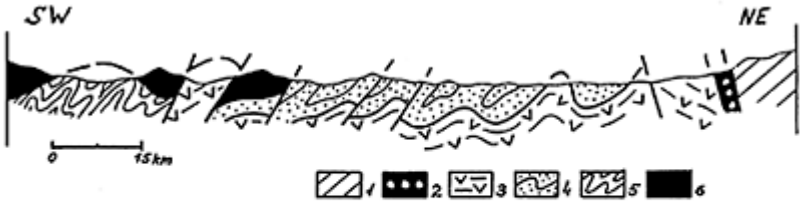

Key: 1—Caledonides of the Mongolian Altai, 2—basalts, cherts (D?) of the Bidzhii Zone, 3—alkali volcanics (D_1–C_1) of the North Barunkhurai Zone, 4—terrigenous and Volcanic-terrigenous deposits (D_2–C_1) of Olunbulak Zone, 5—volcano-terrigenous deposits (D_{1-3}fm) of the Ulanus Zone, 6—basaltoids (D_{1-2}) of the South Barunkhurai Zone.

Figure 31 Geological section of the Barunkhurai Depression.

complicated by N–S and transverse fractures with most of them having a considerable fault component, with elements of wrench faulting. The intensity of deformation increases from north to south. Relatively simple brachyform dislocations dominate in the north, while in the south it is mainly holomorphic folding, with widely developed compressed folds whose hinges rise towards the south-east. As a result, the overall structure opens north-westwards towards the Xinjiang.

It should be noted that no basement rocks are exposed in East Dzungaria, and the age range of the deposits is fairly small: from middle Devonian to early Carboniferous. The

age of the sequences increases to the south. This suggests a regional *décollement* at the base of the Middle Palaeozoic sequences. The *décolle-ment* plunges southward and passes into deepeer structural levels, deforming more and more ancient rock complexes. Outside Mongolia, in Xinjiang, ophiolites (within the Dzakheba-Almantai ophiolitic belt) were entrained into the overthrusting. During its displacement, the detached mass was broken into a series of 'facies' sheets, differentially thrusting one over another. The most southerly and northerly complexes originated in the upper and the lower sheets, respectively. An increase in the intensity of the structure southwards suggests an underthrusting mechanism for its formation. The apparent maximum amplitude of overthrusting of individual sheets reaches 70–80 km (without taking into account secondary folding). The overall size reduction of the structure is estimated as at least 250 km.

In East Dzungaria there are five tectonic zones (from north to south): the Bidzi, North Barunkhurai, Olonbulak, Ulanus, and South Barunkhurai zones.

The Bidzi Zone

This zone, within the Shut-Ula Mountains, is located south of the Mongolian Altai, with which it is contiguous along the Bulgan Fault. Structurally, the zone consists of narrow (0.5–2 km)fault wedges (see Fig. 30). The maximum apparent thickness of the section is about 1 km. Basalt pillow lavas (200–300 m) are exposed at its base. Above this is a horizon (120–150 m) of basaltic tuff and epiclastic rocks, including dolerite sills; the horizon is overlain by a sequence (500–600 m) of variegated siliceous tuffite, siliceous shale, sandstone, and siltstone.

The effusive part of the section consists of mesocratic basalt (f_1 18.5–20.5), of average Al content (*al* ^{1}0.9–l.0), with a stable FeO_x/MgO ratio (1.22–1.54). The rocks being studied differ from typical MORB in their higher TiO_2 (1.3–1.7) and lower MgO and P_2O_5. As a whole this is a poorly differentiated tholeiitic series, showing a low content of rare and trace elements (Table 4). The Bidzi basalts may have been formed in an oceanic trough. However local depletion in rare elements indicates that they could be the basement rocks of ensimatic arcs as well. The constant FeOx/MgO value indicates a calc-alkaline trend in the more acid differentiates.

The North Barunkhurai (Barangin) Zone

This Zone is made up of volcanics, varying in facies from basalts to rhyodacites, with all of them showing high alkalinity. Lavas, various tuffs, and epiclastics are common, and hypabyssal bodies are prominent. Sills of augite-, diopside-augite- and

Table 4 Average chemical composition of the major volcanic rock types of the Barunkhurai region.

Component	1	2	3	4	5	6	7	8	9	10	11
SiO_2	47.80	47.40	53.20	56.40	48.70	60.80	55.60	49.60	59.97	45.72	47.20
TiO_2	1.26	0.93	0.78	0.70	1.08	0.94	1.00	1.06	0.97	1.50	1.95

Al_2O_3	16.00	16.95	17.75	17.75	17.00	13.75	16.90	19.00	16.83	16.14	14.75
Fe_2O_3	2.19	6.29	2.81	1.89	4.02	1.84	2.82	5.07	6.56	3.98	2.13
FeO	8.47	4.55	5.82	4.64	7.36	5.59	4.48	5.25	0.64	7.62	9.13
MnO	0.18	0.21	0.19	0.15	0.22	0.19	0.12	0.22	0.17	0.13	0.20
MgO	7.48	6.35	4.65	2.75	4.56	1.20	4.80	4.15	0.51	8.25	5.15
CaO	10.57	7.98	3.99	3.45	8.93	3.85	4.65	9.83	8.79	10.33	9.03
Na_2O	2.72	2.75	3.58	3.96	3.15	5.16	4.78	2.52	4.18	2.46	4.66
K_2O	0.18	2.62	4.36	5.10	1.23	1.50	0.74	0.30	0.29	0.14	0.24
P_2O_5	0.06	0.38	0.40	0.37	0.47	0.35	0.34	0.21	0.20	0.23	0.31
H_2O^+	1.66	2.54	2.58	1.54	2.26	2.66	2.66	1.98	0.41	3.18	3.38
CO_2	1.30	0.91	—	—	—	2.17	1.11	—	—	—	1.22
Cr	104	29	60	82	17	80	58	53	55	145	95
Ni	24	13	22	38	11	9	16	25	15	50	27
Co	16	12	24	38	9	10	18	23	12	37	35
V	70	58	80	84	66	34	66	60	40	75	70
Sc	15	14	10	14	10	10	14	17	11	15	15
Cu	25	27	90	118	34	30	41	340	30	53	40
Zr	52	30	45	84	8	80	70	28	82	70	80
Y	17	10	20	18	11	23	19	20	32	25	25
Ag	—	1.5	0.8	1	1	1.5	—	—	—	—	—
Be	—	1	1.2	0.8	0.5	1	—	—	—	—	—
Ba	—	65	113	50	56	150	—	20	—	25	—
Ga	—	<1	1.4	1	1	1.2	—	—	—	—	—
Mo	—	10	12	5	10	10	—	—	—	—	—
Nb	—	—	8	<5	10	10	17	—	—	<10	—
n	14	12	4	7	12	11	14	8	6	9	6

Note: 1 basalts of the Bidzi Complex; 2–6 Barangin Complex: 2—high-K trachydolerite, 3—shoshonite, 4—latite, 5—subalkaline dolerite and trachydolerite, 6—trachyandesite; 7—andesitebasalt of the Ulanus Complex; 8–11—Baitak Complex: 8—basalts of the lower sheet, 10—basalts of the upper sheet, 11—differentiated basalts of the upper sheet; *n*—number of analyses.

aegirine-augite porphyries are particularly abundant. All of the above-mentioned rock types show complex spatial relationships. Lavas occur at all levels of the section, although they decrease in volume towards the south age of the exposed section is Devonian to early Carboniferous. In the Sukhaityn-Ovgor-Nuru Mountains (see Fig. 30), a limestone band, enclosed in porphyries, has yielded the remains of the brachiopods *Leptaena* sp. indet., *Xystostrophia umbraculum* (Schl.), *Plicostropheodata* sp. indet., and *Euryspirifer* sp. (D_2).

In the Argalantain Mountains, limestone bands, enclosed in tuff, yielded the remains of the brachiopods *Schizophoria* sp., *Orthotetes* sp. indet, *Rhipidomella* sp., *Syringotheris* sp., *Unispirifer* sp., *Spirifer bukhtarmensis* Gretch., S. *subfrandis* Rot., and *Torynifer* sp. indent. (C_1)

The section changes in composition southwards: lava-tuff sequences are replaced by essentially epiclastic rocks. For instance, the sequences in the Khaistyn-Ula Mountains is dominated by mixed epiclastics (reworked basic, intermediate and acid volcanics) up to 2

km in apparent thickness. In the Khairkhan-Ula Mountains (Fig. 30), Devonian epiclastics and polymictic clastics (containing abundant granitoid pebbles) are overlain by terrigenous-carbonate deposits (containing Viséan brachiopods) up to 700 m in thickness. Father south (in the Gurvan-Khairkhan Mountains), the volcanics and epiclastics contain interbeds and units of greywacke with lenses of brachiopod coquina. The brachio-pods give a Tournaisian to early Viséan age. In places the greywackes form a homogeneous rhythmically bedded sequences (up to 1,200 m), containing individual units of siliceous tuffite and limestone.

Thus a facies series, corresponding with a volcanic dome, including its slope and base can be reconstructed in the northern Barunkhurai Zone. Two rock associations can be recognized in the volcanics of the zone. The southern (Argalantain-Ula and Seriin-Nuru mountains) trachyandesite association consists of trachyandesite, quartz latite, trachydacite, and trachyrhyodacite. They form thick horizons of volcanic-bomb tuff from volcanic necks; lava flows are less common. Sills and sills-flows of pyroxene-trachydolerite porphyrites are widely developed. The rocks have a high iron content (FeO_x 10–12.5%; FeO_x/MgO=2–2.5). They are mesocratic ($f_1$17–18) basalts, characterized by a high Al content ($Al^1$1–1.2) and a moderate titanium content (TiO_2 1–1.4%). They show low Cr, Ni, and Co, and high Ag, Be, Ga, Mo, and Ba (see Table 4). Sills were formed following crystallization differentiation and the eruption of more acid varieties. This resulted in the homogeneous composition of the sills and the porphyritic texture, with phenocrysts accounting for 40% of the total rock.

The total alkalinity is 6.6–7.2 (trachyandesites) and 8.1–8.7 (quartz latites). They are poorer in incompatible elements, but are rich in Zr, Y, Nb, Ag, Be, Ga, and Mo. Trachytes, dacites, and trachyrhyodacites are present only as tuffs whereas trachyandesites-basalts form single flows.

The northern shoshonite-latite association (Barangiin-Nuru Ridge)is also represented by sills and volcanics. Sills are composed of pyroxene-porphyrite (SiO_2 48–53.8; Na_2O+K_2O=4.1–7.2%, Na_2O/K_2O=0.7–1.1, $f_1$17–20, $AL^1$0.9–1.1). Enrichment in light and mobile elements is also observed there (Ag 1.5, Ga and Be up to 1 g/t). Shoshonite for the most part occurs in coarse lithic tuffs.

The petro- and geochemical features of the rocks of both associations suggest that they were formed in regions that possessed a continental crust. Processes of crustal assimilation generated a wide range of rocks. The volcanics in question are characterized by the presence of xenoliths of granite and granosyenite.

The Olonbulak Zone

This Zone is characterized by the presence of carbonaceous rocks. As regards its forms it is a mixed sequence up to 2 km thick. Acid epiclastics, rhyolitic tuff, and numerous subvolcanic bodies of rhyolite and dacite occur at the base of the exposed section. In places there are red beds, and locally grey beds containing lenses of coal. The middle section is made up of ash tuff, lithic acid tuff, and tuffite, while the upper section consists of calcareous sandstone, and rarer limestone. The lower, middle, and upper sections yield Famennian, Tournaisian, and Viséan brachiopods, respectively. There is an abundant assemblage of lepidophytes.

As a whole the section is comparable with that of the southern part of the northern Barunkhurai Zone; however, their relationship is still uncertain. It is tentatively assumed that the Olonbulak deposits accumulated under coastal conditions in the area of the North Barunkhurai dome.

The Ulanus Zone

This Zone is located the Barunkhurai Depression (the following mountains are situated around and within its area: Sertengiin-Ula, Khuran-Bogdo-Nuru, Bandzain-Khuren, Indrengiin-Nuru, Maikhan-Khara, and others). Two rock suites are recognized there: the lower volcanic and the upper flysch suites (Luvsandanzan, 1970).

The lower suite (up to 1.5 km) is a combination of acid and mixed volcanics, rhyolitic tuff, tephroids and tuffites, containing rare, thin layers of limestone. Flows of basaltoids, and interbeds of their tuffs, are present, with their amounts rapidly increasing to the south. The Ulanus volcanics make up a differentiated series, from basalt to rhyolite. Andesite-basalt, andesite and rhyolite are the most common rocks; basalt and dacite are subordinate. They are minly calcalkaline rocks. The age of the sequence is Eifelian to Frasnian. For example, in the Mergen-Khutuliin-Nuru Mountains (Mt Khuren-Dush), the limestone yielded the conodont remains *Polygnathus costatus patulus* Klap., *P. costatus partilis* Klap., *Pelekysgnathus* sp., and *Icriodus ex gr. corniger* Witt (D_2e_1). On the Bandzain-Khuren Ridge (at a height of 1,722.0 m), the limestone yielded the fossil tabulate corals *Thamnopora nicholsoni* (Frech.) and *Cladopora kokscharskaje* Dub (D_2). On the southern side of the Indrengiin-Nuru Mountains, the calcareous sandstone contains the remains of the tabulate corals *Thamnopora cervicornis* (Blainv.), and *Emmosia taltiensis* Janer (D_2). In the same area, about 200 m higher up the section, the calcareous tuffite yielded the remains of the brachiopods *Stropheodonta* cf. *interstrialis* (Phill.), *S. asella* Vern., *Cariniferella tioga* (Hall), *Productella jubaculeata* (Murch.), *Atrypa* sp., and *Cyrtospirifer shelonicus* Nal. (D_3f).

The terrigenous-volcanic suite is overlain by a horizon (50–200 m thick) of siliceous tuffite and ash tuff, which yielded the conodonts *Polygnathus communis communis* Br. *et* Mehl., *Bispathodus stabilis* (Br. et Mehl.), and *Pelecysgnathus* sp. (D_3fm).

The above-described horizon is a marker for the southern zones of East Dzungaria. It passes up section into a thick (up 1.2 km) flysch suite. Its lower part contains thin layers of limestone and tuffite, which yielded Lower Carboniferous conodonts in the area of the Ulan-Us Well.

In addition, in some places (Khukh-Deliin-Nuru, Khundryn-Nuru and other mountains), the remains of Lower Carboniferous brachiopods were collected from the lower part of the flysch section. The flysch suite is a monotonous sequence of rhythmically bedded rocks. The lower section (400–500 m) is dominated by sandy flysch. Polymictic sandstone (various reworked volcanics, limestone and granitoids) contains lenses (up to 100 m) of crinoid-brachiopod calcarenite. The upper section is composed of fairly homogeneous sandy-clayey flysch, which is also very typical of all of the southern zones of East Dzungaria.

The South Barunkhurai (Baitak) Zone

This includes the Baitak and Ikh-Khavtag ridges which extend into China and is also made up of volcanic and terrigenous deposits. The section also consists of two suites there. The lower (Devonian) suite is chiefly represented by volcanics which make up two tectonic sheets. The lower sheet is made up of aphyric basalts pyroxene-porphyrites, plagioporphyry, their tuffs, and epiclastics, up to 1 km thick. The basalts (see Table 4) are leucocratic rocks ($f_1$12–16); they differ from oceanic tholeiites in their low TiO_2, high Fe_2O_3, and their high Al content ($aL^1$1.2–1.9). The andesites ($SiO_2$60–62%) are related to the underlying basalts by a single differentiation trend; they form a tholeiitic andesite-basalt association, which may have been formed within an ensimatic island arc.

The volcanics of the upper sheet are represented by basalts. They are massive flows: pillow lavas up to 400 m in apparent thickness. The basalts are aphyric or porphyritic rocks containing phenocrysts of augite or titanaugite, with less common olivine and anorthite-bytownite. They are normally alkaline, low-K rocks (K_2O 0.15–0.28), with low TiO_2 and P_2O_5, and are melanocratic ($f_1$19–23), and normally aluminiferous ($aL^1$0.7–0.9) rocks. They belong to the tholeiitic series, as shown by their K_2O/TiO_2 ratios (0.1–0.2) and FeO_x/MgO (1.1–1.35). Like MORB, they are poor in incompatible trace elements (Sr 10 and Ba 10–30 g/t) and heavy elements (Zr 60–100, Nb 10 g/t) and rich in Cr (120–200 g/t), Y (20–30 g/t).

The pillow lavas of the upper section are the products of differentiation of oceanic tholeiites. They are noted for their decreased MgO; they show higher Ti, K, and P, lower Cr (80–100 g/t), and Ni (20–30 g/t), and constant values of Zr and Y. They probably mark the initiation of emplacement of the ensimatic island arc.

The Lower Carboniferous deposits of both sheets are represented by flysch which is similar to that in the Ulanus Zone.

Heterogeneous Devonian to Lower Carboniferous complexes occur in the Barunkhurai area of Mongolia (Fig. 32). The Bidzi Complex corresponds with the Variscan palaeo-oceanic basin, probably opening to the north-west towards the Ob-Zaisan Zone.

The more southerly North Barunkhurai Zone is made up of subalkaline volcanics, differentiated from basalts to rhyolites. As a whole this is an orogenic complex, split up along the strike and composed of shoshonite-latite, trachyandesite, and rhyolite associations. The above-mentioned volcanics make up a series of central-type uplifts, some of which have survived (e.g. in the Argalantain-Ula

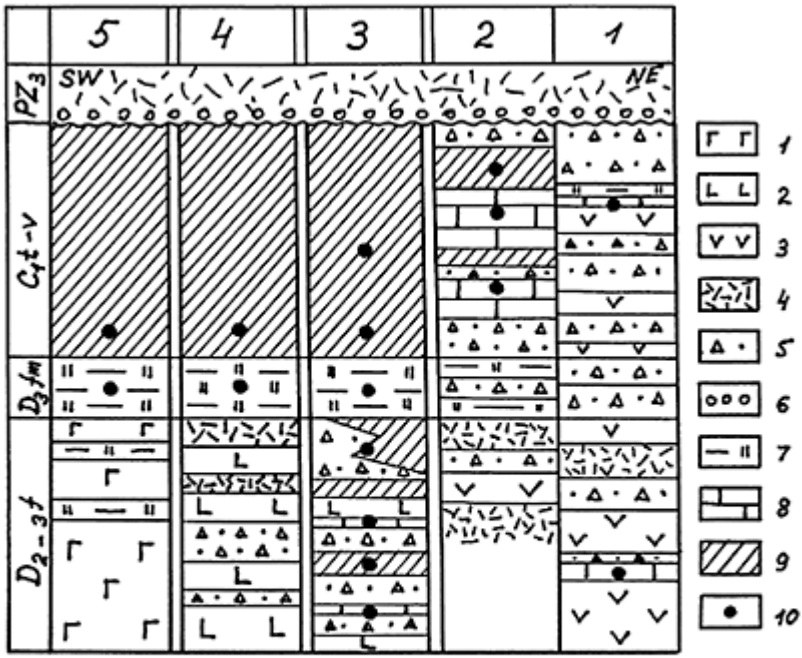

Key: 1—tholeiitic basalt, basaltic andesite, and andesite; 3—shoshonite, trachyandesite, latite, trachydacite, and trachyrhyolite; 4—dacite and rhyolite; 5—tuff and epiclastics; 6—basal conglomerate, 7—tuffite and siliceous tuff; 8—limestone, 9—flysch, 10—fossil sampling sites; Figures on the sections: zone—1—North Bamunkhurai, 2—Olonbulak, 3—Ulanus; 4 and 5—South Barunkhurai Zone (4—lower and 5—upper tectonic sheet or slice).

Figure 32 Correlation of the sections of East Dzungaria.

Mountains). Shallow-water epiclastics, varying from coarse in the north to sandysilty rocks in the south, accumulated on the southern side of the volcanic ridge; they mark the slope and the foot of the dome.

Along with the N–S petrochemical zoning, transverse (NW) zoning is also present to the south, high-K subalkaline volcanics give way to calcalkaline rocks. The above-mentioned fact allows us to consider the North Barunkhurai Zone as a Middle Palaeozoic volcanic belt, formed on pre-Eifelian (probably Caledonian) sialic basement. From the data of Deruelle (1982), it is possible that the shoshonite-latite association was farthest from the edge of the continent and that the rhyolite association was developed along its outer border. In other words, the North Barunkhurai Zone can be regarded as an Andean-type continental margin with a subduction zone with a southern (in present-day co-ordinates) polarity.

The deposits of the Olonbulak Zone are unique. They represent a carbonaceous molasse, formed in coastal conditions. In some of their features they resemble the deposits of the volcanic belt (i.e. an abundance of rhyolites and dacites, epiclastics, and

Lower Carboniferous brachiopod limestones); these allow us to consider the zone as being part of a volcanic belt.

South of the North Barunkhurai volcanic belt, a basin (the Ulanus Zone), infilled with thick volcanic-terrigenous deposits, is located. The deposits were chiefly represented by epiclastics and tuffs in Devonian times and greywacke flysch in Lower Carboniferous times. In the axial part of the section, the flysch units appear at the Devonian level. In the Devonian section, the clastic deposits show a zonal differentiated composition (basic and acid epiclastics), grain size and stratification. The provenance of the deposits can be determined with some certainty. An overall deepening of the basin was accompanied by the mixing and reworking of clastic material; this suggests that the source areas were remote from the sedimentary basin. The occurrence of massive volumes of the products of granite erosion, making the composition of sediments more polymictic, is also significant.

In the southern part of the Ulanus Zone, volcanics (basalts, andesites, rhyolites, their tuffs) and coarse clastics which mark the southern side of the trough and its transition to an island-arc dome, again increased in importance in Devonian times.

The South Barunkhurai Zone was represented by a sequence of differentiated tholeiites (basalts, andesites, and their tuffs) in Devonian times. In their chemistry and structure, the deposits are here regarded as rocks from fore-arc zone of the Baitak island arc. A change in the character of the volcanicism (the replacement of calc-alkaline volcanics by tholeiites to the south) suggests that subduction zone had a southern polarity. The basalts of the upper sheets, whose characteristics are typical of MORB, belong to a pre-arc trough. This palaeotectonic interpretation of the South Barunkhurai Zone is supported by its close spatial relationship with the Dzakheba-Almantai ophiolitic suture, extending into China, near to the southern part of the area being studied. It cannot be ruled out that the above-mentioned suture formed a root for the rocks of the upper sheet of the zone.

The above-mentioned data indicate the following palaeotectonic model of the Mongolian part of East Dzungaria. There the Devonian saw the formation of a complex accretionary system, including, from south to north (in present-day co-ordinates):

1) a pre-arc palaeo-oceanic trough (the upper sheet of the South Barunkhurai Zone);
2) the fore-arc zone of the Baityk ensimatic island arc (lower sheet);
3) the back-arc zone (southern part of the Ulanus Zone);
4) the Ulanus back-arc basin;
5) the North Barunkhurai volcanic belt (an Andean-type continental margin), formed on the eastern continuation of the Caledonian Chenghis-Tarbagataya continent; and
6) the Bidzi palaeo-oceanic basin, probably representing the eastern continuation of the Ob-Zaisan Variscan palaeo-ocean.

The Baitak Arc died out in early Carboniferous times. An extensive single basin, infilled with greywacke flysch, was formed. The position of the southern boundary basin is uncertain because of inadequate information on the geology of adjacent areas of China. The North Barunkhurai volcanic belt continued to develop. The main accretionary processes at that time were concentrated along this belt.

All of the above-mentioned structures probably died out in middle Carboniferous times, due to a collision between the Caledonian continent and the Baitak island arc. The obduction of palaeo-oceanic elements on to the continent, with firstly the deposits of the

back-arc basin and then those of the island arc and the pre-arc trough being overthrust on the continental margin, is well established. The neo-autochthonous orogenic complex there is late Palaeozoic in age.

4
MIDDLE PALAEOZOIC CONTINENTAL MARGIN MAGMATISM OF MONGOLIA

V.V.Yarmolyuk and V.I.Kovalenko

In the middle Palaeozoic, tectonic and igneous activity was widespread and occurred concurrently with the formation of marine basins of the South Mongolian Variscides, along the margin of the bordering North Asiatic Siberian continent. This resulted in the formation of a volcanoplutonic belt up to 300 km wide which stretched for more than 2,000 km (Gordienko, 1987; Yarmolyuk and Kovalenko, 1991). Relics of this belt have been found in the Altai-Sayan fold zone of Russia, in West and North Mongolia, and in the Russian part of Western Transbaikalia. The belt's structure is determined mainly by the composition of its igneous rocks and shows transverse zoning caused by an increase in the alkalinity of the igneous rocks away from the margin of the palaeo-continent.

The central segment of the belt occurs within Mongolia. It is contiguous there with the Irtysh-Zaisan part of the Variscides, with the South Mongolian Hercynides and with the Khangai-Khentei Middle Palaeozoic marine basin (Fig. 33). There is an extensive literature on Devonian continental magmatism (Marinov, 1973; Luchitsky, 1975; Dergunov *et al.*, 1980; Kovalenko and Yarmolyuk, 1990, to mention but a few). The Map of Geological Formations of Mongolia (Yanshin, 1989) provides information on the pattern of distribution of igneous rocks of this age and Figure 33 summarizes these data. The figure shows that Devonian igneous rocks are very common in north-western Mongolia. The above-mentioned zoning found in the distribution of rocks of different composition has enabled us to recognize the following zones in this part of the belt:

1) calcalkaline,
2) subalkaline and
3) subalkaline and alkaline (Gordienko, 1987; Yarmolyuk and Kovalenko, 1991).

4.1 Calcalkaline Zone

This zone occupies the frontal part of the belt, facing the Middle Palaeozoic marine basins. It is characterized by the presence of granitoid masses and fragments of volcanic terrains whose composition is still poorly known.

The igneous zones are most common in the western Mongolian Altai within the Altai Zone and the Delyun-Yustyd Trough, where they are represented by numerous massifs.

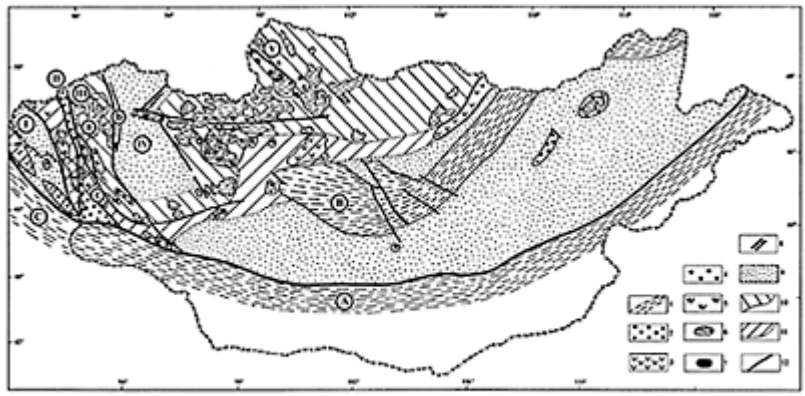

Key: I—Middle Palaeozoic marine basins (A—South Mongolian, B—Khangai-Khentei, C—Irtysh–Zaisan); 2—intracontinental troughs; 3–8—igneous associations: 3 and 4—calcalkaline (3—volcanic, 4—plutonic); 5 and 6—subalkaline (5—volcanic, 6—plutonic); 7—alkali rock masses; 8—bimodal volcanic associations with alkali rocks; 9—non-magmatic areas; 10 and 11—zones of igneous rocks: 10—mainly subalkaline, 11—mainly calcalkaline; 12—faults; I–V—structural zones: I—Altai, II—Delyun-Yustyd, III—Kharkhirin, IV—Lake, V—Prikhubsugul; a–c—geological features: a—Kharkhirin Massif, b—Mort-Ula volcanic field, c—Bulgan Massif.

Figure 33 Location of middle Palaeozoic continental igneous formations in Mongolia.

According to data obtained by A.B.Dergunov, V.Luvsandanzan, and V.S. Pavlenko (1980), these massifs are concordant plutons related mainly to the axial parts of anticlinorial structures. They extend north-westwards, conformable with the trend of the fold structures enclosing Cambrian-Ordovician and Silurian-Devonian sandstones and shales. Their contacts with the enclosing rocks are mainly sharp, showing hornfels zones from several hundreds of metres up to 1.2–2 km wide. Massifs showing diffuse contacts with the enclosing metamorphosed rocks—gneisses and various schists biotite, garnet-biotite, two-mica, less-common amphibole-biotite, plagioclase-and two-feldspar schists (Markova and Fedorova, 1971) are less common, particularly in zones of progressive metamorphism. The massifs range in size from large ones (1,000–5,000 km^2) related to anticlinorial structures to fairly small (a few hundreds of square metres) exposed in the superimposed structures of the Delyin-Yustyd Trough.

Only one example was reported where these granites are overlain by Middle Carboniferous strata. Therefore, based on their similarity in composition and the absence of reliable geological data concerning the upper age limit of the granite, they were all grouped into the Devonian Altai Complex (Marinov, 1973). The K– Ar age of the rocks is 440 to 330 Ma, with the dates most commonly falling into the range, 370–350 Ma (Luchitsky, 1975).

The massifs of the Altai Complex (Dergunov *et al.*, 1980) are composed of fairly homogeneous large porphyry plagiogranites, granodiorites, and granites. Leucocratic two-mica and muscovite tourmaline-bearing granites and granitepegmatites are also present. They form the apical parts of the massifs, and their endocontacts and apophyses, as well as small bodies. A vein series is represented by microgranites, aplites, pegmatites, quartz veins and local occurrences of granite-porphyries. Some massifs contain gabbro-dolerite and lamprophyre dykes. The East Bulgan massif, located in the mountainous part of the Mongolian Altai provides a typical example of the Altai Complex (Luchitsky,

1975). In plan the massif is oval and elongated in a north-westerly direction. Its area is over 3,000 km^2. The contacts with the enclosing Cambrian and Ordovician rocks are uneven and sinuous. The contact surface usually dips under the enclosing rocks. In the exocontact aureole, which is several tens of metres to 1.5–2 km wide, the enclosing rocks are metamorphosed to biotite hornfels, locally accompanied by banded diorite-like rocks showing an irregular taxitic texture.

The massif consists mostly of grey, pale-grey medium-grained and coarsegrained porphyry-like granites and granodiorites, with phenocrysts of pale-grey oligoclase, perthitic microcline, and pink poikilitic orthoclase. The rock has a coarse-and fine-grained groundmass of grey and blue quartz, microcline and plagioclase with subordinate biotite and locally tourmaline. The granites are characterized by the presence of melanocratic diorite and quartz-diorite enclaves. In the endocontact zone, in the vicinity of the roof pendants, the granites become medium- or fine-grained subporphyritic or even aphyric in texture.

The vein rocks of the massif are represented by fine-grained, leucocratic granites, aplites, pegmatites, and lamprophyres. Aplites and pegmatites occur occasionally both in the massif and at exocontacts.

Table 5 Compositions of granitoids of the Altai Complex (Mongolian Altai).

n/n	**1**	**2**	**3**	**4**	**5**	**6**	**7**	**8**	**9**	**10**	**11**	**12**	**13**	**14**	**15**
SiO_2	66.33	73.34	74.32	76.05	67.55	67.30	75.96	73.59	73.76	75.47	72.58	72.62	71.19	67.84	74.69
TiO_2	0.37	0.10	0.26	0.11	0.41	0.31	0.11	0.22	0.19	0.06	0.12	0.35	0.44	0.73	0.12
Al_2O_3	15.02	14.70	12.90	12.70	15.90	15.30	12.60	13.68	13.59	13.43	15.03	13.40	14.39	15.26	13.85
Fe_2O_3	1.61	0.10	0.60	0.40	2.11	1.71	0.11	2.23	2.42	1.24	1.50	3.38	3.27	4.77	1.49
FeO	1.88	0.90	0.90	0.63	1.97	1.25	1.16	1.37	1.80	0.86	0.79	2.51	2.44	3.30	1.04
MnO	0.06	0.03	0.05	0.07	0.07	0.09	0.04	0.07	0.07	0.08	0.03	0.05	0.05	0.07	0.06
MgO	1.70	0.30	0.40	0.30	1.40	1.10	0.20	0.51	0.45	0.09	0.29	0.52	0.91	1.59	0.21
CaO	3.05	1.80	1.30	1.10	3.90	3.80	1.05	0.91	1.05	0.44	0.77	1.35	1.64	2.26	0.61
Na_2O	4.05	4.71	3.87	3.87	4.05	4.05	3.79	3.20	3.25	3.75	3.65	3.13	2.86	2.81	3.76
K_2O	3.48	2.95	4.64	3.51	1.16	3.46	4.34	4.56	4.35	4.50	4.87	4.57	4.29	3.48	4.40
P_2O_5	0.22	0.13	0.17	0.22	0.24	0.22	0.15	0.17	0.17	0.20	0.33	0.12	0.17	0.17	0.15
F	0.13	0.07	0.06	0.03	0.04	0.04	0.03	0.07	0.08	0.01	0.08	0.1	0.15	0.12	0.1
Total	97.77	99.06	99.41	98.96	98.76	98.59	99.51	100.51	101.10	100.12	99.96	102.00	101.65	102.28	100.38
Cr	26	3	5	5	11	8	4	14	9	2	4	10	21	40	2
Ni	n.d.	n.d.	n.d.	n.d.	n.d.	n.d.	n.d.	14	24	3	10	16	19	27	5
Co	11	2	2	2	9	6	2	6	4	1	2	3	8	10	1
Sc	9	2.2	3.8	2.8	7	6.6	5.4	5.9	5	2.8	2.6	7.4	8.5	13.8	4
V	n.d.	n.d.	n.d.	n.d.	n.d.	n.d.	n.d.	48	40	8	11	33	72	160	7
Cu	n.d.	n.d.	n.d.	n.d.	n.d.	n.d.	n.d.	14	16	15	10	17	18	21	15
Pb	n.d.	n.d.	n.d.	n.d.	n.d.	n.d.	n.d.	22	21	19	26	17	22	18	29
Zn	n.d.	n.d.	n.d.	n.d.	n.d.	n.d.	n.d.	37	26	10	25	33	46	53	34
Sn	n.d.	n.d.	n.d.	n.d.	n.d.	n.d.	n.d.	13	17	12	9.2	6.7	7.2	6.7	11
W	n.d.	n.d.	n.d.	n.d.	n.d.	n.d.	n.d.	2.73	6		1.83	4.5	3	9.6	10.5
Mo	n.d.	n.d.	n.d.	n.d.	n.d.	n.d.	n.d.	0.3	0.75	0.3	0.38	1.2	0.39	0.59	0.3

Rb	62	17	73	75	26	40	118	n.d.	218	302	294	186	170	144	480
Cs	1.1	0.2	2.1	2	1.2	3.3	5.4	22	23	15	33	10	11	8	22
Ba	614	1474	856	705	328	473	849	160	160	45	190	580	740	1300	100
Sr	279	324	119	140	363	290	116	60	77	13	60	90	160	210	36
Ta	0.3	0.09	1.1	0.7	0.5	0.5	1.3	1.3	1.5	2.5	2.5	0.9	1	1	6
Nb	3	2	14	6	7	7	12	8	6	2	13	7	n.d.	13	9
Hf	4.2	2.1	6.8	3.3	3.8	3.4	3.7	4	3	1.5	2.5	6	5	8	2
Zr	124	73	167	77	115	102	98	145	95	55	45	180	n.d.	315	50
Y	20	15	29	24	17	18	43	27	26	17	22	49	43	53	67
Th	9.5	0.8	10.8	8.5	2.7	4.2	13	7	6.8	2.3	6	12	11	18.9	6.5
U	1.7	0.3	2.5	2.6	0.8	1	1.5	1.8	2.3	1.6	3.1	2.4	1.6	3.7	5.2
La	19.8	6.2	44.1	23.2	11.8	15	30.2	14.5	11.5	2.1	10.9	30.6	28.2	46.9	10.2
Ce	35	12.2	73.5	38	24.2	29.2	56.8	29.6	23.6	4.9	22.7	62.3	57.3	93	18.3
Nd	16.9	6.7	33.2	16.9	13.8	15.8	29.3	16.8	13.5	3.3	13.2	35.2	32.2	51	9
Sm	3.9	1.7	7.2	3.6	3.6	4	7.12	4.4	3.54	1	3.5	9.2	8.4	13	2.1
Eu	0.8	0.41	1.07	0.53	0.93	0.95	0.94	0.52	0.49	0.03	0.48	1.01	1.08	1.76	0.24
Gd	3.54	1.72	6.01	2.53	3.4	2.87	7.29	4.2	3.5	0.84	3.6	8.6	7.6	10.8	1.6
Tb	0.59	0.29	1.05	0.46	0.57	0.47	1.25	0.71	0.59	0.17	0.49	1.48	1.3	1.79	0.31
Yb	1.72	0.84	3.6	1.81	1.61	1.22	4.08	2.31	1.81	0.94	0.59	4.82	4.13	5.26	1.54
Lu	0.25	0.12	0.53	0.27	0.23	0.17	0.59	0.34	0.26	0.15	0.07	0.7	0.6	0.75	0.24
B	n.d.	n.d.	n.d.	n.d.	n.d.	n.d.	n.d.	22	75	16	110	18	34	17	20
Be	n.d.	n.d.	n.d.	n.d.	n.d.	n.d.	n.d.	2	3.5	1.8	12.5	3.1	1.1	4.15	25

n.d.—not determined.

Table 5 shows the chemical composition of the granitoid rocks of the Altai Complex. Their compositions correlate with the calcalkaline series (Na_2O+K_2O <8%) when the $K_2O>Na_2O$ ratio is normal. Their content of SiO_2 is 66 to 76%, i.e. it corresponds with the granodiorite-biotite leucogranite compositional range.

4.2 The Subalkaline Rock Zone

This zone of calcalkaline rocks is bordered by a terrain (or zone) dominated by subalkaline rock series on the intracontinental side of the marginal belt. This zone is made up of numerous massifs and fragments of strongly deformed volcanic terrains scattered along the eastern part of a ridge system of Mongolian Altai (the Kharkhirin Zone) and within North Mongolia.

The plutonic massifs show different structures in different parts of the zone. Therefore, they have been assigned to the granite-leucogranite association (Luchitsky, 1975; Dergunov *et al.*, 1980; Dergunov and Kovalenko, 1995) or grouped into the Kharkhirin (in Mongolian Altai) and into Tess (North Mongolia) complexes (Marinov, 1973). Two major groups:

1) normal granites in microcline-plagioclase granite facies and

2) leucogranitic and alaskite granites in the subalkaline granite, granosyenite and syenite facies can be recognized among the rocks making up the Kharkhirin Complex (Luchitsky, 1975).

The first group amounts to 20% and the second group, to about 75% of the area of the massifs. Small gabbro-diorite, gabbro-dolerite and monzonite bodies are rare in occurrence.

Three groups of rocks, formed during three successive phases of intrusion, can be distinguished within the Tess intrusive complex (Luchitsky, 1975). The first phase is represented by medium- and coarse-grained biotite and mainly microcline leucocratic granites and granosyenites. Quartz syenites and syenites are subordinate. All the rock types of this phase are connected by facies transitions. The rocks of the second phase owe their appearance to biotite granites that were homogeneous in composition. They consist of K–Na feldspar (38–50%), quartz (20–35%), plagioclase (15–25%), and biotite (2–3%). Finally, phase 3 is represented by leucocratic and alaskite granites and aplites, which are more leucocratic and contain higher amounts of quartz than the rocks of phase 2. They form small bodies intruding the rocks of phase 1 and 2, or form separate massifs.

The massifs of the granite-leucogranite association are Devonian (middle Devonian) in age. They usually intrude the associated volcanic formations, including the fossiliferous Eifelian sedimentary-volcanic strata of the Mongolian Altai (Dergunov *et al.,* 1980). However, pebbles from these massifs occur in sand-conglomerate rocks containing Upper Carboniferous-Lower Permian flora, from North Mongolia, within the Bolnai Ridge (Yarmolyuk *et al.*, 1987). There is also one example where granites of the Tess Complex are overlain by sediments containing Middle-Upper Devonian flora (Blagonravov, 1970). The K–Ar age of the rocks from the different massifs varies within a wide range, from 330 to 390 Ma.

The largest and best-known: the Kharkhirin pluton for which the Kharkhirin Complex is named provides a good example of massifs of this type of asociation. It is located within the north-eastern ridges of the Mongolian Altai, its area is over 3,700 km^2 and it extends north-south for 150 km. The massif is irregular in shape, with geniculate structures that repeat the fold structures in the surrounding Cambrian-Ordovician and Ordovician-Silurian rocks. In general, the pluton plunges gently northwards, with steep southern contacts. Based on gravity data, the massif is plate-like in shape and has a thickness of 5–6 km (Luchitsky, 1975). The massif is composed of megaporphyric normal granites and leucogranites and alaskite granites. The former occur in most eroded part of the massif and up to an attitude of 1,700 m. Mountainous areas at altitudes of 1,700–3,500 m consist of leucocratic and alaskite granites.

The normal biotite and amphibole-biotite granites of the lower horizons of the pluton are massive megaporphyric rocks containing tabular segregations of feldspar 2–5 cm in diameter, dominated by microcline. Locally, they contain numerous *schlieren* of biotite-amphibole and plagioclase. At the endocontacts and in small apophyses, the megaporphyric granites grade into medium-grained and fine-grained granite porphyries; in the fine-grained apophyses they show microgranular recrystallization. The megaporphyric granites are intruded by veins of granite-porphyry, microgranite, and aplite as well as pegmatoid granite. The most common veins are flat lying types.

The leucocratic and alaskite granites are represented by coarse- and mediumgrained two-feldspar granites rich in quartz. The content of biotite and amphibole reaches 1–4%. A steeply dipping series of veins cut the top of the massif.

The relationship between the two groups of granites is determined, on the one hand, by the intrusion of the megaporphyric granites by alaskites and, on the other hand, by the

presence of gradual transitions. Therefore, the granites show a range of facies and phase relations, with the alaskite and leucocratic granites having formed somewhat later.

Tables 6 and 6a and Figure 34 show the compositions of rocks of the graniteleucocratic association. In general, they are marked by a high alkalinity (Na2O+ K_2O)>8% and often show a predominance of K_2O.

Within the zone of subalkaline rocks, the volcanic formations are best preserved within the structures of the Mongolian Altai, where they form fragments of strongly deformed volcanic terrains. The volcanics are commonly associated with sedimentary rocks that yield fossils, therefore their age can be fairly reliably determined as early and middle Devonian (Luchitsky, 1983). Volcanic activity occurred during two stages, which can each be correlated with lavas sequences of different composition.

The early stage (early Devonian) was marked by the formation of an association of basic and intermediate volcanic rocks. The association consists of twopyroxene and pyroxene-plagioclase basalts, andesite-basalts, and andesites together with agglomerates and tuffs derived from these lavas.

Table 6 Compositions of granitoids of the Kharkhirin Complex (Mongolian Altai).

n/n	**1**	**2**	**3**	**4**	**5**	**6**	**7**	**8**	**9**	**10**	**11**	**12**	**13**	**14**	**15**	**16**
SiO_2	69.26	76.21	77.09	75.74	76.55	76.08	76.19	76.65	70.49	77.49	76.17	74.32	74.61	74.79	74.70	76.06
TiO_2	0.63	0.05	0.11	0.14	0.05	0.22	0.07	0.08	0.46	0.07	0.12	0.18	0.56	0.18	0.30	0.28
Al_2O_3	13.60	12.30	11.60	12.00	12.40	12.60	11.50	11.60	14.00	11.65	12.48	12.88	12.30	12.40	12.70	11.90
Fe_2O_3	1.13	0.10	0.80	0.60	0.10	1.01	1.09	1.60	0.81	1.59	1.61	2.85	0.52	0.90	1.10	0.70
FeO	2.77	0.90	0.27	0.63	0.90	0.80	2.06	0.36	1.79	0.65	0.93	1.65	1.78	0.99	0.81	1.17
MnO	0.07	0.03	0.03	0.04	0.03	0.04	0.04	0.03	0.05	0.02	0.03	0.03	0.04	0.05	0.05	0.05
MgO	1.05	0.10	0.10	0.20	0.10	0.30	0.10	0.10	0.70	0.05	0.09	0.23	0.20	0.20	0.30	0.20
CaO	2.10	0.60	0.40	0.60	0.50	0.90	0.60	0.50	1.80	0.36	0.55	0.55	0.97	0.93	1.19	0.83
Na_2O	3.68	3.79	3.65	3.51	3.65	2.90	3.00	3.50	3.70	3.79	3.40	3.33	3.62	4.28	3.56	3.46
K_2O	4.45	4.75	4.76	4.79	4.65	4.04	4.69	4.78	4.57	4.41	4.97	4.90	4.27	4.70	4.65	4.80
P_2O_5	0.26	0.11	0.13	0.17	0.11	0.13	0.12	0.10	0.23	0.01	0.03	0.05	0.02	0.03	0.06	0.02
F	0.06	0.06	0.06	0.07	0.09	0.07	0.05	0.1	0.06	0.35	0.04	0.1	0.02	0.33	0.06	0.03
Total	99.00	98.94	98.94	98.42	99.04	99.02	99.46	99.30	98.60	100.09	100.38	100.97	98.89	99.45	99.42	99.47
Cr	20	4	5	9	6	8	7	8	8	7	4	10	5	5	8	5
Ni	n.d.	n.d.	n.d.	n.d.	n.d.	n.d.	n.d.	n.d.	n.d.	5	4	15	11	14	6	7
Co	9	1	1	2	0	2	1	1	5	1	1	2	3	2	3	1
Sc	12.6	1.7	3.1	4.9	3.9	4.3	2.6	2.2	7.9	0.5	4	5.9	4.2	3.4	3.7	2.6
V	n.d.	n.d.	n.d.	n.d.	n.d.	n.d.	n.d.	n.d.	n.d.	2	3	12	9	8	22	4
Cu	n.d.	n.d.	n.d.	n.d.	n.d.	n.d.	n.d.	n.d.	n.d.	10	10	16	16	10	10	13
Pb	n.d.	n.d.	n.d.	n.d.	n.d.	n.d.	n.d.	n.d.	n.d.	110	36	27	49	17	23	44
Zn	n.d.	n.d.	n.d.	n.d.	n.d.	n.d.	n.d.	n.d.	n.d.	130	110	74	110	30	35	59
Sn	n.d.	n.d.	n.d.	n.d.	n.d.	n.d.	n.d.	n.d.	n.d.	14	8.7	11	8.2	5	11	9.8
W	n.d.	n.d.	n.d.	n.d.	n.d.	n.d.	n.d.	n.d.	n.d.	1.23	2.85	2.73	5.1	0.87	3.6	3
Mo	n.d.	n.d.	n.d.	n.d.	n.d.	n.d.	n.d.	n.d.	n.d.	0.76	0.66	1.6	0.96	1.8	0.83	0.68

Rb	102	264	156	264	186	217	161	251	111	366	180	208	142	152	n.d.	244
Cs	10	17	7.4	16	8.2	18	8.7	8.5	7	14	3	8	4	4	n.d.	10
Ba	640	100	181	125	100	234	100	100	884	80	560	360	650	600	320	130
Sr	105	25	33	43	25	58	28	26	127	10	92	85	90	81	110	30
Li	n.d.	n.d.	n.d.	n.d.	n.d.	n.d.	n.d.	0	0	95	14	22	22	32	n.d.	79
Ta	1.1	3.4	1.8	3.2	1.7	2.3	1.4	2	1.1	7	1.5	1.7	1.4	1.7	2.5	2.1
Nb	13	15	19	19	20	17	17	24	9	42	31	n.d.	n.d.	3	5	n.d.
Hf	9.8	5.4	6.2	5.9	4.6	6.6	6.6	4.4	8.2	13	5	6	6	4.6	5	5
Zr	294	95	131	128	100	142	112	67	263	60	40	n.d.	n.d.	70	90	n.d.
Y	49	26	45	46	20	23	32	32	47	166	45	51	42	33	65	43
Th	16	27	22	36	23	31	39	30	17.5	30	18.7	20	18	15.7	24	28
U	2.9	4	4.5	6.3	3.2	2.8	4.8	4.4	2.2	12.5	3.4	5.7	4.3	2.4	4.2	4.2
La	42.7	5.3	49.6	26.8	18.3	46.2	26.6	20.4	43.8	38.9	44.6	38.9	33.3	25	21.9	22
Ce	82.4	16.8	82.2	54.8	42	80.9	58.2	43.2	78.3	73.4	80.9	79.9	63.3	58	47.5	48
Nd	43.9	14.8	39.8	31.1	27	38.6	35.6	25.4	38.3	38	40.1	45.4	33.1	23.5	28.8	24.2
Sm	10.9	5.5	8	8.1	7.8	8.8	9.9	6.9	8.9	9.3	9.4	11.9	8.12	5.3	8	5.9
Eu	1.54	0.1	0.22	0.32	0.09	0.6	1.17	0.15	1.43	0.09	0.49	0.61	0.81	0.5	0.73	0.3
Gd	11.4	8.1	7.1	8.8	8.4	8.53	11.3	8.24	8.2	11.7	7.3	9.9	6.4	4.2	6.3	4.3
Tb	1.9	1.48	1.29	1.66	1.54	1.57	2.05	1.6	1.42	2.37	1.29	1.73	1.15	0.79	1.23	0.86
Yb	5.51	6.04	5.12	7.91	6.64	6.86	8.39	8.51	4.8	14.8	4.71	6.06	4.37	3.59	6.64	5.1
Lu	0.78	0.92	0.77	1.24	1.02	1.05	1.27	1.36	0.7	2.43	0.7	0.9	0.65	0.56	1.06	0.83
B	n.d.	n.d.	n.d.	n.d.	n.d.	n.d.	n.d.	0	0	2.3	2.9	5.2	6	4.3	11	4.1
Be	n.d.	n.d.	n.d.	n.d.	n.d.	n.d.	n.d.	0	0	13.8	2.9	2.55	1.8	2.3	3.7	2.8

n.d.—not determined.

Table 6a Compositions of the rocks of the Tess Complex (North Mongolia).

n/n	**1**	**2**	**3**	**4**	**5**	**6**	**7**	**8**
SiO_2	73.30	73.80	74.50	62.10	61.25	70.50	73.90	63.50
TiO_2	0.18	0.16	0.18	0.83	0.65	0.30	0.75	0.87
Al_2O_3	14.00	12.50	12.80	17.10	16.30	14.20	12.86	16.44
Fe_2O_3	0.00	1.25	0.63	1.98	1.97	1.24	1.14	2.61
FeO	0.59	1.55	0.98	1.97	3.38	1.53	0.74	2.28
MnO	0.02	0.01	0.05	0.10	0.14	0.07	0.09	0.09
MgO	0.01	0.02	0.03	1.10	0.53	0.52	0.33	1.46
CaO	1.17	1.14	1.42	3.42	3.15	2.45	1.43	3.82
Na_2O	5.77	5.77	3.84	5.12	4.52	4.24	4.40	4.67
K_2O	3.51	2.16	4.54	4.79	6.36	4.52	4.25	3.90
P_2O_5	0.01	0.01	0.01	0.32	0.20	0.06	0.05	0.30
H_2O	0.66	0.85	0.57	0.84	1.01	0.53	0.28	0.34
CO_2	0.84	0.40	0.13	0.17	0.14	0.10	0.00	0.00
F	0.08	0.22	0.04	0.07	0.04	0.03	0.05	0.08
Total	100.07	99.62	99.68	99.84	99.60	100.26	100.22	100.29
Cr	10	18	3	6	9	5	4	9
Co	1	2	2	4	3	3	2	12

Sc	0.3	0.5	3.1	15.9	25.9	3	3.8	8.5
Rb	260	134	88	41	49	91	75	75
Cs	1.3	0.8	2.1	2.1	1.3	2.7	0.8	1.6
Ba	560	670	933	5198	2170	1013	748	1453
Sr	71	93	83	261	140	298	118	740
Ta	2.5	1.2	1	0.6	0.5	1.1	1.2	1.5
Nb	31	19	15	10	8	11	19	18
Hf	7.3	11.2	3.8	8.2	30	5.5	6.6	6.4
Zr	195	346	108	220	1061	155	246	258
Y	45	33	26	26	30	23	33	25
Th	12	5.5	13.8	5.5	11	16.3	6.3	4.8
U	1.9	2.2	3.2	1.1	1.5	1.6	2.1	2.2
La	60.9	43.4	41.1	91.3	333.4	37.4	40.3	36.4
Ce	138.2	107.9	60.2	144.7	422.8	55.9	66.8	63.6
Nd	87.9	75.9	23.5	61.8	141	22.3	30	30.3
Sm	25.2	23.6	4.6	12.9	24.2	4.43	6.5	6.9
Eu	0.39	0.99	0.55	5.56	2.25	0.82	0.47	1.57
Gd	32.9	38.8	2.98	6.99	8.6	2.45	4.7	4.2
Tb	6.1	6.8	0.53	1.13	1.42	0.43	0.85	0.67
Yb	27.21	23.78	2.08	2.5	3.89	1.56	3.3	1.58
Lu	4.19	3.51	0.31	0.34	0.55	0.23	0.48	0.22

A lava sequence in the lower part of the section in the volcanic terrain of Mt Mort Ula (Fig. 35) (Yarmolyuk and Vorontsov, 1993) is a typical example of this type of structural association. The association is composed mainly of lavas and is represented by a series of thin (4–8 m) sheet flows of grey and dark-grey subalkaline basalts. As a rule, the flows are separated by bands of scoria and lapilli tuff. A series (150 m) of thick (≤15 m) lava flows composed of pale-grey and greenish-grey trachyandesites with plagioclase and pyroxene has been found in the middle part of the section. The thickness of the sequence is more than 520 m. The age of the rocks making up this association is inferred from the fact that the tuffstone, gravelstone, and carbonate beds yield abundant Lower Devonian fossils (Luchitsky, 1983).

During the later stage there were formed rocks of the rhyolite-dacite association. It is composed of lava, agglomerates and tuffs of dacites, rhyodacites and rhyolites, with subordinate andesites and andesite-dacites. The rocks of this association form separate volcanic terrains, but they occur mainly together with outcrops of earlier-stage rocks. Therefore Mt Mort-Ula (Fig. 35), acid volcanics rest conformably on basic lavas. Large blocky tuff- and lava-breccia trachyrhyodacite and trachydacite beds (70 m thick) occur at the base of the acid rock section (Yarmolyuk and Vorontsov, 1993). These are overlain by a series of lava sheets (130–150 m) of flow-banded trachyrhyodacites interbedded with tuff breccias (up to 5–6 m thick). The upper part of the sequence is made up of thick (<20 m) sheets of brown and greyish-red flow-banded and spheroidal rhyolites, interbedded with tuffs of the same composition. The section is crowned by a unit (40 m) of brown and beetroot red, fused rhyolite tuffs. The total thickness of the sequence reaches 670 m.

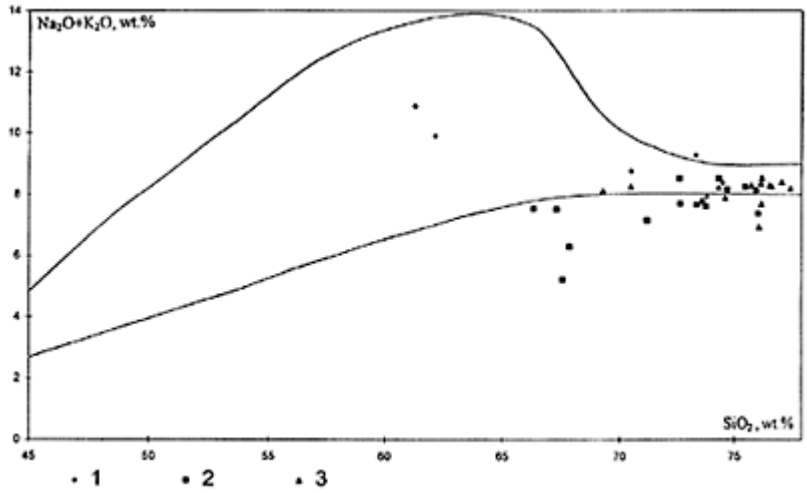

Key: 1–3—assemblages (complexes): 1—Altai, 2—Kharkhirin, 3—Tess.

Figure 34 Compositions of the Devonian granitoids of different assemblages shown on the SiO_2–(Na_2O+K_2O) classification diagram.

It is significant that the acid lava is characterized by massive flow-banded and spherulitic texture. As a rule, lava is aphyric, with a felsitic matrix containing rare quartz, feldspar, and locally biotite phenocrysts.

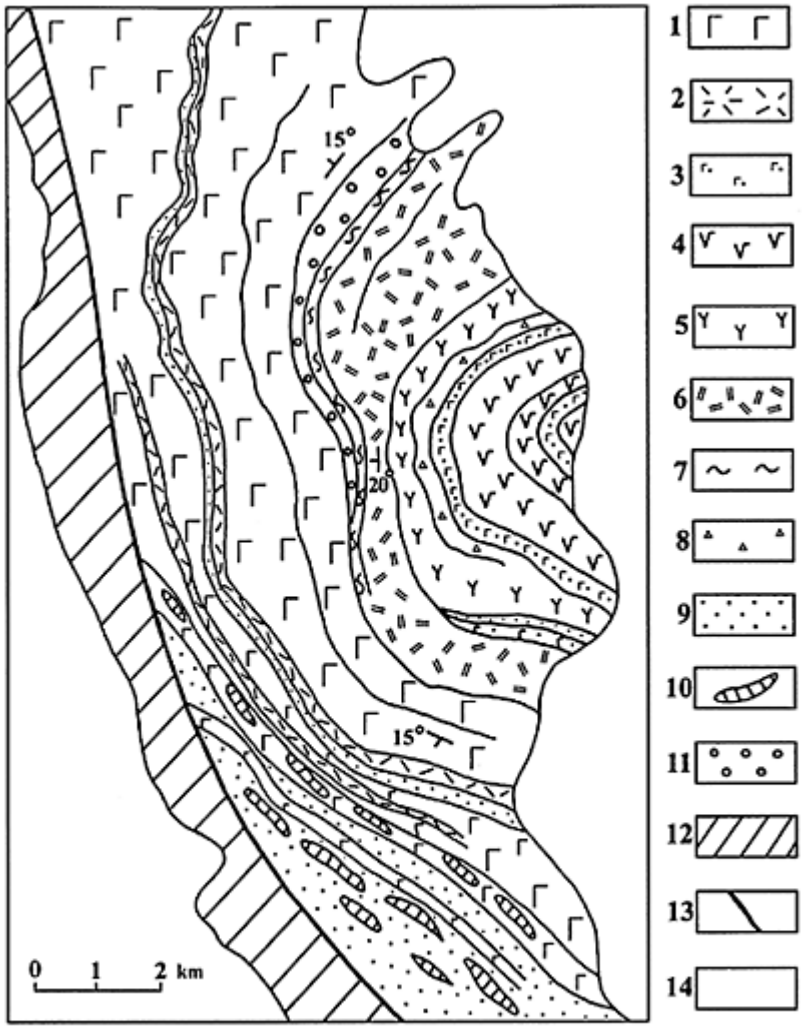

Key: 1 and 2—upper volcanic sequence: 1—subalkaline basalts, 2—trachyrhyolites; 3–8—lower volcanic sequence (differentiated complex): 3—basalt, 4—basaltic andesite, 5—trachyrhyodacite, 6—trachyrhyolite and rhyolite, 7—trachyrhyolitic ignimbrite, 8—lava breccia of trachyrhyodacites; 9—sandstone, siltstone, and gravelstone; 10—carbonate rock lenses; 11—conglomerate; 12—Vendian–Lower Cambrian formations; 13—faults; 14—Unconsolidated deposits.

Figure 35 Geological structure of the Mt Mort-Ula volcanic field ((b) on Fig. 33).

The age of the rocks from the late stage of volcanism is determined as Emsian, on the basis of their relationships with the basic and intermediate volcanites and

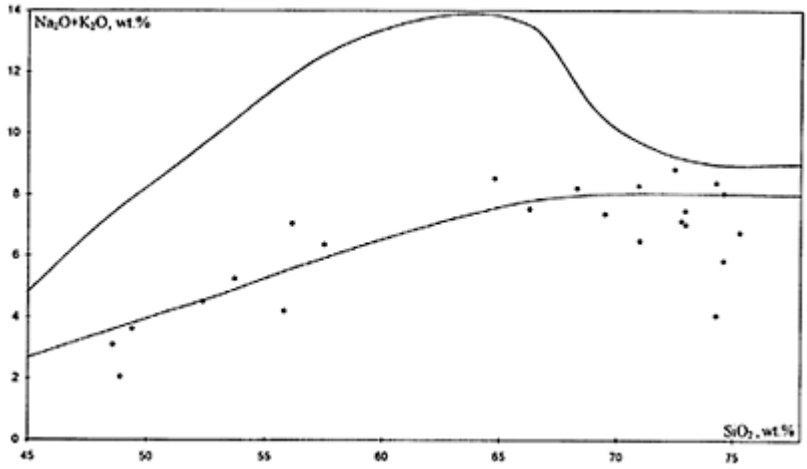

Figure 36 Compositions of the Devonian volcanic rocks in the subalkaline rock zone shown on the SiO_2–(Na_2O+K_2O) classification diagram.

also can be inferred from the fact that in some regions these rocks are overlain by terrigenous rocks yielding Givetian fossils (Luchitsky, 1983).

Table 7 presents the chemical composition of the rocks of the volcanic association. On the diagram (Fig. 36) they fall in the field of high-alkalinity rocks. Of special interest is the unusual composition of the acid volcanics, namely the marked predominance of K_2O, up to ultrapotassic composition. In this respect, the acid volcanics have no equivalents among the acid plutonic rocks of the Mongolian Altai, although the latter are characterized in general by a K_2O/Na_2O ratio greater than one.

4.3 The Subalkaline and Alkaline Zone

This zone embraces the intracontinental back-arc of the Devonian marginal belt. From this part of the belt, in the Prikhubsugul area, Devonian massifs of nepheline syenites and alkaline gabbroids—ijolite-urtites, juvites, and foyaites—have long been reported (Yashina, 1982). However, only recently have the outlines and extent of the subalkaline rock zone been defined, in connection with studies on the eastern margin of the ridges of the Mongolian Altai, in the Ozernaya Zone, where numerous volcanic terrains and intrusive massifs containing alkaline rocks have been found. Three terrains of Devonian volcanic and plutonic alkaline rocks have been recognized, named according to the controlling fault systems: the Tsagan-Shibetin, Khankhukhei, and Agardak volcanic areas (Fig. 37).

The Tsagan-Shibetin volcanic area includes a system of volcanic fields extending for more than 200 km north-south along the Tsagan-Shibetin fault zone.

Table 7 Chemical compositions of Devonian volcanics from the subalkaline zone of the Mongolian Altai.

Component	1	2	3	4	5	6	7	8	9	10	11	12	13	14	15	16	17
SiO_2	48.58	48.90	49.40	55.80	57.50	52.37	53.72	56.12	72.80	69.47	75.29	72.96	72.97	70.92	74.27	74.58	72.50
TiO_2	0.77	0.60	0.67	1.50	1.40	1.81	1.82	1.89	0.42	0.66	0.19	0.29	0.23	0.23	0.37	0.37	0.22
Al_2O_3	11.18	11.20	16.58	13.66	14.70	14.95	14.45	15.21	12.58	14.44	12.42	12.88	13.52	13.66	10.53	10.49	13.69
Fe_2O_3	4.23	2.60	2.32	3.00	2.42	5.00	4.62	9.83	4.77	3.86	3.47	3.09	2.58	3.60	6.32	6.63	3.68
FeO	7.70	8.90	7.28	6.81	5.60	5.88	6.06	2.11	—	—	—	—	—	—	—	—	—
MnO	0.18	0.16	0.15	0.16	0.10	0.40	0.39	0.21	0.03	0.05	0.03	0.02	0.01	0.03	0.03	0.01	0.03
MgO	9.20	10.10	7.10	4.84	3.95	4.42	3.63	2.66	0.65	1.54	0.41	0.45	1.60	1.40	2.01	0.53	0.12
CaO	10.80	11.20	7.50	1.46	4.72	7.25	6.51	1.96	0.40	0.80	0.21	1.11	0.12	0.16	0.16	0.10	0.20
Na_2O	1.30	1.30	2.58	3.00	5.60	3.62	3.17	5.94	4.21	5.25	3.49	3.14	0.20	0.20	0.20	0.20	3.28
K_2O	1.80	0.76	1.04	1.20	0.76	0.89	2.08	1.11	2.93	2.12	3.28	4.34	6.83	8.09	3.86	5.65	5.55
P_2O_5	0.14	0.18	0.18	0.40	0.16	0.22	0.26	0.27	0.07	0.13	0.01	0.03	0.04	0.04	0.02	0.02	0.04
F	0.03	0.03	0.02	0.08	0.04	0.05	0.09	n.d.	n.d.	n.d.	n.d.	n.d.	n.d.	n.d.	n.d.	n.d.	n.d.
LOI	3.72	4.38	4.68	4.72	2.72	2.55	2.46	2.44	1.08	1.65	1.06	1.56	1.98	1.68	2.31	1.49	0.58
Total	99.63	100.30	99.50	99.63	99.67	100.49	99.92	99.75	99.84	99.97	99.86	99.99	99.95	99.98	100.01	100.01	100.02
Li	n.d.	n.d.	n.d.	n.d.	n.d.	42	28	26	10	19	6	9	28	28	34	6	4
Rb	n.d.	n.d.	n.d.	n.d.	n.d.	20	64	20	54	52	74	78	110	96	68	114	76
Zr	n.d.	n.d.	n.d.	n.d.	n.d.	180	200	250	430	360	460	490	260	510	800	780	440

Sr	n.d.	n.d.	n.d.	n.d.	n.d.	290	300	290	60	57	60	22	43	26	11	110	75
Ba	n.d.	n.d.	n.d.	n.d.	n.d.	510	510	510	380	390	440	520	490	440	140	360	880
Sn	n.d.	n.d.	n.d.	n.d.	n.d.	1.9	2.1	3.0	3.1	2.7	2.8	5.0	4.2	4.1	14	10	4.8
Nb	n.d.	n.d.	n.d.	n.d.	n.d.	5.2	5.2	5.2	15	12	14	17	19	29	53	51	57
Sc	n.d.	n.d.	n.d.	n.d.	n.d.	41	n.d.	34	n.d.	11.7	n.d.	9.3	2.9	4.5	0.9	1.0	7.2
Hf	n.d.	n.d.	n.d.	n.d.	n.d.	4.2	n.d.	6.4	n.d.	9.0	n.d.	13	6.5	12.4	19.5	19.6	10.2
Ta	n.d.	n.d.	n.d.	n.d.	n.d.	0.4	n.d.	0.6	n.d.	0.8	n.d.	1.5	1.6	1.9	3.2	3.7	1.5
Th	n.d.	n.d.	n.d.	n.d.	n.d.	3.6	n.d.	5.6	n.d.	8.5	n.d.	11.2	14.5	11.9	12.5	13.5	10.0
U	n.d.	n.d.	n.d.	n.d.	n.d.	0.6	n.d.	2.9	n.d.	1.7	n.d.	3.2	2.2	1.9	2.6	2.3	1.8
La	n.d.	n.d.	n.d.	n.d.	n.d.	16.2	16	18.6	n.d.	7.45	n.d.	41.9	34.6	63.5	42.8	21.0	14.6
Ce	n.d.	n.d.	n.d.	n.d.	n.d.	37.7	32	39.7	n.d.	20.6	n.d.	82.7	58.8	114.8	82.5	54.5	31.6
Nd	n.d.	n.d.	n.d.	n.d.	n.d.	24.6	29	23.6	n.d.	16.4	n.d.	45.2	27.2	51.8	43.9	40.2	19.1
Sm	n.d.	n.d.	n.d.	n.d.	n.d.	7.2	6.7	6.4	n.d.	5.6	n.d.	11.5	6.0	13.3	10.9	13.0	5.3
Eu	n.d.	n.d.	n.d.	n.d.	n.d.	1.94	2.5	1.87	n.d.	0.90	n.d.	1.91	0.59	1.41	1.7	2.1	0.9
Gd	n.d.	n.d.	n.d.	n.d.	n.d.	7.0	6.7	7.4	n.d.	7.5	n.d.	11.5	4.2	7.8	13.0	18.1	5.8
Tb	n.d.	n.d.	n.d.	n.d.	n.d.	1.2	n.d.	1.3	n.d.	1.38	n.d.	2.0	0.76	1.4	2.39	3.20	1.08
Yb	n.d.	n.d.	n.d.	n.d.	n.d.	3.9	4.3	4.58	n.d.	6.10	n.d.	7.45	3.20	5.85	10.0	11.50	4.89
Lu	n.d.	n.d.	n.d.	n.d.	n.d.	0.58	0.55	0.68	n.d.	0.94	n.d.	1.11	0.49	0.89	1.53	1.70	0.76

Note: 1–8—basalt-andesite association, 9–17—rhyolite-dacite association; analyses, 1–5—after Luchitsky (1983).

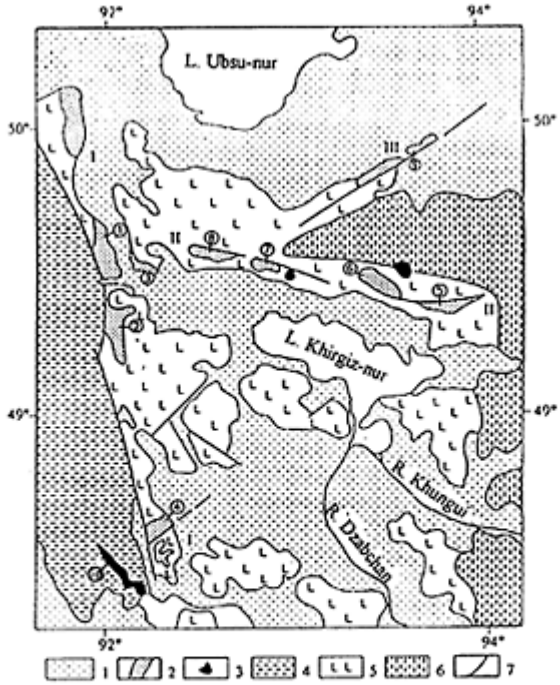

Key: I—Mesozoic–Cainozoic deposits, 2—Devonian volcanic associations, 3—peralkaline granite and syenite, 4—Caledonian structures of the Mongolian Altai, 5—early Caledonides of the Lake Zone, 6—structures of the Precambrian crystalline basement, 7—fault. Volcanic zones: I—Tsagan–Shibetin, II—Khan–Khukhei, III—Agardak; Circled figures: 1—Mort-Ula, 2—Shiveingol, 3—Sharaburidunur, 4—Shargatyn-Ula, 5—Ichetuingol, 6—western Tsagan–Khairkhan, 7—Bomin–Kharin, 8—Ulanushig, 9—Bayan–Erdenet, 10—Khaldzan–Buregtey.

Figure 37 Distribution of the Devonian volcanic associations in the Lake Zone on eastern margin of the Mongolian Altai.

Within this zone, volcanic associations of alkaline rocks rest on the erosion surface, with basal conglomerates, above Lower-Middle Devonian volcanics typical of the subalkaline rock zone (Mt Mort-Ula area, see Fig. 35) or on red and variegated Lower Devonian strata (Yarmolyuk and Kovalenko, 1991). Locally, they are interbedded with, and grade up the section into terrigenous rocks, containing lenses and carbonate rocks yielding bryozoa, corals and brachiopods of EifelianGivetian age (Marinov, 1973).

Within this volcanic area, the southern extremity of the zone is of particular interest. It is marked by a combination of alkali rocks from different facies, including both volcanics (Mt Shargatin-Ula area) and peralkaline granites of the Khaldsan-Buregtey Massif. The volcanic field of the Mt Shargatyn-Ula area forms brachysyncline and NW–SE faults, (Fig. 38). Within the field, the Devonian

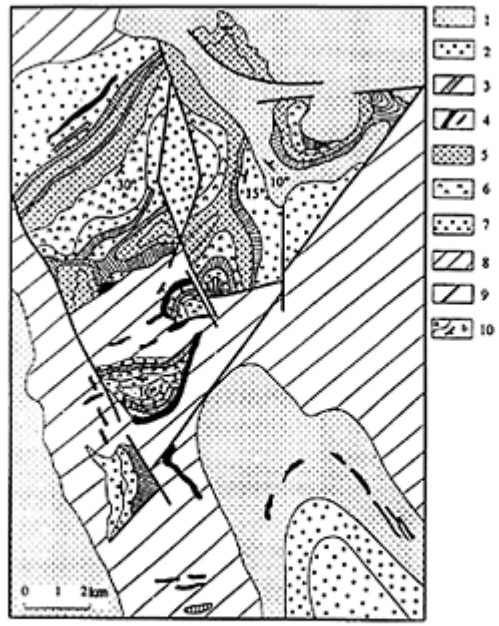

Key: 1—unconsolidated deposits; 2—Upper Devonian and Lower Carboniferous post-volcanic deposits; 3–7—Lower–Middle Devonian formations: 3—basalt, 4—sill, 5—trachyrhyolite, 6—pantellerite, 7—sedimentary rocks; 8—Pre-Devonian basement, 9—fault, 10—geological boundaries (a); elements of occurrence (b).

Figure 38 Geological structure of the Mt Shargatyn-Ula volcanic field ((4) on Fig. 37).

formations unconformably overlie grey Silurian sedimentary deposits (Dergunov *et al.*, 1980).

A sequence of variegated conglomerates, gravelstones, sandstones, and siltstones, ranging in thickness from several metres up to 700 m has been recognized in the lower part of the Devonian deposits (Fig. 39). The changes in sediment composition within this sequence can be attributed to the fact that they are related to two troughs separated by a north-east striking horst-like protrusion. The northern trough (Shargatin) includes part of Mt Shargatin-Ula and the southern one is identified as the Chigertai Trough.

Almost without exception, the Devonian volcanics are related to the Shargatin Trough and its southern margin. The volcanics rest conformably on a terrigenous sequence, with isolated basalt sheet flows in their upper part.

The volcanic sequence commences with a series (70 m) of interbedded sheet flows of dark-grey, aphyric, subalkaline basalts and andesite-basalts and brown flow-banded trachyrhyolites and trachyodacites. Above come acid rock sheets (460 m). Their lower part consist of brown, in the less-altered part bluish-grey, flow-banded trachyrhyolites and their welded tuffs. The upper part is represented

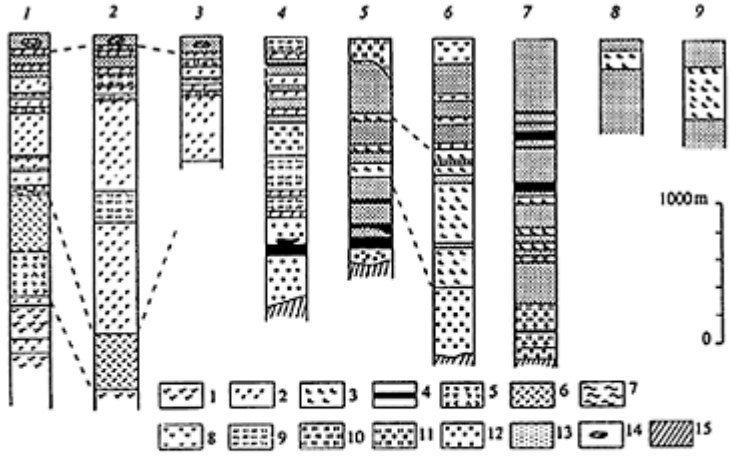

Key: 1—subalkaline basaltic andesite and andesite, 2—subalkali basalt, 3—subalkali and alkali (nepheline-normative and Pseudoleucite-bearing) basalts, 4—teschenite, dolerite, and gabbroid sills; 5—trachydacite and its lava breccia, 6—rhyolite, 7—trachyrhyolite ignimbrite, 8—trachyte, 9—trachyrhyolite, 10—pantellerite, 11—alkali microgranite, 12—conglomerate, 13—terrigenous rocks, 14—carbonate lenses, 15—Pre-Devonian basement; Volcanic field cross-sections: 1—Mort-Ula, 2—Shiveingol, 3—Sharaburidunur, 4—Shargatynula, 5—Ichetuingol, 6—western Tsagan-khairkhan-Ula, 7—Bomin-Kharin, 8—Ulan-Ushig, 9—Bayan-Erdenet.

Figure 39 Correlation of the Devonian volcanic formations of the eastern margin of Mongolian Altai.

by flow-banded blue trachyrhyolites-pantellerites (Table 8). They are overlain by a volcanosedimentary unit more than 360 m thick. This is dominated by variegated sandstones, gravelstones, and siltstones, including calcareous siltstones. About one-third of their volume consists of dark-grey, aphyric, less commonly porphyritic, lavas and basalts that are more or less evenly dispersed within the section of the unit.

The uppermost part of the section is composed of thin sheet flows of subalkaline andesite basalts and also of brown, locally bluish-grey, aphyric trachyodacites, similar in petrographic composition to the rocks of the pantelleritic part of the section. There the thickness of the acid volcanics is more than 180 m. The rocks rest conformably on the lower parts of the section, but, in the western part of the region, there is a volcanic unconformity caused by the dome-like emergence of underlying rocks and the erosion that preceded the eruption of the trachyodacites.

The volcanics show on unusual distribution pattern across the area: the most common are trachyodacites and pantellerites, whose thickness decreases eastwards, north-eastwards, and southwards. The trachyodacites-pantellerites are interbedded with basalts, therefore a section through the volcanics shows a bimodal pattern typical of the flanks of acid volcanoes that formed concurrently with the eruption of basalt lavas (Yarmolyuk and Kovalenko, 1991). This suggests that

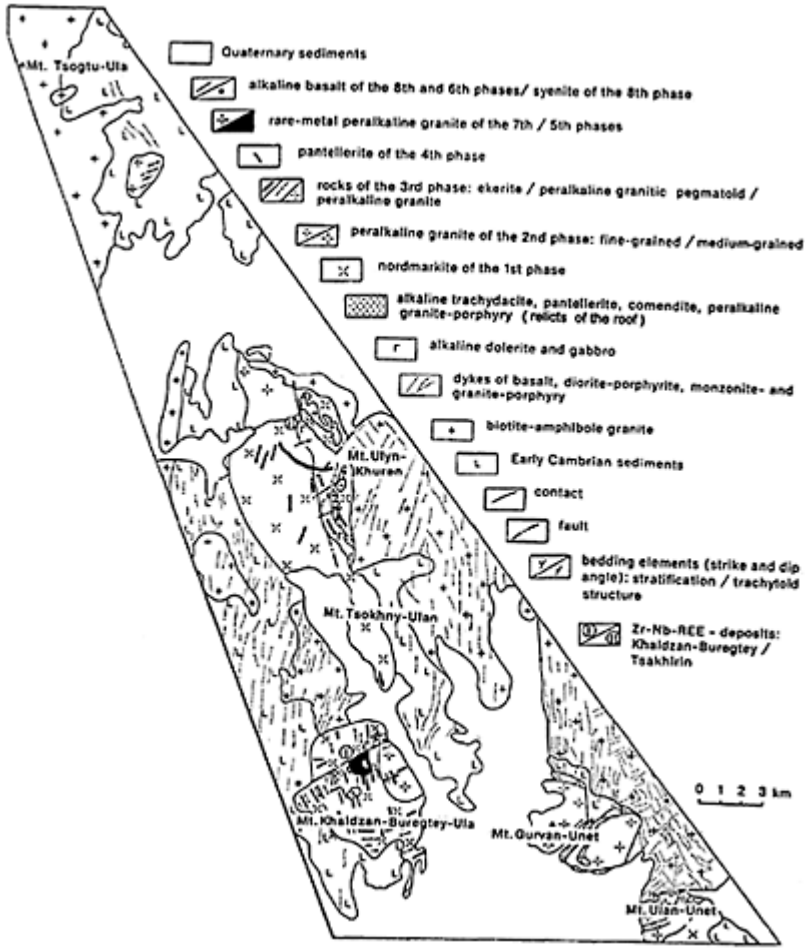

Figure 40 Geological structure of the Khaldzan—Buregtey Massif ((10) on Fig. 37) (after Kovalenko *et al.*, 1995).

the centre of the pantellerite volcano was west of the present boundaries of the volcanic field. There we can observe a volcanic unconformity and see the greatest thickness of the upper series of trachyolite lava flows. It should also be noted that the localities of the Lower–Middle Devonian peralkaline granites of the Khaldzan-Buregtey Massif occur 15 km west of the boundary of the volcanic field.

The Khaldzan-Buregtey Massif of peralkaline granites is a part of chain of eastern ridges of the Mongolian Altai (Kovalenko *et al.*, 1995). It is elongated in NNW direction, following the strike of the Altai structures (Fig. 40). It is 30 km long and up to 8 km wide. The enclosing rocks are Vendian-Lower Cambrian (?)

Table 8 Compositions of volcanic rocks of the Devonian rift associations of north-western Mongolia.

Sample	1	2	3	4	5	6	7	8	9	10	11	12	13	14	15	16
SiO_2	49.87	73.56	46.68	52.18	72.67	47.53	34.44	50.97	46.40	48.94	43.91	47.21	53.72	45.57	49.57	76.19
TiO_2	1.73	0.27	2.03	2.89	0.13	2.09	4.92	3.08	2.29	2.22	4.05	2.64	1.82	1.84	2.77	0.23
Al_2O_3	16.35	12.87	15.20	14.39	11.75	19.30	8.80	13.76	15.93	17.29	15.80	17.15	14.45	16.51	14.74	12.68
Fe_2O_3	5.63	1.20	4.22	9.95	2.50	3.96	18.44	6.86	4.07	3.29	3.82	3.99	4.62	6.09	9.91	1.00
FeO	4.79	1.37	7.14	2.29	2.07	5.63	9.58	5.54	7.78	5.42	10.87	8.69	6.06	5.70	2.83	1.42
MnO	0.27	0.02	0.16	0.19	0.18	0.15	0.23	0.24	0.19	0.15	0.24	0.17	0.39	0.61	0.44	0.02
MgO	5.38	0.39	8.38	3.55	0.30	3.80	14.10	4.60	6.30	4.00	4.91	3.37	3.63	6.64	3.20	0.15
CaO	7.27	0.45	8.33	7.09	0.20	8.20	2.80	5.20	9.20	6.00	8.82	7.70	6.51	7.88	4.89	0.26
Na_2O	4.59	3.04	3.50	3.62	4.68	3.92	1.82	4.52	3.42	3.95	3.42	3.78	3.17	4.17	5.57	6.38
K_2O	0.76	4.68	1.22	1.28	4.27	1.66	0.94	1.55	1.44	3.36	0.85	2.00	2.09	0.41	1.81	1.86
LOI	2.53	0.50	2.01	1.88	0.81	3.37	3.65	2.69	3.29	4.49	2.15	2.06	2.46	3.84	2.95	0.63
P_2O_5	0.20	0.03	0.41	0.53	0.01	0.47	0.28	0.59	0.34	0.96	0.74	0.75	0.26	0.19	1.03	0.03
Total	99.37	99.32	100.19	99.84	99.57	100.04	100.00	99.60	100.65	100.07	99.58	99.51	99.17	99.45	99.67	99.80
Li	26	12	38	15	12	17	10	21	23	9	8	7	28	52	14	18
Rb	8	100	25	21	64	18	8	22	22	38	8	28	64	8	22	22
Zr	180	570	240	200	640	160	130	170	100	190	230	260	200	120	280	640
Nb	5	28	17	10	26	18	15	9	13	30	24	36	8	6	14	26
Hf	3.3	17	6.5	5.4	14.1	4.1	2.9	6	4	6	5.4	15	4.2	3	3.5	16.6
Ta	0.3	1.8	4.8	0.8	2	1.6	1.4	0.6	1.3	3	2	3.5	0.4	0.4	0.6	1.8

Ba	310	1410	700	410	830	270	160	250	410	580	460	730	1,110	240	470	110
Sr	450	180	810	380	80	550	340	540	510	640	730	840	340	190	100	100
Pb	10	12	6.3	6.8	22	1.3	1.4	20	2.4	10	34	9.7	51	803	903	2
Co	36	3	58	38	46	43	120	31	58	35	23	34	25	32	29	25
Ni	63	6	26	28	17	56	260	19	98	17	27	12	32	99	70	14
Cr	39	3	140	12	10	68	300	3	220	3	1	1	40	51	39	7.8
V	200	5	250	300	15	430	400	280	290	170	180	120	200	200	240	4.7
Y	23	48	240	36	76	21	15	35	20	23	24	35	41	23	58	22
Sc	28	5.5	24	33	2	48	10	44	30	13	27	24	41	37	37	4.4
Th	1.1	8.5	4.9	3	10	1.9	1.1	2.8	1	2.8	2.2	4.7	3.6	0.6	2.6	9.3
U	0.6	0.9	1	0.8	1.7	1	0.6	1.1	0.5	0.8	1.8	2.8	0.6	0.5	0.5	1.7
La	7.1	38.1	29.4	21.7	49.5	24.4	13.3	17	16.4	43.1	29.4	63	16.2	8.9	10.9	34.4
Ce	19.3	86.3	54.2	51	103.8	5.8	27.4	42.3	36.4	85.9	59.4	129.5	37.7	22.6	27.3	73.4
Nd	15.1	54.9	27.4	32.4	60.6	29.4	15.8	29.8	22.7	47.5	33.2	73.8	24.6	16.4	19.3	43.6
Sm	5.1	15.8	6.5	9.4	16.2	7.8	4.2	9.3	6.4	12.1	8.6	19.4	7.2	5.2	6	11.9
Eu	1.54	2.99	1.72	2.54	2.45	2.39	1	3	1.91	3.44	2.5	4.77	1.94	1.53	1.58	1.89
Gd	4.9	15.98	4.96	9.3	14.2	6	2.86	8.5	5.7	8.7	7	22.1	7	5.3	6.2	12.6
Tb	0.83	2.93	0.79	1.5	2.48	0.91	0.43	1.45	0.87	1.3	1.07	3.3	1.2	0.91	1.06	2.39
Yb	2.56	12.24	1.85	3.82	8.81	1.75	0.85	4.55	1.79	2.5	2.23	6.16	3.98	2.89	3.45	11.43
Lu	—	—	—	—	—	0.19	0.11	0.66	0.24	0.33	0.3	0.81	0.58	0.42	0.5	1.79
$(^{87}Sr/^{86}Sr)_0$	0.705	—	0.703	0.703	—	0.707	0.704	0.706	0.705	0.704	0.703	0.703	0.706	0.705	0.706	—

Sample	**17**	**18**	**19**	**20**	**21**	**22**	**23**	**24**	**25**	**26**	**27**	**28**	**29**	**30**	**31**	**32**
SiO_2	70.92	68.32	62.10	56.11	49.53	73.00	74.79	46.46	46.18	47.11	70.96	45.61	53.21	44.67	60.42	68.53
TiO_2	0.15	0.27	0.05	0.05	2.52	0.08	0.12	1.57	3.34	3.59	0.10	2.50	1.53	2.26	1.14	0.48
Al_2O_3	12.20	14.00	18.58	19.30	17.30	14.03	11.68	13.22	15.84	15.33	13.20	16.92	16.15	14.44	16.17	15.40
Fe_2O_3	2.33	2.08	1.73	0.98	3.37	0.63	1.07	3.48	13.28	9.05	2.90	5.81	7.09	7.92	2.74	3.10
FeO	2.95	3.05	2.00	3.92	7.78	1.00	2.06	9.11		3.86	1.53	6.72	2.56	5.03	3.66	0.27
MnO	0.10	0.16	0.23	0.13	0.20	0.03	0.07	0.17	0.25	0.20	0.07	0.16	0.14	0.13	0.17	0.09
MgO	0.10	0.10	0.25	n.d.	3.70	0.10	0.16	11.71	4.88	4.57	0.05	5.36	1.63	6.88	1.20	0.23
CaO	0.30	0.51	0.79	0.70	5.50	0.53	0.30	8.06	6.61	5.79	0.15	8.57	3.79	10.60	2.80	0.60
Na_2O	6.21	6.20	8.23	10.01	5.00	5.90	5.63	2.96	3.81	3.78	5.82	2.83	6.25	2.41	4.98	4.73
K_2O	4.25	4.65	4.59	5.17	1.50	3.55	3.94	0.68	1.19	1.61	4.84	1.16	2.67	1.41	4.95	5.89
LOI	0.35	0.20	1.43	4.24	3.43	0.75	0.11	1.28	3.75	3.82	0.39	3.06	3.45	2.93	1.28	0.54
P_2O_5	0.02	0.05	0.03	0.06	0.62	0.02	0.03	0.26	0.88	0.72	0.01	0.43	0.91	0.51	0.42	0.06
Total	99.90	99.95	100.01	100.67	100.45	99.95	99.99	98.96	100.18	99.99	100.02	99.13	99.37	99.34	99.93	99.92
Li	126	48	74	53	37	44	45	6	20	22	3	10	5	13	14	8
Rb	174	128	170	100	15	360	600	10	9	16	240	5	32	13	150	180
Zr	1,831	2,000	1,748	1,500	260	1,940	2,360	110	350	290	910	280	530	210	340	570
Nb	183	300	240	114	38	1,016	1,013	—	—	—	130	17	38	32	28	42
Hf	n.d.	n.d.	n.d.	n.d.	6.5	74	12	2	7	2.7	22	4.2	13	4.8	9.6	16.5
Ta	—	—	—	—	3.5	95	13	1.1	2.5	0.9	11	1.4	3	2.8	2.6	3.2

Ba	22	30	300	77	450	60	50	320	650	470	23	400	700	540	960	760
Sr	16	13	990	180	580	20	22	410	500	500	18	540	300	1300	570	180
Pb	26	25	20	19	6.7	280	58	17	22	7.5	20	3.9	20	2.4	28	11
Co	0.5	0.5	0.5	5.5	34	n.d.	1.9	62	28	23	2.8	54	12	47	4.9	—
Ni	11	4.1	3	4.6	6.4	—	6.1	270	81	11	31	64	10	150	1	—
Cr	16	1	5	1	1	—	3.8	400	101	10	25	10	5	180	26	—
V	1	3	4	9.6	60	—	1	160	120	140	2.9	200	47	210	—	—
Y	86	130	160	77	22	240	330	—	—	—	70	18	45	26	46	51
Sc	n.d.	n.d.	n.d.	n.d.	13	0.2	0.4	20	23	34	0.3	20	16	25	17.5	7.3
Th	—	—	—	—	3.4	99	86	1.9	2.7	1.2	22	1.7	4.9	3	8.5	15
U	—	—	—	—	1	9	4.2	1.4	—	0.8	3.1	0.6	1.8	1.1	2.5	3.3
La	210	160	240	465	35.8	51.4	33.6	13.6	39.6	44.1	99.9	20.1	63.2	28	48.9	52.8
Ce	450	270	360	250	71	117.7	63.8	29.1	81.6	83.6	189.7	43.7	126.1	54.5	94.6	97.8
Nd	230	170	130	97	38.9	75.8	33.6	17.4	46.7	43.9	99.1	25.4	69.6	29.5	50.4	49.6
Sm	n.d.	n.d.	n.d.	n.d.	9.9	22	8.2	4.7	12.3	10.8	24.3	6.8	17.8	7.4	12.6	11.9
Eu	—	—	—	—	2.9	0.34	0.31	1.33	3.33	2.48	0.66	1.98	4.2	2.27	2.72	0.83
Gd	—	—	—	—	7.4	25.2	8.8	4.1	10.7	6.5	18.9	5.3	14.4	5.7	9.85	8.1
Tb	—	—	—	—	1.17	4.8	1.64	0.6	1.66	0.93	3.34	0.64	2.24	0.91	1.63	1.4
Yb	18	12	14	8.3	2.69	22.86	7.5	1.05	3.49	1.45	12.2	2.5	4.87	2.21	4.61	5.31
Lu	n.d.	n.d.	n.d.	n.d.	0.37	3.58	1.16	0.14	0.47	0.18	1.81	0.28	0.66	0.31	0.65	0.79
$(^{87}Sr/^{86}Sr)_0$	—	—	—	—	0.705	—	—	0.703	0.706	0.703	—	0.703	—	—	—	—

Note: Rocks sampled from volcanic fields: 1–2 Shiveingol, 3–5 Shargatinulin, 6–10 Ulanushig, 11–12 Bayan-Erdenet, 13–16 Mortulin, 17–23 Bominkhorin (22–23 peralkaline granite of the Ulan-Tologoi), 24–27 Ichetuingol, 28–32 Tsagan-Khairkhan.

biotite-amphibolic, granite with biotite and amphibole two-feldspar granites and older ofiolites.

The contact between the granitoids of the massif and their enclosing rocks is intrusive, with distinct, often sinuous, boundaries including some that cut the bedding at almost 90°. Locally, the roof sags of the massif are metamorphosed to hornfels.

The massif has a multiphase structure. The sequence of intrusion phases is:

1) nordmarkites of phase 1,

2) peralkaline granites of phase 2,

3) ring dykes of peralkaline granite pegmatites, ekerites, and fine-grained peralkaline granites of phase 3,

4) north-south dykes of pantellerites of phase 4,

5) medium-grained rare-metal peralkaline granite of phase 5,

6) dykes of alkali gabbroids and basaltoids of phase 6,

7) fine-grained miarolitic peralkaline rare-metal granitoids of phase 7,

8) dykes of leucite basaltoids and stock-like bodies of leucosyenites of phase 8.

The intrusion of basaltoid magma apparently occurred repeatedly during the formation of the granites. Therefore, dyke-like globular basaltoid segregations, with chilled contacts, occur in the nordmarkites of phase 1 and the alkali granites of phase 2. Their formation is attributed to the intrusion of ‘hotter’ basaltoid magma into relatively ‘cold’ peralkaline granite magma (Kovalenko *et al.*, 1995).

The massif consists mostly of porphyritic fine- and medium-grained nordmarkites of phase 1. A decrease in volume is evidenced by the relationships of the rocks of the subsequent intrusion phases. Of special interest are the rare-metal peralkaline granitoids of phases 5 and 7. They form stock-like bodies with steep intrusive contacts. Compositionally, they are coarse-grained microcline-albite granites consisting of K-Na feldspar, albite, quartz, arfvedsonite, aegirine, fluorite, and various rare-metal minerals. Ore exotic minerals (upto 25 vol.%) are represented by elpidite, gittinsite, zircon, pyrochlore, rare-earth fluorcarbonate, monazite, and polylithionite. The content of rare elements is (in wt %): Zr—5.3, Nb—0.8, REE—0.4, and Y—0.3. Apart from this, the granites are enriched in Be, Sn, and Rb, and locally in Li, Pb, Zn, Hf, and Ta. Melt-inclusions studies revealed enrichment in the element of magma of the rare-metal granites (Kovalenko *et al.,* 1995). Geochemical analysis of the variation in rare-element contents with Zr in the entire rock sequence of the massif suggests that fractional crystallization was responsible for formation of the rare-metal melts.

Table 9 presents the compositions of the rocks of the massif. It shows that all of the products of the alkali-granite magmas are highly alkaline, with an agpaitic coefficient of ≥1. The rare-metal geochemical specialization is apparent within the entire range of compositions and drastically increases in the rocks of the raremetal phases of intrusion.

Table 9 Chemical composition of representative samples of rocks from the Khaldzan-Buregteg Massif (after Kovalenko et al., 1989).

	1	2	3	4	5	6	7	8	9
SiO_2	64.66	66.14	73.14	72.17	74.09	70.22	72.17	69.69	41.92
TiO_2	0.56	0.37	0.10	0.45	0.22	0.10	0.31	0.30	2.65
Al_2O_3	13.07	12.80	10.00	7.56	8.20	10.90	10.76	10.40	13.90
Fe_2O_3	8.76	2.16	2.14	2.96	4.92	2.82	3.13	3.72	6.13
FeO	—	5.63	3.66	6.38	2.69	4.40	1.26	0.62	6.78
MnO	0.25	0.19	0.15	0.24	0.10	0.18	0.05	0.16	0.44
MgO	0.14	0.08	0.18	0.33	0.10	0.09	0.02	0.09	6.40
CaO	1.50	1.22	1.64	0.69	0.50	0.30	0.26	2.90	10.20
Na_2O	5.99	6.03	4.42	4.21	4.28	5.02	4.66	5.36	2.47
K_2O	4.85	4.68	3.20	3.97	4.71	2.94	4.44	2.82	1.83
P_2O_5	0.11	0.06	0.14	0.07	n.d.	n.d.	0.10	n.d.	0.41
LOI	0.16	0.05	0.55	0.08	0.06	0.65	1.32	1.60	5.88
F	n.d.	0.04	0.035	0.13	0.05	0.25	0.50	1.00	0.40
H_2O	n.d.	0.02	0.01	0.06	0.02	0.10	0.20	0.42	0.16
CO_2	n.d.	n.d.	n.d.	0.01	0.07	0.11	0.01	0.35	1.46
Total	100.05	99.47	99.365	99.31	100.01	98.08	99.19	99.43	101.03
a.c.	1.2	1.2	1.1	1	1.5	1.1	1.2	1.2	0.4

Note: 1 and 2—nordmarkites (phase I); 3—peralkaline granites (phase II); 4 and 5—veined series (phase III): *4*—peralkaline granite pegmatoids, 5—ekerites; 6—pantellerites (phase IV); 7–8—rare-metal peralkaline granites (phases V and VII); 9—alkali basalts (phase VI).

The Rb-Sr age of rocks from the Khaldzan-Buregtey Massif was found to be 375±17 Ma, i.e. late middle Devonian. The primary $^{87}Sr/^{86}Sr$ ratio in the source was estimated to be 0.7046. The Sm-Nd isotope systematics of the rocks show that, based on their ε_{Nd} values (for 380 Ma) their compositions range from +4.3 to +7.6. Taking into account that the average composition of the Caledonian crust at that time had about ε_{Nd}=+7.25, we can assume that the products of the mixture from two isotope sources—mantle and crustal—took part in the formation of the massif.

Therefore, in their time of emplacement, in the alternating supply of acid and basic melts, and in the similarity in the compositions of their magmatic products, the rocks of the Khaldzan-Buregtey Massif and those of the volcanic fields of Shargatyn-Ula can be considered as equivalent. This suggests that the formation of both magmatic areas was related to a common igneous centre and to some of its plutonic and volcanic facies.

The Khan-Khukhei volcanic area comprises volcanic fields and peralkaline granitoid massifs related to a system of E-W faults affecting the southern face of the Khan-Khukhei Ridge. In their present structure the volcanics are associated with isolated troughs mostly infilled by terrigenous rocks yielding Lower and Middle Devonian flora (Dergunov, 1989; Yarmolyuk and Kovalenko, 1991). The neighbouring troughs are marked by the similarity in their sections and the type of deformation. This allows us to relate them to at least two *en échelon*, conjugated, graben-like WNW-ESE-trending troughs—the Tsagan-Khairkhan-Ula and Bomin-Kharbin troughs.

The Tsagan-Khairkhan-Ula trough stretches for about 50 km and consists of the western and eastern (Ichetuingol) terrains of Devonian volcanosedimentary rocks. The Devonian deposits rest uncomformably on dislocated Vendian-Lower Cambrian rocks, with a sequence (up to 500 m) of red conglomerates, gravelstones, and sandstones at the base of the section (Fig. 41).

The basal conglomerates are overlain by a volcanosedimentary sequence whose terrigenous part consists of thin-bedded sandstones, siltstones, and gravelstones. The volcanic rocks show an irregular distribution across the section and make up individual sheets or their series, being most common in the western part of the trough. The lower part of the section is represented there by a thick (about 1,000 m) series of thin sheet flows of aphyric, less-common porphyry, subalkaline basalts (including normative nepheline-bearing), with subordinate beds of terrigenous rocks.

The upper part of the sequence (above 650 m) is composed of terrigenous rocks containing sheet flows of grey porphyry trachytes with large (up to 1 cm) feldspar phenocrysts. A bed of trachytes (200 m), formed by a series of extrusive mushroom-shaped bodies occurs in the uppermost part of sequence.

In the eastern (Ichetuingol) part of the trough, there is a decrease in the content volcanics (Fig. 39). The volcanosedimentary sequence is more than 1,000 m thick and contains individual basalt sheet flows or series of flows, the thickest (≤60 m) of them, as in the western part of the trough, is related to the lower part of the

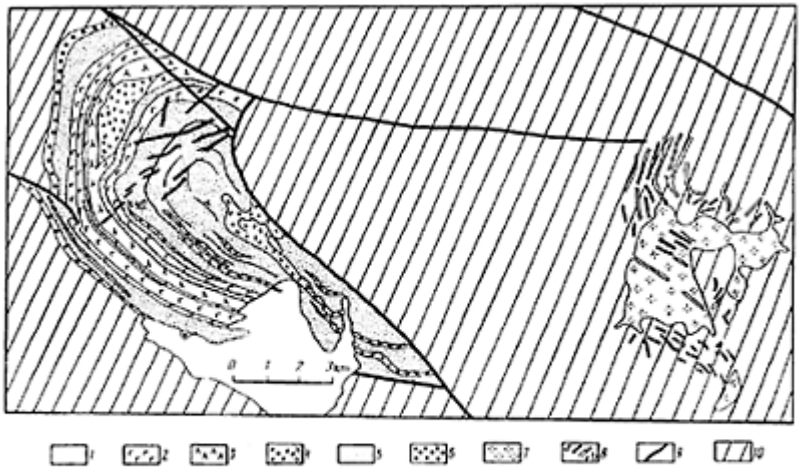

Key: 1—Cainozoic deposits; 2–8—Devonian rocks: 2—subalkali basalt and subordinate trachybasalt, 3—mainly normative nepheline bearing trachybasalt, 4—trachyte, 5—red beds, 6—conglomerate, 7—alkali syenite, 8—dykes (a—basalt, b—mariupolite, alkali granite, and syenite); 9—fault, 10—pre-Devonian formations.

Figure 41 Distribution of the Devonian alkali rocks of the Mt Tsagan-Khairkhan-Ula area ((6) on the Fig. 37).

sequence. The section is capped by a thick (>400 m) sequence of flow-banded pantellerites, recrystallized in their central parts to microgranites (Table 8).

In this part of the volcanic trough, subvolcanic bodies—basalts, trachytes and pantelleritic dykes—as well as teschenite and dolerite sills—are very common. A massif of alkali syenites with an alkali granite phase and pantellerite, comendite and mariupolite dykes, is related to the northern slope of the trough (Yarmolyuk and Kovalenko, 1991). The identical compositions of the massif rocks and the volcanics (syenites-trachytes, peralkaline granites-comendites) suggests that they belong to different facies of a single igneous centre.

Of particular note are the structural features of the Ichetuingol terrain, which indicate the tectonic conditions during the deposition of the Devonian layered complexes (Fig. 42). The western part of the terrain is divided into three subparallel grabens by exposures of Vendian-Cambrian carbonate and siliceous-volcanic rocks. They differ in the thickness of the lower conglomerate sequence and that of the lower series of basaltic sheets and in the composition of their clastic material, especially in the basal parts of the sequence. The composition of the clasts depends on that of the source rocks bordering each of the grabens. This suggests that the grabens mapped within the Ichetuingol terrain are primordial in nature and cannot be interpreted as fragments of some large basins; in this case the composition of the clastic material could be attributed to distant source areas.

However, we can suggest how the grabens were formed and the relationship of the volcanism to graben formation.

The Bomin-Kharin Trough differs structurally from the Tsagan-Khairkhan-Ula Trough, primarily due to the presence of numerous sills of differing compositions. The occurrence of Devonian igneous activity is also associated with various types of sedimentary rocks. In the Mt Bomin-Kharin-Ula area, a stratified

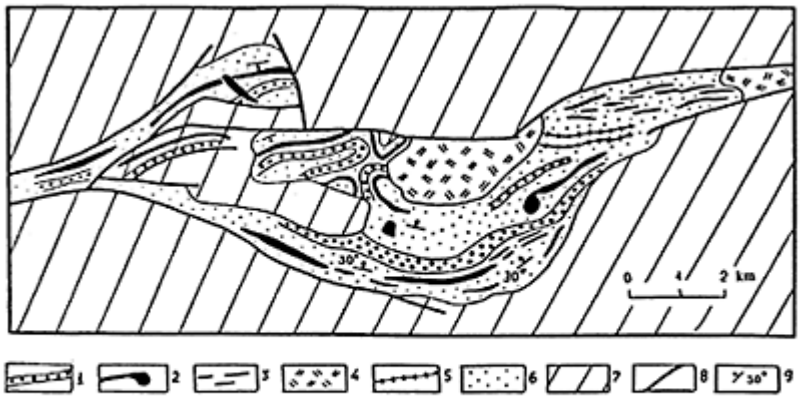

Key: 1–6—Devonian formations: 1—basalt, 2—teschenite and dolerite sills, 3—basalt dyke, 4—pantellerite, 5—pantellerite and trachyte dykes, 6—sedimentary rocks; 7—pre-Devonian basement; 8—faults; 9—bedding elements (strike and dip angle).

Figure 42 Geological structure of the Ichetuingol volcanic field ((5) on Fig. 37).

Devonian complex is folded into an elongated E-W-trending trough. Structurally, the trough is dominated by sedimentary rocks forming the following section. Its lower part (400–500 m thick) consists of redstone sandstones and gravelstones with a calcareous cement. Up section they grade into a unit (700 m thick) of thinly interbedded buff and yellow calcareous and occasionally pale-grey arkoses. The upper part of the section (above 600 m thick) is represented by interbedded buff-grey and pale-grey fine-pebble conglomerates.

At all levels, the section contains numerous dykes, sills, and sheets of igneous rocks (Fig. 43). The lower part is marked by a series of closely spaced sills of light-blue, blue, and brownish grey pantellerites and peralkaline microgranites. The rocks contain phenocrysts of alkali feldspar, the matrix is massive or flow-banded, or locally microspherulitic. The matrix also contains numerous micro-crysts of dark-coloured alkaline minerals.

In the middle part of the section, several sheets of aphyric subalkaline olivine basalts, with easily discernible amygdaloidal upper scoria layers occur among the buff-grey sandstones. Their total thickness does not exceed 40–50 m.

A thick (≤50 m) microcrystalline peralkaline mariupolite sill is related to the upper horizons of the middle part of the section. The upper contact of the sill is a wavy surface, and a similar type of deformation is retained in overlying rocks, implying that they were fairly plastic at the time of intrusion. Near the endocontact, the mariupolites are oxidized, becoming buff in colour, contain abundant vesicles, and show blocky jointing, locally resembling ropy lava. In the central part of the sill, the rocks are grey and massive, and show a spotted appearance

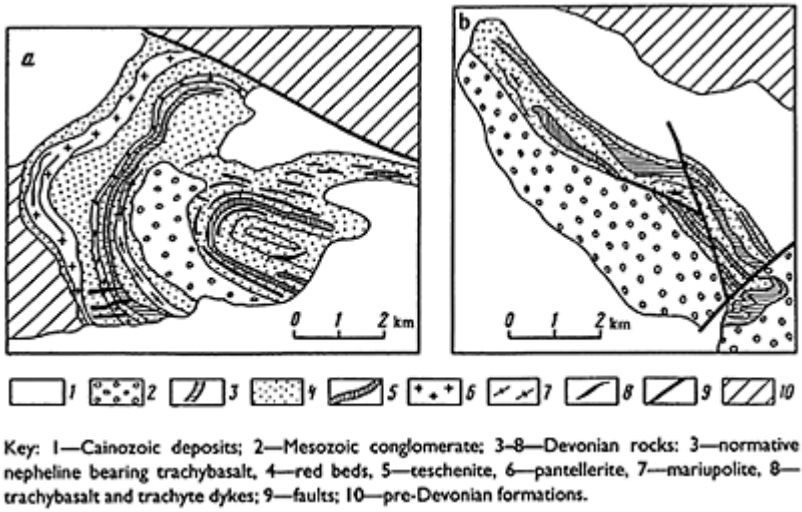

Figure 43 Structure of the Devonian troughs in the areas of the Bomin-Khara-Ula (a) and Ulan-Ushig-Ula (b) mountains ((7) and (8) on Fig. 37).

when fresh due to the development of spherical nepheline segregations in a groundmass of fine-grained albite-aegirine.

Alkali basaltoid and teschenite sills are very common in the upper part of the section of this terrain. The largest teschenite sill is up to 49 m thick, and is characterized by a pronounced differentiation from kaersutite-pyroxene varieties containing analcite in the chilled endocontact to medium-grained olivine-hornblende teschenites. Table 8 presents the rock compositions for this terrain.

The higher horizons of the Bomin-Kharin Trough occur in the Mt Ulan-Using-Ula area (see Fig. 43). The Mt Bomin-Kharin section is made up by a unit of interbedded red sandstones and siltstones up to 300–350 m thick. It is overlain by a series of thin (1–3 m) subalkaline basalt and leucite trachybasalt sheet flows alternating with sandstones. The leucite trachybasalts are massive or show a pillowed structure. Round hummocks, 1 cm across, are leucite segregations replaced by secondary minerals. The thickness of this series is more than 50 m.

It is significant that, like other troughs, the Bomin-Kharin Trough contains plutonic alkali rocks. For example, an peralkaline-granite stock is exposed in the basement inlier on the eastern slope of the trough. In composition, it is similar to the sill pantellerites and differs in its high content of rare metals, as evidenced by high Zr, Nb, and Ta. Table 8 presents the compositions of the rocks in the trough.

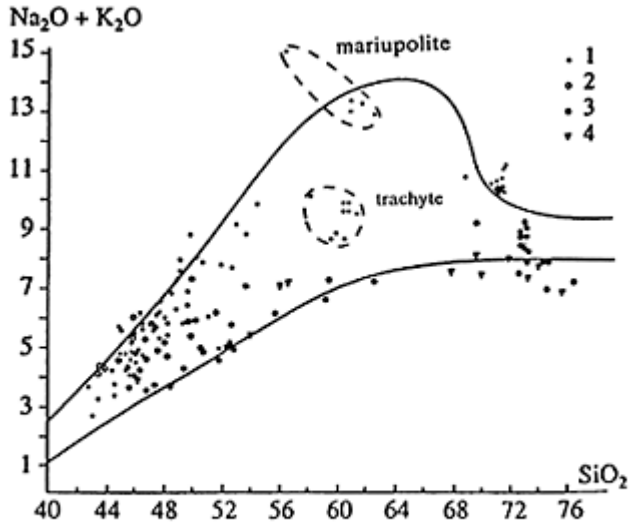

Key: compositions of rocks of 1—the Khan-Khukhei Zone; 2—Agardak Zone; 3 and 4—Tsagan-Shibetin: of—3: trachyrhyolite–trachybasalt and trachybasalt–trachyrhyolite–pantellerite association, 4—trachybasalt–trachyandesite and trachyrhyodacite–rhyolite association.

Figure 44 Location of the Devonian volcanics of the Lake Zone on the SiO_2–(Na_2O + K_2O) classification diagram.

The Agardak volcanic region is a chain of small volcanic fields related to the Agardak Fault. Structurally, the fields are represented by volcanics interbedded with red beds. They are dominated by tephrites; basalts are less common. They form thin (3–5 m) lava flows, and the total thickness of the volcanic rocks reaches 400–450 m.

4.4 Chemical Composition

Petrochemically, the rocks of the associations discussed above belong to the K-Na subalkaline and alkali petrochemical series (Table 8 and 9). On the diagram (Fig. 44), their compositions are located at the boundary separating fields of subalkaline and alkali rocks. The diagram also shows that the associations are characterized by compositions plotting mainly within the range of SiO_2 45–52% and SiO_2 60–70%.

High alkalinity as indicated by the petrographic composition of rocks including the alkali minerals (analcite, nepheline, pseudoleucite, aegirine, arfvedsonite, and barkevikite), is reflected in the norm. Therefore the majority of the main volcanics are characterized by the presence of normative nepheline. Normative nepheline and acmite were recorded in the salic rocks.

Along with nepheline-normative basalts, hypersthene-normative basalts are common among the basic rocks, but quartz-normative basalts are rare. In terms of trace elements, the above associations are characterized by a high content of lithophile elements, making them compositionally similar to the alkali rock associations of present-day rift zones. Figure 45 shows the distribution of minor elements. A marked enrichment in light REE is evident throughout the entire range of compositions. Differentiation in the basic rock series led to REE enrichment in their leucocratic derivatives. In this case, REE distribution does not change during the transition to mariupolites and pantellerites that show a tenfold enrichment in REE with respect to the poorly differentiated basalts. The enrichment remains the same with respect to the poorly differentiated basalts. It also stays the same with respect to Rb, Zr, and Sn.

The variations in the rock composition are to some extent due to regional factors. Higher alkalinity is recorded in the rocks of the Agardak and Khankhukhei volcanic areas containing associations of alkali basic (nepheline-normative and pseudoleucitic basalts) and salic (trachytes, mariupolites, and pantellerites) rocks. The Tsagan-Shibetin volcanic area is dominated by subalkaline basalts and trachyrhyolites.

4.5 On the Nature of Marginal Belt Magmatism

Regarding the formation of the Devonian marginal belt we need to consider the processes operating at that time in Central Asia, and in particular in Mongolia. Within the area of the South Mongolian and Irtysh-Sayan arms of the palaeo-

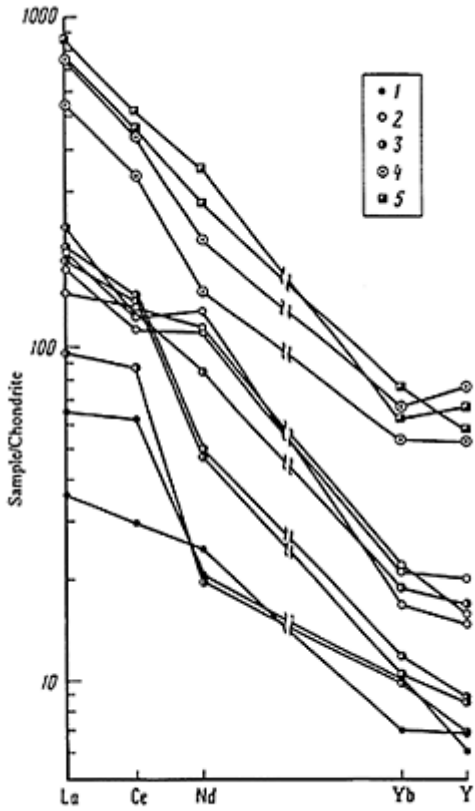

Key: 1—subalkaline basalt, 2—alkali basalt and teschenite, 3—trachyte, 4—mariupolite, 5—pantellerite.

Figure 45 REE content in rocks of the Devonian volcanic associations of the Lake Zone.

Tethys, formation of island arcs and marginal seas took place, implying the subduction of an oceanic plate. Apparently, subduction also took place beneath the continental plate. For example, regional metamorphism in the southern Mongolian Altai, in the zone of the present boundary of Caledonian and Variscan structures occurred in the rearly and Middle Devonian. Based on the data of I.K. Kozakov (1986) the zircon age of metamorphism was estimated as 380±20 Ma. The same age range was found for the igneous processes within the marginal belt. Its structures are characterized by a successive increase in alkalinity away from the continental margin. In this respect, the marginal belt is similar to the volcanic belts of active Andean-type continental margins. This interpretation is shared by most researchers on Central Asian magmatism (Kovalenko *et al.,* 1983; Gordienko, 1987; Yarmolyuk *et al.,* 1991, 1995; and Kovalenko *et al.,* 1995).

According to this interpretation, the nature of the alkali rock zone is of particular interest. These rocks are marked by a distinct intraplate mineral assemblage, reflected in the bimodal composition of the igneous associations, the high alkalinity and the wide range of minor elements. Similar compositional features are typical of other geodynamic environments whose magma sources lie beneath the lithosphere, i.e. rift zones and mantle hot-spot areas. The formation of alkaline igneous rocks zones was controlled by tensional structures such as grabens and fault depressions. The area of their distribution seems to correlate with a zone of homogeneous sublithospheric tension or rifting. The isotopic composition of the basalts from this zone provides some data about the diapiric structure responsible for the tensional rifting (Vorontsov, 1994). Figure 46 shows that the compositional distribution pattern correlates with the structure of this diapir, with the isotopically different segments, with their boundaries oriented across the strike of the marginal belt.

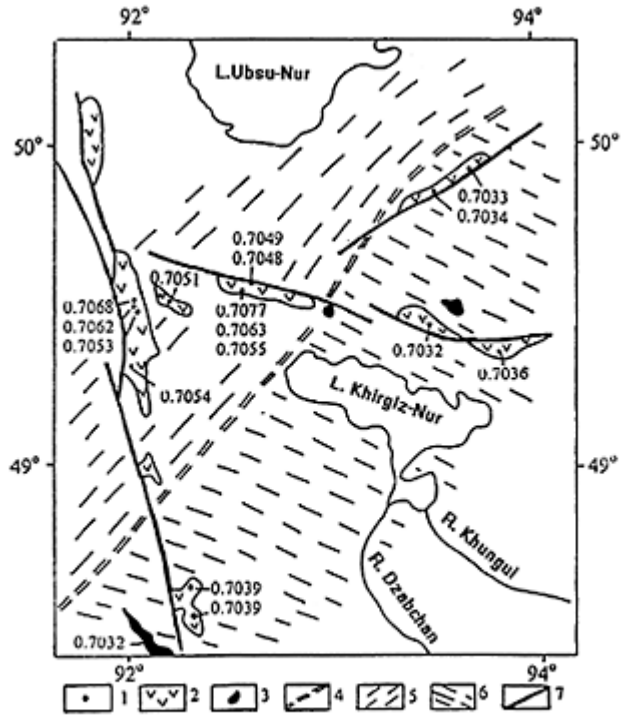

Key: 1—sampling localities and I^{o}_{Sr} value for basalt; 2—riftogenic volcanic associations; 3—alkali granite; 4–6—the hypothetical boundary between areas of igneous sources with different composition, 5—mantle with elevated I^{o}_{Sr}; 6—mantle with reduced I^{o}_{Sr}; 7—fault.

Figure 46 Isotopic compositions of basalts of the Devonian riftogenic associations of NW Mongolia.

Despite the unusual compositions and structures of the rocks of the subalkaline and alkaline zones, it should be noted that the time of rifting within the zone correlates with the period of existence of the Devonian continental margin, and the lateral series of igneous associations of the marginal belt, and that the rift associations regularly replace the calcalkaline and subalkaline associations. Hence the rift associations can be assigned to the marginal belt formations. Therefore, their origin should be considered together with the processes responsible for the generation of active plate margins. In addition, the alkaline zone can be identified as a back-arc rift zone, typical of an Andean type plate margin (Yarmolyuk and Kovalenko, 1991).

5
THE INDO-SINIDES OF INNER MONGOLIA

S.V.Ruzhentsev

The Indo-Sinian fold belt of Inner Mongolia occupies the extreme south-eastern part of the MPR (Mongol Popular Republic) stretching along the frontier of China for a distance of 650 km and with a maximum width of 70 km. Spatially, the Indo-Sinides are related to mountains such as the Bulgan-Ula, Dalantin-Ula, Agui-Ula, Khetsu-Ula, Ikh-Shara-Khad, Dzherem-Ula, Sudzniin-Nuru, Baga-Shary-Khad, Uran-Del, and Nomt-Ula (South Gobi and East Gobi Aimak (district)). This complex nappe-fold structure was formed at the early/middle Triassic boundary, at the site of a system of troughs infilled with diverse Upper Palaeozoic formations. From north to south, the Lugingol and Solonker zones can be recognized there. The former consists of a Permian flysch series and the latter is a set of tectonic sheets overlying the flysch and composed of diverse rock types (including ophiolite), ranging in age from middle Carboniferous to late Permian. The neo-autochthonous cover is Triassic-Jurassic in age.

5.1 The Lugingol Zone

This zone is a band of Upper Palaeozoic flysch. The flysch series is characterized by either a tectonic or transgressive contact with the rocks of the underlying South Gobi Zone.

The zone is subdivided into three subzones: The northern Bulgan subzone (Figs. 47 and 48) consists of dolomitic marble, stromatolitic limestone, quartzite, and phthanite (R_3) overlain transgressively by basal conglomerates (50–70 m) followed by a sequence (400–450 m) of variegated lithic (rhyolitic) tuff interbedded with basalt, epiclastics, and cherty tuffite (R_3-V?).

The middle complex, which transgressively overlies the lower one is composed of:

1) Conglomerate and gravelstone (50 m) made up of fragments of quartzite, marble, Ordovician, Devonian and Carboniferous limestone, rhyolitic tuff, porphyrite, and epiclastics.

2) Limestones (90–100 m) grey, bedded, and biogenic, yielding crinoids and bryozoos, brachiopods *Jakovlevia mammatiformis* (Fred.), *Alispiriferella litha* (Fred.), *Mogousia sinuata* (Fred.), *Spiriferella keilhaviiformis* (Fred.), *Liostella* sp., and *Kochiproductus* sp. ($P_2u–kz_1$).

3) Interbedded mudstones and biogenic limestones (70–80 m) containing Upper Permian brachiopods.

The upper complex consists of three sequences. The lower sequence (1,000–1,200 m thick) is represented by interbedded conglomerate (containing the pebbles and boulders of various granitoids, quartz porphyries, acid and basic tuffs, dolerites porphyrites, jaspers, cherts, tuffites, diverse sandstones, and carbonate rocks), gravelstones and sandstones. Fossils such as *Paracalamites striatus* (Schmal.), *Callipteris advensis* Zab., *Pecopteris ex gr. anthriscifolia* (Goepp.), and *Composteris* sp. (P_2) were collected from the lower part of the section.

The middle sequence (400–500 m thick) consists of interbedded polymictic conglomerate, sandstone, shale, and limestone, and the upper sequence (up to 1500 m thick) is a homogeneous sandy-clayey flysch.

The above-mentioned deposits (especially the lower and middle sequences) mark the northern slope of the flysch trough. The lower sequence is post-

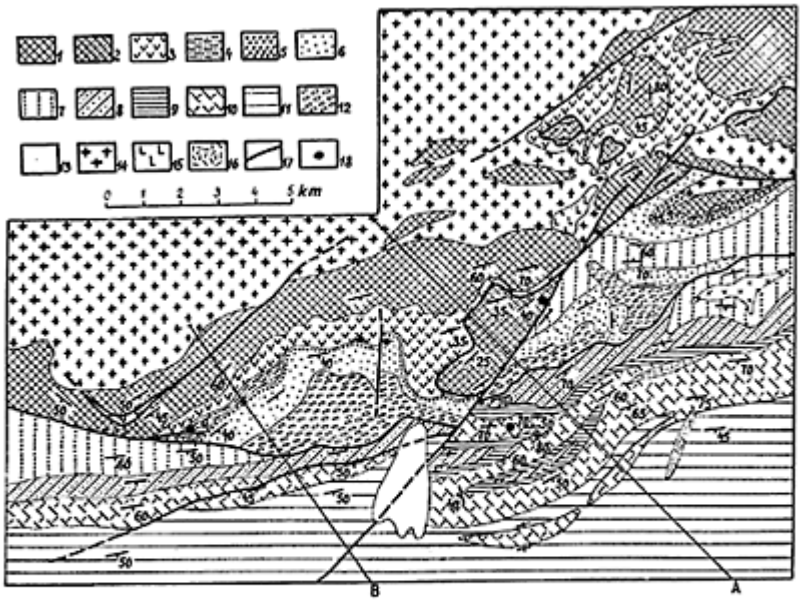

Key: 1—marble and quartzite (R_3); 2—the same in allochthonous occurrences; 3—rhyolite, dacite, andesite, and tuff (R_3–V); 4—limestone (P_2u–kz_1); 5—limestone conglomerate (P_2kz); 6—sandstone (P_2kz); 7—polymictic conglomerate, sandstone (P_2kz–t); 8—sandstone (P_2–T_1?); 10—limestone (P_2–T_1?); 11—terrigenous flysch (T_1?); 12—polymictic conglomerate (T_3); 13—Quaternary deposits; 14—granite (Pz_3); 15—basalt (K); 16—quartz-porphyry (K); 17—fault; 18—fossil sampling sites.

Figure 47 Geological map of the Bulgan-Ula Mountains (for location see Fig. 1-㊷), E 107°–N 43°).

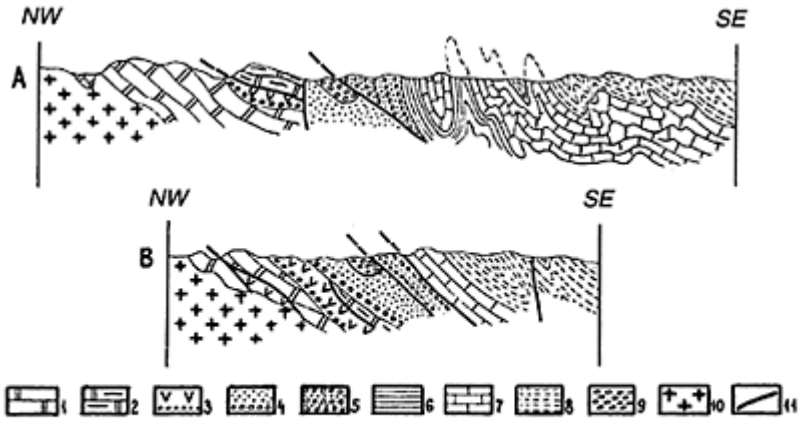

Key: 1—marble and quartzite (R_3); 2—the same in an allochthonous occurrence; 3—rhyolite, dacite, and andesite (R_3–V); 4—conglomerate and sandstone (P_2u–kz_1); 5—conglomerate (P_2kz); 6—sandstone and limestone (P_2–$T_1?$); 7—limestone (P_2–$T_1?$); 8—flysch ($T_1?$); 9—conglomerate (T_2); 10—granite (PZ_3); 11—fault.

Figure 48 Geological profiles across the Bulgan-Ula Mountains.

Kazanian in age and also Permian, i.e. Tatarian. The age of much of the upper sequence is possibly early Triassic.

Apart from the above-described deposits, conglomerates are very common in the foothills of the Bulgan-Ula Mountains. They rest unconformably on rocks of all the three sequences. These coarse-pebble and boulder varieties are massive, red, and polymictic, although the clasts are mainly limestone in composition. The pebbles are composed of both Riphean-Vendian marble and Upper Permian limestone. Based on this, and their similarity to the conglomerates of the Noyen-Somon type section, these varieties were tentatively assigned to the middle-late Triassic.

The Lugingol subzone is adequate in general to the axial, most downwarped, part of the Lugingol Trough. Mainly Upper Permian monotonous flysch deposits are present, containing no distinctive horizons. The flysch series is folded into a system of morphologically diverse cleavage folds. Fairly small, north and north west dipping and overturned closed folds complicated by shearing are the predominant fold type here. The base of the flysch series is exposed only in the most south-westerly part of the zone, in the Dalantin-Ula Mountains, where it occurs together with Permian flysch. Riphean rocks are also very common (Fig. 49).

Structurally, the area is made up of a series of folded tectonic sheets (Fig. 50). The middle (Bestuli) sheet is characterized by the presence of the most complete section. There, unconformably overlying variegated marble, quartzite, quartzsericite schist (R) are the following:

1) Conglomerate (100–120 m) variegated. Contains coarse pebbles and boulders (fragments of marble, quartzite, chert, granites, and quartz porphyries).

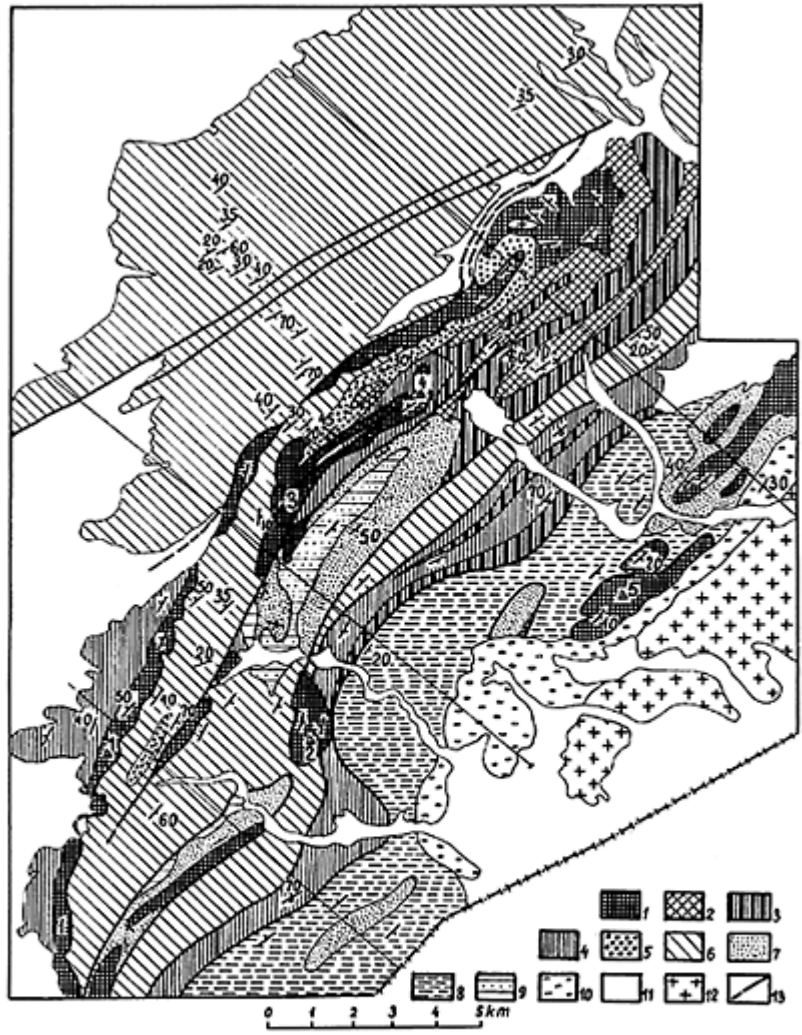

Key: 1—marble and quartzite (R_3); 2—variegated dolomite (R_3); 3—marble, chlorite–sericite slate (R_3); 4—marble, quartzite, and carboniferous chart (R_3–V); Lugingol subzones: 5—conglomerate, sandstone, and limestone (P_2u–kz_1); 6—flysch (P_2kz–t); Dzherem subzone: 7—conglomerate (P_2); 8—flysch (P_2); 9—rhyolite and its tuff (T?); 11—Quaternary deposits; 12—granite (PZ_3–T_1); 13—fault; Figures on the map: 1—Mt Dalan-Ula; 2—Mt Mant-Ula; 3—Mt Best-Ulan-Ula; 4—Mt Khangan-Ula; 5—Mt Bichigt-Ula.

Figure 49 Geological map of the Dalantin-Ula Mountains (for location see Fig. 1-㊸), E 105°–N 42°).

Key: 1—marble (R_3); 2—mica schist (R_3); 3—conglomerate (P_2); 4—flysch, P_2 (Bichiktin sheet); 5—flysch P_2 (Best-Ula and Dalan-Ula sheets); 6—conglomerate (T_2).

Figure 50 Geological section across the Dalantin-Ula mountains.

2) Rhythmically interbedded polymictic sandstone, siltstone, mudstone (300–350 m), and sandy limestone; fossils include ammonites (*Daubuchites* sp.) and brachiopods *(Retimarginifera* sp.) indicating a late Permian, apparently Ufimian age.

3) Sandy-silty flysch (up to 2,000 m thick).

The Dzherem subzone is (located on the southern slope of the Lugingol flysch trough). The authors studied a section in the Dzherem-Ula Mountains (Fig. 51).

1) The turbidite sequence (up to 600 m thick) is made up of rhythmically inter-bedded polymictic sandstones, from coarse- to fine-grained, containing conglomerate lenses (marble, quartzite, jasper, chert, tuffite, pebbles of acidic tuffs and epiclasts of granite, sandstone, Lower Carboniferous limestone).

2) Sandy-clay flysch (250–300 m).

3) Limestones (2–5 m) clay, biogenic; brachiopods: *Jakovlevia mammiformis* (Fred.), *Alispirifirella litha* (Fred.), *Spiriferella* sp., *'Neospirifer' striatoplicatus* (Toula), *Lammianmargus peregrina* Fred. (P2u-kz1).

4) Rhyolitic and dacitic tuff (70–90 m).

5) Pyroxene porphyry and variolite (20–100 m).

6) A variegated sequence (up to 1,200 m) of interbedded buff, red, and grey polymictic sandstones, gravelstones, and conglomerates (pebbles of granitoids, diorites, quartzes, and plagioclase porphyries, dolerites, quartzites, quartz-mica schists, and marbles).

To summarize, the Lugingol Zone is an extensive flysch of the South Gobi microcontinent. The flysch was deposited mainly in the late Permian. The authors interpret the Lugingol Trough as a marginal trough. This is evidenced by its sedimentary infill (flysch with elements of marine molasse) and its general trend of development, as reflected in the migration of the trough axis northwards, towards the inner part of the microcontinent. In the axial part of the trough, the flysch series is mainly Ufimian-Kazanian in age, but in the north (within the Bulgan subzone) its age is Tatarian-early Triassic.

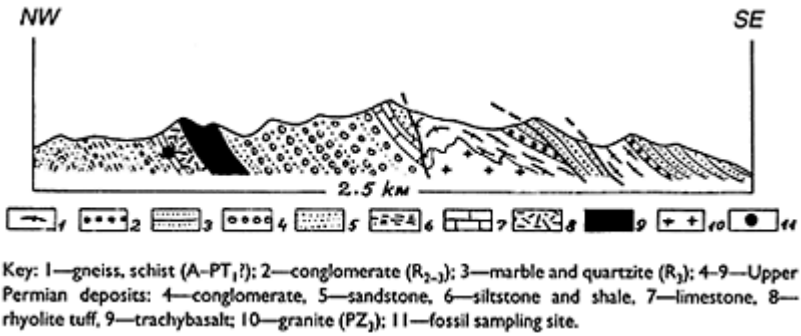

Figure 51 Geological section across the Dzherem-Ula Mountains (for location see Fig. 1-㊹), E 108° 30'–N 42° 40').

5.2 The Solonker Zone

The Solonker Zone extends along the border of China, as a narrow band, for a distance of about 120 km. It is mainly located in China, where it is known as the Solunshan-Linsi Zone (Hu and Zhu, 1991). Within Mongolia, the Solonker Zone is represented by a series of rootless tectonic nappes, resting either on the Precambrian basement or on the Lungol flysch (Fig. 52). Six nappes (in ascending order) can be recognized:

1) Sharaula—marble and quartzite (R), and rhyolite and basalt (R_3–V_1), plus a terrigenous sequence (P_2);

2) Khetsu-Ula—basalt, jasper (P_1), a terrigenous sequence (P_2), a tuff-terrigenous sequence (P_2);

3) Nomt-Ula—basalt and jasper (P_1), and mixtite (P_2);

4) Agui-Ula—limestone (C_2–P_1);

5) Tavan—sandstone and limestone (C_{2-3}), volcanics (P_1);

6) Sudzniin—ophiolite(Ruzhentsev *at al.*, 1989).

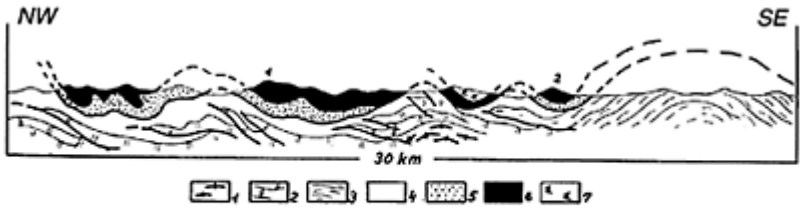

Key: 1—gneiss and schist (A–PT_1?); 2—marble (R_1); 3—quartzite, ferruginous quartzite, and marble (R_2); 4—Lugingol flysch (P–T_1) 5—Nomt-Ula and Khetsu-Ula Nappe; 6—Aigui-Ula and Tavan nappe; 7—Sudzhiin ophiolite nappe.

Figure 52 Structural section across the Solonker Zone.

The above-listed sheets infill the western (Agui-Ula Massif) and eastern (Sudzhiin-Ula, Tavan and Nomt-Ula Mountains) synforms (Fig. 53). A brief description of the sections of the above-mentioned sheets is given below.

The Shara-Ula Nappe

The base of the section is made up of marbles interbedded with microquartzites overlain by a sequence of rhyolite tuff, epiclastics, and basalt (R–V_1 up to 1,200 m) intruded by numerous dolerite dykes. Above this come basal conglomerate and a sequence (up to 1,500 m) of polymictic sandstone (grains of quartz, plagioclase, potassic feldspar, and mica, and lithic clasts, i.e. granitoids, and basic and acid volcanics (1–5 m) interbedded with pebbles of the Asselian, Sakmarian and Artinskian fusulinid limestones, indicating that the age is post-Artinskian).

The Khetsu-Ula Nappe (Khetsu-Ula Mountains)

At the base of the section of this nappe basalts (<600 m thick), are exposed, interbedded with coarse lithic tuff, epiclastics that begin to dominate the upper part of the sequence containing siliceous tuffite and ash tuff units. Above these comes a series (≤200 m thick) of sandy-silty turbidites containing lenses (up to 50 m) of massive, coarse-grained sandstone, gravelstone, and conglomerate (containing limestone, quartz-porphyry, and granite pebbles). There are also mixtite beds made up of Middle Carboniferous-Artinskian fusulinid limestone blocks. The mixtite beds considerably increase in number southwards. The turbidites are overlain by calcareous sandstones yielding the brachiopods *Jakovlevia mammatiformis* (Fred.), *Alispiriferella* sp. and *Liostella* sp. (P_2u–kz_1); above these comes a sequence (up to 500 m thick) of dacite tuff, epiclastics with limestone blocks containing the brachiopods *Spiromagnifera* sp., *Hustedea longirostris* Lich (P_2kz) allowing the sequence to be dated as as Kazanian or even Tatarian.

The Nomtula Nappe

This consists of two sheets. The sequence of the lower sheet (Uran-Del and Nomt-Ula Mountains) is as follows:

1) Aphyric basalt, plagioclase and pyroxene-plagioclase porphyritic pillow lava (50–60 m).

2) Bedded jasper (130 m) containing Lower Permian fusulinid limestone boulders and blocks.

3) Polymictic sandstone, gravelstone, and conglomerate (230–250 m) forming complex lenses in the section; they also contain fusulinid limestone blocks up to 15–20 m in size.

4) Mixtites (up to 600 m); these form a massive or coarsely bedded mass of unsorted polymictic sandstone and gravelstone, packed with boulders and blocks of fusulinid limestones, ranging in age from middle Carboniferous to early Permian. Apart from limestone, blocks of sandstone, basalt, jasper, tuffite, quartz-porphyry,

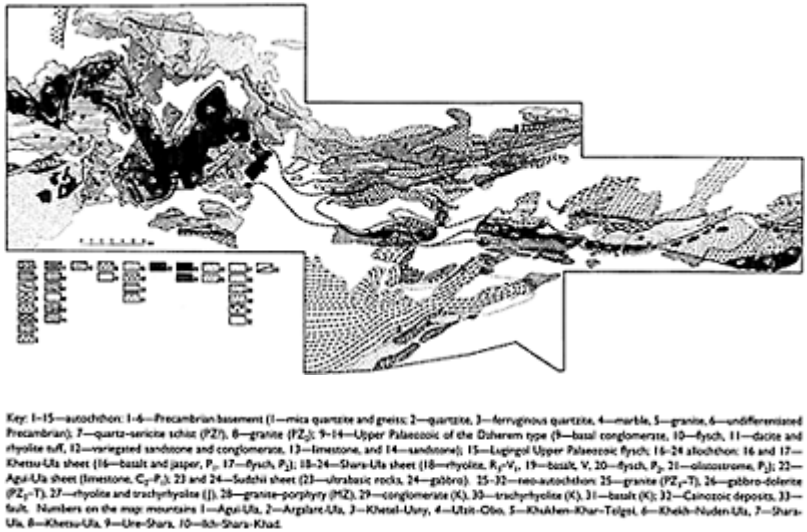

Key: 1–15—autochthon: 1–6—Precambrian basement (1—mica quartzite and gneiss; 2—quartzite, 3—ferruginous quartzite, 4—marble, 5—granite, 6—undifferentiated Precambrian); 7—quartz-sericite schist (PZ?), 8—granite (PZ_3); 9–14—Upper Palaeozoic of the Dzherem type (9—basal conglomerate, 10—flysch, 11—dacite and rhyolite tuff, 12—variegated sandstone and conglomerate, 13—limestone, and 14—sandstone); 15—Lugingol Upper Palaeozoic flysch; 16–24 allochthon: 16 and 17—Khetsu-Ula sheet (16—basalt and jasper, P_1, 17—flysch, P_2); 18–24—Shara-Ula sheet (18—rhyolite, R_2-V_1, 19—basalt, V, 20—flysch, P_2, 21—olistostrome, P_2); 22—Agui-Ula sheet (limestone, C_2-P_2); 23 and 24—Sudzhi sheet (23—ultrabasic rocks, 24—gabbro). 25–32—neo-autochthon: 25—granite (PZ_3-T), 26—gabbro-dolerite (PZ_3-T), 27—rhyolite and trachyrhyolite (J), 28—granite-porphyry (PZ), 29—conglomerate (K), 30—trachyrhyolite (K), 31—basalt (K); 32—Cainozoic deposits, 33—fault. Numbers on the map: mountains 1—Agui-Ula, 2—Argalant-Ula, 3—Khetel-Uuny, 4—Ulzit-Obo, 5—KhuAhen-Khar-Tolgoi, 6—Khekh-Nuden-Ula, 7—Shara-Ula, 8—Khetsu-Ula, 9—Ure-Shara, 10—Ikh-Shara-Khad.

Figure 53 Geological map of the Angui-Ula, Khetsu-Ula and Ikh-Khara-Shad massifs (for location see Fig. 1-㊺), E 108°–N 42°10′).

and granite also occur. The blocks are locally 10 m in size and the upper part also contains olistostromes extending for several kilometres and up to 100 m thick.

The upper sheet of the nappe (in the Targany-Nuru Mountains) is made up of aphyric basalt pillow lavas (350–370 m), locally interbedded with jasper and silicic tuffites. The basalts are overlain there by a sequence of mixtites (up to 1,100 m), differing from

mixtites of the lower sheet in the presence of larger blocks and the appearance of acid tuffite and tuff bands in the upper third of the section. Apparently the mixtites there can be correlated with the terrigenous sequences of the Khetsu-Ula Nappe.

The Agui-Ula Nappe (Agui-Ula, Baga-Shara-Khal, Uran-Del, Dzhun-Mand Mountains)

These are composed of homogeneous grey, bituminous, bedded limestone yielding abundant Kasimovian, Gzhelian, Asselian, Sakmarian, and Artinskian fusulinids. On the whole, the rocks at the base of the nappe are young in a northerly direction. The limestones form a chain of diverse tectonic relics, locally represented by secondary folds. The largest of them (Agui-Ula Mountains) is 10 km across. The thickness of limestones in each particular case does not exceed 400–500 m.

The Tavan Nappe

This is present only in the eastern part of the zone. The following rocks crop out there:

1) Intercalated (600–700 m) of recrystallized banded limestones, forming beds up to 30 m thick, coarse-grained epiclastics of lavas and acid and intermediate intrusive rocks. Locally the calcareous sandstones contain lenses of brachiopod limestones (containing the remains of *Laniputula* sp. and *Cancrinella alazeica*, C_{2-3}).

2) Lithic andesite tuff (250 m).

3) Andesites (up to 800 m), forming massive flows, intercalated with, epiclastites, tephroids, and tuffites.

4) Interbedded andesite tuff, epiclastics, dacite tuff, ash tuff and tuffite (300–400 m). Limestone bands (0.5–9.7 m) appear in the upper part of the sequence; they contain the brachiopods *Spiriferella* sp., *Waagenoceras* sp., *Megausia* sp., and *Paramagnifera nativa* Manakov (P_1k).

The Sudzhiin Nappe

This consists mainly of ultrabasic rocks. They are very common in the Sudzhiin-Ula Mountains, where they form a thick sheet, resting on the sandstones, mixtites, and limestones of the Khetsu-Ula, Nomt-Ula, and Agui-Ula nappes. Within Mongolia, the nappe is made up of harzburgites. Blocks of wehrlite, banded gabbro, and massive gabbro occur locally. In the western part of the zone, the gabbros crop out over an extensive area. The nappe has not been strongly *mélanged*.

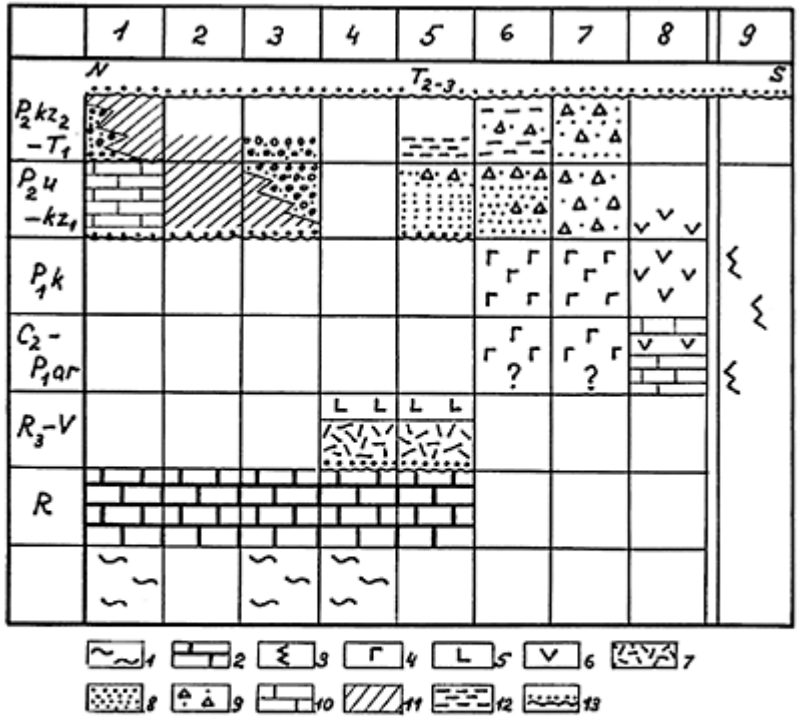

Key: 1—gneiss, schist; 2—marble and quartzite; 3—ultrabasites and gabbro; 4—tholeiitic basalt; 5—alkali basalt, 6—basaltic andesite and andesite; 7—rhyolite, dacite, and tuff; 8—sandstone, sandy–shaly turbidites; 9—mixtites; 10—limestone; 11—flysch; 12—tuffite and tuffaceous siltstone; 13—Triassic molasse (neo-autochthon). Numbers on the sections: 1—Lugingol Zone: 1—Bulgan, 2—Lugingol and 3—Dzherem subzones; Solonker Zone: 4—autochthon; 5—Shara-Ula, 6 and 7—Khetsu-Ula (6—lower and 7—upper sheets); 8—Agui-Ula and Tavan, 9—Sudzhiin nappes.

Figure 54 Correlation of the main complexes of the Indo-Sinides of Mongolia.

A neo-autochthonous complex is represented by a sequence (300–350 m) of red conglomerates and sandstones (continental molasse), tentatively assigned to the Triassic. These deposits show a polymictic clast composition sandstone, limestone, granite, various volcanics, gabbro, and ultrabasites. The red molasse is intruded by Triassic granites.

The above-listed complexes of deposits represent a series of allochthonous masses displaced northwards. Figure 54 shows their original locations. The facies relationships between the Lugingol flysch and protrusions of the Precambrian rocks along the northern periphery of the Solonker Zone can be easily established. South of the protrusions, similar relationships are evident for the Permian terrigenous deposits of the Shara-Ula Nappe. The similarities between the Shara-Ula, Khetsu-Ula, and Nomt-Ula sections

suggests that part of a single tectonic zone formed in the late Permian. It is not so obvious in the case of the Agui-Ula and Tavan nappes. It can be only stated that the formation of the Carboniferous-Permian and underlying nappes began in Ufimian times and continued into the late Permian, as evidenced by the composition and age of the mixtites in the Khetsu-Ula and Nomt-Ula Mountains. Based on the above evidence, a palaeotectonic cross-section for the Indo-Sinides of Mongolia may be shown as follows (from north to south):

1) the Lugingol flysch foredeep,

2) a protrusion of the Precambrian basement (the autochthon of the Solonker Zone),

3) the Solonker Trough (Shara-Ula, Khetsu-Ula, and Nomt-Ula nappes),

4) the limestones of the Agui-Ula and Tavan nappes are tentatively identified as deposits of the southern margin of the Solonker Trough,

5) ophiolites form the southernmost element.

The data available for the Mongolia do not make it possible to unambiguously interpret the position of the ophiolites within the belt palaeostructure. The data for contiguous areas of China are contradictory. Some workers (Tang, 1990) assign ophiolites at the Mongolia-China border to the Ondersum (Vandermyao) Belt, identifying them as Cambrian formations, others (Hu and Zhu, 1991) identify the Solunshan-Linsi Devonian-Lower Carboniferous ophiolite suture there; this is a relict structure of the Variscan ocean basin. The data presented above and data from the Upper Palaeozoic deposits of Chinese Inner Mongolia (Mueller *et al.*, 1991) imply the existence of a Carboniferous-Permian ocean basin. It could well have been generated by the superimposition of rifting processes on the ancient Ondersum ophiolite suture (Ruzhentsev *et al.*, 1992b).

The following palaeotectonic interpretation may be proposed for the deposits of the Solonker Zone. Flysch infilled the Lugingol foredeep, which was emplaced during the late Permian at the margin of the South Gobi microcontinent. The foredeep developed as a compensatory structure, due to the northward movement of the folded front of the Indo-Sinides of Inner Mongolia. The more southerly Solonker Trough was infilled by a thick sequence of Upper Permian polymictic clastic rocks. Two parts are recognized within the trough. In the northern (Shara-Ula Nappe) part, the Permian deposits rest on the Precambrian cover of the microcontinent; the basement is not exposed in the southern (Khetsu-Ula and Nomt-Ula) part. However, volcanics are very common there.

The basalts of the Khetsu-Ula Nappe and the lower sheet of the Nomt-Ula Nappe belong to the weakly differentiated tholeiite series. Based on their petrochemistry, the following rocks are recognized (Table 10): olivine basalt (aL^{l}—0.68–0.75, f^{1}—20–21.3), mesocratic basalts (aL^{1}—0.78–1, f^{1}—16.7–19.2) and leucobasalt (aL^{1}—0.78–1, f^{1}—16.7–19.2). In general, the basalts of the upper sheet of the Nomtula Nappe are very similar to them. These are also rocks of the tholeitic series. The latter differ mainly in their high alkalinity. The petrochemical types described above are also recognized there. A high TiO_2 content (2%) indicates magma generation within an oceanic rise or incipient island arc. In their Co, Cr, Ni, Cu, and Yb contents, the basalts are similar to those of an intra-oceanic volcanic rise.

Above the volcanic horizon of the Solonker Trough are situated the polymictic sandstones associated with huge masses of blocky mixtites. Genetically, these are olistostrome formations, which resulted from the overthrusting of the Agui-Ula and

Tavan nappes, caused by the gradual closure of the trough in the late Permian. The emplacement of island-arc volcanics took place during the late Carboniferous and early Permian, implying the existence of synchronous crust. The Solonker Trough was only emplaced in the later early Permian, and so we can regard it as a newly formed structure,

The closure of the Solonker Basin began in Ufimian times. Island-arc series were overthrust on the Solonker deposits. The onset of the process is marked by the substitution of silicic volcanic deposits for polymictic sandstones, and the appearance of the first mixtite beds in the section. Overthrusting of the Agui-Ula, Tavan, and Sudzhiin allochthons continued during the Kazanian and Tatarian. A flysch basin was formed at that time around the outer periphery of the Indo-Sinides. In the early Triassic, collision processes continued farther north. The strata infilling the Solonker Trough gave rise to the formation of the lower nappes (Shara-Ula, Khetsu-Ula, and Nomt-Ula) already lying within the microcontinent. Their minimum visible distance of the displacement of the allocation is 40 km.

Thus, the development of the Indo-Sinides of Inner Mongolia was caused by three processes

1) the opening of the Inner Mongolian palaeo-ocean as a result of the rifting of the Eurasian Variscan continent in the Carboniferous,

2) the formation of an accretionary system (formation of an island-arc and back-arc trough, C_3–P_1),

3) continental collision (closure of the palaeo-ocean and the appearance of nappes obducted on to the margin of the South Gobi microcontinent, P_2–T_1).

6
UPPER PALAEOZOIC CONTINENTAL MARGIN MAGMATISM OF MONGOLIA

V.V.Yarmolyuk and V.I.Kovalenko

By the beginning of the late Palaeozoic the continental part of Mongolia had been extended by the addition of the South Mongolian Hercynides, within which continental crust had been formed by that time. The boundary with the palaeo-Tethys moved to the south (according to present-day co-ordinates), to the Solonker Zone, where complexes of marine basins, including ophiolites, were formed in late Palaeozoic times (Ruzhentsev *et al.*, 1990).

The continental part of Mongolia was affected by large-scale igneous processes in late Palaeozoic times (Fig. 55). This resulted in the creation of a huge igneous region, covering about 90% of the country. The structure of the province is governed by:

1) linear volcanic belts, following the continental boundary;
2) granitoid intrusions associated with the belts; and
3) the Khangai granitoid batholith: Mongolia's largest.

The igneous region was formed in two stages (Yarmolyuk, 1983; Yarmolyuk and Kovalenko, 1991): an early stage (later early Carboniferous to middle-late Carboniferous) and a late stage (the end of the Late Carboniferous to the Permian).

6.1 Early-Stage Magmatism

Throughout almost the whole of the Carboniferous, igneous activity was confined to the area of the South Mongolian Hercynides, where a vast E–W South Mongolian volcanic belt was formed (Fig. 56). Recent hypotheses regarding the structure of the volcanic belt are based on the studies of Sinitsin (1956), Mossakovsky and Tomurtogoo (1976), Durante (1976), Yarmolyuk (1978, 1983), and many others. The data obtained suggest that volcanic activity began almost ubiquitously within the belt at the end of the Tournaisian, and continued up to the late Carboniferous (Fig. 57). The belt consists of two large segments, separated roughly along the 104° meridian, with their constituent volcanic suites differing in composition. The *western segment* is made up of both basic-intermediate and acid suites. This can be exemplified by the structure of a volcanic terrain, which is associated with the Noyen and the Tost ridges, and is the most extensive volcanic field

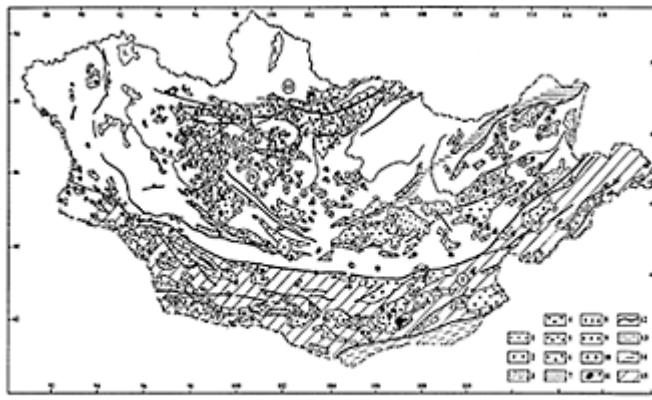

Key: 1–3—calcalkaline volcanics: 1—basaltic andesite and andesite, 2—andesite and dacite, 3—rhyolite; 4–6—subalkaline volcanics: 4—trachyandesite, 5—trachyrhyolite, 6—subalkaline basalt, 7—volcanics of bimodal (basalt–comendite and basalt–pantellerite) associations; 8—diorite and granodiorite; 9—granite; 10—leucogranite and granosyenite; 11—alkali granite; 12—fault; 13—marine assemblages of the Solonker Trough; 14—marine assemblages of the Dzhargalantuin Trough; 15—South Mongolian Hercynides; Circled figures are igneous belts: I—South Mongolian, II—Central Mongolian, III—North Mongolian, IV—Khangai Batholith.

Figure 55 Distribution of Upper Palaeozoic igneous rocks in Mongolia.

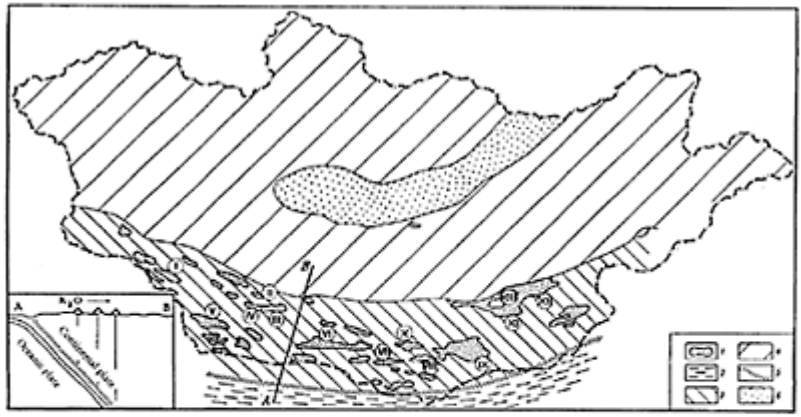

Key: I—belt of volcanic exposures; 2–6—structural complexes: 2—Indo-Sinides, 3—Variscides, 4—Caledonides, 5—reconstruction of a palaeo-subduction zone exposure, 6—Khangai–Khentei superimposed trough. Volcanic fields and areas: I—Bor–Khavtsagal Stow (Urochishche), II—Sumen–Khairkhan Ridge, III—central Edrengiin–Nuru Ridge, IV—western Edrengiin–Nuru Ridge, V—Arslan–Khairkhan Ridge, VI—Noen–Tost Ridge, VII—Khaldzan-Ula Mountains, VIII—Bayan–Obo district, IX—Khan–Bogdo district, X—Tsokhiotuin–Khida district, XI—Ulugei–Khida district, XII—Mandakha district, XIII—Tsagan–Suburgin district. Inset map. Reconstruction of a palaeo-subduction zone, based on an increase in the K_2O content in rocks along the A–B section (Yarmolyuk, 1983).

Figure 56 Location of the Carboniferous volcanic formations of Mongolia.

within the belt. It stretches E–W for 250 km, with a width of more than 30 km (Fig. 58).

The sequence of Carboniferous volcanics is made up of three suites: the lower suite comprises a series of rhyolite tuffs and lava breccias; the middle suite is made up of andesite-basalt- and andesite porphyrites; and the upper suite is made up of rhyolite-and rhyolite-dacite normal and welded tuffs and tuffaceous-sedimentary rocks (Yarmolyuk, 1978).

The suite of rhyolite tuffs and lava breccias is exposed in the central part of the Tost Ridge, in the core of an anticline structure, cross-cut by the Takhilga-Obo granite intrusion. The suite is made up of monotonous greenish-grey rhyolite tuffs and lava breccias, forming a number of thick (≤40 m) laterally extensive beds; south of the intrusion its visible thickness is over 600 m. Subordinate to the tuff and lava breccia are single lava flows of andesite porphyries and thin layers of terrigenous rocks which are especially numerous in the upper part of the sequence. A Viséan fossil flora was observed in these beds (Durante, 1976).

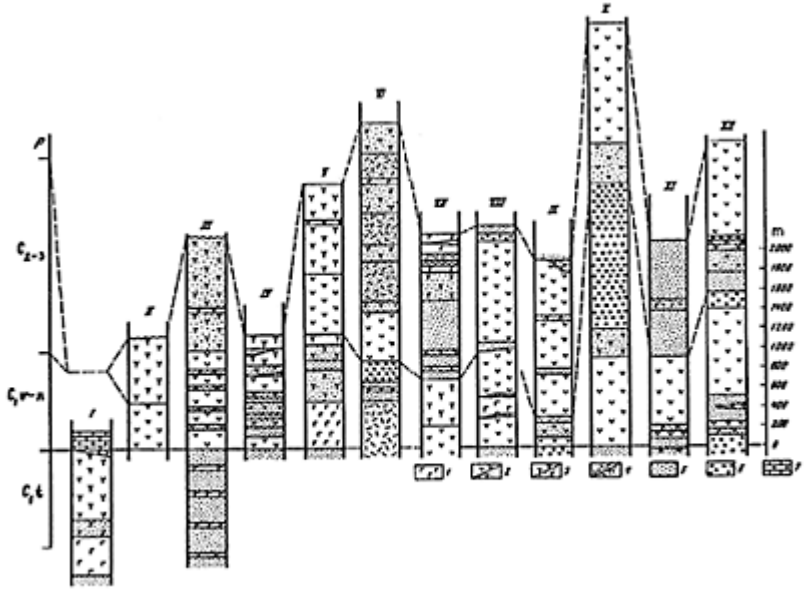

Figure 57 Correlation of the Carboniferous volcanic formations of Mongolia. (The numbering of the sections is the same as that of the volcanic fields in Fig. 56, where these sections were studied).

The distribution of rhyolite tuffs and lava breccias is probably localized. The fact that acid volcanics are absent in other areas of Mongolia, where the bases of the volcanic sections can be observed, and also the way in which the overlying andesite porphyries rest directly on the folded basement suggest the distribution of the rhyolite is restricted and that it was probably associated with an isolated volcanic focus. The sequence of rhyolite tuffs and lava breccias is disconformably overlain by a suite of alternating tuffaceous-sedimentary rocks, conglomerate and gravelstone, replaced at the top by a suite of andesite-basalt- and andesite porphyries. The tuffaceous-sedimentary rocks contain the impressions of fossil plants, typical of the Lower to Middle Carboniferous (Yarmolyuk, 1983).

The suite of andesite-basalt- and andesite porphyries is made up of sheets of lava flows, their tuffs, and tuffaceous-sedimentary rocks, intercalated with volcanics. Outcrops of all of the rocks were found in the areas adjacent to the volcanic terrain, where the deepest horizons of the igneous association can be found.

A series of lava sheet flows, displaying well-developed zones of red and violet scoria, as well as coarse bomb and lapilli tuff, occurs in the east of the volcanic terrain. The lower and upper parts of the suite are dominated by tuffs and rather homogeneous lava sheet flows, respectively. The suite of andesite-basalt- and andesite porphyries is underlain by schists of possibly Silurian age; therefore, in this area its section commences with saprolites (formed by the weathering of the schists) followed by conglomerates and tuff conglomerates, with fragments of lava, occurring together with pebbles of schist. The thickness of the suite of andesite-basalt- and andesite porphyries there is in excess of 600 m.

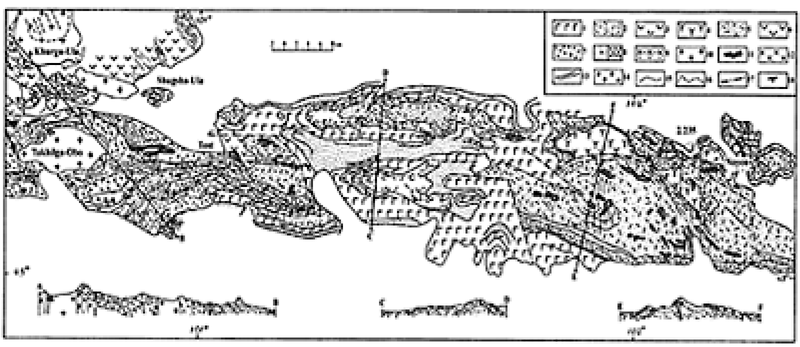

Key: 1–3—contrasting volcanic sequence: 1—basalts and their tuffs, 2—trachyrhyolite and comendite, 3—rhyolite–dacite ignimbrite, 4—andesite–dacite and dacite, 5—sequence of common and welded rhyolite tuff, 6—basaltic andesite–andesite porphyry sequence, 7—rhyolite tuff and tuff lava sequence; 8—sandstone, siltstone, tuffaceous–sedimentary rocks (a), conglomerate (b); 9—folded basement, 10—granite, 11—granite–porphyry, 12—diorite, 13—andesite porphyry, granite–porphyry and felsite–porphyry dykes, 14—rocks metamorphosed to hornfels, 15—geological boundaries; 16—structural lineaments in granitoid massifs (inferred from aerial photographs); 17—faults, 18—dips and strikes.

Figure 58 Geological structure of the Upper palaeozoic volcanic formations of the Noen and Tost ridges (VI on Fig. 56) (after Yarmolyuk, 1978).

Another area showing multiple andesite porphyry outcrops is located on the northern, eastern, and south-eastern slopes of the Tost Ridge (within the area of the Takhilga-Obo-Khurgu-Ula Mountains). The suite of andesite-basalt- and andesite porphyries there shows the greatest thickness and has a two-part structure. Tuffs of mixed and andesite composition, including a few lava flows occur in its lower part. A Lower to Middle Carboniferous flora was found in the finegrained tuff (Table 10). The upper part of the sequence, over 600 m thick, is composed almost entirely of lavas.

In different areas of Mongolia the rocks of the suite show a similar petrography and are represented mainly by plagioclase-, or, less commonly, pyroxene-plagioclase porphyries, which are compact, massive, bluish-grey, violet, and buff rocks.

Table 10 Distribution of fossils in the late Palaeozoic volcanic rock sections of the Noyen and Tost ridges.

Age	Strata	Tost Ridge, SE slope	Somon Noyen, (2 km NE)	Noyen Ridge Southern slope (2,235 m)
Early Permian	Bimodal volcanics	*Dicranophyllum?* sp. Leaves of the Ginkgophyte, *Ginkgophyllum vsevolodi* Zal. type	*Barakaria* sp. *Angaropteridium* cf. *Cardiopteroides* (Schm.) Zal. *Adiantites?* sp.	*Ryfloria,* with fine dorsal grooves
Late Carboniferous			*Dicranophyllum* sp. *Rufloria* sp. *Cordaites* cf. *zalesscyi* Durante	
Middle Carboniferous	Rhyolitedacite and dacite tuff	Small finecushioned lepidophyte with leaf		
	Andesite porphyrite	*Abacanidium* sp. vel *Angaropteridium* sp.		
Early Carboniferous	Tuffstone and conglomerate	*Abacanidium* ex. gr. *ligulaeformis* (Such.) Durante, *Abacanidium* sp. vel *Angaropteridium* sp.		

The first appearance of the suite of andesite-basalt- and andesite porphyries was caused by the beginning of regular volcanic activity within the Noyen and the Tost ridges. During the eruptions of this cycle, about 4,200–5,200 m^3 of lavas and tuffs were erupted. They covered much of Mongolia (an area of 7,000–7,500 km^2) with a layer 600–700 m thick (Luchitsky, 1983).

A suite of normal and welded rhyolite tuffs and tuffaceous-sedimentary rocks occurs between the underlying suite of andesite-basalt- and andesite porphyries and the overlying bimodal volcanic suite. The latter is dated as late Carboniferous to early Permian (Yarmolyuk, 1983), therefore the age range of the formation of the rhyolite tuff suite is narrowed down to the middle Carboniferous-earlier late Carboniferous. This is consistent with the Carboniferous flora found in the tuff (Table 10).

In the eastern part of the volcanic terrain, the thickness of the suite exceeds 2,600 m. It conformably overlies the porphyritic lava flows with tuffs of mixed composition, containing andesite porphyry fragments. A few lava flows of andesite porphyry still occur in the lower horizons of the suite.

The following features, which show how it was formed, can be noted in the structure of the suite. Its lower part, about 400–500 m thick, contains alternating rhyodacite and rhyolite tuffs, ignimbrites, and tuffaceous-sedimentary rocks. The upper 1.5 km of the section are saturated with relatively thin beds of variously coloured, acid, welded tuffs. All of these rocks are dominated by fragments of plagioclase crystals. Quartz is uncommon. The ashy material within the welded tuffs shows a eutaxitic structure; it has been recrystallized to form a finely crystalline quartz-feldspar aggregate. Upwards the suite is replaced by a thick (300–400 m) undifferentiated sheet of green welded tuff, overlain by a unit of variegated tuff sandstone. Basalt lava flows and sporadic thin laterally extensive beds of violet, brown trachyrhyolite ignimbrite, typical of the overlying suite of bimodal volcanics, appear in the upper horizons of the unit.

In the west of the area, within the Tost Ridge, the suite of rhyolite tuffs and tuffaceous-sedimentary rocks is most completely represented in the south-eastern part of the ridge. There a unit of tuffaceous-sedimentary rocks, more than 100 m in thickness, overlies the andesite porphyries without apparent disconformity. It is dominated by normal and welded rhyolite- and rhyolite-dacite tuff. Thin layers of tuffaceous sandstone and tuffaceous siltstone are subordinate. Welded tuff occurs mainly in the lower and middle horizons of the suite. It is represented by compact, buff, pink, and dark-grey rocks, similar to the eutaxitic lavas in structure. Topographically they form extensive scarps, where the rocks show columnar jointing and platy parting. In places the beds of welded tuff form series, composed of a group of beds, similar in thickness, overlain by a bed of normal tuff.

Even higher up the sequence, the horizons of the suite are made up of green vitric and crystal welded tuffs, which form a very thick bed. The composite thickness of the suite there is about 2,300–2,500 m. The suite as a whole is similar in structure to the volcanics occurring in the east of the volcanic terrain.

Despite differences in the composition of the suite, a generalized sequence can be reconstructed. The lower parts of the suite are dominated by tuffaceous-sedimentary rocks and poorly stratified vitric tuff. Higher up the section are welded tuffs, intercalated with tuffaceous-sedimentary rocks, volcanic breccia, or forming moreor-less thick series of beds. The upper parts of the suite are dominated by thin beds of compact, buff, violet,

and grey welded tuff. In places, the separate beds can be grouped to form complex composite beds with no boundaries between them. A similar process is probably characteristic of the beds of welded tuffs, which probably formed at about the same time, and whose boundaries are blurred due to high-temperature alteration and the lithostatic pressure of the overlying beds.

All of the rocks of the group under consideration are markedly leucocratic in appearance. They contain crystal fragments, which are predominantly acid plagioclase; quartz is subordinate and orthoclase is rare. Dark minerals are usually absent; biotite or pyroxene have only been noted from a few rocks. The latter are probably fragments of phenocrysts from basalts; fragments of the same basalts can also be seen in the rocks.

The rocks show various relict textures: lithoclastic, eutaxitic, and pseudoflow. The latter occur in facies of the welded tuff where the ash particles and individual fragments of glass are flattened and drawn out into thin, elongate, parallel lenticules.

The total volume of erupted material within the rhyolite tuff suite, accumulated during its formation, is approximately 14,000 to 17,000 m^3 (Luchitsky, 1983).

In the *eastern segment* of the volcanic terrain, Carboniferous volcanics are chiefly represented by basic and intermediate rocks, while the more acid rocks are markedly subordinate and are usually associated with volcanic vents or small extrusions.

The volcanic terrain of the Tsokhiotuin-Khida area (Fig. 59) can be considered as a typical volcanic field of this segment (Durante, 1976; Yarmolyuk, 1978). The section is made up of the following units, in ascending order: tuffaceous-sedimentary, lower andesite porphyry, sandstone-conglomerate, tuffaceous, and upper andesite porphyry suites. The contained plant remains indicate a Tournaisian age for the tuffaceous-sedimentary suite. The lower andesite porphyry suite is assigned to the Viséan and probable lower Serpukhovian (Durante, 1976). It is dominated by sheets of andesite and andesite-basalt porphyries, alternating with tuffs and tuff conglomerates, as well as with sandstones, siltstones and siliceous sinter. The thickness of this suite is 1,200–1,500 m.

The suite of andesite porphyries is overlain by a suite (≤1,700 m thick) of conglomerate, gravelstone and sandstone, containing numerous plant remains, typical of the Serpukhovian-lower Middle Carboniferous. Tuffs, tuff sandstones and tuffaceous conglomerates are widely represented high up in the conglomerate sequence. The rocks, which reach 500 m in thickness, are grouped together as a tuffaceous member. This member is overlain by the alternating upper andesite porphyry suite: an assemblage of subaerial andesite and basalt porphyry, showing unusual red scoria zones in the upper parts of the lava flows. The lava flows are intercalated with tuffs and agglomerates, as well as with volcanic grey gravelstones and rudaceous sandstones. The thickness of the suite is over 2,000 m. Its concordant relationship with the underlying rocks suggests that the porphyry is middle Carboniferous to early late Carboniferous in age.

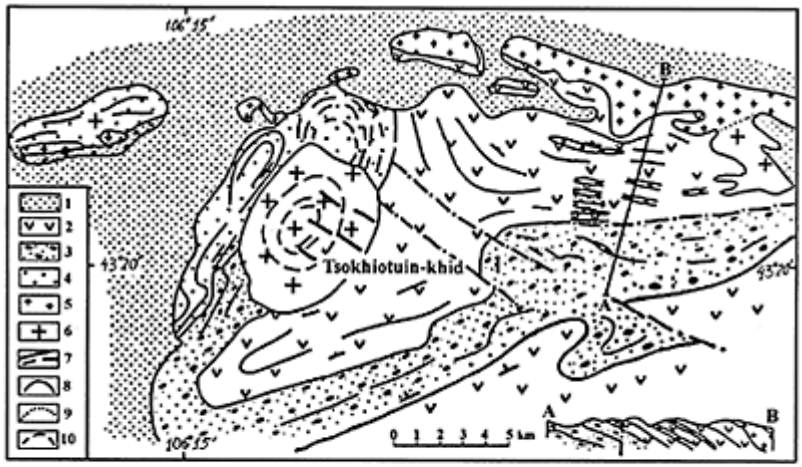

Key: 1—Upper Cretaceous and Cainozoic deposits, 2—andesite porphyry, 3—conglomerate, 4—Middle Palaeozoic folded formations, 5—granite-porphyry and rhyolite; 6—granodiorite, 7—syenite-porphyry dykes, 8—geologic boundaries, 9—facies boundaries, 10—structural lineaments plotted from aerial photographs.

Figure 59 Geological structure of the Tsokhiotuin-Khid district (⊗ on Fig. 56) (after Yarmolyuk, 1978).

It is evident from a correlation chart of the sections (Fig. 57) that other volcanic terrains, from different areas of Mongolia, are similar in structure. It should be noted that the age range of the sequences is reliably confirmed by numerous Carboniferous plant remains from the thin sedimentary layers within the volcanics (Durante, 1976). By and large, currently available data suggest that the volcanic activity in this part of the volcanic belt took place mainly after Viséan times. Lavas *sensu stricto* usually make up two rock series, one of which was formed during the late early or probably early middle Carboniferous; the other being middle to late Carboniferous in age. Volcanics of different ages are still similar in composition; they are represented by andesite and andesite-basalt and, to a lesser degree, basalt.

The chemistry of the Carboniferous volcanics has been studied in detail by Marinov, (1973), Yarmolyuk (1978), and Luchitsky (1983). Table 11 gives some examples of the chemical composition of the rocks. As a whole, the volcanics belong to the calcalkaline petrochemical series (Fig. 60). The volcanics show relatively high Na_2O contents and Na_2O/K_2O ratios greater than one. As a whole, petrochemical series are consistent with a successive up-section change in composition of the igneous rock series, from basalt through andesite to dacite and rhyolite, thus suggesting a homodromous direction of igneous differentiation during the development of the Carboniferous volcanicism.

Table 11 Chemical composition of representative rocks of the Carboniferous volcanic associations of the South Mongolian volcanic belt.

	1	2	3	4	5	6	7	8	9	10	11	12	13	14	15	16	17
SiO_2	54.96	53.33	51.06	48.64	55.06	60.32	63.14	64.65	64.83	56.70	57.00	55.66	72.40	71.20	73.90	75.50	77.05
TiO_2	0.83	0.77	0.73	0.92	0.76	0.61	0.65	0.53	0.82	0.74	0.74	0.94	0.43	0.41	0.36	0.26	0.18
Al_2O_3	16.10	16.45	17.17	17.56	18.86	16.80	18.25	17.04	15.49	18.00	18.00	17.10	13.60	14.80	13.80	12.60	12.80
Fe_2O_3	4.80	1.65	1.79	2.56	4.94	1.23	0.30	0.63	1.62	2.83	5.24	3.61	1.39	1.69	0.87	0.74	0.91
FeO	2.69	7.48	8.49	8.70	2.69	4.63	5.73	2.80	2.40	4.24	3.02	3.95	1.09	1.09	0.84	0.73	0.58
MnO	0.12	0.28	0.22	0.19	0.13	0.11	0.19	0.11	0.12	0.16	0.12	0.13	0.06	0.09	0.07	0.07	0.04
MgO	4.66	4.58	3.58	4.58	2.89	3.85	1.89	0.99	1.14	4.47	5.60	4.91	0.96	0.64	0.24	0.36	0.36
CaO	6.99	9.00	8.83	9.12	6.82	4.04	1.79	2.08	3.17	3.70	4.63	5.37	0.90	1.70	1.10	0.70	0.65
Na_2O	3.16	3.32	2.84	2.88	3.38	3.83	2.76	4.80	5.00	3.51	3.08	3.55	5.27	3.82	4.11	2.77	2.7
K_2O	2.32	1.36	2.46	1.90	2.68	2.95	2.19	4.34	2.40	1.90	0.57	0.29	2.19	2.47	2.82	4.86	3.38
P_2O_5	0.99	0.34	0.53	0.40	0.38	0.31	0.36	0.20	0.16	0.49	0.52	0.40	0.16	0.02	0.08	0.09	0.10
LOI	3.72	1.59	2.50	2.92	1.50	2.26	3.00	2.45	1.63	3.68	2.24	2.52	1.16	1.02	1.38	1.16	1.00
Total	100.34	100.15	100.20	100.37	100.09	100.94	100.25	100.62	98.78	100.42	100.76	99.43	99.61	99.05	99.57	99.84	99.82

Note: 1–9 volcanic field of the Edrengiin-Nuru Ridge, Ridge, rocks were sampled up the section (Luchitsky, 1983): 1–6—andesite—basalt sequence, 7–9—dacite sequence, 10–17—volcanic field of the Noyen Ridge, rocks were sampled up the section (Yarmolyuk, 1978): 10–12—andesite-basalt sequence, 13–17—dacite rhyolite sequence.

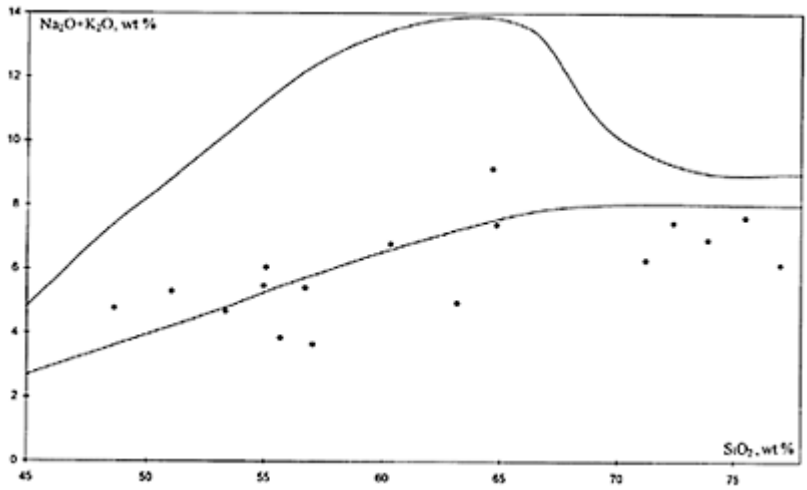

Figure 60 Compositions of volcanic rocks of the southern Mongolian volcanic belt, plotted on an SiO_2–(Na_2O+K_2O) classification diagram.

Plutonic Rock Associations

Together with the volcanics, various granitoids, grouped together to form associations of granodiorite-granite, granite, leucogranite, and monzonite-syenitegranosyenite, participated in the structure of the Carboniferous volcanic belt of southern Mongolia. As a rule, the granitoid bodies occur in anticlinal structures and mainly intrude the lower parts of the Carboniferous igneous suites. Nowhere are they covered by the Permian igneous and Permo-Triassic molasse sequences, which are relatively common in South Mongolia. Therefore their age is tentatively determined as Carboniferous. Table 12 gives the chemical composition of this rocks.

To conclude our discussion of the Carboniferous magmatism of South Mongolia, it should be noted that conspicuous zoning in the distribution of volcanics of different of alkalinity, first of all K_2O, was found across the whole of the volcanic region. In rocks of similar type and age the K_2O content increases from south to north, i.e. from the edge of the palaeocontinent inwards (Yarmolyuk and Kovalenko, 1982) (Fig. 61, see Fig. 56). These changes have been interpreted from the viewpoint of the formation the volcanic belt above the subduction zone which dived under the Late Palaeozoic North Asiatic continent at an angle of 45°. It should be noted that the volcanic belt was situated at the edge of the continent; this position, taking into account the petrochemical zoning within the belt demonstrates its similarity with volcanic belts of Andean-type active continental margins.

Table 12 Compositions of the late Palaeozoic granites of the South Mongolian volcanic belt.

n/n	**1**	**2**	**3**	**4**	**5**	**6**	**7**	**8**	**9**	**10**	**11**	**12**
SiO2	74.88	72.07	72.99	74.56	73.90	76.60	72.32	67.88	68.88	69.33	71.03	70.12
TiO2	0.18	0.44	0.24	0.38	0.10	0.12	0.12	0.35	0.50	0.55	0.55	0.48
Al_2O_3	12.70	13.50	13.90	13.70	13.14	12.39	13.50	15.63	14.35	13.88	13.64	14.30
Fe_2O_3	0.90	1.50	1.35	1.00	0.76	0.73	0.55	1.78	1.76	0.33	0.90	1.33
FeO	1.35	1.80	0.81	0.36	1.15	0.57	1.70	1.73	1.45	2.59	1.94	1.05
MnO	0.06	0.08	0.06	0.04	0.05	0.02	0.07	0.10	0.08	0.08	0.05	0.07
MgO	0.40	0.50	0.70	0.30	0.09	0.00	0.32	0.07	0.72	0.81	0.65	0.56
CaO	2.98	2.40	2.25	1.10	0.83	0.51	1.82	2.90	2.45	2.67	1.98	2.35
Na_2O	4.42	4.72	3.61	3.23	3.76	3.76	4.25	4.44	4.29	3.91	3.91	5.05
K_2O	0.83	2.27	2.78	3.89	5.12	4.76	4.27	3.24	4.23	4.45	3.80	3.41
P_2O_5	0.03	0.10	0.07	0.09	0.02	0.00	0.08	0.11	0.17	0.11	0.09	0.11
H_2O	n.d.	n.d.	n.d.	n.d.	0.45	0.31	0.81	1.23	0.81	n.d.	n.d.	n.d.
CO_2	n.d.	n.d.	n.d.	n.d.	n.d.	n.d.	0.06	0.14	0.20	0.18	0.14	0.07
F	0.02	0.02	0.05	0.02	0.09	0.3	0.04	0.03	0.06	0.1	0.08	0.04
Total	98.73	99.38	98.76	98.65	99.36	99.77	99.87	99.60	99.88	98.88	98.68	98.90
Cr	6	4	9	4	86	2	14	14	13	12	121	9
Ni	8	18	13	9	n.d.	n.d.	n.d.	n.d.	n.d.	n.d.	n.d.	n.d.
Co	5	8	5	3	1	0	3	7	5	6	7	3
Sc	4.1	8.5	6.2	3.5	4.4	1.5	2.5	5.4	6.9	10	8.8	3.4
V	27	35	44	20	n.d.	n.d.	n.d.	n.d.	n.d.	n.d.	n.d.	n.d.
Cu	13	11	8	8	n.d.	n.d.	n.d.	11	8	n.d.	n.d.	n.d.
Pb	13	6	19	33	n.d.	n.d.	n.d.	20	20	n.d.	n.d.	n.d.
Zn	23	35	29	13	n.d.	n.d.	n.d.	31	56	n.d.	n.d.	n.d.
Sn	8.7	2.9	43.1	n.d.	n.d.	n.d.	n.d.	n.d.	n.d.	n.d.	n.d.	n.d.

W	1.08	1.68	0.99	0.87	n.d.	n.d.	n.d.	n.d.	n.d.	n.d.	n.d.	n.d.
Mo	0.41	0.95	0.3	0.34	n.d.	n.d.	n.d.	n.d.	n.d.	n.d.	n.d.	n.d.
Rb	n.d.	n.d.	n.d.	n.d.	237	580	151	67	103	145	135	75
Cs	0.2	0.4	3	2	12.5	31	4	1.1	3	8.2	9	0.9
Ba	150	310	450	430	105	100	721	757	577	557	296	641
Sr	210	160	160	160	52	36	209	348	210	175	129	226
Li	n.d.	n.d.	n.d.	n.d.	n.d.	n.d.	n.d.	n.d.	n.d.	n.d.	n.d.	n.d.
Ta	0.2	0.3	0.7	0.2	2	6	1	0.6	1	1.6	0.8	0.7
Nb	n.d.	1	7	1	20	11	15	9	14	24	13	10
Hf	3.6	5	3.6	3.6	6	9	8	4	7	9	5	5.8
Zr	90	120	145	60	158	131	309	171	239	388	185	226
Y	16	36	23	21	85	256	51	22	32	66	40	22
Th	4	3.5	8	9.5	29	48	12	7	10	15	13	8
U	0.6	1.1	2.5	2.2	5	5.2	3.7	1.8	3.2	2.3	2.1	3.1
La	15	15.9	17.1	14.9	49.8	19.5	30.4	19.6	30	57.6	30.2	23.8
Ce	25.4	34.6	32.4	27.1	103.9	48.7	56.1	33.7	53.2	103	58	41.2
Nd	11.7	21.1	16.8	13.5	60.2	34.4	28.4	15.8	25.8	50.5	30.7	19.4
Sm	2.6	5.9	4.1	4.1	16	10.8	6.8	3.5	5.9	11.8	7.6	4.4
Eu	0.81	0.88	0.73	0.7	0.45	0.07	0.5	0.77	1.1	1.7	0.76	0.7
Gd	1.66	5	3	2.8	12.7	12.5	5.7	2.2	4	8.7	5.4	2.8
Tb	0.31	0.94	0.55	0.5	2.2	2.5	1.02	0.41	0.7	1.48	0.95	0.5
Yb	1.53	4.3	2.28	1.85	7.5	14.2	3.9	1.83	2.57	5.7	3.61	1.98
Lu	0.24	0.67	0.35	0.28	1.17	2.3	0.59	0.28	0.38	0.68	0.54	0.3
B	5.2	3.1	3.2	4.9	n.d.	n.d.	n.d.	n.d.	n.d.	n.d.	n.d.	n.d.
Be	0.75	1.1	1	n.d.	n.d.	n.d.	n.d.	n.d.	n.d.	n.d.	n.d.	n.d.

n.d.—not determined.

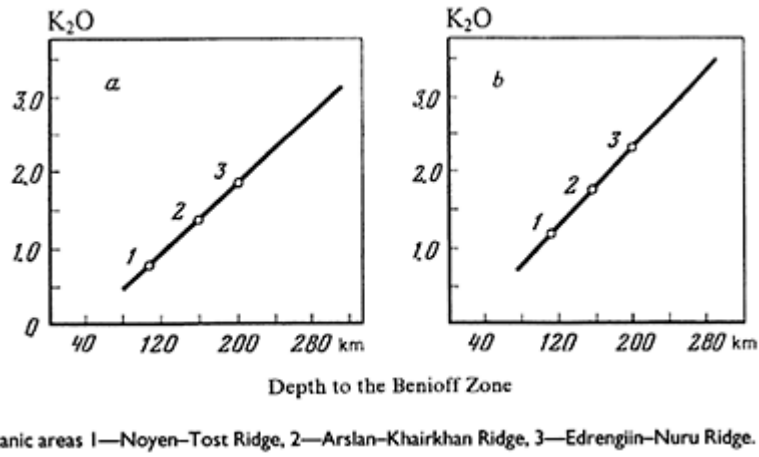

Figure 61 The K_2O content of the rocks (a—SiO_2=55%, b—SiO_2=60%) versus depth to the subduction zone (after Yarmolyuk, 1983).

6.2 Late-Stage Magmatism

In Mongolia, since the end of the late Carboniferous and throughout the Permian, igneous activity has occurred mainly within the northern Caledonian megablock. Two complexes of igneous rock associations were formed at that time. They differ in their rock composition, spatial distribution, and structural setting. According to their dominant rock associations, one of them can be considered as a differentiated complex and the other as a bimodal complex (Yarmolyuk and Kovalenko, 1991).

Rock Associations of the Differentiated Complex

The associations of this group are part of the structure of the Central and the North Mongolian volcanoplutonic belts and the separating Khangai granitoid batholith, which is the largest in Mongolia. The volcanoplutonic belts join along the western flank of the batholith. This allows them to be considered with the batholith as a single volcanic area. The distribution pattern of rocks of different composition in the volcanic suites of both belts is governed by an up-section increase in silica. Therefore these igneous rock associations, like the Carboniferous associations of the South Mongolian belt, were recognized as being part of the differentiated volcanic complex (Yarmolyuk, 1983). In addition, granitoids of various composition also form part of the structure of the belts.

The Central Mongolian volcanoplutonic belt consists of a series of volcanic fields that lie to the south of the Khangai-Khentei ranges in a gently sloping arc. It extends for 1,700 km, and its width varies from 100–200 km in the west to 350 km in the east. The most

complete sections of volcanic rocks are located on the southern and south-eastern slopes of the Khangai batholith. The volcanics are underlain by Middle-Upper Carboniferous sandstone-conglomerate sequences. The volcanics contain thin layers of terrigenous deposits, containing a Lower Permian flora (Mossakovsky and Tomurtogoo, 1976). The volcanics are overlain by Upper Permian deposits. These relationships unambiguously indicate an early Permian age for the volcanics (Mossakovsky and Tomurtogoo, 1976). Andesites, dacites, and rhyolites are the commonest rocks (Kepezhinskas and Luchitsky, 1973; Kovalenko, 1991). They form sequences (up to 2,500 m thick) of different compositions, with two distinct types of sections, namely rhyolite and andesite types. According to the type of section, the volcanics also form associations of andesitebasalt-andesite, andesite-dacite-rhyolite, dacite-rhyolite, and dacite-trachyrhyolite. In both types of section the distribution pattern of the rocks is determined by the predominant geochemical trend, namely, by the replacement of more basic by more acid rocks at higher levels in the volcanic sequences. All the rocks from the rhyolite type of section, including the subordinate andesites, are leucocratic (Kepezhinskas and Luchitsky, 1973). The rhyolite is made up of quartz, plagioclase, and orthoclase in different abundance ratios. Dark minerals are locally represented only by biotite. The same rocks of the andesite-dacite-rhyolite series are more melanocratic in the andesite type of section; they contain different femic minerals (pyroxene, amphibole, and biotite).

In their chemistry, the rocks of the differentiated igneous complex of the Central Mongolian belt (Table 13, Fig. 62) show Na_2O+K_2O of 6–8%, with roughly equal Na and K ratios (Yarmolyuk and Kovalenko, 1991). These contents are typical of the calcalkaline series. In their Al_2O_3 content, the andesites of the belt are similar to those of high-Al series of modern active continental margins.

Diverse granitoids such as granodiorites, granites, leucogranites, and granosyenites are closely related structurally to the volcanics. They intrude the volcanic suites but do not affect the Upper Permian deposits. This indicates that they are early Permian in age. The granitoids of the belt are dominated by rocks that form an association of granites-leucogranites with granosyenites (Dergunov and Kovalenko, 1995). The composition of the rocks of the association points to regional differences, as indicated by the abundance ratios of the various phases, the petrochemical and geochemical features of the rocks, their relative ages and the sizes of the intrusions. Nevertheless, the granitoid intrusions do show strong similarities at different localities within the belt. Many intrusions are as large as 1,000 km^2 in area. As a rule, two phases of injection were responsible for the formation of these bodies (Kovalenko, 1991). Biotite-, biotite-hornblende granites, adamellites, and subordinate granodiorites were characteristic of the first phase. The rocks are medium- to coarse-grained, equigranular or porphyritic. The rocks of the second phase include medium- to fine-grained leucocratic and biotite subalkaline granites and granosyenites. Anorthoclase dominates in the compositions of the rocks of both phases (40–55%). In addition, plagioclase (10–30%), quartz (30–40%), and biotite (up to 5%) are present. In the granosyenites, the content of anorthoclase reaches 60–75%, and the amount of femic minerals increases to 5–10%.

Table 13 Representative compositions of volcanic rocks of the differentiated complex of the western Central Mongolian volcanic belt (after Kovalenko, 1991).

	Butsugan Depression										**Chandoman Depression**			
SiO_2	50.21	52.50	55.44	55.36	59.89	65.93	66.85	69.42	70.60	72.27	53.47	59.47	67.96	73.79
TiO_2	1.19	0.80	1.39	1.30	0.76	0.47	0.68	0.71	0.31	0.24	0.94	0.97	0.54	0.21
Al_2O_3	18.41	18.70	14.76	18.06	17.32	16.00	15.70	14.95	13.17	14.62	17.99	15.68	15.04	12.99
Fe_2O_3	5.75	3.60	6.29	4.36	3.68	2.67	2.04	2.20	2.11	1.53	5.77	4.25	2.08	1.17
FeO	4.57	5.17	3.25	3.98	3.03	1.87	1.94	1.73	2.12	1.00	2.11	3.99	1.96	0.98
MnO	0.26	0.20	0.13	0.12	0.18	0.13	0.11	0.09	0.08	0.08	0.12	0.10	0.18	0.02
MgO	4.45	3.70	3.14	2.92	2.21	1.17	0.78	0.66	n.d.	0.45	3.50	1.84	1.16	0.19
CaO	7.54	7.20	6.80	7.00	4.68	2.09	1.81	1.47	1.54	0.72	6.72	4.93	2.18	1.16
Na_2O	3.81	3.60	4.37	3.68	4.05	5.54	5.83	5.74	4.59	3.69	5.03	5.60	4.20	4.58
K_2O	1.52	1.88	1.51	1.33	2.92	2.55	2.64	1.80	4.72	4.30	1.57	2.08	2.62	4.40
P_2O_5	0.31	0.22	0.60	0.38	0.31	0.15	0.17	0.18	0.02	0.06	0.31	0.35	0.10	0.04
F	0.03	0.04	0.09	0.03	0.04	0.04	0.02	0.02	0.02	0.02	0.02	0.06	n.d.	0.02
Total	98.05	97.61	97.77	98.52	99.07	98.61	98.57	98.97	99.28	98.98	97.55	99.32	98.02	99.55
Li	14.8	16.5	25	13	15.9	11.1	12.2	11.6	9.3	16.7	10	8.5	8	3
Rb	31.4	31.4	31	34.4	46.5	66.5	51.4	35.9	67.5	89.4	30	25.5	43	96
Sr	301	483	495	571	622	414	305	195	232	101	817	696	175	65

Ba	681	707	515	530	701	794	440	661	1184	897	745	711	150	935
Zr	130	249	185	177	185	285	321	294	268	168	270	144	300	380
Be	1.7	2	1.5	2.3	1.6	3	3.1	2.1	1.5	2.4	3	2.5	2	3
Sc	20.2	14.8	27.5	19.5	16.5	14.5	13.4	10	16	6.7	24	12	13	5
B	11.75	11.4	21.5	13.6	12.5	15	9.7	16.6	17.2	12.2	8	12	11	11
Sn	2.7	4.3	3.5	2.45	2.3	3.9	6.4	2.6	1.8	4.3	7	2.5	4	1.5
Mo	1.1	1.2	2	1.45	1.9	0.9	1.5	0.7	0.8	1.1	1	1.1	2	2
Cu	48.2	26.8	45.5	59.35	29.3	11.4	14.1	11.9	22.2	6.7	50	34	16	15
Pb	15.8	22.6	22.5	22.2	24.2	28	34.7	37.2	20.6	32	17	14	15	20
Zn	106	112	110	92.5	120	77.5	70	62	68	56	90	49	40	60
Cr	60	12	11	19	19	16	22	12	13	9	8	12	6	6
Ni	37	4.3	9	13	6	5	4	3	5	3	11	15	2	2
Co	30	11	26	18	11	4	4	2	6	2	22	13	3	1
V	178	79	270	161	91	34	52	38	8	5	280	105	8	14

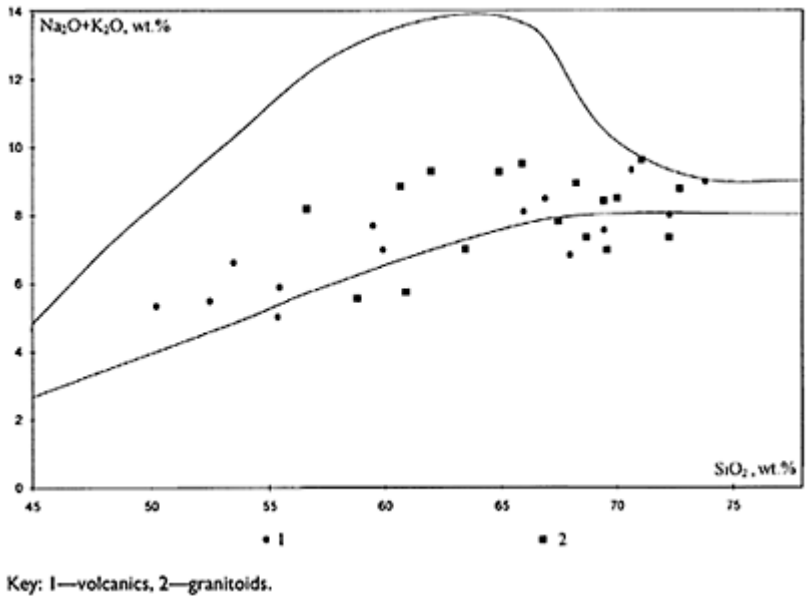

Key: 1—volcanics, 2—granitoids.

Figure 62 Compositions of rocks of the differentiated complex of the Central Mongolian volcanic belt plotted on a SiO_2–(Na_2O+ K_2O) classification diagram.

The chemistry of the rocks of the association is consistent with the calcalkaline and the subalkaline petrochemical series (Table 14, Fig. 62). The rocks of the early phase of intrusion belong mainly to the calcalkaline series, whereas the predominant rocks of the

second phase fall into the subalkaline series. The rocks Xshow a moderate Al content (12–16%) and $Na_2O/K_2O<1$.

The North Mongolian volcanoplutonic belt is represented by large terrains of volcanics and granitoid intrusions which occur along the northern slope of the Khangai-Khentei ranges and continue ENE into adjacent areas of Russia. The belt extends for over 2,000 km including its extent in Russia with its width reaching 250–350 km. Its structure is defined by vast, up to 200–300 km long, volcanotectonic depressions (Fig. 63), containing great thicknesses of volcanics in their central portions and reduced thicknesses on the margins of the depressions (Yarmolyuk and Kovalenko, 1991) (Fig. 64).

The differentiated igneous complex of the North Mongolian volcanic belt is composed of three concordant suites. They are:

1) a suite of basic and intermediate lavas;
2) a suite of acid volcanics; and
3) a volcanosedimentary suite (Yarmolyuk and Kovalenko, 1991).

Table 14 Mean composition of the late Palaeozoic granitoids of the western Central Mongolian volcanic belt.

	Dzabkhan Zone				**Khantaishir Trough**				**Argalintin Trough**	**Butsagan Trough**		**Chandoman Trough**					
	1	**2**	**3**	**4**	**5**	**6**	**7**	**8**	**9**	**10**	**11**	**12**	**13**	**14**	**15**	**16**	**17**
SiO_2	56.60	61.90	68.20	71.04	60.63	64.86	65.85	69.40	69.53	67.43	69.97	60.85	58.78	63.39	68.65	72.25	72.69
TiO_2	0.82	0.55	0.41	0.33	0.82	0.50	0.46	0.45	0.45	0.54	0.32	0.62	0.58	0.54	0.35	0.26	0.24
Al_2O_3	19.12	17.77	14.24	14.69	16.09	16.46	16.21	15.38	14.79	15.45	14.73	15.82	17.92	15.48	14.64	14.13	13.47
Fe_2O_3	2.66	2.66	1.72	0.97	3.29	2.13	1.82	1.65	1.36	1.35	1.59	2.78	2.98	2.89	1.95	1.29	1.42
FeO	3.46	2.64	2.01	1.22	2.67	2.47	2.31	1.58	2.00	2.69	1.27	3.79	3.59	2.06	1.84	1.58	0.91
MnO	0.17	0.14	0.09	0.05	0.07	0.07	0.08	0.23	0.05	0.10	0.08	0.08	0.15	0.06	0.05	0.05	0.02
MgO	1.81	1.34	1.15	0.22	2.98	0.97	0.71	0.94	1.04	1.00	0.58	2.98	2.89	2.09	0.86	0.54	0.07
CaO	5.61	2.87	2.40	1.20	3.14	2.43	2.18	1.96	2.35	2.25	1.81	5.94	6.96	4.95	3.35	1.68	1.29
Na_2O	4.50	4.74	4.54	4.35	4.67	4.62	4.56	3.79	3.37	4.05	4.55	3.57	4.04	4.38	3.93	3.93	4.35
K_2O	3.68	4.55	4.40	5.27	4.18	4.65	4.95	4.63	3.60	3.77	3.95	2.17	1.53	2.62	3.42	3.41	4.42
P_2O_5	0.40	0.26	0.18	0.05	0.31	0.13	0.12	0.12	0.08	0.20	0.13	0.24	0.12	0.20	0.15	0.08	0.11
F	0.08	0.04	n.d.	0.04	0.08	n.d.	0.09	n.d.	n.d.	0.04	0.03	0.11	n.d.	0.06	0.15	0.14	0.10
Total	98.91	99.46	99.34	99.43	98.93	99.29	99.34	100.13	98.62	98.87	99.01	98.95	99.54	98.72	99.34	99.34	99.09
Li	16	11	12	13	15.5	16	9.8	18	10	18	21	10.3	10.5	13.2	20.5	20	15
Rb	30	140	80	165	20	152	262	190	125	130	137	63	42	71	87	108	161
Sr	470	270	200	n.d.	300	265	150	160	297	120	176	227	250	307	222	200	119
Ba	n.d.	n.d.	n.d.	n.d.	n.d.	580	n.d.	470	775	1361	606	776	483	863	976	745	635

	Dzabkhan Zone				Khantaishir Trough				Argalintin Trough	Butsagan Trough		Chandoman Trough					
	1	**2**	**3**	**4**	**5**	**6**	**7**	**8**	**9**	**10**	**11**	**12**	**13**	**14**	**15**	**16**	**17**
Zr	110	320	190	n.d.	165	390	324	n.d.	170	192	266	137	127	174	204	135	145
Be	1	2	1	n.d.	2.7	3	4.6	n.d.	2.5	3	2.3	1.4	1.3	1.7	2	2.7	2.6
Sc	20	10	5	n.d.	40	10	5.8	n.d.	3.7	3	5.3	16	21	10	7.5	3.4	2
B	11	9	10	n.d.	16	13	13.6	n.d.	18	n.d.	n.d.	19	14.3	15.5	18	21	18
Sn	4	1.5	3	n.d.	3	3	4.6	n.d.	2.2	1.8	5.2	2.1	4	2.6	2.5	2.1	1.7
Mo	1	0.5	0.5	n.d.	2	2	1	n.d.	0.7	0.8	1.3	1.6	1.3	1.9	1.4	1	1.7
Cu	57	3	7	n.d.	37.5	20	25.6	n.d.	5.7	16	16.6	67	63	36	26	24.6	18
Pb	32	25	48	n.d.	16.5	23	34.6	n.d.	29.5	20	22.6	24.6	14	27	26	36	40
Zn	120	30	15	n.d.	60	30	37	n.d.	22	49	70	67	60	52	37	28	17
Cr	21	13	12	n.d.	121	10	45	n.d.	605	8	20	62	14	53	27	18	10
Ni	2	2	2	n.d.	41	5	3	n.d.	2	2	4	14	7	10	6	3	2
Co	20	4	1	n.d.	25	6	5	n.d.	3	2	4	18	13	12	8	4	1
V	210	62	58	n.d.	150	37	50	n.d.	34	13	54	169	197	74	66	34	12

Note: 1—syenodiorite; 2, 5, and 14—monzonite; 3, 7, and 10—granosyenite; 4—subalkaline granite; 6—syenite; 8, 9, 11, and 16—granite; 12 and 13—diorite; 15—granodiorite; 17—leucogranite.

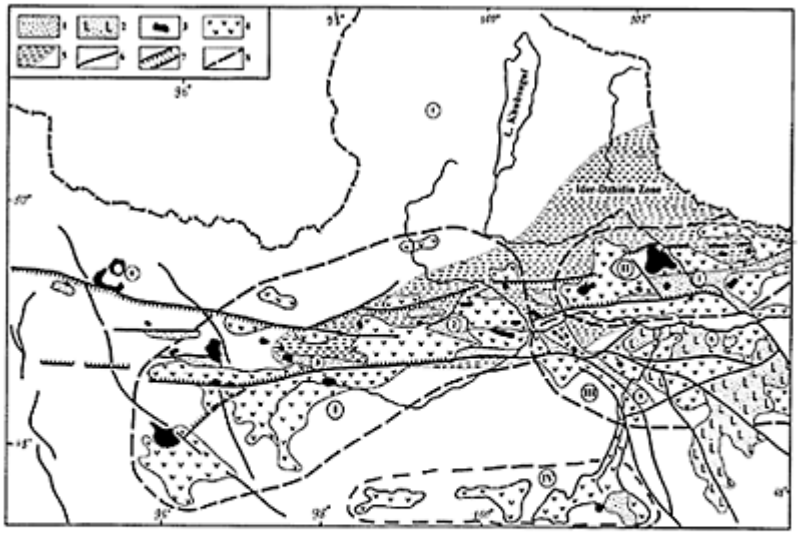

Key: 1–3—riftogenic associations: 1—bimodal, 2—subalkaline basalt of the Orkhon–Selengin Trough, 3—alkali granitoid, 4—fields of rocks of the differentiated volcanic complex; 5—Vendian–Lower Cambrian ophiolite terrain, 6—fault; 7—rift-zone boundary faults; 8—boundaries of volcanic troughs. Volcanic trough: I—North Khangai, II—Dzhelturin, III—Orkhon–Selengin, IV—Central Khangai. Volcanic field (circled numbers): ①—Tarbagatai-Gol and Eglin-Gol district, ②—Bugsein-Gol district, ③—Toson–Tsengel district, ④—Dzun–Khangai district, ⑤—confluence of the Khanui-Gol and Khunei-Gol rivers, ⑥—Erdenet deposit.

Figure 63 Distribution of the late palaeozoic igneous formations in North Mongolia.

The age of the suites is reliably substantiated as early Permian from the abundant plant remains (Table 15).

The suite of basic and intermediate volcanics is made up of basalts, andesitebasalts and andesites, all showing high alkalinity; in places they are intercalated with tuffaceous sandstones, siltstones, and gravelstones. Pyroclastic varieties are relatively rare, and locally tuff and, less commonly, lavas of andesite-dacite and rhyolite composition also occur within the suite. The thickness of the suite varies from a few hundred metres to 2,000 m in the central parts of the volcanotectonic depressions. The rocks of the suite yielded imprints of *Cordaites*, suggesting later late Carboniferous-earlier early Permian age for the rocks (Durante, 1976).

The suite of acid volcanics (or rhyolite-trachyrhyolite association) is composed of lavas, and also normal and welded tuffs of trachydacitic, trachyrhyolitic and, to a lesser extent, trachyrhyolitic composition. They contain phenocrysts of orthoclase, oligoclase, and quartz. The pyroclastic rocks show the same suite of phenocryst. These phenocrysts are cemented by fine ashy material. Basic and intermediate lavas are subordinate. The acid volcanics rest conformably on the underlying rocks; they are separated by units of tuffaceous-sedimentary rocks

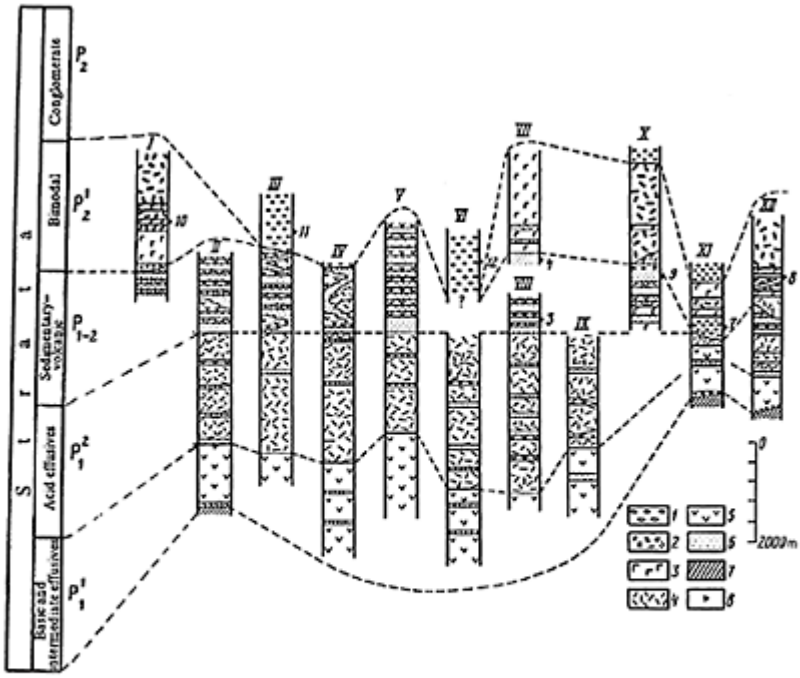

Key: I—conglomerate, 2—trachyrhyolite, pantellerite, and comendite; 3—subalkaline basalt; 4—trachydacite and trachyrhyodacite; 5—trachyandesite; 6—tuffaceous-sedimentary rocks; 7—pre-Permian basement; 8—the occurences of fossil flora in the sections: the number corresponds with that in Table 15 and 23. I–III—the eastern extremity of the trough, IV–VIII—central part of the trough, IX–XI—the western extremity of the trough, XII—the northern slope of the trough.

Figure 64 Correlation of the Permian sections of the North Khangai volcanic trough.

and tuffs of mixed composition. Their contained flora indicates an early Permian age (Yarmolyuk *et al.*, 1986). The thickness of the suite varies from 1,500–2,000 to 3,500–4,000 m.

The sedimentary-volcanic suite has a complex facies structure, caused by the irregular pattern of distribution of sedimentary, volcanosedimentary and volcanic rocks in the sections. The suite has a different structure in the different volcanotectonic depressions. In some depressions (Orkhon-Selenga) the suite is dominated by tuffites, in others (North Khangai and Central Khangai depressions) by lavas (Yarmolyuk and Kovalenko, 1991). Basalt, andesite, trachyte, and trachydacite, and tuffs of mixed composition, are present in the suite in roughly equal amounts. In places the volcanics account for 70% of the rocks. The thickness of the suite varies from 5,000 m in the axial parts of the volcanotectonic depressions to complete thinning at the margins (Fig. 64). Plant remains indicate an age range from

Table 15 Distribution of plant remains over sections of the Permian differentiated complex, North Khangai Zone, North Mongolia (after Yarmolyuk and Kovalenko, 1991).

	Upper Phytohorizon III	4. *Cordaites* cf. *singularis*	5. *Rufloria* with fine dorsal grooves, *Cordaites* ex. gr. *concinna*	6. *Glottophyllum sp., Cordaites* ex. gr. *gracilentus, Cordaites* aff. *singularis, Cordaites* ex. gr. *concinna*
		Volcanosedimentary strata		
Permian	Phytohorizon II	3. *Rufloria with f*ine dorsal grooves, Rufloria aff. *kerulenica, Cordaites* ex. gr. *concinna*		
		Acid volcanic rocks		
	Lower Phytohorizon I	1. *Rufloria* aff. *theodirii, Cordaites* ex. gr. *singularie, Paragondwanidium* sp.	2. Decorticated trunks of the pteridophytes *Angaropteridium, Paracalamites sp. Rufloria* sp.	
		Conglomerates at the base of acid and intermediate volcanic rocks		

Numbers are those for the occurrences of fossil flora in sections, as shown in Figure 64.

the end of the early Permian to the beginning of the late Permian (Yarmolyuk and Kovalenko, 1991).

The volcanics of the differentiated complex of the North Mongolian belt as a whole fall into the subalkaline petrochemical series (Table 16, Fig. 65). They have a higher alkalinity as compared with the volcanics of the Central Mongolian belt, due to an increase in the contents of both K_2O and Na_2O, with the latter being predominant (Yarmolyuk and Kovalenko, 1991).

Numerous granitoid intrusions of various compositions make up the northern Mongolian volcanoplutonic belt. They form associations of:

1) gabbro and syenite-diorite;

2) diorite-granodiorite-granosyenite-granite (Selenga Complex);

3) gabbro-monzonite and granosyenite-granite (Shivotin Complex); and

4) porphyritic ore-bearing (Cu-Mo) intrusions (Erdenet Complex) (Kovalenko, 1991).

The most widespread intrusions are those of the Selenga Complex. The general order of formation is as follows (Kovalenko, 1991):

1) amphibole gabbro-diorites, diorites, and less-common gabbros;

2) amphibole-biotite granitoids of mixed composition: quartz-diorites, granodiorites, monzogranodiorites, granosyenites, adamellites, and granites;

3) granites, leucogranites, and microgranites of dykes and veins.

Table 16 Compositions of rocks of the Permian differentiated volcanic complex of the Central Khangai volcanic Trough (North Mongolian volcanic belt)

	BTs-5	BTs-6	BTs-7	BTs-8	BTs-10	BTs-11	BTs-12	BTs-13	BTs-14	BTs-15	BTs-1
	1	2	3	4	5	6	7	8	9	10	11
SiO_2	59.06	57.93	56.34	52.36	56.55	53.99	58.86	55.53	56.64	59.11	73.28
TiO_2	1.07	1.40	1.40	1.99	1.31	1.54	1.00	1.36	1.33	1.22	0.16
Al_2O_3	15.70	16.20	16.30	16.20	16.30	16.60	15.80	16.10	15.45	15.85	13.30
Fe_2O_3	4.28	3.52	5.28	4.91	4.95	5.67	2.82	4.54	5.03	4.62	1.39
FeO	2.36	3.59	2.36	4.95	3.02	3.00	3.68	3.39	2.59	2.42	1.09
MnO	0.10	0.10	0.12	0.12	0.11	0.12	0.10	0.11	0.09	0.09	0.08
MgO	2.30	2.08	2.95	3.25	2.77	3.26	2.83	3.32	3.35	2.25	0.23
CaO	3.80	4.00	4.70	6.10	4.90	6.00	4.20	4.90	5.55	5.10	0.43
Na_2O	3.67	3.86	4.67	3.10	3.75	3.48	3.50	3.35	2.81	4.04	3.78
K_2O	5.52	5.30	3.13	3.39	4.26	3.31	4.54	4.03	4.18	2.65	5.67
P_2O_5	0.54	0.73	0.84	1.24	0.77	0.79	0.46	0.72	0.70	0.46	<0.02
F	0.21	0.17	0.19	0.25	0.19	0.25	0.23	0.19	0.05	0.22	0.11
LOI	1.14	1.26	2.01	2.28	1.63	2.20	1.99	2.34	1.88	0.05	0.67
Total	99.75	100.14	100.29	100.14	100.51	100.21	100.01	99.88	99.65	98.08	100.19
Rb	156	138	84	84	116	91	127	111	129	63	261
Zr	348	335	373	451	428	299	440	330	461	320	239
Nb	16	17	15	22	18	16	16	14	18	10	23
Hf	8.6	8.6	n.d.	12	11	n.d.	n.d.	8.4	n.d.	5	7.9
Ta	1.2	1.4	n.d.	1.5	1.1	n.d.	n.d.	1.1	n.d.	0.5	1.9
Ba	526	1,780	<100	1,317	1,372	1,029	<100	1,076	1,150	885	136
Sr	758	1,203	1,195	1,118	996	1,567	912	1,252	751	759	165
Co	17	18	n.d.	23	20	n.d.	n.d.	22	n.d.	19	1.8
Cs	2.7	2.1	n.d.	1.7	1.3	n.d.	n.d.	4.2	n.d.	1	4.5
Y	29	32	27	37	35	28	34	26	36	23	36
Sc	10.8	11.3	n.d.	15	13.5	n.d.	n.d.	13.4	n.d.	12.2	3.7
Th	13	11	n.d.	6	6	n.d.	n.d.	5	n.d.	6	36
U	3.1	3.5	n.d.	2.1	2.3	n.d.	n.d.	2.2	n.d.	1.3	3.7
La	81.3	86.9	n.d.	105	84.4	n.d.	n.d.	69.3	n.d.	32.9	61.1
Ce	122	146.4	n.d.	175	135.4	n.d.	n.d.	111.2	n.d.	58.7	104
Nd	49	67	n.d.	78.5	58.7	n.d.	n.d.	48.2	n.d.	28.6	44
Sm	9.7	14.8	n.d.	17.1	12.4	n.d.	n.d.	10.9	n.d.	6.6	7.5
Eu	2.05	2.49	n.d.	3.6	2.5	n.d.	n.d.	2.35	n.d.	1.67	0.47
Gd	7.8	8.7	n.d.	13.7	10.4	n.d.	n.d.	8.6	n.d.	5.5	6.65
Tb	1.1	1.25	n.d.	1.9	1.46	n.d.	n.d.	1.21	n.d.	0.85	0.97
Yb	1.74	1.98	n.d.	3	2.1	n.d.	n.d.	1.83	n.d.	1.84	2.63
Lu	0.22	0.25	n.d.	0.38	0.26	n.d.	n.d.	0.23	n.d.	0.25	0.36

	BTs-3	BTs-4	BTs-17	Kh-89/9	Kh-89/10	Kh-89/11	Kh-89/12	Kh-89/13	Arg-89/3	Arg-89/4
	12	13	14	15	16	17	18	19	20	21
SiO_2	71.04	71.70	74.28	56.56	56.87	68.32	71.34	57.41	62.20	70.10
TiO_2	0.30	0.40	0.14	1.44	1.39	0.72	0.46	1.34	0.99	0.50
Al_2O_3	14.90	14.70	10.65	16.25	16.10	14.85	13.85	16.25	16.15	14.35
Fe_2O_3	1.65	1.35	2.23	4.13	6.12	2.72	1.72	5.23	3.23	2.12
FeO	1.49	1.04	2.77	3.31	1.52	0.89	1.07	1.96	1.96	0.80
MnO	0.05	0.03	0.10	0.16	0.14	0.07	0.07	0.12	0.11	0.07
MgO	0.44	0.40	0.20	3.15	3.10	0.95	0.55	1.85	2.10	0.75
CaO	0.60	0.33	0.20	4.10	2.65	0.85	0.80	3.25	2.20	0.35
Na_2O	3.78	4.08	4.53	3.63	3.98	3.69	3.44	4.26	4.34	4.09
K_2O	5.60	5.52	3.84	4.45	4.25	5.35	6.02	4.03	4.42	4.62
P_2O_5	0.03	0.03	0.04	0.79	0.82	0.20	0.11	0.76	0.43	0.14
F	0.10	0.07	0.35	1.83	2.83	1.46	1.01	2.92	2.09	1.38
LOI	0.37	0.87	0.25	0.15	0.20	0.15	0.10	0.30	0.10	0.10
Total	100.71	100.52	99.58	99.95	99.97	100.22	100.54	99.68	100.32	99.37
Rb	230	210	695	122	122	213	255	115	180	163
Zr	252	246	2,155	349	366	414	333	368	345	361
Nb	20	18	227	16	15	22	24	14	20	17
Hf	7.7	7.5	82.9	8.6	9.3	11.6	n.d.	9.2	9.7	9
Ta	1.6	1.5	23.3	1.1	1.1	1.6	n.d.	1.1	1.5	1.7
Ba	119	538	1,133	1451	1550	1099	721	1,526	1394	1451
Sr	180	173	40	1003	917	340	187	1,020	314	741
Co	3.3	1.5	1	19	21	5	n.d.	18	11	3
Cs	8.4	6.8	5.1	9.3	12.1	11.1	n.d.	9.6	10.2	10.7
Y	33	24	339	33	30	35	34	30	32	28
Sc	3.4	2.4	0.5	12.7	13.1	6.1	n.d.	12.9	9	5.4
Th	34	34	164	11	8	28	n.d.	10	18	31
U	5	4	36	4.5	5	5	n.d.	3	4	9
La	68.1	24.2	147	72.7	85	73.6	n.d.	78	78	33
Ce	114	30.1	284	128	127	118	n.d.	135	128	54.5
Nd	42.2	9.8	151	61	51	51	n.d.	64	57	24.4
Sm	7.4	1.65	37.6	14	10.2	10.8	n.d.	14.4	12.2	5.3
Eu	0.95	0.27	0.99	2.88	2.48	1.58	n.d.	2.42	2.12	1.04
Gd	6.3	1.52	41	8.5	9.3	7.1	n.d.	9.7	7.9	6.0
Tb	1.13	0.28	7.2	1.3	1.3	1.1	n.d.	1.39	1.2	1.00
Yb	2.3	1.31	25.3	2.3	2.2	2.3	n.d.	2.2	2.3	3.0
Lu	0.33	0.2	3.7	0.3	0.29	0.32	n.d.	0.28	0.3	0.43

Note: rocks sampled up the section of volcanic sequences: BTS—in the Bat-Tsengel area 1–10 basic and intermediate volcanics, 11–14 acid volcanics; Kh and Arg—in the middle part of the Khanui River—sedimentary-volcanic strata; LOI—ignition losses, n.d.—not determined.

The intrusions are dominated by the rocks of the second phase. Early diorites and gabbroids make up 10–20% of the area of the intrusions and individual small bodies. The Erdenet intrusion is the most prominent example of the association (Fig. 66). It is dominated by granitoids, characterized by high basicity; the granitoids grade into granosyenite, but locally they are intruded by granosyenites. Hybridization and orthoclasization are typical of the rocks of the intrusion. The rocks of the association as a whole are moderately siliceous and aluminiferous

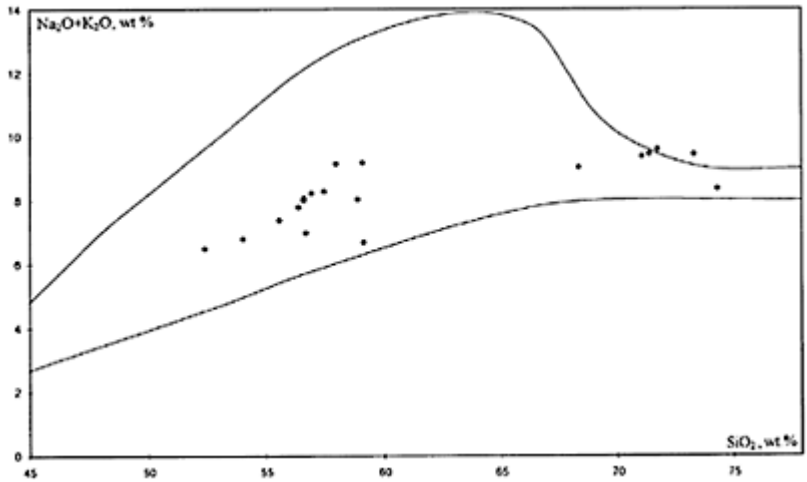

Figure 65 The rock compositions of the differentiated complex of the Central Khangai Trough plotted on an SiO_2–(Na_2O+K_2O) classification diagram.

(Table 17). Most of the rocks show variations of SiO_2 within 66–68% and Al_2O_3 within 15–17%. An Na_2O/K_2O ratio of greater than one is typical of these rocks, but an increase in the K_2O content to the point at which subalkaline granites make their appearance ($Na_2O/K_2O<1$) is noted in the age series. The rocks of the association as a whole belong to the subalkaline K-Na petrochemical series.

Here we will compare the compositions of the igneous rocks of the Central Mongolian and the North Mongolian-Transbaikalian volcanoplutonic belts. The belts were formed at the same time, in the early Permian, within a single igneous area and they show similar associations of igneous rocks. The range of compositional variations of:

1) volcanic rocks is determined by $52\% \leq SiO_2 \leq 73\%$ and

2) intrusive rocks by 60–76% SiO_2.

Other petrochemical parameters, such as the contents of Al_2O_3, CaO, MgO, and other oxides are also similar. Differences in composition are caused by increasing in the alkalinity of the rocks, K_2O for the most part, from the south to the north of the igneous

region (Yarmolyuk, 1983). These variations are observed within each belt. In total, they lead to the higher alkalinity of the rocks of the North Mongolian belt as compared with the rocks of the Central Mongolian belt. The tendencies observed are explained from the viewpoint of the formation of both belts above the palaeo-subduction zone, gently plunging (12–15°) northwards (Kovalenko *et al.*, 1983; Yarmolyuk and Kovalenko, 1991). This inference is in good agreement with the hypothesis that the Lower Permian igneous area was associated with the active continental margin of the North Asiatic continent, at its boundary with the palaeo-Tethys (Mossakovsky, 1975).

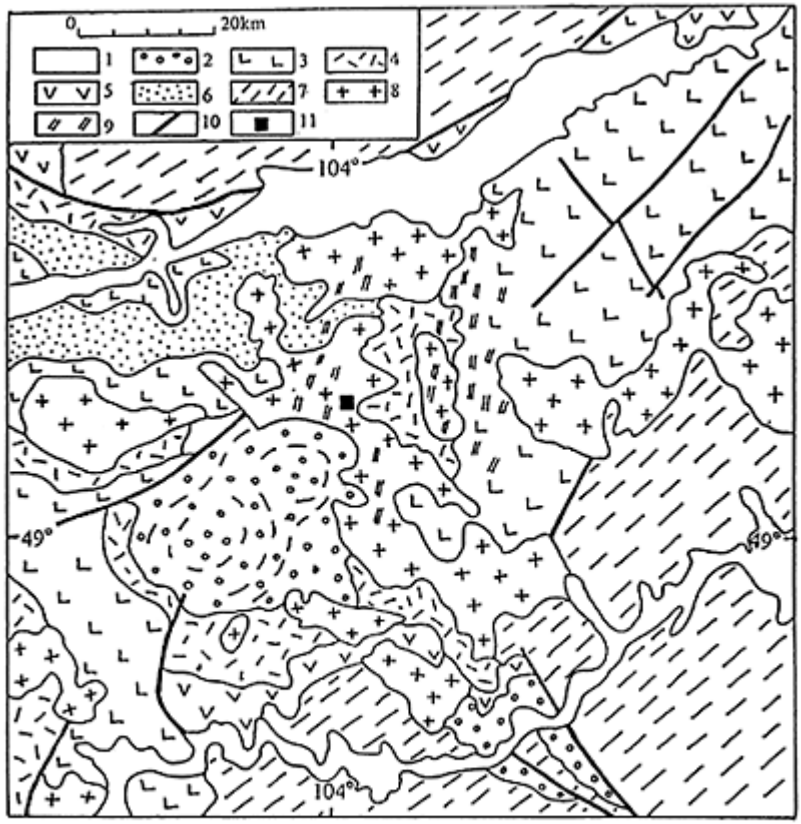

Key: 1—Quaternary deposits; 2—Mesozoic deposits; 3–6—Permian sequences: 3—basalt (P_2), 4—acid volcanics (P_1), 5—basic and intermediate volcanics (P_1), 6—volcanic–sedimentary (P_{1-2}); 7—folded basement complexes; 8—granitoid; 9—dyke; 10—fault; 11—Erdenet deposit.

Figure 66 Geological structure of the Erdenet deposit (after Kovalenko, 1991).

The Khangai batholith occupies a special place in the structure of the Permian igneous region (see Fig. 55). It is represented by a system of large intrusions, which form a wide arc around the periphery of the Khangai Synclinorium. The total area of exposure of its intrusions is about 100,000 km^2. The batholith is made up of a variety of granitoids, which form two multiphase intrusive complexes: the early (Khangai) and the late (Sharausgol) complexes (Marinov, 1973). The age of batholith formation is determined from stratigraphic relationships and from isotopic dating. The granitoids of the batholith intrude Carboniferous terrigenous deposits, which infill the Khangai Synclinorium and in places cross-cut Lower Permian volcanic suites. In turn they are intruded by Lower Mesozoic granitoids. Therefore the age of batholith formation as a whole is determined as late Permian.

Table 17 Chemical composition of the igneous rocks of the Selengin Complex in the Erdenet area (after Kovalenko, 1991).

	Egingol Massif		**Tsokhingol Massif**		**Erdenet Massif**							**Massifs of the southern Orkhon-Selengin Trough**				
	1	**3**	**1**	**2**	**4**	**1**	**2**	**2**	**3**	**6**	**5**	**2**	**3**	**4**	**5**	**7**
SiO_2	47.20	66.85	45.35	54.50	70.10	50.40	57.90	61.90	66.57	65.74	72.85	55.25	67.91	70.74	74.35	70.00
TiO_2	1.50	1.00	1.12	1.05	0.30	0.77	0.66	0.44	0.77	0.41	0.16	0.78	0.47	0.36	0.34	0.02
Al_2O_3	18.00	17.40	21.04	19.03	15.76	18.08	17.47	17.90	16.03	15.06	13.70	18.40	15.31	14.56	12.90	15.30
Fe_2O_3	1.68	1.04	3.15	2.15	1.27	3.63	3.40	1.78	1.98	1.65	0.73	4.32	2.10	1.44	1.62	0.60
FeO	8.30	2.85	7.55	5.70	1.56	5.20	3.44	1.72	1.84	1.72	1.30	3.40	1.51	0.89	0.64	1.70
MnO	0.11	0.08	0.11	0.14	0.04	0.14	0.08	0.04	0.06	0.05	0.03	0.09	0.06	0.08	0.05	0.04
MgO	6.30	1.25	7.76	3.09	0.82	7.12	3.53	2.35	1.38	1.87	0.53	3.75	1.68	1.11	0.51	0.04
CaO	9.35	1.70	10.02	7.50	1.90	7.92	4.90	3.93	2.93	2.40	1.21	6.22	2.33	1.22	0.87	1.54
Na_2O	3.03	3.75	2.10	4.05	3.83	3.31	4.47	5.40	4.61	4.81	3.47	3.85	4.41	5.24	4.15	4.70
K_2O	1.24	4.10	0.45	1.30	4.10	1.22	2.24	2.30	2.80	3.38	4.91	1.35	3.41	3.50	4.20	4.40
P_2O_5	0.52	0.22	0.02	0.11	0.06	0.16	0.29	0.16	0.13	0.19	0.05	0.09	0.12	0.10	0.02	0.02
F	0.06	0.04	0.04	0.05	0.02	0.07	n.d.	n.d.	0.035	n.d.	n.d.	n.d.	n.d.	0.036	n.d.	n.d.
Total	97.29	100.28	98.71	98.67	99.76	98.02	98.38	97.92	99.14	97.28	98.94	97.50	99.31	99.28	99.65	98.36
Li	28	14.5	8	5.5	6	12	14	7.3	10	4.1	14.5	16.3	11.75	7.8	n.d.	n.d.
Rb	27	122	7	19	69	39	60	57	66	90	33	96	62	111	n.d.	n.d.
Sr	720	315	1,022	482	296	625	750	411	405	258	317	239	300	100	n.d.	n.d.
Ba	n.d.	n.d.	n.d.	390	n.d.	275	359	450	646	605	715	425	598	492	n.d.	n.d.

Zr	150	20	10	150	170	116	185	215	190	297	145	355	280	263	n.d.	n.d.
Be	1	2	3	1.5	1.3	0.7	1	2	1	2	2	2.3	2.6	3	n.d.	n.d.
Sc	8	3.5	16	27	13	26	16	4.7	6.5	5	15	7.9	4.3	4.3	n.d.	n.d.
B	6	18.5	18	4.5	18.7	7	27	7	12.5	6	17.5	16.3	12.7	9.3	n.d.	n.d.
Sn	6	5.5	2.2	1.5	2.8	3.5	1.5	1.5	2.7	2	3	3.2	2.5	3.2	n.d.	n.d.
Mo	2	2.5	0.7	1	1	0.7	1	1.3	1	1	1	1.3	1.3	1	n.d.	n.d.
Cu	2	17	53.5	58.5	10	49	320	30	70	121	184	184	57	51	n.d.	n.d
Se	0.01	0.025	0.09	0.07	0.03	n.d.	n.d.	n.d.	n.d.	n.d.	n.d.	n.d.	n.d.	n.d.	n.d.	n.d
Pb	17	41.5	8.5	11.5	33.3	11	17	16	37	23	14	26	24	26	n.d.	n.d.
Zn	170	65	155	175	70	85	135	37	215	90	220	211	97	147	n.d.	n.d
Cr	91	13	532	21	7	125	61	6	42	23	86	68	48	69	n.d.	n.d
Ni	98	6	130	9	3	62	15	25	11	10	28	22	12	10	n.d.	n.d.
Co	22	5	76	19	3	32	10	8	5	2	22	8	6	2	n.d.	n.d.
V	280	315	1,575	1,058	30	195	49	62	30	9	89	35	40	6	n.d.	n.d.

Note: 1—gabbro, 2—diorite, 3—granodiorite, 4—granite, 5—leucogranite, 6—granosyenite, 7—subalkaline granite.

The U-Pb concordia zircon and sphene ages (unpublished data) for the batholith rocks are in the range of 250–254 Ma, i.e. the end of the late Permian: thus they are consistent with estimates from stratigraphic relationships.

For the most part, the Khangai Complex is made up of hornblende-biotite- and biotite granodiorites and granites (Fedorova, 1977). Tonalites, quartz-diorites and gabbro-diorites are subordinate. The complex includes intrusions of either essentially granitic or granodioritic composition, therefore the rocks as a whole are placed in the granodiorite-granite association. Intrusions displaying a zonal structure, in which more basic varieties occur around the periphery of the intrusions are fairly common. Eruptive contacts locally observed between rocks of different composition suggest that the complex was formed in two successive phases. The first phase was represented by granodiorites, with subordinate quartz-diorites and tonalites, and the second phase by adamellites and granites. As a whole the dyke bodies are atypical. They consist of fine-grained granodiorite and aplite-granite. Granodiorite- and granite-porphyries, and plagioclase porphyric diorites, are less common.

The granodiorites of the complex are rather similar in their general compositions. The mineral assemblage of the rocks consists of plagioclase, orthoclase, quartz, biotite, and hornblende. Variations in the abundance ratios of rock-forming minerals gave rise to gradual transitions between the main rock types. The rocks of the complex are grey in colour and medium- to coarse-grained in texture; as a rule, they have a distinct porphyritic texture. The porphyritic appearance is imparted by thick tabular phenocrysts (1.5–2 cm in diameter) of microcline and plagioclase, which make up 20–25% of the rock.

The chemistry of the rocks is consistent with the calcalkaline petrochemical series (Table 18). The rocks show $Na_2O+K_2O<8\%$ and a Na_2O/K_2O of greater than one. The rocks are weakly oversaturated with alumina, and they have fairly high contents of alkali-earth elements; the agpaitic coefficient is usually lower than 0.7.

The granitoids of the Sharaus-Gol Complex form intrusions that alternate with those of the Khangai Complex. In most cases, the intrusions of the Sharausgol Complex are

similar in size to the batholiths and show intricate contacts with their country rocks. Their elongate shape is due to the fact that they follow the major fractures that bound the Khangai depression.

The Sharaus-Gol Complex was formed in two phases. The granites of the earlier phase are rather homogeneous, and are represented by pale-pink medium- to coarse-grained leucocratic and biotite granites. The average composition of the granitesis: plagioclase 28%, orthoclase 39%, dark-grey or smoky quartz 30.5%, biotite 1.3%, accessory minerals 1.2% (Dergunov and Kovalenko, 1995).

The second (later) phase of the complex is represented chiefly by fine-grained pinkish-grey leucocratic and biotite granites. The rocks form small stocks and dykes up to a few square kilometres in size; they have sharp contacts with the granitoids of the first phase. The granites of the second phase are similar in composition to those of the first phase, but differ from them by containing the products of autometasomatic processes of albitization and muscovitization.

Table 18 Compositions of rocks of the Khangai Complex.

n/n	**1**	**2**	**3**	**4**	**5**	**6**	**7**	**8**	**9**	**10**	**11**	**12**
SiO_2	60.60	71.90	70.40	70.70	61.30	66.40	68.70	68.40	66.62	71.30	67.80	71.71
TiO_2	0.73	0.21	0.12	0.20	0.81	0.45	0.43	0.46	0.57	0.81	0.82	0.48
Al_2O_3	16.80	14.40	16.70	15.40	18.70	15.70	14.75	15.90	16.20	13.93	14.88	13.35
Fe_2O_3	2.32	0.94	0.14	0.69	2.09	1.94	0.79	1.61	2.41	1.71	1.28	0.57
FeO	3.63	0.87	1.39	1.41	2.24	1.91	1.96	1.16	1.70	1.18	1.80	1.52
MnO	0.16	0.02	0.09	0.09	0.20	0.07	0.06	0.11	0.09	0.05	0.05	0.03
MgO	1.89	0.32	0.21	0.40	1.26	1.71	1.46	0.70	1.20	0.54	1.60	0.55
CaO	6.15	1.71	2.96	3.19	4.27	3.48	2.67	1.65	2.80	1.57	3.08	2.09
Na_2O	4.18	3.64	5.43	4.29	6.26	4.00	3.69	4.92	3.75	4.14	3.93	3.55
K_2O	1.75	4.93	2.22	2.63	1.52	3.57	4.49	3.84	2.94	4.27	4.21	4.54
P_2O_5	0.32	0.09	0.06	0.09	0.19	0.13	0.13	0.21	0.30	0.11	0.14	0.14
H_2O	1.17	0.78	0.63	0.72	1.24	0.92	0.93	0.00	n.d.	0.40	0.52	n.d
CO_2	0.11	0.10	0.13	0.11	0.10	0.07	0.10	0.00	n.d.	n.d.	n.d.	0.15
F	0.03	0.03	0.02	0.03	0.05	0.05	0.06	0.03	0.06	0.08	0.08	0.08
Total	99.81	99.91	100.47	99.93	100.18	100.35	100.16	98.96	98.58	100.01	100.11	98.68
Cr	3	5	3	3	3	18	21	8	5	6	21	8
Co	11	2	1	3	5	9	8	4	7	5	9	4
Sc	11.7	2.6	2.3	3.2	12.6	8	7.6	4.5	7.4	3.3	7.7	3.1
Rb	34	162	32	30	19	97	154	72	67	189	175	196
Cs	0.9	6.5	0.6	1	0.8	10	15	2.3	2.3	7	12	4.2
Ba	895	1,267	940	1603	1,512	651	644	1,645	1,244	621	626	642

n/n	1	2	3	4	5	6	7	8	9	10	11	12
Sr	416	272	372	374	393	236	243	295	391	273	293	236
Ta	0.6	1.3	0.6	0.5	0.5	1	1.2	0.6	0.6	2	1.1	2.5
Nb	5	10	7	7	8	8	8	8	6	17	8	13
Hf	5.2	5.3	2.2	3.8	13.2	5.4	6.4	7.8	5.5	6	5.5	9
Zr	144	151	71	128	402	156	157	165	181	196	191	332
Y	23	23	16	18	24	27	31	20	25	32	36	40
Th	4.6	20.6	3.6	2.4	1.6	16.6	33	8.5	9.5	30	30	56
U	1.2	1.4	0.5	0.4	0.4	1.9	4.7	1.5	1.7	4.9	2.4	3.8
La	30.1	47.8	11.4	26.7	23	26.8	45	37.4	32.3	49.8	38.1	92.6
Ce	56.3	69.2	19.4	39.4	46.2	47.4	75	58.7	54.3	78.7	65.7	144
Nd	29	26.7	8.9	15.5	25.7	22.9	33.9	24.8	24.8	33.5	30.8	61.1
Sm	7	5.15	1.97	3.05	6.6	5.31	7.4	5.14	5.47	7	6.9	12.6
Eu	1.7	0.66	0.64	0.82	3.06	0.91	0.88	1.07	1.2	0.9	0.87	0.99
Gd	4.48	2.8	1.76	1.63	5.43	4.09	5.05	2.84	2.91	4.1	3.9	5.4
Tb	0.79	0.44	0.32	0.31	0.92	0.7	0.84	0.51	0.53	0.65	0.67	0.87
Yb	2.83	0.97	1.41	1.49	2.85	2.31	2.43	2.07	2.2	1.5	2.14	2.21
Lu	0.42	0.13	0.22	0.23	0.41	0.34	0.35	0.31	0.33	0.21	0.31	0.31

n.d.—not determined.

Geochemically, the rocks of the complex belong both to the calcalkaline and the subalkaline petrochemical series (Table 19). Their alkali content varies between 7.0 and 8.5%. The sodium/potassium ratio is variable but, on the whole, $K_2O<Na_2O$. The agpaitic coefficient (Na_2O+K_2O/Al_2O_3) varies from 0.6 to 0.9. Compared with the rocks of the Khangai Complex, these rocks are richer in Rb and Th and poorer in Sr and Ba.

Rock Associations of the Bimodal Complex

The bimodal complex of the Upper Palaeozoic igneous region is made up of igneous bimodal associations (basalt-trachyrhyolite, basalt-comendite or pantellerite) after which the complex is named, as well as granite and syenite.

The distribution of the associations is related to linear systems of grabens, which are controlled by the largest W-E faults in Mongolia. Five systems or zones are recognized (Fig. 67). Two of them are located in the Hercynian terrain (the Gobi-Tien Shan Zone and the zone of the Main Mongolian lineament) and three are found in the Caledonian megablock (Gobi-Altai, North Gobi, and North Mongolian zones). The geology of the largest zones is outlined below.

The Gobi-Tien Shan Zone represents a chain of volcanic terrains and intrusions of alkali granites; it is controlled by a system of adjacent faults of the same name, which are concentrated in a 60–75-km-wide belt. The volcanic rocks of the bimodal

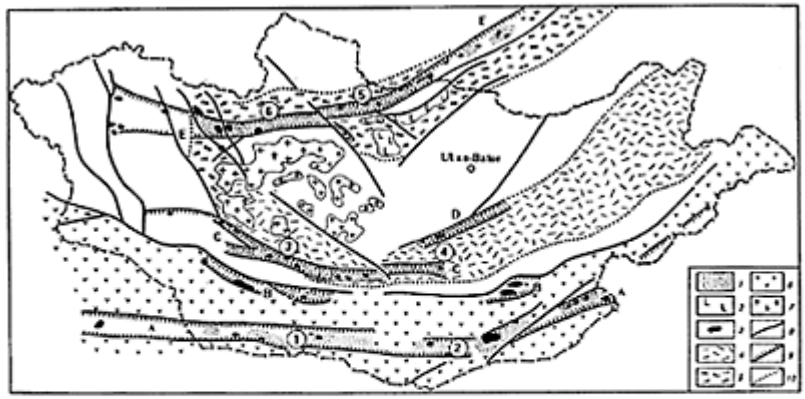

Key: Rift zone: A—Gobi–Tien Shan, B—Main Mongolian lineament, C—Gobi-Altai, D—North Gobi, E—North Mongolian–Transbaikal. Districts: 1—Tost, 2—Nomgon, 3—Chandoman, 4—Ulziit, 5—Teshig, 6—Bugsein-Gol. 1—bimodal basalt-pantellerite–comendite associations; 2—subalkaline basalt; 3—peralkaline granite; 4–6—terrains of rocks of the differentiated complex: 4—the Lower Permian of the Central Mongolian belt, 5—the Lower Permian of the North Mongolian belt, 6—Carboniferous of the South Mongolian belt; 7—the granite of the Khangai batholith; 8—fault, 9—rift-zone boundaries; 10—boundary of the volcanic areas.

Figure 67 Distribution of Upper Palaeozoic rift zones in Central Asia (after Yarmolyuk and Kovalenko, 1991).

Table 19 Compositions of rocks of the Sharaus-Gol Complex.

n/n	**1**	**2**	**3**	**4**	**5**	**6**	**7**	**8**	**9**	**10**
Sample	**SHAR4475**	**XAH4478**	**XAR4490**	**ZX5020**	**ZX5021**	**ZX5023**	**ZX5025**	**ZX5026**	**1715a**	**1715w**
SiO_2	75.30	68.90	73.10	72.05	74.65	75.23	73.01	70.86	75.19	71.18
TiO_2	0.13	0.49	0.20	0.24	0.21	0.11	0.22	0.33	0.20	0.48
Al_2O_3	13.40	14.20	13.26	14.10	13.60	12.20	13.55	14.15	12.60	12.98
Fe_2O_3	0.50	1.43	1.69	0.11	0.80	0.10	1.30	0.51	0.66	2.32
FeO	1.09	1.84	1.93	1.16	0.45	0.90	0.27	2.24	0.56	1.21
MnO	0.09	0.06	0.06	0.05	0.04	0.13	0.06	0.04	0.05	0.09
MgO	0.15	0.57	0.24	0.30	0.30	0.20	0.25	0.25	0.08	0.34
CaO	0.63	2.06	1.75	1.20	0.90	0.65	0.80	0.70	0.28	1.14
Na_2O	4.26	4.28	4.43	4.31	3.50	4.76	4.81	4.36	4.40	4.17
K_2O	4.14	4.51	2.75	4.78	4.20	4.95	4.69	5.30	4.93	5.07
P_2O_5	0.01	0.20	0.09	0.16	0.19	0.11	0.13	0.14	0.06	0.09
H_2O	0.10	0.81	0.69	n.d.	n.d.	n.d.	n.d.	n.d.	0.08	0.08
F	n.d.	0.07	0.03	0.04	0.03	0.03	0.03	0.07	0.1	0.05
Total	99.80	99.35	100.19	98.46	98.84	99.34	99.09	98.88	99.08	99.15
Cr	3	7	6	6	3	38	4	24	2	4
Co	1	4	2	3	2	1	1	3	1	3
Sc	3.5	4	8.4	3.6	2.3	1.1	2.8	4.2	1.2	4.7
Rb	96	148	71	146	170	140	91	154	315	194
Cs	5.3	3.6	3	4.8	8.3	4.3	2.2	2.8	10	7.5

Ba	564	730	549	688	556	185	532	425	100	238
Sr	74	270	100	178	192	62	85	64	52	96
Ta	0.9	1.7	0.9	0.8	0.8	1.2	0.8	1.7	5	4
Nb	10	16	9	9	9	11	11	17	43	39
Hf	3.6	6.5	5.8	7.4	4.2	3.6	5.5	10.4	7	18
Zr	70	170	165	214	125	92	173	268	185	520
Y	23	27	36	33	24	32	25	12	35	48
Th	10.3	27	7.8	33	21	18	12.6	27.5	32	57
U	1.3	3.9	2	7.9	4	1.6	2.2	3.5	8.2	10.5
La	15.01	51.1	23.4	39.3	26.9	29.1	35.2	49.9	31	54.5
Ce	25.8	80.9	45.6	63.3	38.9	45.4	57.2	105.5	53.6	90
Nd	12.1	34.6	24.5	27.5	15	19.1	25.1	62	25.2	40.2
Sm	2.72	7.2	6.16	5.8	2.9	3.9	5.36	16.7	5.7	8.7
Eu	0.28	1.01	0.94	0.62	0.49	0.34	0.64	0.91	0.18	0.63
Gd	2.54	4.88	5.25	3.29	2.04	3.27	3	13.5	3.9	5
Tb	0.47	0.77	0.98	0.6	0.37	0.6	0.57	2.2	0.74	0.91
Yb	1.96	1.84	4.46	2.52	1.49	2.44	2.83	6.17	3.48	3.82
Lu	0.3	0.25	0.69	0.38	0.23	0.37	0.45	0.87	0.54	0.58

complex usually occur concordantly with the rocks of the Carboniferous differentiated complex. However, as a rule, they are separated by erosion surfaces or by tuffaceous-sedimentary rocks. The late Carboniferous-early Permian age of the volcanics of the bimodal complex is supported by finds of plant remains of appropriate age in the volcanic rocks of some areas of the volcanic zone (Table 11). The Rb-Sr ages of the peralkaline granites of the zone fall in the range 286–297 Ma (Wang and Han, 1994; Kovalenko *et al.*, 1995). The granites are associated with the magma chambers of comendite volcanoes (Yarmolyuk, 1983) and thus support a late Carboniferous-early Permian age for the magmatism.

Figure 68 shows the structure of the bimodal association of the Tost Ridge area and Figure 69 shows sections of the volcanic suites, which reach 2,000 m in thickness. Sections through the suite display alternating layers of basalts, on the one hand, and comendites and trachyrhyolites, on the other (Yarmolyuk, 1983). The latter form large lenses near volcanic vents and thus are associated with palaeostrato volcanoes. The basalts occur within the lava plateaux. It should be noted that the formation of the bimodal complex was related to the creation of a W–E trend belt of dykes of basalts and comendites. Table 20 gives the composition of the rocks.

The *Gobi-Altai Zone* includes a chain of grabens, infilled with the rocks of the bimodal complex, which, in the present structure, extend along the northern flank of the Gobi Altai ridges and farther east for over 1,000 km. At present the grabens reach a maximum width of 15 km. The zone may have formed during the second half of the early Permian, as suggested by the following data. Firstly, the thin sedimentary layers, found within the volcanic suites, yield early Permian flora (Table 21). Secondly, the bimodal volcanic suites rest disconformably, or with basal conglomerates, on the volcanics of the differentiated complex (which are also dated as early Permian from their contained plant remains). Thirdly, the rocks of the bimodal complex are locally overlain by conglomerates, which yield lower Upper Permian flora (Table 21).

Figure 70 is a chart of the largest area of the rocks of the bimodal complex, associated with the Khara-Argalinty, Dund-Argalinty, and Bakhar-Ula ridges. The complex is composed of subalkali basalts, comendites, pantellerites, and trachyrhyolites. The thickness of the suites varies from 1,500 to 2,000 m (Yarmolyuk, 1983). The rocks show an obvious heterogeneity in their distribution, and differ in their composition. Acid rocks, namely, comendites, pantellerites, trachyrhyolites, form lenses of various sizes, associated with strato volcanoes or individual extrusive domes. As in the Gobi-Tien Shan Zone, the basalts form lava plateaux. The development of the graben was related to the formation of a W–E dyke belt, whose relics can be seen in the basement inliers and the lower horizons of the volcanic suite.

Table 22 gives the composition of the rocks of the bimodal complex of the Gobi-Altai Zone.

The *North Mongolian Zone* is controlled by the distribution of rocks of the bimodal complex and intrusions of peralkaline granites within a system of E-W faults, stretching from the ridges of the Mongolian Altai along the Khan-Khukhei

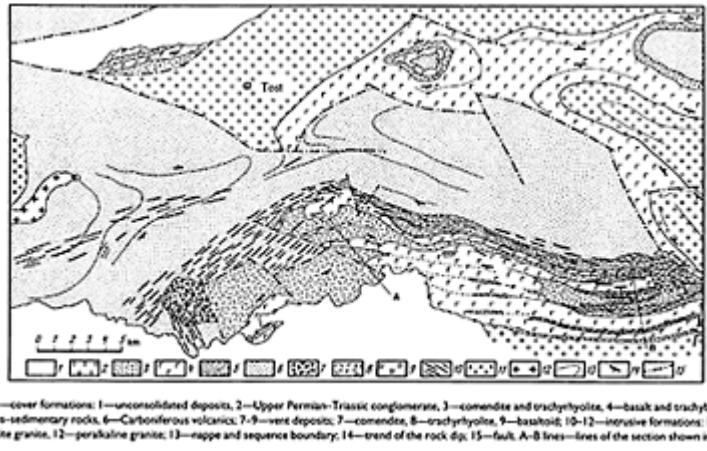

Key: 1-6—cover formations: 1—unconsolidated deposits, 2—Upper Permian-Triassic conglomerate, 3—comendite and trachyrhyolite, 4—basalt and trachybasalt, 5—tuffaceous-sedimentary rocks, 6—Carboniferous volcanics; 7-9—vent deposits; 7—comendite, 8—trachyrhyolite, 9—basaltoid; 10-12—intrusive formations: 10—dyke, 11—biotite granite, 12—peralkaline granite; 13—nappe and sequence boundary; 14—trend of the rock dip; 15—fault; A-B lines—lines of the section shown in Fig. 69.

Figure 68 Geological structure of the north-eastern extremity of the Tost Ridge (on Fig. 67).

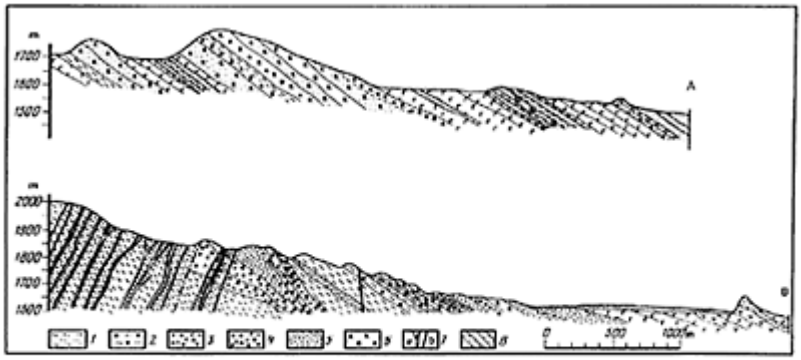

Key: 1—comendite ignimbrite, 2—comendite lava breccia; 3—orthoclase-phyric trachyrhyolite, 4—trachyrhyolite lava breccia, 5—trachyrhyolite, 6—comendite, 7—comendite dyke (a), basaltoid dyke (b); 8—tuffaceous-sedimentary rocks. Lines of section are shown in Fig. 68.

Figure 69 Volcanic sections on the south-eastern slope of the Tost Ridge.

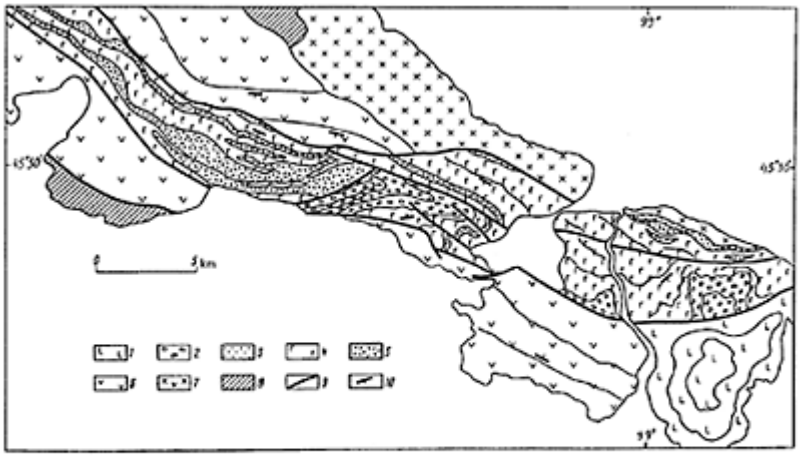

Key: 1—Cretaceous basalt; 2—Upper Permian conglomerate; 3—crumbly breccia; 4 and 5—volcanics of the bimodal complex: 4—trachybasalt, 5—trachyrholite, comendite, and trachydacite; 6—volcanics of the differentiated complex; 7—pre-Permian granitoid; 8—Lower Palaeozoic folded formations; 9—fault; 10—dips and strikes.

Figure 70 Geological structure of the Upper Palaeozoic volcanic formations of the Khara- and Dund-Argalintu Ridge (after Yarmolyuk, 1983).

and the Bolnai ridges farther east, and thence into Russia. Within the zone, the volcanics of the bimodal complex rest with a disconformity and basal conglomerates on the volcanic suites of the Lower Permian differentiated complex. The plant remains found in the terrigenous layers suggest a late Permian age for the

Table 20 Compositions of the volcanics of the bimodal complex and the alkali granites of the Tost Ridge (Gobi-Tien Shan rift zone).

	1	2	3	4	5	6	7	8	9	10	11	12	13	14	15	16
SiO_2	73.39	71.78	71.49	72.04	71.60	73.59	66.66	71.90	74.60	65.74	72.55	75.00	66.64	60.17	50.17	50.17
TiO_2	0.56	0.45	0.40	0.55	0.48	0.38	0.82	0.78	0.27	1.10	0.26	0.34	0.55	1.50	1.90	2.70
Al_2O_3	9.78	10.00	10.00	10.20	10.00	9.80	15.00	10.08	9.75	14.18	13.60	9.00	14.75	15.60	16.63	15.56
Fe_2O_3	2.16	2.92	2.70	2.60	2.70	4.51	—	2.56	—	—	—	—	—	—	—	—
FeO	3.97	3.95	4.05	3.96	4.05	1.71	4.40	4.28	5.71	6.23	3.36	6.54	5.60	7.48	10.77	11.56
MnO	0.27	0.20	0.25	0.20	0.22	0.21	0.12	0.28	0.16	0.18	0.07	0.16	0.13	0.15	0.26	0.11
MgO	0.05	0.34	0.34	0.24	0.20	0.20	1.32	0.08	0.10	1.05	0.22	0.30	1.08	1.90	4.26	4.46
CaO	0.39	0.76	0.86	0.69	0.56	0.39	2.10	0.50	0.52	1.85	0.73	0.35	0.73	2.88	7.20	8.25
Na_2O	3.96	4.05	3.78	4.43	4.40	3.62	5.90	3.76	3.56	5.99	6.70	2.73	3.87	5.17	4.69	3.72
K_2O	4.33	4.09	4.19	4.19	4.12	4.12	1.36	4.69	4.20	2.30	1.52	5.16	4.50	3.62	1.86	1.29
P_2O_5	n.d.	n.d.	0.48	0.42	0.67	0.51	0.12	n.d.	n.d.	0.20	0.01	n.d.	0.06	0.49	0.45	0.62
F	0.11	0.12	0.08	0.12	n.d.	0.10	n.d.	0.11	n.d.	n.d.	n.d.	—	n.d.	n.d.	n.d.	n.d.
LOI	0.70	1.39	0.93	0.78	1.03	0.37	1.52	0.52	0.52	0.88	0.58	0.14	2.16	0.78	2.38	1.68
Total	99.67	100.05	99.55	100.42	100.03	99.51	99.32	99.54	99.39	99.70	99.60	99.72	100.07	99.74	100.57	100.12
a.c.	1.15	1.11	1.08	1.16	1.17	1.06	0.75	1.12	1.07	0.87	0.93	1.15	0.73	0.8	0.59	0.48
Li	23	n.d.	15	9	10	83	n.d.	n.d.	15	n.d.	n.d.	n.d.	n.d.	n.d.	n.d.	n.d.
Rb	98	n.d.	72	74	74	76	n.d.	n.d.	91	n.d.	n.d.	n.d.	n.d.	n.d.	n.d.	n.d.
Sr	47	n.d.	48	46	42	47	180	n.d.	80	240	90	n.d.	n.d.	n.d.	n.d.	900
Ba	85	n.d.	120	90	140	110	500	n.d.	83	600	400	n.d.	n.d.	n.d.	n.d.	600
Be	5.8	n.d.	7.9	8.6	8.7	9.5	3.1	n.d.	3.1	2.7	0.7	n.d.	n.d.	n.d.	n.d.	1.6
B	21	n.d.	21.5	18	17	11	10	n.d.	12	11	9	n.d.	n.d.	n.d.	n.d.	20

	1	2	3	4	5	6	7	8	9	10	11	12	13	14	15	16
Sn	13	n.d.	6.8	6.3	8.7	6.6	2.3	n.d.	8.5	2.6	6.3	n.d.	n.d.	n.d.	n.d.	3
Pb	28	n.d.	24	26	33	17	10	n.d.	30	13	22	n.d.	n.d.	n.d.	n.d.	7
Zn	294	n.d.	91	86	126	79	110	n.d.	210	105	138	n.d.	n.d.	n.d.	n.d.	178
Cr	25	n.d.	32	46	37	3	32	n.d.	40	66	66	n.d.	n.d.	n.d.	n.d.	50
Ni	12	n.d.	9	17	20	5	6	n.d.	11	25	26	n.d.	n.d.	n.d.	n.d.	50
Co	3	n.d.	1	2	1	1	4	n.d.	1	7	8	n.d.	n.d.	n.d.	n.d.	35
V	8	n.d.	11	10	6	7	36	n.d.	5	50	21	n.d.	n.d.	n.d.	n.d.	250
La	n.d.	78	74	72	72	n.d.	18	n.d.	77	35	50	66	79	36	22	14
Ce	n.d.	190	160	170	170	n.d.	44	n.d.	140	61	77	180	100	50	46	32
Nd	n.d.	57	61	59	53	n.d.	27	n.d.	75	43	46	82	79	45	32	20
Sm	n.d.	20	15	16	15	n.d.	6	n.d.	17	9	12	17	10	6	6	5
Eu	n.d.	2.3	2.2	1.8	1.9	n.d.	2	n.d.	2.5	4.3	1.2	2.4	3.7	2.5	2	2
Gd	n.d.	24	20	23	23	n.d.	n.d.	n.d.	20	14	15	27	19	n.d.	n.d.	n.d.
Dy	n.d.	17	17	18	16	n.d.	n.d.	n.d.	30	14	16	33	20	n.d.	n.d.	n.d.
Yb	n.d.	20	19	20	19	n.d.	3.6	n.d.	20	5	8.2	21	12	4.6	2.9	n.d.
Y	n.d.	100	97	100	100	n.d.	40	n.d.	120	48	65	110	88	42	31	23

Note: 1 and 6—comendite; 2–5—peralkaline granite; 7—trachydacite; 8–16—rocks sampled up the section of the bimodal complex in the Khoshatu-Ula area: 8—pantellerite, 9—comendite, 10—trachydacite, 11 and 12—comendite, 13—peralkaline trachydacite (altered), 14—trachyte, 15 and 16—basalt of the upper part of the section; a.c.—agpaitic coefficient; n.d.-not determined; LOI—losses of ignition.

Table 21 Distribution of fossils over sections of Permian rocks, Gobi-Altai volcanic zone (after Yarmolyuk, 1983).

Age	Strata	Somon Chandoman and Olonbulak	Khara- and Dund-Argalinty ridges		
			2 km north of mount 2,005.7 m	Mount Shovkh Ula area	South of Mt Noyen-Bogdo-Ula
Late Permian	Sand-conglomerate locally containing	Upper horizons 1. *Rutfloria* cf. *delicata* Durante 2. *R. cf. synensis* (Zal) S.Meyen 3. *Cordaites*	Middle horizons 1. *Cordaites* cf. *graculentus* (Gorel.) S. Meyen 2. *C. cf.*		Lower horizons 1. *Rutfloria* ex. gr. *derzavinii* (Neub.) S. Meyen 2. *Cordaites* aff. *latifolius* (Neub.) S.Meyen

		aff. *gorelovae* S.Meyen 4. *C. cf. oblo*nga Radcz. 5. *C.* cf. *angustifolius* Neub. 6. *Crassinervia* ex. gr. *pentagonata* Joreb.	*minax* (Gorel.) S.Meyen		3. *C. ex. gr. pra*lincisa (Gorel.) S.Meyen 4. *C. cf. suica*tus (Neub.) S.Meyen 5. *C. cf. kuznetskia*nus (Gorel.) S.Meyen
Early Permian	Bimodal volcanic complex (late-stage)			1. *Cordaites* cf. *singularis* (Neub.) S.Meyen 2. *Rutfloria* with fine dorsal grooves	
	Differentiated volcanic complex (early-stage)		Lower Permian flora		

Table 22 Compositions of rocks of the bimodal complex in the Khara-Argalintu-Chandoman (Gobi-Altai rift zone) area.

	1468–2	**1468–3**	**1468–4**	**1468–5**	**1468–7**	**1468–9**	**1468–10**	**1468–11**	**1468–12**	**1469–7**
	1	**2**	**3**	**4**	**5**	**6**	**7**	**8**	**9**	**10**
SiO_2	48.91	44.78	73.18	46.38	70.22	75.40	50.00	75.25	72.33	71.99
TiO_2	1.25	1.33	0.46	1.60	0.45	0.21	1.46	0.33	0.54	0.37
Al_2O_3	17.47	16.12	11.83	16.23	12.75	11.43	17.31	9.93	10.53	13.40
Fe_2O_3	4.08	3.55	3.58	4.55	5.61	2.44	5.77	5.37	4.79	2.11
FeO	5.05	4.75	1.13	5.00	0.52	0.40	3.30	0.31	0.39	0.72
MnO	0.14	0.12	0.02	0.15	0.04	0.07	0.12	0.02	0.04	0.06
MgO	6.11	6.10	0.14	8.23	0.07	0.06	4.90	0.02	0.14	0.21
CaO	8.60	10.51	0.06	8.66	0.20	0.06	7.44	0.09	0.38	0.72
Na_2O	3.29	2.62	2.89	3.28	4.19	2.39	3.47	2.88	5.12	4.41
K_2O	0.94	0.23	5.73	0.53	4.75	6.33	2.88	5.00	4.33	5.01
H_2O^-	0.26	0.30	—	0.46	—	0.18	0.26	0.16	0.18	0.08
H_2O^+	2.56	3.85	1.09	3.65	0.93	0.55	2.19	0.28	1.09	0.71
P_2O_5	0.27	0.32	0.06	0.38	0.05	0.07	0.53	0.10	0.08	0.06
CO_2	1.01	4.94	0.36	1.03	0.14	0.35	0.54	0.46	—	—
Total	99.94	99.52	100.53	100.13	99.92	99.94	100.17	100.20	99.94	99.85

La	14.6	14.9	65.9	8.3	64.7	91.5	31.7	69	122	83.4
Ce	30	30.5	134	20.7	130	168	59.8	140	237	148
Nd	17.2	17.4	75.9	14.6	72.5	84	31	78.7	127	71.9
Sm	4.6	4.6	19.8	4.6	18.7	20	7.6	20.4	32	16.6
Eu	1.39	1.47	1.28	1.49	0.65	0.39	1.87	2.39	1.6	1.12
Gd	5.1	5.2	13.8	3.3	13.7	17.3	4.81	15.8	25.2	10.5
Tb	0.85	0.86	2.5	0.6	2.52	3.4	0.83	2.87	4.6	2
Yb	2.48	2.48	9.64	2.21	10.7	19.9	2.68	11.6	19.5	9.9
Lu	0.35	0.35	1.45	0.33	1.64	3.23	0.39	1.75	2.98	1.56
Sc	29	27	1.9	33	6.2	1	24	0.9	0.7	53
Cr	79	177	n.d.	165	17	9	47	18	17	25
Co	37	37	0.3	42	0.43	0.5	29	0.4	0.4	0.6
Cs	1.6	4.4	0.8	2.8	2.3	3	1	1.7	5.5	27
Hf	3.2	3.6	14	3.2	20	32	4.7	17	31	19
Ta	0.3	0.4	1.5	0.2	1.8	5.7	0.5	1.6	3.3	2
Th	2	2.3	13	1	11	42	2	13	25	13
U	1.4	0.3	3	n.d.	4	8	n.d.	3	6	4

	1470	**1471–4**	**1474–7**	**1474–8**	**1476–1**	**1476–2**	**1476–3**	**1481–3**	**1483–3**	**1483–5**
	11	**12**	**13**	**14**	**15**	**16**	**17**	**18**	**19**	**20**
SiO_2	64.72	50.10	75.75	75.24	73.58	50.40	74.33	66.07	50.05	51.52
TiO_2	0.70	1.67	0.31	0.27	0.36	2.59	0.30	0.68	1.49	1.16
Al_2O_3	14.72	16.81	10.26	10.24	13.46	14.73	10.63	16.19	17.91	17.47
Fe_2O_3	3.99	6.61	3.08	2.95	0.87	5.26	3.44	2.11	4.65	7.21
FeO	1.07	2.95	1.06	1.46	1.64	6.02	1.28	0.99	3.93	2.47
MnO	0.15	0.14	0.06	0.09	0.05	0.16	0.09	0.11	0.15	0.12
MgO	0.48	5.28	0.04	0.04	0.11	4.11	0.14	0.42	4.25	3.04
CaO	1.63	7.68	0.12	0.42	0.20	6.41	1.01	0.76	7.43	6.16
Na_2O	5.08	3.75	4.34	5.13	5.19	4.57	4.24	5.87	3.84	5.22
K_2O	5.13	1.65	4.23	3.18	3.46	2.52	3.59	5.51	2.30	2.34
H_2O^-	0.10	0.16	0.06	0.11	0.02	0.20	n.d.	0.08	0.39	0.19
H_2O^+	1.01	1.66	0.61	0.57	0.92	1.69	0.58	0.84	2.91	2.59
P_2O_5	0.12	0.83	0.03	0.04	0.11	0.74	0.04	0.16	0.71	0.52
CO_2	1.01	0.20		0.20	n.d.	0.18	0.10	0.15	0.54	0.35
Total	99.91	99.49	99.95	99.94	99.97	99.58	99.77	99.94	100.55	100.36

La	45.8	n.d.	81.7	91.1	58.7	37.2	58.9	n.d.	n.d.	n.d.
Ce	91	n.d.	147	164	111	72.7	118	n.d.	n.d.	n.d
Nd	49.5	n.d.	71.9	80.4	57.3	39.2	65.6	n.d.	n.d.	n.d
Sm	12.6	n.d.	16.8	18.8	14	9.9	16.9	n.d.	n.d.	n.d
Eu	2.02	n.d.	0.62	0.73	0.56	2.78	0.93	n.d.	n.d.	n.d
Gd	8.91	n.d.	9.4	12.1	9.2	10.7	11.8	n.d.	n.d.	n.d
Tb	1.58	n.d.	1.9	2.3	1.73	1.74	2.1	n.d.	n.d.	n.d
Yb	5.94	n.d.	11.7	12.3	8	4.6	8.8	n.d.	n.d.	n.d
Lu	0.89	n.d.	1.92	1.97	1.25	0.64	1.33	n.d.	n.d.	n.d
Sc	16.6	n.d.	2.6	2.8	3.8	30	2.4	n.d.	n.d.	n.d
Cr	22	n.d.	15	21	14	25	17	n.d.	n.d.	n.d
Co	0.8	n.d.	0.4	0.5	1.4	29	0.4	n.d.	n.d.	n.d
Cs	1.8	n.d.	2.1	0.8	1.3	0.81	0.8	n.d.	n.d.	n.d
Hf	10	n.d.	23	24	15	6	18	n.d.	n.d.	n.d
Ta	1.1	n.d.	2.1	2	1.6	0.8	1.7	n.d.	n.d.	n.d
Th	5	n.d.	18	17	20	3.5	16	n.d.	n.d.	n.d
U	4	n.d.	4	6	7	1	0.9	n.d.	n.d.	n.d

Note: Rocks sampled up the section of volcanic strata in the areas of the ridges: 1–11—Chandoman, 12–17—Khara-Argalintu, 18–20—Dund-Argalintu.

volcanics (Table 23). The Rb-Sr ages of the volcanics fall in the range 260–250 Ma (Yarmolyuk *et al.*, 1990, 1995c), i.e. they are in agreement with the data.

The composition and distribution of the rocks of the complex can be illustrated by the area of the confluence of the Tarbagatai-Gol and the Eguin-Gol rivers (Fig. 71). The volcanic bodies of the complex are concentrated there within an E–W-trending graben, and form a volcanic suite with a complex facies structure. Intrusions of peralkaline granites and syenites occur along the margins of the graben and within it. The exposed volcanic section reaches 3,000 m in thickness. The volcanic suite is composed of subalkaline basalts, pantellerites, and alkali trachydacites. These volcanics, which differ in their composition, occur in the suite in comparable amounts. They are distributed more or less irregularly over the section, thus suggesting that the foci of the basalt and pantellerite-alkali trachydacite eruptions existed there at the time the suite was formed. Local accumulations of alkali-sialic rocks, forming large lava lenses, are the probable products of centraltype volcanoes. This can be exemplified by the volcanic terrain of Mt Butelin-Ula. There a stock of alkali quartz-syenite intrudes the lower part of the volcanic suite. In the endocontact zone, the syenites are fine grained in texture and resemble alkali trachydacite lava flows. It should be stressed that the position of

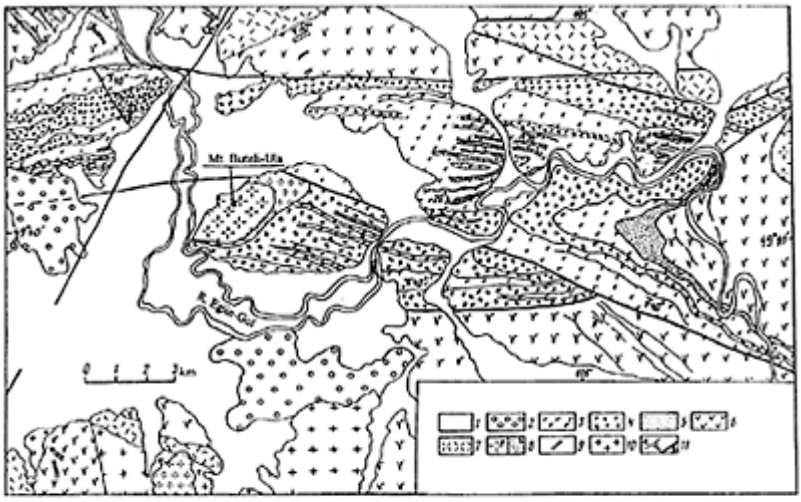

Key: 1—Quaternary deposits; 2—conglomerate (J_{1-2}); 3 and 4—rocks of the bimodal complex (P_2): 3—subalkaline basalt, 4—pantellerite, comendite, alkali trachydacite; 5—tuffaceous-sedimentary rocks; 6–7—differentiated volcanic complex (P_1) 6—trachyandesite basalt and trachyandesite, 7—trachydacite, trachyrhyolite; 8—peralkaline granite and syenite (P_2) medium-grained (a), fine-grained (b); 9—comendite, pantellerite, alkali-granite–porphyry dykes; 10—granosyenite and leucogranite (P_1); 11—attitude (a), fault (b).

Figure 71 Geological structure within the confluence of the Tarbagatai and Fgiin-Gol rivers (5 on the Fig. 67 and on the Fig. 63) (after Yarmolyuk and Kovalenko, 1991).

Table 23 Distribution of plant remains within sections of Upper Permian rocks, North Khangai Zone, North Mongolia (after Yarmolyuk and Kovalenko, 1991).

	Phytohorizon V	12. *Cordaites* cf. *clercii, Cordaites* ex. gr. *gracilentus, Lepidophyllum* ex. gr. *rotundatum, Niazonaria* sp. Conglomerates				
Late Permian	Phytohorizon IV	11. *Rufloria ex. gr. brevifol*ia, R. cf. *delicata, Rufloria* aff. *ullannurica* Conglomerates				
	Phytohorizon III	7. *Cordaites* ex. gr. *gracilentus, C.* aff. *kuznetskianus, C.* cf. *sulcatus*	8. *Rufloria* sp., *Cordaites* cf. *gracilentus*	9. *Cordaitea* cf. *singularis, C.* cf. *kuznetskianus*	10. *Cordaites* cf. *kuznetskianus*	

Bimodal volcanic complex

Numbers are those for the occurrences of fossil flora in the sections, shown in Figure 64.

the stock is determined by the thickest (≤3,000 m) part of the terrain of alkalisialic rocks, and the presence of *lahar* accumulations, typical of the slope facies of central-type volcanoes, which can be found in a section through the volcanics. Therefore there is good reason to believe that the terrain in question is part of a central-type volcano, fed by the stock described above.

Table 24 gives the compositions of the rocks of the complex of the North Mongolian Zone.

Taking into consideration the Upper Palaeozoic magmatism of the bimodal complex as a whole, it should be noted that the bimodal igneous associations possess similar structures in the various zones where they are found (Yarmolyuk and Kovalenko, 1991). They are composed of subalkaline basalt, trachyrhyolite, comendite, and pantellerite, as well as markedly subordinate trachyandesite, trachydacite, and trachyte. The rocks of the associations form large volcanic terrains, some of which reach a few thousand square kilometres in area. The terrains are very variable in structure. It is not unusual to find that individual localities are composed of either essentially acid or essentially basic rocks, but an alternation of acid and basic rocks is rather more common. The character of the sections changes rapidly along the strike of the volcanic terrains, thus indicating that the volcanic processes were rather complex in character, resulting in the formation of igneous associations.

As a rule, the basaltic part of a particular section was represented by a succession of hundreds of basalt lava flows, varying in thickness from a few metres to 20–25 m. Their original position was flat-lying, i.e. they correspond with plateau eruptions. The basalt lava flows contain intercalated thin layers and units of tuffaceous-sedimentary rocks, as well as rare lenses of trachyrhyolites and comendites or extensive bodies of acid tuffs and ignimbrites. These sections reach 1,500–2,000 m in thickness.

The distribution of acid lavas in the structure of the volcanic terrains is associated with large lava lenses, reaching 10–20 km across. The central parts of the lenses can exceed 2,000 m in thickness. At their margins, the proportion of acid volcanics decreases and they alternate with basic rocks. This highly variable type of section is peculiar to bimodal igneous associations and suggests the simultaneous formation of acid and basic volcanic products. The lenses of acid volcanics are undoubtedly products of the activity of large stratovolcanoes and caldera volcanoes (Yarmolyuk, 1983). The central parts of the stratovolcanoes contain relics of vents, made up of intricately combined stocks, extrusive dome bodies, and radiating and ring dykes of comendites, peralkaline granites, and basalts. These relationships suggest that not only acid, but also basic, melts were erupted (Yarmolyuk and Kovalenko, 1980). The structure of these volcanoes is dominated by lava flows, but lava breccias, tuffs and ignimbrites are also present there. The latter also occur outside the stratovolcanoes and form separate horizons in plateaubasalt sections.

As regards their structure, the bimodal igneous associations infill grabens of varying sizes, stretching along the strike of zones of bimodal volcanicism. The bodies occurring beneath the volcanic complex (dykes and alkali granites), which

Table 24 Variation in rock composition up the section of the volcanic sequence of the bimodal complex in the Egiin-Gol River basin.

	1614–3	1614–8	1614–9	1614–10	1614–12	1614–13	1614–14	1617–1	1617–2	1617–3	1626–1	1626–4	1626–7
	1	**2**	**3**	**4**	**5**	**6**	**7**	**8**	**9**	**10**	**11**	**12**	**13**
SiO_2	49.20	46.99	47.77	67.08	67.43	68.39	47.50	48.62	65.63	70.00	65.36	68.30	60.69
TiO_2	1.81	1.85	2.13	0.76	0.74	0.73	2.02	2.59	1.47	0.64	0.56	0.57	0.89
Al_2O_3	16.76	16.49	15.85	14.47	14.67	14.42	16.22	15.04	15.41	14.70	15.98	13.17	17.84
Fe_2O_3	3.80	5.14	5.08	2.84	3.13	4.33	5.60	6.59	4.57	3.49	2.16	4.50	3.15
FeO	6.37	5.85	6.81	2.11	1.56	0.90	5.90	5.28	—	0.10	2.22	2.15	1.73
MnO	0.17	0.16	0.21	0.16	0.14	0.12	0.17	0.17	0.19	0.15	0.11	0.25	0.11
MgO	5.06	5.11	5.17	0.57	0.40	0.05	4.57	6.24	0.11	0.10	0.29	0.24	0.87
CaO	7.19	7.78	8.20	0.31	0.34	0.18	7.73	8.51	0.56	0.10	0.34	0.26	1.93
Na_2O	3.65	3.70	3.65	5.76	5.76	5.18	3.54	3.20	5.95	4.94	6.72	5.18	6.30
K_2O	2.60	1.63	1.00	5.20	4.91	4.96	2.14	1.43	5.05	5.25	5.41	4.56	5.13
H_2O^-	0.23	0.37	0.21	0.22	0.24	0.11	0.66	1.44	0.80	0.22	0.20	0.14	0.20
H_2O^+	1.83	2.91	2.48	0.43	0.49	0.38	2.44	—	—	—	0.54	0.48	0.50
P_2O_5	0.88	0.74	1.26	0.10	0.17	0.23	1.38	0.76	0.30	0.01	0.24	0.14	0.36
CO_2	0.33	1.19	0.00	0.31	0.00	0.00	0.00	0.20	0.14	0.25	0.14	0.14	0.00
F	0.04	0.04	0.05	0.06	0.04	0.04	0.07	0.03	—	—	0.07	0.04	0.04
Total	99.92	99.95	99.87	100.38	100.02	100.02	99.94	100.10	100.18	99.95	100.34	100.12	99.74
La	37.3	25.4	37.7	69.5	89.5	91.6	30.5	21.8	79.6	101.2	123.7	105.3	51.9
Ce	80	57	77	138	191	204	64	48	180	2.16	320	230	113
Nd	44	36	43	79	92	87	35	30	79	95	135	101	58
Sm	10.3	8.5	9.5	15.9	18.9	17	7.9	6.7	16.2	19.2	29.2	19.4	11.3
Eu	2.9	2.6	2.5	1.88	1.78	1.67	2.3	2.18	1.3	1.56	2.2	1.9	2.8
Gd	5.5	4.8	7	12.1	15.6	14	5.7	5.8	14.6	15.4	24.6	16.8	10.6

	1614–3	1614–8	1614–9	1614–10	1614–12	1614–13	1614–14	1617–1	1617–2	1617–3	1626–1	1626–4	1626–7
	1	**2**	**3**	**4**	**5**	**6**	**7**	**8**	**9**	**10**	**11**	**12**	**13**
Tb	0.95	0.81	1.16	2.06	2.46	2.45	0.9	0.8	2.23	2.5	4.04	2.6	1.5
Yb	2.8	2.7	3	8.1	10.3	10	2.4	1.9	9.5	11.5	17.5	10.5	4.8
Lu	0.35	0.4	0.43	1.1	1.4	1.3	0.3	0.34	1.2	1.4	2.2	1.4	0.6
Sc	28.1	28.3	23.9	7.7	8.6	4.7	24.1	24.5	6.7	6.7	5.8	7.1	9.8
Co	29.2	40.1	36.3	1.7	1.25	3	38.7	39	2.1	1.9	0.7	1.2	2.5
Hf	4.9	4.2	5.6	19.3	24.2	23.2	4.1	3.5	20.7	27	41	26.2	9.5
Ta	0.7	0.5	0.8	1.8	2.5	2.6	0.4	0.4	2.4	2.9	4.3	2.8	1.2
Cr	124	123	263	199	157	61	300	151	42	51	23	41	15
Cs	1	1.5	1.2	1	0.8	0.7	0.6	1.5	1.8	0.8	0.6	0.8	0.6
Th	2.2	1.1	2.2	9.4	12.1	12.3	1.7	1.2	10.5	12.2	20.2	12.4	4
U	0.8	0.3	1	0.9	3.1	3	0.6	0.5	2.7	3.9	1.9	2.4	1.7
Zr	294	246	325	703	894	841	253	241	761	985	1364	985	397
Nb	14	7	12	27	50	43	8	6	49	57	87	57	24
Y	34	25	33	78	87	80	24	21	80	116	162	99	43
Sr	800	789	943	54	32	54	850	1004	59	40	31	33	131
Rb	63	16	27	118	96	135	36	12	121	134	118	140	60
Ba	1781	735	281	236	135	627	934	212	823	144	100	120	1103

could indicate the position of eroded volcanic terrains, are absent outside the margins of the grabens. This indicates a probable relationship between the formation of the grabens and the generation of the bimodal associations.

Dykes of trachybasalts, trachyrhyolites, comendites and peralkaline granites represent an important feature of the structure of volcanic terrains (Yarmolyuk *et al.*, 1981). They are represented by parallel bodies, usually lying normal to the occurrence of volcanic suites and forming dyke belts. The latter extend along the strike of the volcanic grabens for many kilometres. Dykes are particularly numerous beneath volcanic terrains (inside the basement), where they are represented by hundreds of bodies and where they account for 20–25%, locally 70% of the Earth's crust (Fig. 72). In terms of the overall width of the grabens, an area of at least a few kilometres wide is occupied by dykes. This space was created by regional crustal extension, which accompanied the bimodal magmatism and the formation of grabens.

The recognized zones of bimodal associations are considered as rift zones (Yarmolyuk, 1983). This inference is based on data on the composition of igneous associations, similar to those of modern continental rifts, and on their distribution in relation to the grabens. These rift zones form the Upper Palaeozoic rift system of Central Asia (Yarmolyuk and Kovalenko, 1991).

The composition of the rocks of bimodal associations depends only slightly on their geographical position and age of formation. Basic rocks show a relatively constant suite of phenocrysts minerals, dominated by plagioclase (andesilabradorite and labradorite), olivine, and clinopyroxene (augite or titanaugite). The content of phenocrysts is usually low (up to 15–20%). Different variations in the abundance of the minerals in the phenocrysts and the groundmass are consistent with the following main petrographic

varieties: olivine-basalt, aphyric basalt, pyroxene-plagioclase- and plagioclase porphyry-basalt and andesine-basalt.

There are also a wide variety of acid rocks. Their composition is determined by the presence of perthitic alkali feldspar (Ab_{60-50} Or_{40-50}), and quartz. The latter can be observed in graphic intergrowths with alkali feldspar. Plagioclase is atypical of the rocks and is present in only some of the subalkaline trachytes, trachyrhyodacites, and trachyrhyolites. The groundmass is made up of a quartz-alkali-feldspar aggregate. The groundmass of the alkali varieties also contains fine prismatic and acicular grains of alkali amphibole and aegirine, as well as irregular segregations of ore minerals and fluorite.

Variations in the contents of the rock-forming minerals and the composition of the groundmass generate the main rock types: comendite, pantellerite, alkali trachydacite, trachyrhyolite, trachyrhyodacite, and trachyte. All of the alkaline rocks (comendite, pantellerite, and alkali trachydacite) contain alkali femic minerals or the products of their alteration, alkali feldspar, and quartz. The latter varies from 5–7% in the comendites to 1–2% in the pantellerites. In the alkali trachydacites, quartz is present only in the groundmass.

The rocks of the bimodal igneous associations fall into the subalkaline and alkaline potassium-sodic petrochemical series (Yarmolyuk and Kovalenko, 1991). On a (Na_2O+K_2O/SiO_2 diagram, representative plotted points, showing

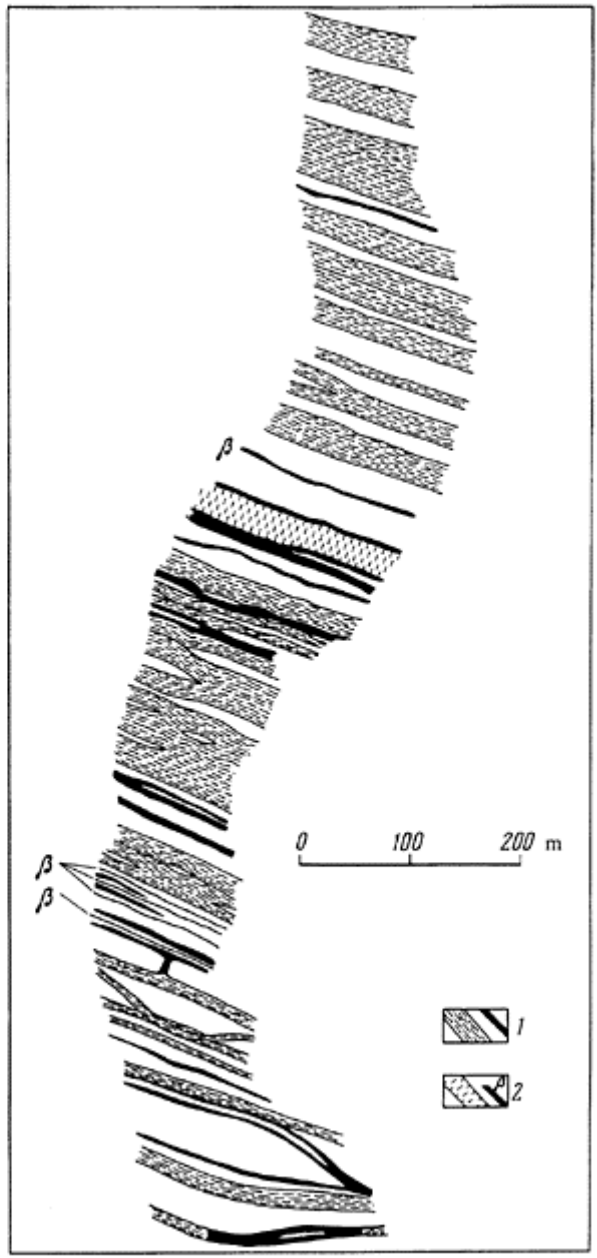

Key: 1—comendite, trachyrhyolite; 2—basalt.

Figure 72 Structure of a dyke belt on the southern slope of the Dund-

Argalintu Ridge (after Yarmolyuk, 1983)

the composition of the rocks of the associations, form two different fields (Fig. 73). One of them is presented by basic rocks (53% SiO_2); the compositions of the other field lie mainly within the range of 66%≤SiO_2≤77%. The rocks of the basic series show high alkalinity and local undersaturation with silica. They have high TiO_2(>1.8%).

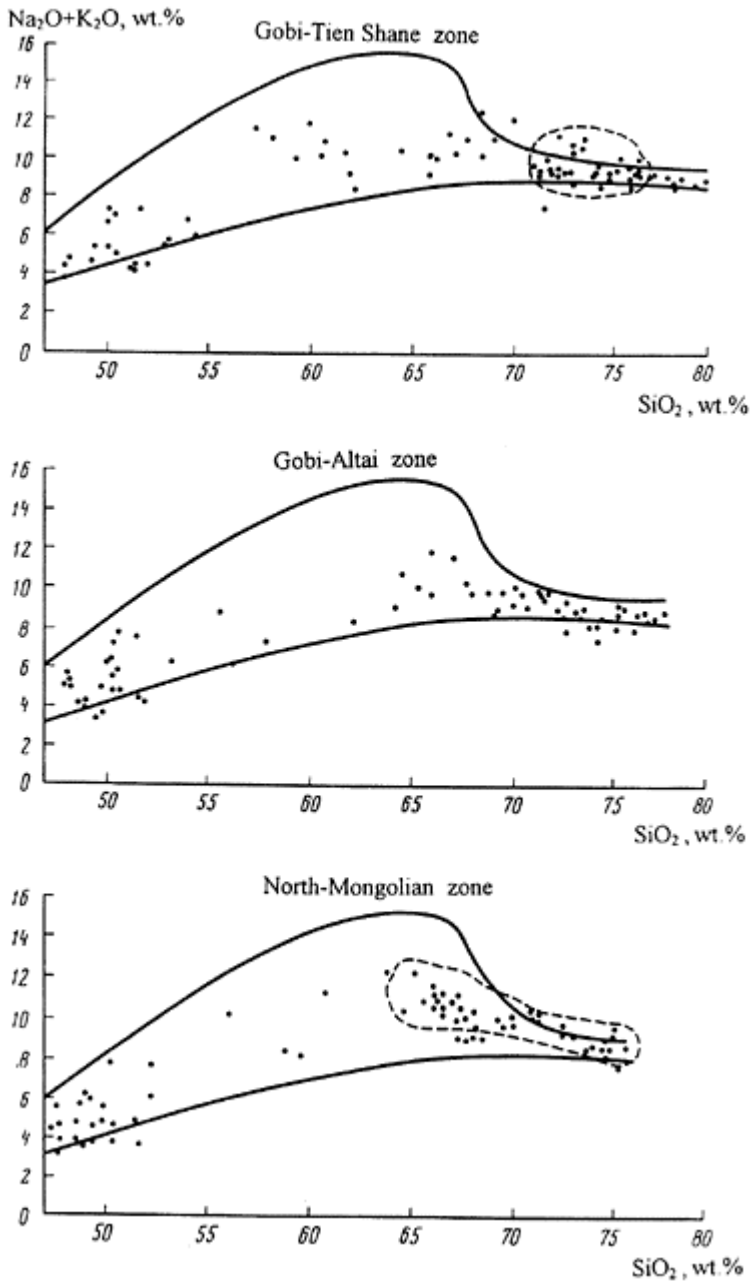

Figure 73 Rock compositions of the bimodal complex of the Late aleozoic

rift zones plotted on an SiO_2–(Na_2O+K_2O) classification diagram.

The rocks of the acid group have a high silica content (up to 77%), low CaO (averaging 0.2%), and Al_2O_3 (9 to 13.5%). They have high Na_2O and K_2O (≤13%) with their ratios being approximately equal. The agpaitic coefficient is close to 1 even in the subalkaline rocks and greater than 1 in the alkali rocks. The rocks are rich in REE, Y, Zr, Nb, and Rb. We have obtained data on the isotopic composition of the volcanic complex as a whole; the results were obtained for the Burgultuin-Gol volcanic area (Yarmolyuk *et al.*, 1990b). I°Sr is: 0.70478–0.70496 in basalts; 0.7054–0.7064 in trachyrhyolites and comendite welded tuffs; and 0.71180–0.71202 in the pantellerites and comendites of the extrusive domes.

In the bimodal complex, the intrusive rocks are represented almost entirely by peralkaline granites and syenites. In addition, leucocratic lithium-fluoric raremetal granites have also been found in the eastern part of the Gobi-Tien Shan Zone only, where the zone is superimposed on the pre-Hetcyniah complexes of the Totoshan inlier (Yugodzir W-Mo ore field).

Peralkaline granitoids from the various structural zones of Mongolia differ somewhat in their composition. For instance, in southern Mongolia (in the Gobi-Tien Shan Zone and the zone of Main Mongolian lineament) is dominated by the most acid peralkaline granitoids and alkali leucogranites (on average, SiO_2>73%). In the Gobi-Altai Zone, the typical rocks are peralkaline granites and granosyenites (on average, 69<SiO_2<73%). In the North Mongolian Zone, the leading rock variety is peralkaline granosyenites (on average, SiO_2<71%), associated with alkali syenites and normal syenites containing just one feldspar (anorthoclase) (Yarmolyuk and Kovalenko, 1991). As a rule, intrusions of peralkaline granites were formed by complex multiphase processes. This can be exemplified by Mongolia's largest Khanbogdin peralkaline granitoid intrusion, which is also of interest because it contains rare-metal granites (Table 25) (Kovalenko, 1977). The intrusion, situated in the Gobi-Tien Shan rift zone, has a ring structure; it is surrounded by suites of comendites and pantellerites, for which it may have served as

Table 25 Compositions of peralkaline granites of the Khanbogdin Massif, (after Kovalenko, 1977).

	1	2	3	4	5	6	7	8	9
SiO_2	74.45	73.84	76.90	73.76	71.90	71.28	67.40	71.96	66.20
TiO_2	0.16	0.18	0.18	0.25	0.42	0.44	0.66	0.26	0.87
Al_2O_3	11.62	11.35	12.10	10.77	8.58	8.55	5.36	9.04	4.17
Fe_2O_3	1.90	2.10	0.65	2.43	8.30	7.67	5.28	5.94	12.00
FeO	2.43	2.25	1.35	1.98	n.d.	n.d.	4.76	0.27	0.89
MnO	0.15	0.18	0.08	0.20	0.27	0.28	0.47	0.21	0.31
MgO	0.03	0.02	0.01	0.40	0.16	0.28	0.01	0.03	0.02
CaO	0.05	0.06	0.05	0.58	0.45	0.58	0.16	0.07	0.16
Na_2O	4.61	4.61	4.31	4.93	5.14	5.04	4.17	5.32	5.54
K_2O	4.59	4.80	4.69	4.77	3.53	3.95	4.69	3.99	3.90
F	0.13	0.08	0.04	0.13	n.d.	n.d.	0.34	0.18	0.03

H_2O	n.d.	0.22	0.22	0.52	0.98	1.32	1.90	0.90	1.95
ZrO_2	n.d.	n.d.	n.d.	n.d.	n.d.	n.d.	5.40	1.06	5.14
Total	100.12	99.69	100.58	100.72	99.73	99.39	100.60	99.23	101.11
a.c.	1.08	1.11	1	1.22	1.65	1.73	2.22	1.44	3.17

Note: 1–6—granites of the main phase, 7–9—rare-metal granites.

a feeder. The following phases (from earlier to later) occurred in the formation of the intrusion:

1) alkali granites of the main intrusive phases;

2) dykes of ekerite, ekerite-porphyry, 'bedded' peralkaline granitic rocks, pegmatoid peralkaline granites, and pegmatites;

3) fine-grained aegirine peralkaline granite;

4) dykes of pantellerite;

5) dykes of peralkaline-granite porphyry; and

6) dykes of fine-grained syenite and monzonite.

Dykes of ekerite, pegmatite, rockallite, and 'bedded' alkali-granitic rocks contain rare metals, found in the following rare-metal minerals: elpidite, astrophyllite, neptunite, armstrongite, synchisite, milarite, polylithionite, and various titanosilicates and silicates of niobium, Zr and rare-earth elements (Vladykin *et al.,* 1981). As a result, the rocks are sharply enriched in REE, Y, Zr, Hf, Nb, Ta, Sn and Be and poor in Sr and Ba. It is not unusual to find high contents of Li, Rb, and Be in the rocks of the intrusion.

The Rb-Sr age of the Khanbogdin intrusion is 282±21 Ma (Vladykin *et al.,* 1981). This is in agreement with the geological data, suggesting a late Carboniferous to early Permian age for the comendites and pantellerites of the bimodal volcanic complex. The initial $^{87}Sr/^{86}Sr$ ratio is estimated to be 0.7076 for the rocks of the intrusion.

As a whole, when characterizing the intrusions of peralkaline granites associated with the bimodal complex, it should be noted that these are usually alkalifeldspar and leucocratic rocks. The mineralogy of the rocks includes alkali feldspar, quartz, and alkali femic minerals (aegirine, arfvedsonite, and riebeckite). The rock textures only vary slightly within each intrusion. The rocks contain a wide suite of accessory minerals, such as sphene, apatite, zircon, titanomagnetite, ilmenite, and fluorite. The rare-metal granitoids contain monazite, rare-earth fluorine carbonates, elpidite, and titanosilicates and many exotic minerals. In places they contain economic concentrations (Kovalenko, 1977). Chemically, the rocks show low Al_2O_3 and high alkalis, hence the agpaitic coefficient is greater than 1, as a rule. They also show low contents of alkali-earth elements. The main geochemical features of the rocks are high in REE, Y, Zr, Nb, Hf, Ta, Zn, and Sn, and low in Sr and Ba (Kovalenko, 1977).

Thus, the Permian bimodal igneous complex differs greatly from the coeval differentiated complex. These differences are the result of both the compositions of the rocks of the igneous associations and the structural setting of their formation. The formation of the bimodal association was related to the emplacement of the graben, caused by high-amplitude regional extension (rifting).

The similar ages of the riftogenic bimodal complex and the differentiated complex suggest that they were both formed within California-type continental margin (Zonenshain *et al.,* 1976). The formation of this type of margin in the late Paleozoic of Central Asia has been discussed by a number of authors (Kovalenko *et al.,* 1983;

Yarmolyuk, 1983; Yarmolyuk and Kovalenko, 1991). Data on the propagation of rifting with time from the continental boundary (the Carboniferous/Permian boundary in the Gobi-Tien Shan Zone) inwards (at the end of the Permian in the North Mongolian Zone) indicate that a spreading centre of the late Hercynian palaeo-Tethys, was progressively overlapped by the active margin of the North Asiatic continent. The successive passage of this spreading centre under the continent activated continental breakup along zones of weakness in the lithosphere: the sites of ancient suture zones (Yarmolyuk and Kovalenko, 1991), and this led to a progressive shift in the age of rifting, observed across the active margin, as well as the replacement of the rocks of the differentiated complex with those of the bimodal complex.

At present, the sources of magma for the bimodal complex can be defined using data on the Sr and Nd isotopic compositions of the basic rocks of the complex (Yarmolyuk *et al.*, 1997). Figure 70 shows the way in which the rocks were sampled, and Table 26 gives the results of isotopic data. In accordance with the abovementioned age data for computing initial isotopic compositions, the age of the rocks is estimated at 290 Ma for the Gobi-Tien Shan Zone, 270 Ma for the Gobi-Altai Zone, and 250 Ma for the North Mongolian Zone.

Figure 74 presents the results of isotopic measurements. They suggest that the majority of the isotopic compositions of the basalts from the individual rift zones

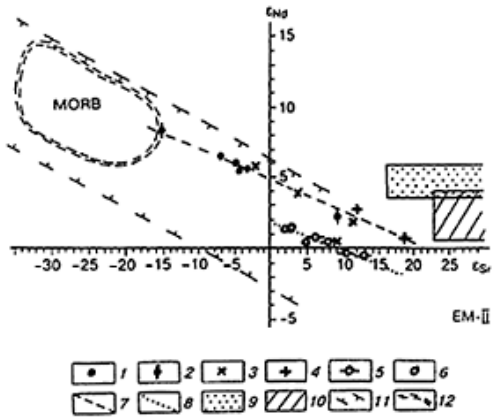

Key: 1–6—basalt compositions of rift-zone: 1 and 2—Gobi–Tien Shan (district: 1—Tost, 2—Nomgon); 3 and 4—Gobi-Altai (district: 3—Chandoman, 4—Ulziit); 5 and 6—North Mongolian–Transbaikal (district: 5—Teshig, 6—Bugsein–Gol); 7 and 8—correlation lines of rift-zone basalt compositions: 7—Gobi–Tien Shan and Gobi-Altai, 8—North Mongolian–Transbaikal; 9 and 10—isotopic composition of continental crust (after Kovalenko *et al.*, 1996): 9—Hercynides, 10—Caledonides; 11 and 12—composition field of: 11—mantle rocks, 12—MORB.

Figure 74 Isotopic compositions of Upper Palaeozoic bimodal basalt associations of plotted on an ε_{sr}–ε_{Nd} diagram.

Table 26 Isotopic composition of basalts in the Upper Palaeozoic rift zone of Central Asia.

Sample no.	Area	T Ma	Rb	Sr	$^{87}Rb/^{86}Sr$	$^{87}Sr/^{86}Sr$	ε_{Sr} (T)	Nd	Sm	$^{147}Sm/^{144}Nd$	ε_{Nd}
Gobi-Tien Shan Zone											
HT 1/9	Tost	290	10.80	718.9	0.0435	0.703967	−5.3	23.23	5.319	0.13844	+6.0
HT 2/3		290	6.60	666.2	0.0287	0.704018	3.7	31.13	7.200	0.13981	+5.8
HT 2/8		290	15.50	552.5	0.0811	0.704150	−4.9	26.39	5.939	0.13605	+5.8
HT 2/10		290	8.90	470.8	0.0547	0.703851	−7.6	21.05	5.088	0.14614	+6.5
HM 1/16	Nomgon	290	33.30	1857.0	0.0526	0.705005	+8.9	90.86	15.69	0.10438	+2.2
HM 1/19		290	24.70	376.8	0.1896	0.703859	−15.4	75.75	16.97	0.13540	+8.1
Gobi-Altai Zone											
ULD 2/3	Uldziit	270	14.8	689.8	0.0620	0.705231	+11.5	26.89	6.221	0.13982	+2.8
ULD 3/3		270	51.8	820.7	0.1828	0.706156	+18.1	39.87	8.253	0.12514	+0.8
1468/2	Chandoman	270	11.9	501.7	0.0688	0.705206	+10.8	19.34	4.493	0.14046	+1.9
1468/3		270	1.9	474.2	0.0116	0.704463	+3.3	20.96	4.755	0.13714	+3.8
1468/5		270	6.13	369.0	0.0481	0.704170	−2.8	16.39	4.296	0.15848	+5.9
1468/10		270	53.3	1,023.0	0.1506	0.705363	+8.5	34.70	6.750	0.11759	+0.2
North Mongolian-Transbaikal Zone											
1656/1	Bugsein-Gol	250	72.3	842.2	0.2485	0.705398	+4.4	45.52	9.666	0.11800	+0.4
1656/3		250	41.3	667.9	0.1791	0.704969	+1.8	50.41	10.38	0.12452	+1.5
1656/4		250	19.7	923.9	0.0616	0.704584	+2.2	36.79	7.742	0.12721	+1.6
1660/6	Teshig	250	29.7	1034.0	0.0832	0.705039	+7.6	43.32	8.448	0.11788	+0.6
1660/7		250	30.3	786.0	0.1116	0.705006	+5.7	33.06	6.453	0.11798	+0.9
1668/2		250	27.6	958.2	0.0832	0.705231	+10.3	36.40	7.625	0.12665	−0.2
1668/9		250	12.2	823.2	0.0429	0.705213	+12.1	24.81	5.347	0.13027	−0.5

Note: Isotopic analyses of Nd and Sr were performed using a MAT-262 2mass-spectrometer. The accuracy of the element ratios was 0.2 rel. % and 0.5 rel. % for $^{147}Sm/^{144}Nd$ and $^{87}Rb/^{86}Sr$, respectively. The following parameters of the undifferentiated Earth's mantle were used in calculating ε_{Nd} and ε_{Sr}: $^{143}Nd/^{144}Nd$—0.512638, $^{147}Sm/^{144}Nd$—0.1967 (CHUR) and $^{87}Sr/^{86}Sr$—0.7045, $^{87}Rb/^{86}Sr$—0.0825 (UR).

are more or less stable along the strike of the zones, and form relatively compact 'fields' when plotted on a diagram. However, the basalts from the various zones differ in their composition. As a whole, they are consistent with successive changes in the isotopic sources of basalt melts across the Central Asiatic rift system, from sources depleted in lithophile elements, such as Rb (low $^{87}Sr/^{86}Sr$ values) and Nd near the border of the Upper Palaeozoic North Euroasiatic continent, to sources rich in these elements in the interior of the continent.

The linear dependence of the distribution of isotopic compositions of the basalts from a particular zone, when plotted on a diagram (Fig. 74), can be interpreted using a mixing model for two sources of melts, of very different composition. The diagram also shows the fields of isotopic compositions of Hercynian and Caledonian continental crust, estimated for the late Palaeozoic in accordance with data on isotopic parameters of granite protoliths from appropriate structural zones (Kovalenko *et al.*, 1996). The diagram shows that trends in the variations of isotopic composition in the basalts lie outside the fields for crustal compositions. Hence, crustal material could not have participated in the formation of the basalt melts, and therefore the composition of the latter was governed by mantle sources, which had different isotopic parameters. One of them is similar in composition to a moderately depleted source of MORB (Zindler and Hart, 1986). Another source is consistent with a mantle source enriched in radiogenic strontium (EM-II-type mantle). The former source controlled the formation of the basalts of the Gobi-Tien Shan rift zone, whereas the latter source primarily controlled the formation of the Gobi-Altai Zone basalts. The compositions of the basalts of the North Mongolian-Transbaikalian rift zone plot on a line parallel to the correlation line describing the rock compositions of the Gobi-Altai Zone, but shifted towards more neodymium-rich compositions. The second mixing component may have been similar to depleted mantle. The contribution of the latter is similar to that for the Gobi-Altai Zone, as suggested by similar variation in the isotopic compositions of the rocks along the ε_{Sr} axis.

The variability in the isotopic parameters of magma sources of the Upper Palaeozoic Central Asian rift system reflects the compositional heterogeneity of the mantle. However, it could also be a function, within certain limits, of geodynamic factors. In line with the above-mentioned geodynamic model, the successive combined subsidence of the oceanic plate and the mantle diapir—causing spreading—to great depths must have entrained deeper and deeper mantle horizons which were then melted by the diapir. In this case, the variation in the composition of the melt sources may have been related to the compositional stratification of the mantle (Fig. 75). It is conceivable that the compositional similarity of the basalts of the Gobi-Tien Shan rift zone with depleted sources of the MORB type, resulted from slight subsidence of the diapir near the border of the continent and the primary involvement of depleted lithospheric mantle in the melting. The composition of the lithospheric mantle in Central Asia is reliably documented from data on mantle xenoliths (Kovalenko, Yarmolyuk, 1990). For the Gobi-Altai and northern Mongolian-Transbaikalian zones the position of the mantle diapir is fixed at a deeper level. It is correlated with the emergence of a source rich in radiogenic

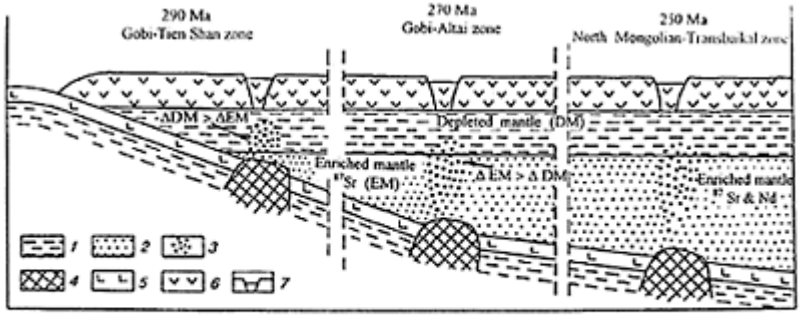

Key: 1 and 2—mantle sources of the melts: 1—depleted mantle (DM), 2—enriched mantle (EM); 3—region of melt generation; 4—mantle diapir of the buried spreading centre; 5 and 6—crust: 5—oceanic, 6—continental; 7—rift zone.

Figure 75 Model showing the interaction of mantle sources of different composition during the formation of igneous rocks of the late Palaeozoic rift system. The different parts of the figure reflect age intervals and rift zones. The contribution of source rocks of different composition is determined by the Δ value.

strontium (Fig. 75), which can tentatively be correlated with the asthenospheric mantle. The composition of the latter is not homogeneous and, in particular, an area enriched in neodymium occurs there beneath the North Mongolian-Transbaikalian rift zone. During the formations of the basic melts of this zone, the proportion of the enriched mantle source was approximately equivalent to, or greater than, that of the depleted mantle.

7
THE MESOZOIC-CAINOZOIC OF MONGOLIA

V.V.Yarmolyuk and V.I.Kovalenko

From the Triassic onwards, the whole of Mongolia developed within an intra-continental regime. The Mesozoic and Cainozoic structures of the country rest with structural unconformity on the basement rocks of varying ages. The structures were formed over several stages, which were consistent with periods of external tectonism on the continent.

The early Mesozoic history of Mongolia ($T–J_{1–2}$) was largely influenced by continental collisions during the closure of the Mongol-Okhotsk marine basin, represented in Mongolia by the Dzargalantuin trough, which is attenuated to the west. A large arched uplift developed in the collision zone within the present-day Khentei Uplands to the south, north, and west the uplift was bounded by systems of troughs, infilled with terrigenous, coal-bearing molasse, whose thickness varies from a few hundreds of metres to 4–5 km (Yanshin, 1975).

Unlike the Hercynian structures, which have an overall E-W trend, a N-S arrangement of rock complexes, of different ages, is peculiar to the early Mesozoic structures as a whole (Yanshin, 1975). Thus, igneous associations of this age are dominant in East Mongolia, where numerous granitoid intrusions are concentrated, whereas in stratified successions terrestrial volcanics alternate with continental molasse, in various combinations. In West Mongolia usually only amagmatic terrigenous deposits are present. The boundary between the two regions is drawn between the 100° and 105° meridians, and is contiguous with the limit beyond which collisional processes were negligible.

Rift-related processes had a pronounced effect on the structure of Mongolia in late Mesozoic times. They led to separation of the early Mesozoic arched uplifts and troughs into blocks, and led to the formation of extensive, narrow, rift structures, systems of grabens and grabens-synclines, and wide and flat basins. The tectonic depressions formed the sites of formation of lava plateaux, as well as volcanotectonic ring structures and subvolcanic intrusions of trachyrhyolites, granitoids, and basaltoids. Late Mesozoic deposits vary from 0.2 to 2 km in thickness (Dergunov and Kovalenko, 1995).

The end of the early Cretaceous saw the progressive cessation of tectonic processes throughout the whole of Mongolia, and the late Cretaceous-Palaeogene saw a period of development similar to platform evolution (Yanshin, 1975). In northern Mongolia, a gently sloping uplift, showing the preserved erosion surfaces, emerged at this time, while red sand-siltstone beds, with thicknesses of less than 500 m accumulated in southern Mongolia, within the South Gobi plate. In places, the beds contain sheets, sills, and stocks of basaltoids, which formed repeatedly throughout the late Cretaceous and Palaeogene.

Tectonic processes became more active in the late Cainozoic, occurring chiefly in the western part of the country, where the alpine ridges of the Mongolian and Gobi-Altai, the Khangai arched block uplift, a system of seismic fractures, and rift grabens, all developed. The tectonism was caused by the collision of Hindustan and the Asiatic continent, creating the largest collision belt in Central Asia, including the whole of Mongolia (Molnar and Tapponier, 1975; Zonenshain and Savostin, 1980; Yarmolyuk *et al.*, 1991). The formation of the collision belt was accompanied by large-scale basaltoid magmatism, associated with hot-spot activity (Yarmolyuk *et al.*, 1995). The tectonic and volcanic activity in the region remains the same at the present time. As late as the twentieth century, three disastrous earthquakes occurred there: the Bolnay (1905), Gobi-Altai (1957) and Mogod (1967) earthquakes (Florensov, 1963; Florensov and Khilko, 1979). Volcanic eruptions have occurred in the Khangai Uplands (Central Mongolia) throughout the history of humankind. Information about them is given in ancient chronicles (Luchitsky, 1983).

Throughout the Mesozoic and the Cainozoic, Mongolia constituted an area of intense igneous activity, leading to the development of large igneous regions. Igneous activity was concentrated within two periods, namely the early Mesozoic and the late Mesozoic-Cainozoic. These two periods differed in the geodynamic mechanisms of their igneous activity.

7.1 Early Mesozoic Magmatism

In early Mesozoic times, igneous activity was concentrated mainly in eastern Mongolia (Fig. 76). The activity was correlated in time and space with the structures of the Mongo-Okhotsk belt, which was being formed at that time. Local igneous events, which occurred in the west of the country, led to the creation of small volcanic terrains, and subvolcanic and hypabyssal intrusions, which were unevenly scattered over a vast area. They were dominated by alkali rocks, which are typical of intraplate environments.

Due to the differences in the influence of geological structures on the distribution of igneous rocks within Mongolia, we will now consider the typical features of early Mesozoic magmatism within collisional and intraplate environments.

Early Mesozoic Collisional Magmatism

This type of magmatism covers a vast area in the east of Mongolia, where it shows a zonally symmetrical structure (Fig. 76). The Dzargalantuin marine trough, which occurs in the western, attenuated part of the Mongol-Okhotsk marine basin, is located in the axial part of the area.

The core of the igneous area coincides with the Khentei Mesozoic Uplift (Yanshin, 1975). The core is made up of large granitoid intrusions of the granodiorite-

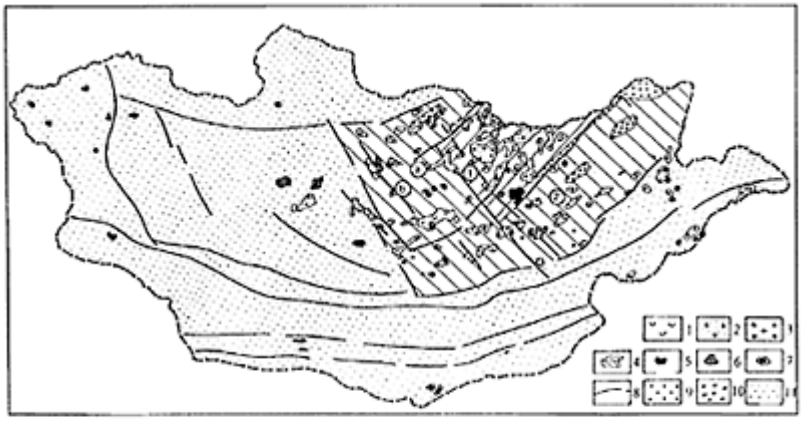

Key: 1–4—igneous association of the continental-collision zone: 1—volcanic, 2—granodiorite–granite, 3—granite–leucogranite, 4—granite–leucogranite containing granosyenite; 5—alkali granite and syenite, nepheline and pseudoleucit, syenites, and comendite; 6 and 7—intraplate igneous associations: 6—subalkaline and alkali basalt, phonolite, and trachyte, 7—anorogenic pluton (granosyenite, leucogranite granite, and lithium–fluorine granite); 8—fault, 9—marine deposits of the Dzhargalantuin Trough; 10—continental molasse; 11—non-magmatic area; Structural zones of the collision belt (circled numbers): ①—Core of the batholith, ②—zone of scattered igneous activity; Ore bearing massifs (circled letters) ⓐ—Modotin, ⓑ—Baga–Gazryn.

Figure 76 Distribution of Early Mesozoic igneous rocks in Mongolia.

granite association, plus smaller bodies of leucocratic granites, which are united in Khentei batolith to the north, west and, most obviously, to the south, the core of the area is bounded by a zone of separate small intrusions, dominated by intrusions of leucocratic granites. The intrusions decrease in size away from the granitoid core of the area; they change in shape from platy to linear, and are controlled by fractures. The character of the contact metamorphism also varies in the same direction. Thus, in the central parts of the Khentei Uplift, the intrusions are accompanied by areas where the country rocks are intensely granitized, and around its periphery the intrusions are rimmed by thick aureoles of hornfels, whereas granitization is only observed in the xenoliths (Koval *et al.*, 1982).

The margin of the igneous area is composed of volcanic terrains and relatively small intrusions of granitoids, which are scattered throughout the area. The zone coincides with an area of troughs around the Khentei Uplift. In the literature it is known as a zone of ‘diffuse’ magmatism; the name reflects the discrete, dispersed type of distribution of the igneous rocks (Zaitsev and Tauson, 1971). The granitoids of the zone include alkali granitoids, granosyenites, amphibole-biotite leucocratic granites and alaskite varieties containing only one type of feldspar, as well as lithiumfluoric granites. Granophyric, locally miarolitic, rock varieties are typical of almost all of the granitoids. A progressive transition of granites through granite-porphyries to rhyolites has been recognized in some places. The granitoids of the zone as a whole show geological and petrographic evidence of formation near the surface.

Thus, the zonal distribution of granitoids of different composition, affects the structure of the area. For the most part, they include: granitoids of the granodiorite-granite association in the core; rocks of the granite-leucogranite association in the outer zone; and various granitoids, mainly subalkaline and alkaline in composition, and lithium-fluoric granites in the marginal zone (the zone of 'diffuse' magmatism).

Plutonic Rock Associations

Rocks of the *granodiorite-granite association* form large, multiphase intrusive bodies. In the adjacent part of Russia, rocks of this association intrude PermianTriassic deposits (Zaitsev and Tauson, 1971). The K-Ar ages of the rocks fall in the range 230–180 Ma (Tauson, 1982). The intrusions are diorites, quartz-diorites, granodiorites, and granites (Dergunov and Kovalenko, 1995). Porphyritic, and, less commonly, equigranular biotite-amphibole granodiorites, as well as the later biotite granites within the multiphase intrusions are the most widespread. Diorites and quartz-diorites formed the earliest batches of magma in the intrusions; it is not unusual to find them as xenoliths in the granodiorites.

Numerous dykes of fine-grained granites, granite-aplites, and pegmatites are associated with the granodiorites. They tend to be localized in the endo- and exo-contact zones of the intrusions. The rare pegmatoid veins are usually fairly thin. Molybdenite and cassiterite are among the accessory and ore minerals found within the pegmatoids.

The chemical composition of the rocks varies within the calcalkaline series, from diorite to granite (Table 27; Fig. 77). The rocks are oversaturated with silica

Table 27 Chemical composition of representative rocks of the early Mesozoic granite-granodiorite formation of Mongolia (after Koval *et al.*, 1980).

	1	**2**	**3**	**4**	**5**	**6**
SiO_2	64.77	66.27	68.29	70.97	74.59	74.27
TiO_2	0.78	0.54	0.40	0.25	0.12	0.22
Al_2O_3	16.95	16.22	17.41	14.99	13.84	12.76
Fe_2O_3	1.77	0.91	0.46	1.40	0.84	0.72
FeO	2.05	2.64	1.98	1.28	0.99	1.25
MnO	0.12	0.05	0.09	0.05	0.03	0.08
MgO	1.39	1.21	0.84	0.42	0.28	0.27
CaO	3.02	3.09	1.63	1.85	0.82	0.91
Na_2O	4.94	4.61	4.33	3.54	3.76	3.56
K_2O	3.59	2.92	3.88	2.95	4.28	4.83
P_2O_5	0.18	0.12	0.14	0.01	0.06	0.02
LOI	0.59	0.47	0.54	0.36	0.51	0.48
Total	100.15	99.05	99.99	98.07	100.12	99.37

Note: 1–3—granodiorites; 4–6—granites.

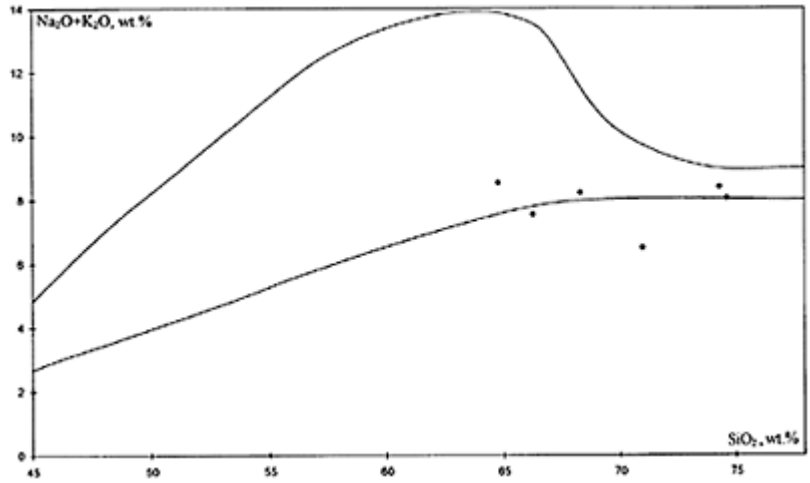

Figure 77 Granitoid average compositions of the Khentei batholith plotted on an SiO_2–(Na_2O+ K_2O) classification diagram.

and alumina and are undersaturated with calcium. As regards sodium predominates over potassium.

The granitoids of the *leucogranitic association* basically tend to be localized in the marginal zone of the batholithic core of the early Mesozoic igneous region. The intrusions regularly decrease in size towards the periphery of the area. The geological relationships indicate that the rocks of the granodiorite-granite association were intruded by these leucocratic granitoids. The few available Rb–Sr ages for these leucogranites fall in the range 190 to 230 Ma. The K-Ar dating provides a wider range of values, overlapping with the age of the rocks of the granodioritegranite association (Tauson, 1982).

The leucogranites are the most common rocks in the south-western part of the marginal zone of the batholithic core. Their most typical representatives are well known as ore-bearing rare-metal intrusions such as the Ongon-Khairkhan, Zhanchivlan, Gorikhin, and Abdar intrusions, etc. (Table 28) (Zaitsev and Tauson, 1971; Kovalenko, 1977). The intrusions are relatively small in size (a few hundreds of square kilometres) and dome-, stock-, or plate-shaped in form.

As a rule, the intrusions show a two-phase structure. The first phase includes medium-grained and generally equigranular, or, less commonly, porphyritic biotite-granites. They are made up of plagioclase (35–50%), orthoclase (23–35%), quartz (25–35%), and biotite (2–5%). Muscovite, garnet, and tourmaline are common components of the rocks.

The second phase involved dykes of fine-grained, commonly, pegmatoid leucogranites. In places these form small intrusions. Pegmatites of both *schlieren* and

Table 28 **Compositions of granitoids in the zone of diffuse magmatism of the early Mesozoic igneous region.**

n/n	**1**	**2**	**3**	**4**	**5**	**6**	**7**	**8**	**9**
SiO_2	70.50	76.60	70.52	74.40	71.80	75.50	76.00	71.73	73.42
TiO_2	0.47	0.21	0.15	0.29	0.41	0.30	0.22	0.30	0.28
Al_2O_3	13.39	12.33	15.50	13.01	14.18	12.78	11.60	13.57	12.45
Fe_2O_3	1.25	0.95	2.46	1.05	0.83	0.56	0.42	1.38	0.24
FeO	2.54	0.44	0.76	1.67	1.89	1.12	2.05	1.77	1.83
MnO	0.06	0.08	0.16	0.05	0.05	0.06	0.04	0.05	0.04
MgO	0.72	0.16	0.61	0.19	0.44	0.20	0.06	0.29	0.19
CaO	1.88	0.48	0.03	0.81	1.50	0.77	0.46	1.51	1.24
Na_2O	3.63	4.15	0.33	3.91	3.67	3.53	3.48	3.91	3.68
K_2O	4.18	3.95	5.68	4.29	4.60	4.49	4.52	5.06	5.15
$^{P}2O5$	0.09	0.04	0.18	0.05	0.16	0.04	0.02	0.09	0.06
H_2O	0.97	0.53	3.20	0.34	0.55	0.46	0.65	0.41	0.00
F	0.08	0.06	0.31	0.11	0.1	0.09	0.39	0.13	0.18
Total	99.68	99.92	99.58	100.06	100.08	99.81	99.53	100.14	98.65
Cr	11	1	2	9	5	3	13	12	131
Co	6	1	1	2	4	2	8	3	3
Sc	7.3	2.5	3.1	3.7	6	3.9	2.2	3.6	4.9
Cu	n.d.	n.d.	18	n.d.	n.d.	n.d.	n.d.	n.d.	n.d.
Pb	n.d.	n.d.	100	n.d.	n.d.	n.d.	n.d.	n.d.	n.d.
Zn	n.d.	n.d.	54	n.d.	n.d.	n.d.	n.d.	n.d.	n.d.
Sn	n.d.	n.d.	n.d.	n.d.	n.d.	n.d.	n.d.	n.d.	n.d.
Rb	155	145	476	164	183	315	591	367	358
Cs	13	2.5	11	5.1	15	23	37	12	20
Ba	450	693	426	122	417	132	100	416	203
Sr	183	79	38	73	143	66	41	105	70
Ta	1.2	1.2	1	1	2	4	5	4	4
Nb	14	14	18	11	14	19	34	22	29
Hf	6	4	4	9.5	6	4.5	7	5	7
Zr	221	114	113	269	211	134	149	156	194
Y	37	24	80	67	36	55	212	60	118
Th	15	17	10	57	23	27	50	29	44
U	2.7	3	5.1	7.4	3.7	8.2	8.6	5.3	7.4
La	33.7	27.1	12.4	106	36.4	21.5	45.3	40.3	43.7
Ce	62.7	44.7	22.1	172.3	66.6	44.2	86.3	68	88.9
Nd	32	20	10.8	75.7	33.4	25.2	45.3	31.1	50.1
Sm	7.7	4.3	2.44	16.2	7.9	6.6	11.1	6.9	13.1
Eu	1.2	0.5	0.22	0.5	0.8	0.3	0.17	0.55	0.58
Gd	5	3.2	2.6	10	4.7	4.8	9.9	6	10.8
Tb	0.88	0.6	0.52	1.65	0.74	0.88	1.96	0.98	1.96
Yb	3.23	2.83	2.77	4.5	1.76	3.68	11.1	2.61	8.2
Lu	0.48	0.44	0.44	0.64	0.24	0.56	1.8	0.37	1.27

n/n	**10**	**11**	**12**	**13**	**14**	**15**	**16**	**17**
SiO_2	75.40	73.30	75.50	75.23	75.20	77.50	75.20	68.30
TiO_2	0.01	0.01	0.06	0.01	0.03	0.25	0.32	0.37
Al_2O_3	12.94	12.32	13.04	12.81	12.76	12.09	13.54	18.46
Fe_2O_3	0.62	4.52	1.10	0.51	1.69	0.16	0.18	0.00
FeO	1.05	0.34	1.00	1.03	0.86	0.76	0.62	0.39
MnO	0.01	0.02	0.01	0.06	0.02	0.02	0.03	0.04
MgO	0.01	0.00	0.00	0.08	0.01	0.01	0.01	0.01
CaO	0.29	0.31	0.12	0.64	0.16	0.15	0.20	0.12
Na_2O	4.76	4.68	4.81	3.67	4.38	4.24	4.79	6.81
K_2O	4.09	4.02	3.89	4.41	4.44	4.08	4.07	3.60
P_2O_5	0.00	0.02	0.00	0.23	0.00	0.01	0.01	0.08
H_2O	0.20	0.47	0.12	0.98	0.46	0.40	0.29	0.78
CO_2	n.d.	n.d.	n.d.	0.06	0.00	0.00	0.00	0.00
F	0.22	0.22	0.28	0.06	0.17	0.13	0.44	0.75
Total	99.38	100.01	99.66	99.72	100.01	99.67	99.26	98.96
Cr	18	25	6	4	5	8	6	27
Co	1	3	0	1	n.d.	1	n.d.	1
Sc	0.1	0.2	0.2	3.8	0.7	0.8	1.1	1.1
Cu	n.d.	n.d.	n.d.	24	n.d.	n.d.	n.d.	n.d.
Pb	n.d.	n.d.	n.d.	60	n.d.	n.d.	n.d.	n.d.
Zn	n.d.	n.d.	n.d.	44	n.d.	n.d.	n.d.	n.d.
Sn	n.d.	3.1	n.d.	n.d.	n.d.	n.d.	n.d.	n.d.
Rb	669	653	1137	373	801	688	591	1720
Cs	12	14	25	18	17	12	30	13
Ba	100	100	100	100	100	100	100	100
Sr	34	34	35	49	34	36	41	35
Ta	6	5	13	3	10	7	16	62
Nb	91	88	84	23	77	46	34	85
Hf	15	11	18	4.5	8	7	9	13
Zr	186	161	113	123	72	67	149	21
Y	266	260	330	118	283	190	212	408
Th	45	36	30	26	25	18	17	6
U	10.6	5.1	6.6	19.6	8.9	8.4	16	17.6
La	10.3	8.6	12.1	14.6	15.5	12.1	13.7	4.5
Ce	27.7	22.8	28.3	34.8	44.3	32.1	37.8	8.5
Nd	21.3	17.3	18.6	23.4	36.4	24.1	30	4.5
Sm	7.2	5.7	5.5	7	12.8	7.9	10.3	1.1
Eu	0.01	0.02	0.01	0.15	0.01	0.01	0.02	0.01
Gd	9.4	9	6.1	8.5	13.3	7.1	10.3	0.9
Tb	1.95	1.83	1.4	1.59	2.7	1.5	2.2	0.19
Yb	13.8	11.7	15.7	7.3	18.4	11.6	17.6	1.84
Lu	2.3	1.93	2.82	1.14	3.1	1.9	3	0.33

Note: 1–9—leucogranite, 10–17—lithium-fluoric granite.

vein type, and the presence of muscovite, garnet, and tourmaline in the rock composition are especially typical of the granites.The formation of second-phase granites was followed by a stage of metasomatic formation of muscovite greisens and quartz veins containing tin and tungsten mineralization, which is typical of Mongolia (Zaitsev and Tauson, 1971).

The chemistry of the rocks of the association (Fig. 78) shows a fairly wide scatter in the SiO_2 content (66–77%). However, the leucogranites, which affect the appearance of the intrusions, are usually high-silica rocks (SiO_2>73%). The alkali content is about 8%, which is higher than that of most of the leucogranites. Therefore the rocks of the association as a whole are assigned to the subalkaline series. Practically everywhere the K_2O content is rather higher (in places it is substantially higher) than the Na_2O content. The rocks have high Rb and Sn contents, and, in some intrusions, higher Li, Be, and W as well (Table 28). The rocks are characterized by the appearance of a europium minimum in the REE, where enrichment in light REE occurs (Fig. 79).

Lithium-fluoric granites form a subgroup within the leucocratic granites, because of their high rare-metal contents: primilarily of lithium, but also fluorine (Kovalenko, 1977).

In Mongolia, lithium-fluoric granites occur repeatedly, in particular within the late Palaeozoic, early Mesozoic and late Mesozoic. Early Mesozoic granites are the most common. Their relative age is determined by their relationships with the early Mesozoic leucogranites that they intrude; in the geochemical succession of compositional variations, they are consistent with the most highly differentiated products of the

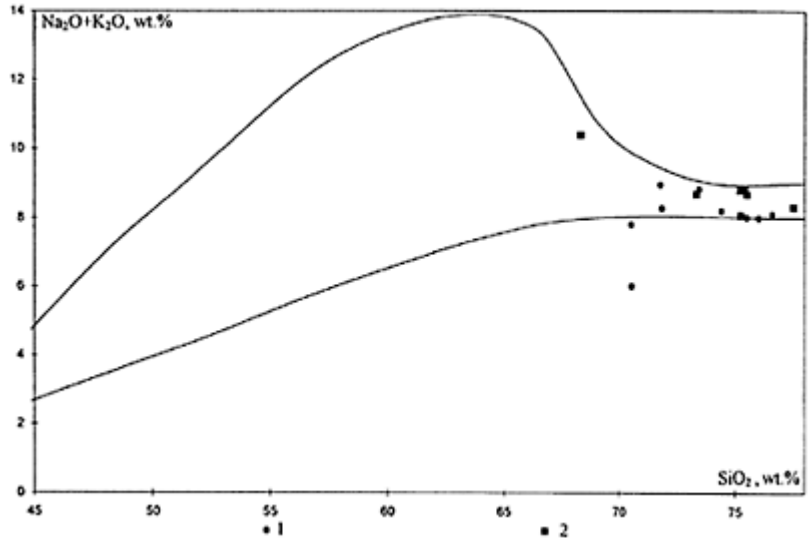

Figure 78 Compositions of rocks of the granite-leucogranite association (1) and lithiumfluorine granite (2) plotted on an Si_2O–(Na_2O+K_2O) classification diagram.

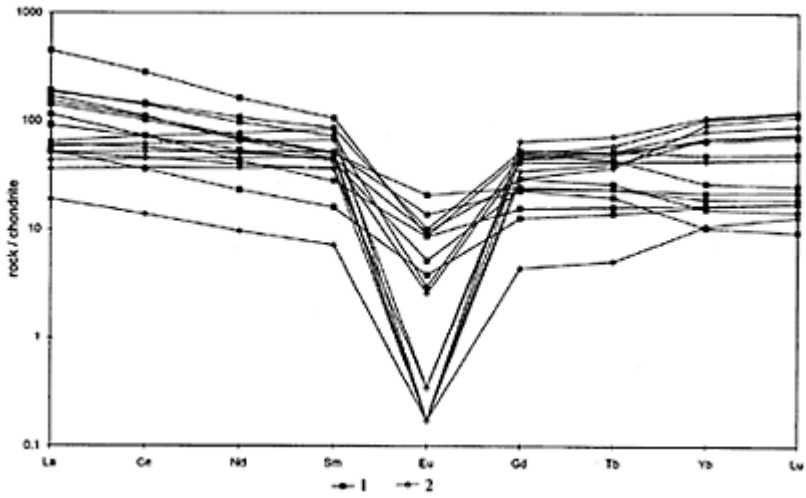

Figure 79 Types of REE distribution in rocks of granite—leucogranite association (1) and lithium—fluorine granite (2).

leucocratic magmas (Kovalenko, 1977). The similarity in the ages of the leucogranites and the lithium-fluoric granites is also marked by the Rb–Sr dates of both, particularly those obtained for the Zhanchivlan intrusion. The leucogranites of the latter are dated at 190 Ma, and the lithium-fluoric granites as 187 Ma.

Intrusions of lithium-fluoric granites occur in the marginal zone of the igneous region (the zone of 'diffuse' magmatism). The granites form small bodies (usually not more than a few hundreds of square kilometres in area); as stated above, they are associated with intrusions of the leucogranitic association (Zaitsev and Tauson, 1971). An important morphological feature of these intrusions is their domed shape; dykes of this composition also occur locally. Multi- and single-phase intrusions are known. They share one feature in common—the presence of amazonite granites or pegmatites in their composition.

Many intrusions of lithium-fluoric granites are zoned in structure (Kovalenko, 1977). In the most obvious type of zoning, the deeper levels of the intrusions are composed of biotite leucogranites, similar to the rocks of the leucogranite association. Towards the apical parts of the intrusions, the leucogranites are successively replaced by microcline-albite- or amazonite-albite granites containing protolithionite, zinnwaldite, and, nearer to the top, lepidolite. Locally the zoning may be incomplete; in this case, the intrusions are made up of one of the above mentioned rock types. Where these granitoids show cross-cutting relationships, the lithium-fluoric type, which contain the most lithian mica, prove to be younger.

The lithium-fluoric granites are represented by two petrographic varieties, namely, one-feldspar and two-feldspar types (Kovalenko, 1977). The one-feldspar granites are usually granophyric in texture. They are composed of perthitic orthoclase (60–70%) and

quartz (30–40%). The less-common minerals include mica, with accessory fluorite, zircon, magnetite, and martite.

The intrusions of two-feldspar lithium-fluoric granites contain a more mixed set of rocks, dominated by leucogranites containing biotite; apart from this, microcline-albite granites containing protolithionite and topaz, and amazonitealbite granites containing lepidolite are also present. The main minerals of the rocks are: plagioclase (Ab_{5-15}–23%), orthoclase (Or_{73} Ab_{27}–35%), quartz (39%), biotite (2.5%), and accessories (0.5%). The latter include fluorite, topaz, zircon, monazite, rare magnetite, columbite, cassiterite, and ilmenite.

Petrochemically, the lithium-fluoric granites are acid rocks that are very poor in calcium and rich in alumina (Table 28). They also have an unusually high fluorine content (usually 0.2–0.4%).

The geochemical properties of the rocks are determined by the increased contents of lithium and fluorine (two to eight and four to five times their clarke content, respectively), as well as Rb (300–750 ppm), Sn (4–12.5 ppm), Be (4–11 ppm), Ta, and Hf. Their barium and Sr contents are abnormally low (6–84 and 4–21 ppm, respectively). The initial $^{87}Sr/^{86}Sr$ ratio varies from 0.7107 (in the Yudugyin intrusion) to 0.7177 (in the Under-Khan intrusion) (Kovalenko, 1977; Koval, unpublished data). Their I_0^{Sr} ratio can be more or less 0.706. The lithium-fluoric granites show a symmetrical REE distribution with a deep europium minimum (Fig. 79).

The plutonic rocks of the zone of ‘diffuse’ magmatism also include subalkaline rocks (monzonite, granosyenite, and syenite) and peralkaline granitoids. These subalkaline rocks are generally associated with leucogranites: together they form a granite-leucogranite association together with the granosyenites. Alternatively they can be associated with peralkaline granites and form an association of peralkaline granites and syenites (Yanshin, 1989).

Associations of peralkaline granites and syenites are represented by intrusions of different shapes and sizes; they tend to be localized around the outer periphery of the area. To the north, they form the Malokunalei Complex, which is mainly located in adjacent parts of Russia. In the southern part of the area, the rocks of the association form a group of intrusions, including the huge Bayan-Ulan intrusion, (about 1,500 km^2 in area).

The age of the peralkaline granitoids was determined from geologic field relationships. In both the northern and southern parts of the area, they intrude Lower Triassic strata and are overlain disconformably by Upper Jurassic to Lower Cretaceous lavas (Zaitsev and Tauson, 1971).

The intrusions of peralkaline granitoids are both complex (multiphase) and simple in structure. The latter are more typical of the south-western margin of the area. The cores of the intrusions are usually made up of more acid rock types, such as granites, whereas the marginal portions are composed of granosyenites and syenites. In the multiphase intrusions, the less-silicic rocks are younger. A lot of dykes occur in the granite and they consist of alkali and subalkaline microsyenites, microgranites, grorudites, syenite pegmatites, and granite aplites (Table 29).

The peralkaline granitoids of the association are, as a rule, one-feldspar rocks, i.e. they are almost completely lacking in plagioclase. The quartz content of the granites is as high as 25%; and quartz is completely absent in some of the syenites.

Table 29 Chemical composition of the rocks of the Dashibalbar Massif of early Mesozoic peralkaline granites (peralkaline granite and syenite formation) (after Zaitsev and Tauson, 1971).

	1	2	3	4	5	6	7	8
SiO_2	74.49	73.01	74.58	75.49	73.35	75.52	75.22	76.36
TiO_2	0.07	0.07	0.07	0.07	0.07	0.04	0.07	0.02
Al_2O_3	11.74	11.55	11.68	12.05	11.38	10.53	10.87	10.61
Fe_2O_3	0.46	0.24	0.54	1.08	0.91	1.94	0.51	0.47
FeO	2.37	2.73	2.05	0.93	2.95	1.67	2.00	2.51
MnO	0.03	0.05	0.03	0.01	0.03	0.01	0.02	0.03
MgO	—	0.11	—	—	0.04	—	—	—
CaO	0.20	0.52	0.33	0.08	0.52	0.13	0.59	0.17
Na_2O	5.21	5.30	5.06	4.25	5.02	4.33	4.52	4.78
K_2O	4.88	4.97	4.41	4.71	5.01	4.85	4.96	4.72
F	0.13	0.13	0.12	0.08	0.03	0.03	0.04	0.34
LOI	0.72	0.81	0.56	0.91	0.28	0.64	1.22	0.10
Total	100.30	99.49	99.43	99.66	99.59	99.69	100.02	100.11

Note: 1 and 2—riebeckite-aegirine granite; 3–6—riebeckite-aegirine granophyre; 7—spherulitic granite porphyry with aegirine; 8—pegmatite.

The dark minerals includes aegirine, aegirine-augite, riebeckite, and arfvedsonite. In the subalkaline rock types dark minerals include normal hornblende and very rare biotite.

Geochemically, the rocks belong to the syenite-alkali syenite and syenitealkali-granite series. They show high alkali contents (>8%), low calcium and magnesium, and reduced Al_2O_3 (11–13%); the agpaitic coefficient is almost one (in the subalkaline rocks) or just over one (in the peralkaline rocks). Unlike the Upper Palaeozoic peralkaline granites, the rocks are poor in rare alkalis, fluorine, and lithophile elements such as Sn, Be, W, and Mo. They contain anomalously low Sr(<25 ppm).

Average compositions were calculated for the Mesozoic granitoids of the Mongolian segment of the Mongol-Okhotsk belt, from the geochemical types (Koval *et al.*, 1980) shown in Table 30. The zoned structure of the area of Lower Mesozoic plutonic magmatism in this part of the belt is clearly defined from the results of trend analysis on the petrogenic components (Koval *et al.*, 1980). As shown on Figure 80, the rocks of the batholithic core of the area are poorer in SiO_2 and Na_2O+K_2O, as compared with the plutonic rocks of its periphery (zones of ‘diffuse’ magmatism).

Volcanic Rock Associations

Unlike the above-mentioned plutonic rocks, Lower Mesozoic volcanic rocks are not widely distributed within the Mongolian segment of the collisional belt. Their outcrops are observed only in the peripheral zone of the igneous area (in the zone

Table 30 Average composition of the Mesozoic plutonic rocks of Mongolia (Tauson, 1982).

Number	Association	SiO_2	TiO_2	Al_2O_3	Fe_2O_3	MnO	MgO	CaO	Na_2O	K_2O	P_2O_5	Total
1	2	3	4	5	6	7	8	9	10	11	12	13
					Early Mesozoic							
Mzi-1	Gabbro-dioritic	53.88	0.95	15.85	8.93	0.14	6.02	7.82	2.88	1.48	0.21	98.16
Mzi-1a	Gabbro	53.59	0.96	15.79	9.13	0.14	6.15	7.94	2.79	1.42	0.21	98.12
Mzi-1b	Diorite	58.44	0.89	16.83	5.92	0.09	4.06	6.36	3.28	2.22	0.24	98.33
Mzi-2	Granodiorite-granitic	68.73	0.41	15.68	3.27	0.07	0.91	2.03	4.26	3.76	0.12	99.24
Mzi-3	Granite-leucogranitic	73.13	0.31	13.66	2.43	0.06	0.39	1.08	3.70	4.38	0.07	99.21
Mzi-4	LiF granitic	74.31	0.17	12.78	2.04	0.04	0.09	0.59	4.12	4.47	0.09	99.30
Mzi-5	Peralkaline granitic	73.20	0.28	12.62	2.89	0.07	0.25	0.58	4.46	5.22	0.08	99.65
Mzi-5a	Syenite	65.66	0.64	16.61	3.22	0.16	0.63	1.06	5.83	5.39	0.21	99.41
Mzi-5b	Solvus granitic	75.40	0.22	11.44	2.53	0.06	0.13	0.44	4.06	5.17	0.05	99.50
Mzi-5b1	Biotitic alaskitic	74.10	0.26	13.19	2.05	0.07	0.24	0.81	3.56	4.74	0.07	99.09
Mzi-$5b_2$	Peralkaline alaskitic	75.76	0.15	11.03	2.65	0.04	0.11	0.35	4.17	5.27	0.04	99.57
Mzi-6	Calcalkaline	71.69	0.33	14.31	2.70	0.06	0.55	1.38	3.94	4.16	0.09	99.21
Mzi-7	Peralkaline	71.88	0.32	14.02	2.72	0.06	0.51	1.28	4.01	4.30	0.08	99.25
Mzi-8	Plutonic rocks	71.42	0.34	14.14	2.88	0.06	0.65	1.44	3.98	4.22	0.09	99.22

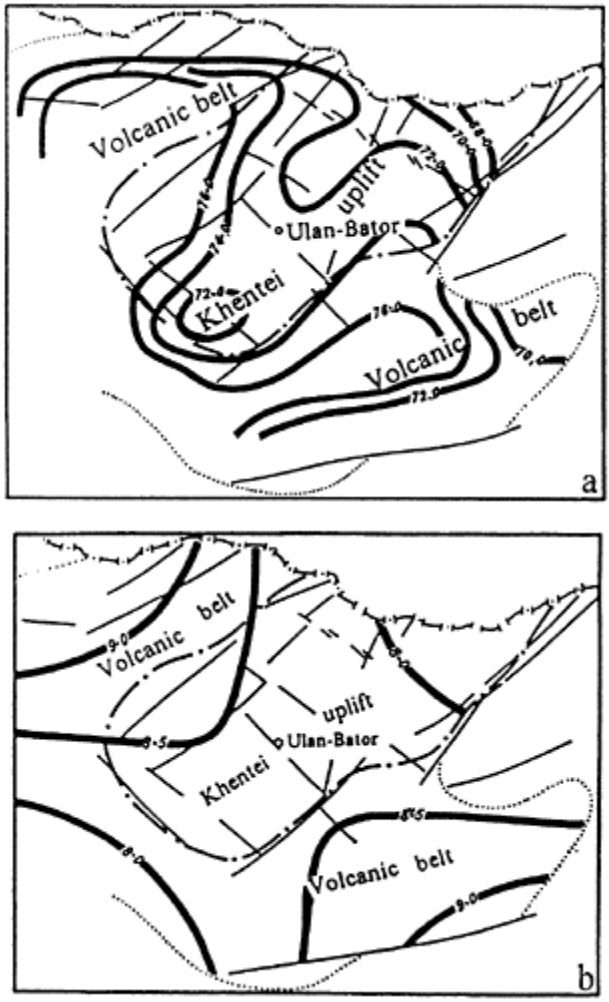

Figure 80 Trend of silica: (a) and total alkalinity (Na_2O+K_2O): (b) of the Lower Mesozoic granitoids of north-eastern Mongolia (after Koval et al., 1980).

of diffuse magmatism). The volcanics form part of the structure of the Lower Mesozoic troughs; they also occur more rarely as homogeneous lava sequences in areas that have suffered no structural deformation. Their age is established from their geological relationships with Upper Palaeozoic and Upper Mesozoic rock complexes; in some cases the age is indicated by Upper Triassic and Lower Jurassic flora found in the terrigenous sediments that occur between the volcanics (Mossakovsky and Tomurtogoo, 1976). The

volcanic terrains are small in size and scattered. Their constituent rock types show a wide range of compositions, from basalts to rhyolites (Luchitsky, 1983). An example of this is a volcanic association on the right-hand bank of the River Selenga (in the north-west of the area), as described by Kepezhinskas and Luchitsky (1974). The volcanic rocks rest disconformably on Upper Permian volcanics (dated by their contained plant fossils). The section commences with andesite tuff (200 m), overlain by trachyandesite lavas,

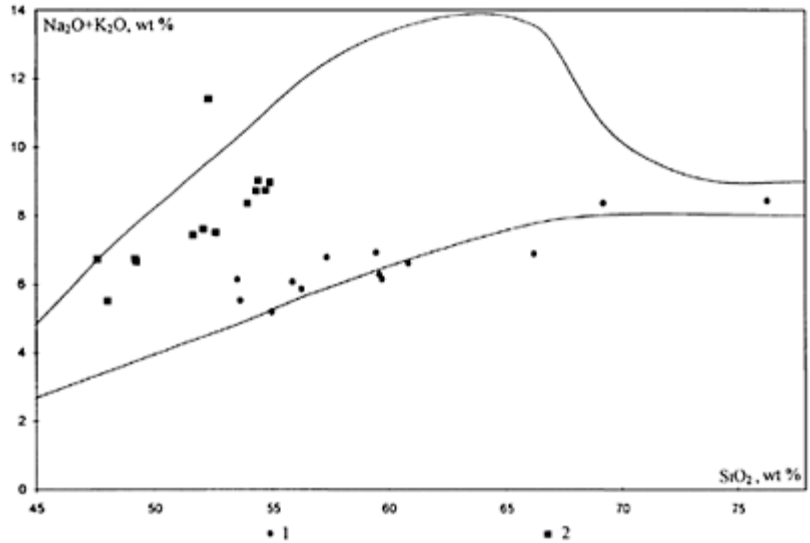

Figure 81 Compositions of rocks of the Lower Mesozoic volcanic associations: (1) of the area of continental collision, and (2) of the area of intraplate magmatism.

containing separate interbeds of andesite-dacite tuff, and dacite lavas. This part of the section reaches up to 2,500 m in thickness. The uppermost part of the section comprises 70 m of basalts and andesite-basalts. As noted by Frikh-Khar and Luchitskaya (Luchitsky, 1983), rock associations similar in composition occur along the south-western and southern fringe of the igneous region as well. The different terrains differ only in the relative abundances of rocks of different compositions.

The investigators (Frikh-Khar and Luchitskaya, 1978; Luchitsky, 1983), who reconstructed the type of volcanic activity prevailing in early Mesozoic times, stress that the volcanic products of this period were associated with isolated depressions; this explains the abundance of clastic facies in the sequences infilling some depressions.

Along with the above-mentioned, there are also occurrences of essentially rhyolitic volcanicism, represented by extrusive domes (Kepezhinskas and Luchitsky, 1974). They occur as small intrusive bodies, extrusive domes, and necks, ranging in size from

100×500 m to 300×900 m. They occur scattered over the whole area, i.e. their distribution is not affected by structural features; therefore they are known to occur both in troughs and on uplifts.

Petrochemically, the Lower Mesozoic rocks as a whole can be included in the calcalkaline and subalkaline series (Table 31; Fig. 81).

Lower Mesozoic Intraplate Magmatism

Occurrences of intraplate magmatism occur chiefly in the west of Mongolia, although rocks consistent with them in composition are observed in the structure

Table 31 Chemical composition of representative rocks of the early Mesozoic volcanic associations.

	1	2	3	4	5	6	7	8	9	10	11	12	13
SiO_2	53.47	53.59	54.95	55.84	56.22	57.30	59.45	59.58	59.70	60.79	66.16	69.18	76.29
TiO_2	0.93	1.68	1.05	0.97	1.19	1.17	0.84	0.78	1.11	0.85	0.51	0.20	0.12
Al_2O_3	17.99	16.69	18.30	18.25	17.39	18.75	16.88	16.55	16.60	15.90	15.84	12.39	12.51
Fe_2O_3	3.62	6.88	2.41	2.21	4.32	1.28	5.00	2.09	0.80	2.29	1.41	1.67	0.63
FeO	3.96	2.48	4.24	5.59	2.01	3.99	1.44	3.25	5.04	2.44	2.36	2.00	0.88
MnO	0.11	0.08	0.13	0.11	0.10	0.10	0.08	0.10	0.11	0.07	0.06	0.01	0.02
MgO	4.61	6.96	3.05	3.36	6.40	2.47	2.23	4.51	3.50	3.20	1.90	0.78	0.18
CaO	7.34	2.10	7.90	6.28	3.04	6.23	4.85	4.74	5.10	4.18	2.88	0.49	0.39
Na_2O	4.60	3.18	3.43	4.02	4.20	4.37	4.52	3.61	4.45	3.87	3.49	4.71	3.49
K_2O	1.53	2.34	1.76	2.04	1.65	2.40	2.39	2.67	1.69	2.74	3.39	3.65	4.94
P_2O_5	0.33	0.99	0.39	0.32	0.27	0.41	0.36	0.23	0.44	0.22	0.17	n.d.	0.02
LOI	1.75	3.92	1.99	1.44	1.91	1.59	1.86	2.76	1.96	3.21	1.94	4.25	0.66
Total	100.24	100.89	99.60	100.43	98.70	100.06	99.90	100.87	100.50	99.76	100.11	99.33	100.13

*Note: 1–8—ro*cks of andesite association: 1–5—after Mossakovsky et al., 1973, 6 and 7—after Tauson (1982), 8–10—after Kepezinskas and Luchitsky (1974); 9–13—rocks of the trachyandesite-dacite-trachyrhyolite association (after Koval *et al.,* 1982).

of the collisional belt. As mentioned above, they are represented by separate intrusions, dyke swarms, and small volcanic terrains. The amount of igneous bodies mapped has increased recently because of increased work on the isotopic dating of igneous rocks of Mongolia and rock complexes of similar composition in the adjacent areas of Russia.

In the extreme west of Mongolia, in the Mongolian Altai, small intrusions of rare-metal granites, including those of the lithium-fluoric type, are considered to be Lower Mesozoic bodies. An isochron Rb-Sr age of 200 Ma characterizes the spodumene granites of the Alakhin intrusion, located in Russia near the Mongolian border (Yu.A.Kostitsyn, unpublished data). The U-Pb age of the Kobdo-Gol tungsten-bearing intrusion is estimated at 170 Ma (from the data of D.P.Minin). Fields of dykes and explosion pipes, composed of alkali basaltoids (kersantites, minettes, pseudoleucitic basaltoids, shonkinites, and solvsbergites) are early Mesozoic in age (Obolenskaya, 1971). The dykes intrude Lower Jurassic deposits; their K-Ar ages in the adjacent areas

of the Gorno-Altai Region and Tuva fall in the range 170–220 Ma (Volochkovich and Leontiev, 1990).

In south Mongolia, dykes of comendites and basalts from the Tost Ridge are assigned by the authors to a Lower Mesozoic intraplate complex. The dykes intrude Upper Permian to Lower Triassic conglomerates: their K-Ar ages fall in the range of 160–190 Ma (Yarmolyuk, 1983). The Lugin-Gol intrusion of pseudoleucitic syenites with REE-carbonatites, intruding Upper Permian rocks, is also probably early Mesozoic in age (Kononova, 1981).

The most thoroughly studied rocks are the Lower Mesozoic intraplate volcanic successions in the Central Khangai Uplift on the River Khanui and in the basin of the River Khoit-Tamir (Table 32), as well as to the south (near the Ongiin-Khuduk Well) and the eastern (Mogod area) fringes of the Khangai Uplift.

At the above localities of the Central Khangai Uplift the Early Mesozoic volcanic rocks, containing weathering crusts and reworked sediments at the base, rest on Permian granites and stratified bodies. The sediments occur within the volcanic sequences, and yield Lower Jurassic flora (Marinov, 1973): the K-Ar ages of the rocks fall in the range of 180–220 Ma. The volcanic successions contain tephrites, phonolites, subalkaline, including nepheline-normative, basalts, and trachytes. A similar rock association, also containing trachyrhyolites has been found near the Ongiin-Khuduk Well. Its K-Ar age is estimated as 190 Ma.

Confirmed occurrences of Lower Mesozoic intraplate magmatism can be found in the Mogod area (Mogod Formation). These volcanics overlie the conglomerates of the Abzog formations (T_{2-3}) and contain Upper Triassic to Lower Jurassic flora in their interbeds (Mossakovsky and Tomurtogoo, 1976).

The section of the Mogod succession starts with trachyandesite lava- and tuff conglomerates, reaching 500m in thickness. Higher up the section they give way to a succession of lava flows, alternating with lithoclastic tuffs of similar composition. The most common volcanic rocks there are subalkaline, including nepheline-normative basalts, which form a lava suite up to 400–500 m thick. In addition, there are subalkaline andesiticbasalts and trachyandesites; in places, the

Table 32 Chemical composition of early Mesozoic intraplate volcanic activity in the Khangai Uplift.

	1	2	3	4	5	6	7	8	9	10	11	12	13
SiO_2	54.33	54.25	54.65	52.25	54.85	53.88	49.16	52.56	47.56	51.61	52.05	48.00	49.22
TiO_2	1.30	1.47	1.39	1.66	1.42	1.44	1.97	1.62	2.14	1.70	1.70	2.00	2.00
Al_2O_3	16.72	17.17	17.30	16.00	16.97	17.11	15.71	16.37	15.34	16.49	16.22	15.52	16.10
Fe_2O_3	3.20	3.60	4.05	3.60	3.60	3.95	3.32	4.24	3.65	4.44	4.41	4.37	5.92
FeO	3.50	4.10	3.90	3.20	4.70	5.10	6.37	4.11	7.01	4.31	4.28	6.19	4.32
MnO	0.08	0.11	0.04	0.05	0.06	0.10	0.14	0.12	0.15	0.12	0.13	0.15	0.14
MgO	2.38	2.90	2.70	2.80	2.57	2.48	5.78	4.28	6.55	4.60	4.57	6.63	5.23
CaO	4.96	5.09	4.61	4.85	4.33	4.97	7.23	5.72	7.03	6.03	5.91	7.37	7.06
Na_2O	4.64	5.28	5.13	5.85	5.40	5.36	3.95	4.35	4.38	4.30	4.40	3.20	4.30
K_2O	4.39	3.45	3.61	5.55	3.58	3.00	2.79	3.16	2.35	3.14	3.21	2.32	2.36
P_2O_5	0.97	1.11	1.10	1.19	0.95	0.94	1.09	0.93	1.10	1.00	1.00	1.09	1.10

LOI	3.64	1.44	1.60	3.00	1.34	1.66	1.85	2.12	1.91	1.83	1.50	2.41	1.61
Total	100.11	99.97	100.08	100.00	99.77	99.99	99.36	99.58	99.17	99.57	99.38	99.25	99.36

Note: 1–6—trachyte-phonolite-alkali-basalt association, sampled at sites on the middle Khanui-Gol River; 7–13—alkali-basalt association sampled at sites on the River Khoit-Tamir.

upper horizons of the sections contain lava lenses of trachytes and trachyrhyolites. Tuffs, some containing volcanic bombs, are common in all the horizons, but they tend to be subordinate. The aggregate thickness of the succession is 1,000–1,500 m. The lavas are usually well-crystallized, distinctly porphyritic, and in places amygdaloidal. The phenocrysts are represented by andesine, augite, and less commonly olivine and hornblende; this enables proper petrographic rock varieties to be recognized.

Bimodal basalt-comendite associations, discovered in the western part of the collisional igneous area (on the western fringe of the Khentei Uplift), are also considered to be intraplate igneous rocks; the associations may have formed by both collisional and intraplate types of magma genesis. In particular, it is here that a terrain of Lower Mesozoic peralkaline granites, described when considering the collisional igneous area, is located.

The bimodal associations are still poorly known. They are composed of subalkaline olivine-basalts, alkali feldspathic trachyrhyolites and comendites. This association was found on the margin of the Dashibalbar intrusion of peralkaline rocks. It consists of numerous subvolcanic bodies (sills, stocks, and dykes), the petrography of which varies from peralkaline granites to vitreous comendites, similar to lava flow comendites. Together the data suggest that both plutonic and volcanic magmatism led to the formation of the bimodal volcanic rocks.

General Trends in the Development of Lower Mesozoic Magmatism

The above overview of the Lower Mesozoic magmatism of Mongolia suggests the existence of two igneous areas, differing radically in their composition, scale and geodynamic nature. The eastern area is clearly related to the structures of the Mongol-Okhotsk belts, from both the age of the collisional processes and the pattern of distribution of the igneous rocks, which are symmetrically zoned around the collisional suture (Dzargalantuin Trough). This area is distinguished by the predominance of calcalkaline rocks, the widespread development of anatectic granitoids, and also an increase in alkalinity of the rocks on the margins of the area, which is typical of a subduction environment. These features have, for a long time, indicated that collisional processes were taking place (Yanshin, 1975).

The second, western, area is notable for the markedly alkaline composition of its constituent rock types. They include alkali and subalkaline basalts, phonolites, trachytes, nepheline, and pseudoleucitic syenites, peralkaline granites, and comendites. These rocks were formed in the interior of the Lower Mesozoic Asiatic continent, and are characterized by a random distribution, independent of the major structures of that time. Therefore we can relate the formation of the western area to intraplate sources of magmatism.

Thus, the general trends of development of magmatism in the early Mesozoic were controlled by two independent origins for the magma sources, namely collisional and intraplate.

7.2 Late Mesozoic-Cainozoic Intraplate Magmatism

Until recently, geologists believed that there was evidence of two independent stages of magmatism, namely, the Upper Jurassic-Lower Cretaceous and the Cainozoic stages, in the Upper Mesozoic-Cainozoic rocks of Mongolia (Marinov, 1973). This belief was based on data from widespread volcanic bodies of this age. These bodies form huge volcanic regions, such as the Upper Jurassic-Lower Cretaceous East Mongolian and Gobi-Altai volcanic belts, and the Upper Cainozoic volcanic plateaux and terrains of the Dariganga, the Central and South Khangai Ridge, and the Lake Khubsugul area (Fig. 82), as shown on the geological maps of Mongolia (Yanshin, 1973, 1989).

Extensive geological research, largely based on the K-Ar isotopic ages of the volcanic successions and their compositions, has been done recently. This has shown that igneous activity has continued almost without interruption for the past 160 Ma in Mongolia. In addition, it has been shown that this long-term igneous activity was associated with mantle hot-spots, while the scale of magmatism and its particular tectonic setting were determined by the activity of mantle plumes (Yarmolyuk *et al.*, 1995a). At the present day, volcanic regions related to the South Khangai, Dariganga, and South Baikal hot-spots, have been recognized in Mongolia.

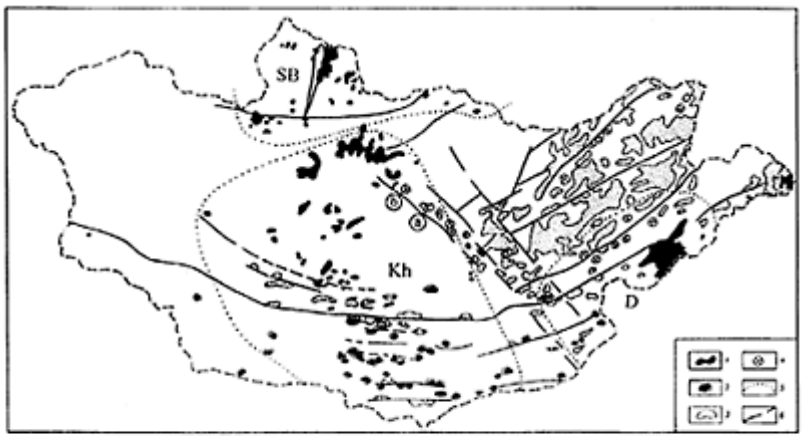

Key: 1–3—volcanic sequence: 1—Upper Cainozoic, 2—Upper Cretaceous and Lower Cainozoic, 3—Upper Jurassic–Lower Cretaceous; 4—granitoid massif (a—Ikh-Khairkhan, b—Ongon-Khairkhan); 5—boundaries of igneous terrains controlled by hot-spots: Kh—South Khangai, SB—South Baikal, D—Darigang; 6—transregional fault, Ore-bearing massifs (circled letters) ⓐ—Ikh-Khairkhan, ⓑ—Ongon-Khairkhan.

Figure 82 Distribution of Upper Mesozoic-Cainozoic igneous rocks in Mongolia.

The South Khangai Hot-Spot

A terrain of Upper Mesozoic-Cainozoic igneous rocks in the Central and Southern Khangai Ridge and in the adjacent areas of South Mongolia (Fig. 83) is correlated with this hot-spot (Yarmolyuk *et al.*, 1994). The igneous rocks of the region were mainly generated by multiple, recurrent volcanic eruptions. They have the following features in common: occurrences of rocks of different ages in the same structures; successive eruptions separated by only short periods of time and similar petrological compositions: mainly subalkaline and alkali basic rocks.

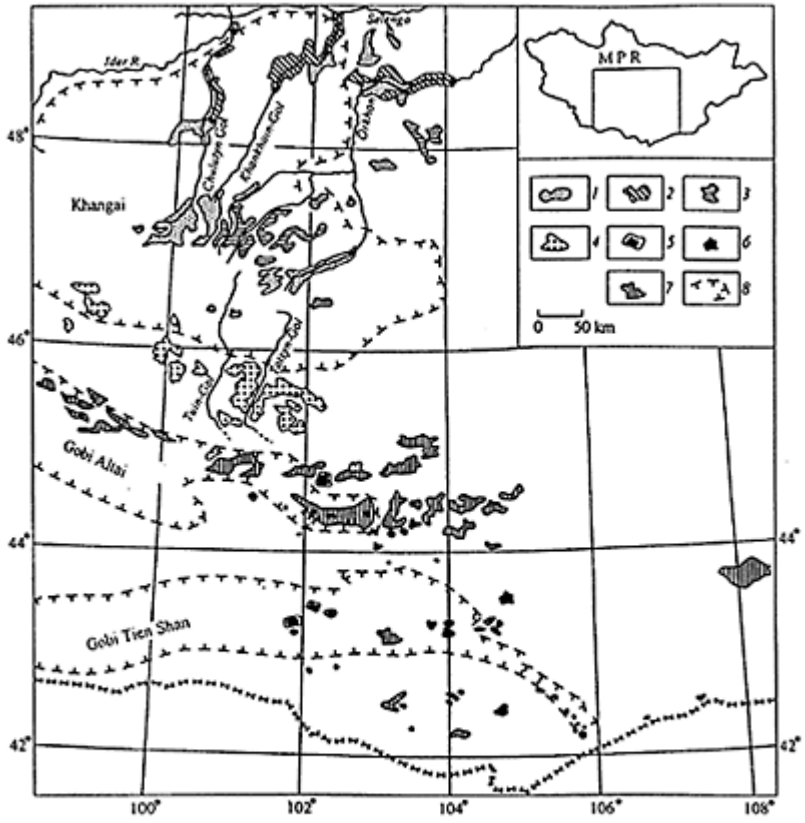

Key: 1–7 igneous rock complex: 1—Eocene–Holocene, 2—Pliocene, 3—Middle Miocene, 4—Upper Oligocene and Lower Miocene, 5—Paleocene–Eocene and Lower Oligocene, 6—Upper Cretaceous; 7—Upper Jurassic-Lower Cretaceous, 8—boundaries of orogenic structures. The inset map shows the location of this area within Mongolia.

Figure 83 Distribution of Upper Mesozoic-Cainozoic igneous rocks in the South Khangai volcanic area (after Yarmolyuk *et al.,* 1994).

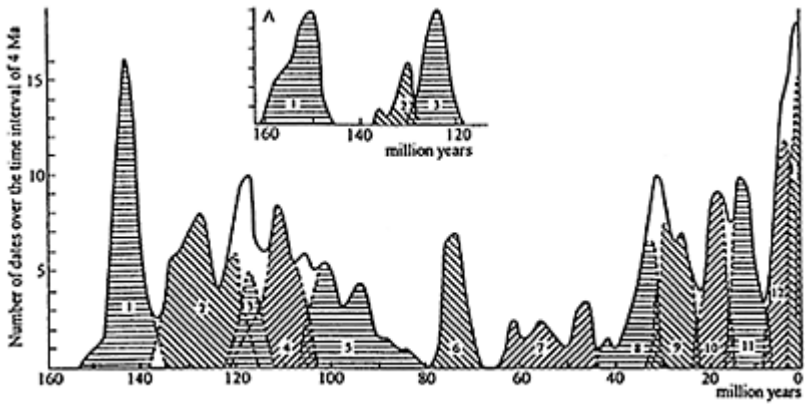

Figure 84 Accumulation histogram of K-Ar dates for Late Mesozoic-Cainozoic igneous rocks of Central and South Mongolia (solid line). Inset map: A—the same for the eastern segment of the Gobi-Altai rift zone. Shaded fields with a dotted boundary include dates on rocks from separate stages of volcanism (after Yarmolyuk *et al.,* 1994). The number of fields corresponds with number of stages of formation of the South Khangai igneous region.

The various stages of development of the hot-spot were recognized by grouping the igneous rocks into associations, each characterized by a similar age of formation and a common structural environment. The age of the rocks was determined on the basis of their relationship with fossiliferous strata (Devyatkin, 1981; Shuvalov and Nikolaeva, 1985), and from K-Ar dating (Yarmolyuk *et al.,* 1995b) (Fig. 84).

Stages of formation of the South Khangai igneous region: spatial, structural, and compositional features

1) The late Jurassic stage (J_3) corresponds with the beginning of the formation of the igneous region (Fig. 85). This stage is consistent with the formation of complexes of high-alkali rocks (Samoilov and Kovalenko, 1983), consisting of melanephelinites-melaleucitites, phonolites, subalkaline trachytes, latites, trachydacites-trachyrhyodacites, and their subvolcanic equivalents: shonkinite-porphyry, nepheline syenite, alkaline and

subalkaline syenite and quartz-syenite. Figure 86 shows the variations in their composition. The formation of ore-bearing, initially, apatitic rocks—as well as carbonatite rocks, rich in rare-earth elements, strontium, barium, and in some case fluorite and lead, was associated with the subalkaline bodies (Samoilov and Kovalenko, 1983).

In terms of their structure, the igneous rocks tend to be localized within the Upper Mesozoic Gobi-Altai rift zone (Yarmolyuk, 1986). The rift zone can be divided into three segments: eastern, central, and western, which to some extent differ in their subsequent history of magmatism (see Fig. 85). Upper Jurassic

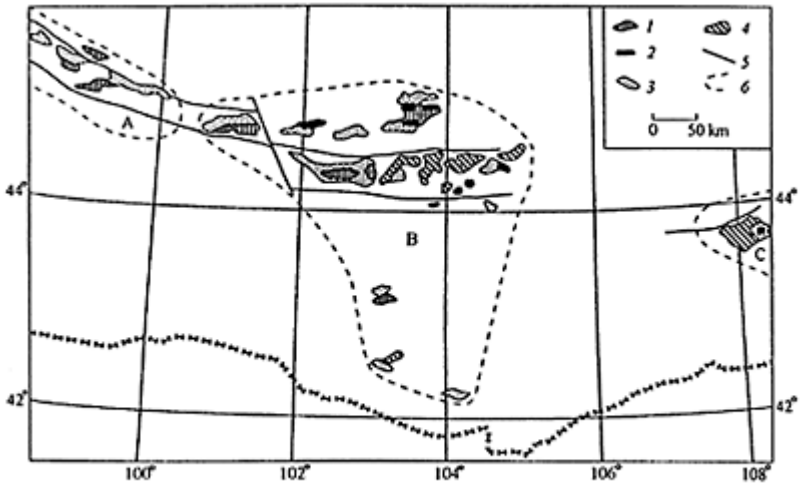

Key: 1–4—age group of: 1—late, 2—middle and 3—earlier early Cretaceous, 4—late Jurassic; 5—fault; 6—boundaries of divisions of the volcanic areas (A—western, B—central, C—eastern).

Figure 85 Distribution of Upper Jurassic-Lower Cretaceous rock associations.

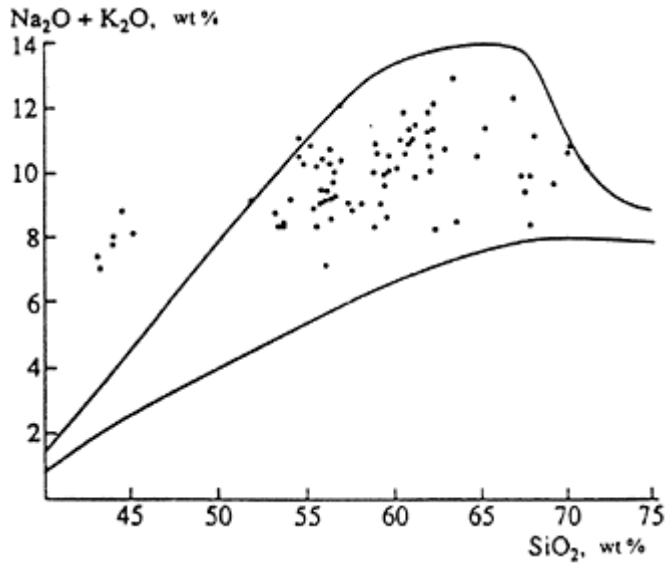

Figure 86 Compositions of Upper Jurassic rocks, plotted on a classification diagram. Lines here and in the following figures delineate a field of subalkaline-series rocks.

igneous rocks occur in spatially separated areas, in the eastern and central segments.

The age of the volcanic rocks is indicated by the late Jurassic fossiliferous sedimentary rocks that occur intercalated with them (Kovalenko *et al.*, 1984). The upper age limit is determined from the unconformably overlying lower Lower Cretaceous volcanics. The numerous K-Ar age data, falling in the range 155–138 Ma, agree with the age estimates based on field relationships.

2) The earlier early Cretaceous stage (K_1^1) is noted for its large-scale outpourings of basalts. The basalts occur largely in extensive grabens, which form a linear WNW-trending chain (see Fig. 85). To a large extent, the chain is related to the ridges of the Gobi-Altai, therefore it is recognized as the Gobi-Altai rift zone.

The volcanic successions of this stage are completely dominated by subalkaline basalts (Fig. 87). Their SiO_2 content varies from 47 to 53%. The Na_2O+K_2O content varies from 4.8 to 9.5%, with $Na_2O/K_2O=0.9–2.2$. In places, the basalts contain small (1–2 cm) inclusions of spinel Iherzolite. The volcanic sections vary in thickness from a few tens of metres in the volcanic terrains of the western and eastern segments of the rift zone, to 600 m in the terrains of the central segment.

The age of the rocks of this stage is mostly determined on the basis of early Neocomian organic remains in sedimentary beds found intercalated with the volcanics (Shuvalov, 1988). The basalts disconformably overlie Upper Jurassic lavas and are

overlain by middle Lower Cretaceous acid volcanics. The K-Ar ages of the rocks fall in the range 134–119 Ma.

3) The middle early Cretaceous stage (K_1^2) is represented by successions of acid volcanics. Their age is determined by reference to fossiliferous lower Lower Cretaceous and upper Lower Cretaceous sequences. The former are disconformably overlain by acid volcanics or by basal units of tuffaceous-sedimentary rocks. The latter conformably or disconformably rest on rhyolites. The K-Ar ages, which fall in the range of 128–115 Ma (Samoilov, 1989), suggest an early Cretaceous age for the acid rocks.

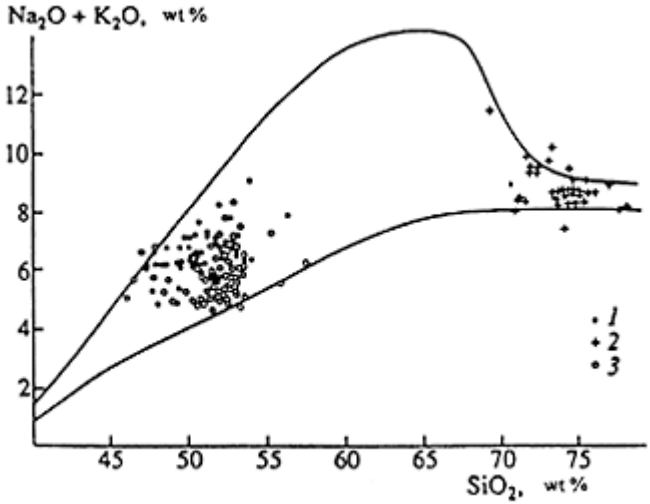

Key: 1–3—age of the rocks: 1—early, 2—middle and 3—later early Cretaceous.

Figure 87 Compositions of Lower Cretaceous volcanics, plotted on the classification diagram.

The volcanic successions of this stage are composed of flow-banded and pillowed lavas, glass, and pyroclastic rocks of trachyrhyolite-ongorhyolite composition. They contain 69–79% (generally over 72%) SiO_2 and up to 10.5% total alkalis (Kovalenko *et al.*, 1979) (see Fig. 87). In the flow-banded lavas, the K_2O/ Na_2O ratio is greater than one; inverse ratios are observed in glasses. The rocks are commonly rich in fluorine, the content of which is a high as 0.83% in ongonites and 1.75% in their glasses. The ongonites show increased concentrations of some rare elements (Kovalenko *et al.*, 1979).

Structurally, the occurrence of acid volcanicism is controlled by the Gobi-Altai rift zone (see Fig. 85). The largest volcanoes, forming groups of edifices, occur in its central part. Only relatively small isolated lava domes and stocks can be observed on the flanks of the rift zone. The acid rocks occupy a total area of about 90–100 km^2; their volume is estimated as 25–30 km^2.

4) The late early Cretaceous stage (K_1^3) is characterized by the development of volcanic successions and numerous subvolcanic bodies of subalkaline basalts and andesitic basalts (see Fig. 87) (Samoilov, 1989).

The distribution of the rocks is controlled by the structures of the Gobi-Altai rift zone. The rocks are usually separated from the earlier early Cretaceous basalts by units of marls, laminated mudstones and siltstones or, less commonly, acid volcanics. The composite thicknesses of the volcanics reach 350 m, averaging about 100 m. The sedimentary strata at the base of the volcanics are saturated with subvolcanic bodies, sills, and dykes. The dykes can form swarms, extending along the grabens.

The age of the rocks of this stage is determined as Aptian to Albian, mostly from the fossil remains, found in the beds of sedimentary rocks (Frikh-Khar *et al.*, 1982), and from K-Ar dating (118–105 Ma).

5) The earlier late Cretaceous stage (K_2^1) is represented by small, central-type basalt edifices and accompanying stocks, laccoliths, and necks. Outcrops of these occur over a huge, roughly circular area, offset southwards from the central part of the Gobi-Altai rift zone (Fig. 88). It is clear that the distribution of volcanic rocks was controlled by specific structures, but only in the northern part of the area, where a chain of volcanic terrains, stocks, and laccoliths is concentrated in the grabens of the rift zone. In the more southerly parts of the area, the volcanic rocks are scattered throughout the area.

The rocks are dominated by subalkaline olivine-basalts, although andesitic basalts are also present (Fig. 89). The volcanics of this stage either overlie or cut through Aptian-Albian deposits; they are overlain by Senonian deposits (Kovalenko *et al.*, 1984b). The K-Ar ages of the rocks fall in the range 105–88 Ma.

6) The later early Cretaceous stage (K_2^2) The volcanic rocks are scattered over a subcircular area, offset south-eastwards from the volcanic area of the preceding stage (see Fig. 88). Volcanics occur in small (roughly 10 km^2 in area) plateau-basalt terrains and slag-bomb cones, covering the plateaux, as well as in dykes, stocks and laccoliths. The products of volcanic activity (Fig. 89) are totally

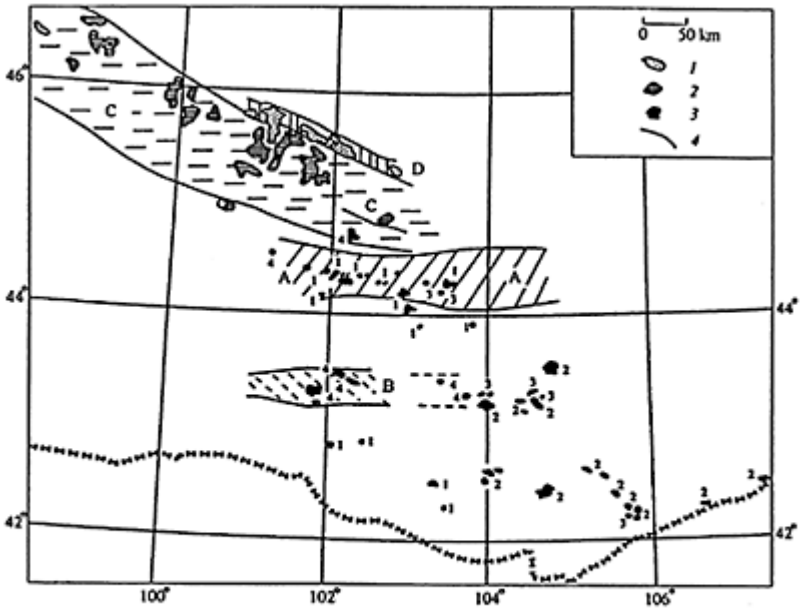

Key: 1–3—rock association: 1—Lower Miocene, 2—Upper Oligocene, 3—another association, whose age is determined by an index (1—early and 2—later late Cretaceous, 3—Paleocene–Eocene, 4—Lower Oligocene); 4—fault. Grabens (shaded) of: A—Gobi-Altai rift zone, B—Gurvantes, C—Dolinoozersky, D—Bayanteg.

Figure 88 Distribution of Upper Cretaceous—Lower Miocene rock associations.

dominated by aphyric subalkaline olivine-basaltic and basanitic lavas, containing large (up to 20 cm) inclusions of Iherzolite and pyroxenite.

The age of the rocks is determined by their occurrence overlying Upper Cretaceous fossiliferous sedimentary rocks. The K-Ar ages of the rocks fall in the range 84–72 Ma, but are mainly concentrated between 75 and 71 Ma.

7) The Palaeocene-Eocene stage $(₱_{1-2})$ A number of small volcanic terrains and individual dykes and stocks belong to this stage. They are scattered within a NW-SE-trending belt, which coincides in part with the volcanic terrain of the preceding stage (see Fig. 88).

In their chemistry, the volcanics (see Fig. 89) show only minor variations in SiO_2 (47–49%) and total alkalis (5–6.5%). The age of the rocks is determined by their local conformable superposition on Upper Cretaceous and Palaeocene deposits (Shuvalov and Nikolaeva, 1985). Their K-Ar ages fall in the range 62–47 Ma.

8) The early Oligocene stage $(₱_3^1)$ is represented by a number of basalt terrains (see Fig. 88), made up of thin (≤10 m) sheets, as well as volcanic stocks, domes, and dykes.

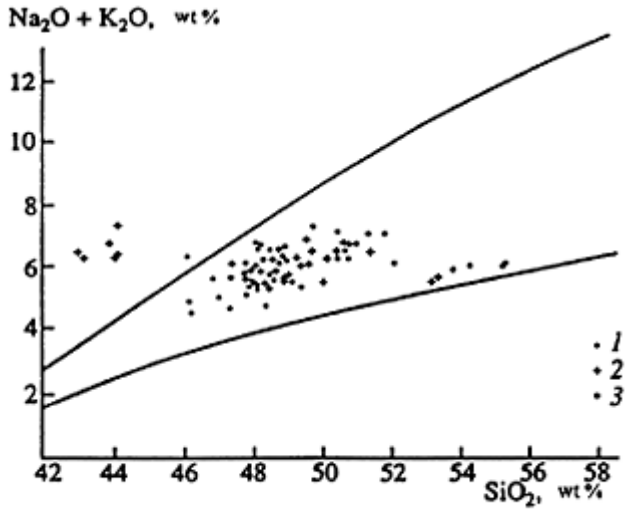

Key: 1–3 age group of: 1—earlier and 2—later late Cretaceous, 3—Paleocene–Eocene.

Figure 89 Compositions of Upper Cretaceous and Paleocene-Eocene volcanics plotted on a classification diagram.

In their composition, the rocks are consistent with aphyric subalkaline Nenormative basalts and alkali basaltoids, locally containing inclusions of Iherzolite. The rocks show the following variations in their composition: SiO_2 47–52.5% and (Na_2O+K_2O) 6.2–8.2% (Fig. 90). The rocks are distinguished by their high K_2O,

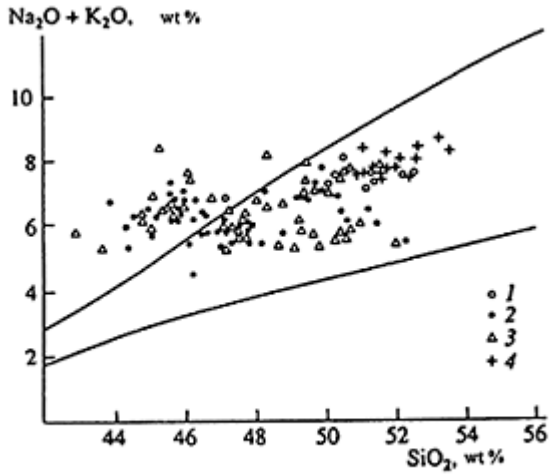

Key: 1–4—age groups: 1—early Oligocene, 2—late Oligocene, 3—early Miocene, 4—middle Miocene.

Figure 90 Compositions of the Oligocene and Miocene volcanics plotted on the classification diagram.

3–4.20%. Their K-Ar ages fall in the range 44–32 Ma, placing them in the early Oligocene.

9) The late Oligocene stage (P_3^2) is typical of the volcanic terrains concentrated in the Dolina Ozyer (Lake Valley) area (see Fig. 88).

Compositionally, the rocks are basanites, hawaiites, mugearites, and subalkaline basalts. They contain Iherzolite inclusions, showing wide variations in their composition (Kepezhinskas, 1979). Their SiO_2 contents vary from 44 to 48%, and their Na_2O+K_2O between 5 and 8% (see Fig. 90).

The age of the rocks of this stage is determined from their occurrence within late Oligocene sedimentary deposits (Devyatkin, 1981). The K-Ar ages of the rocks are mainly concentrated within the range 30–26 Ma (Devyatkin, 1981).

10) The early Miocene stage (N_1^1) Volcanics of this stage tend to be localized on the margins of the Upper Oligocene Dolina Ozyer graben (see Fig. 88).

The early Miocene volcanic complex contains a wide range of rocks, from basanites to subalkaline olivine-basalts (Kepezhinskas, 1979), including small inclusions of Iherzolite. Their SiO_2 contents vary between 43 and 52%, and their $Na_2O + K_2O$ between 5 and 8.5% (see Fig. 90). The K-Ar ages of the rocks fall in the range 22–16 Ma.

11) The middle Miocene stage (N_1^2) is represented by volcanic successions, which were primarily formed in the time interval 15–11 Ma. Their main terrain is the central part of the Khangai Ridge. In places, the sections reach 600 m in thickness, but average about 200m thick.

The volcanics of this stage are dominated by subalkaline olivine-basalts (SiO_2 50–52% and Na_2O+K_2O=7.2–8.5%) (see Fig. 90).

12) The Pliocene stage (N_2) is associated with volcanics dated at 6.4–3.0 Ma. Their terrain occurs in an east-west-trending area, offset north-eastwards from the Central Khangai Ridge (see Fig. 83). The volcanics crop out along some river valleys, where they form high terraces where the thickness of the volcanic sections varies from 50 to 100 m (Devyatkin, 1981). The largest volcanic occurrences are observed in the central part of the area, in the Khanui River basin. There the volcanics form a large lava plateau and infill the entire valley of the lower part of the river. The volcanics occupy an area of about 700 km^2. The thickness of the sections, on average, is 50–70 m.

The products of volcanic activity are dominated by aphyric subalkaline olivinebasalts (Fig. 91), locally containing inclusions of Iherzolite. In composition, they contain from 44 to 50% SiO_2 and 4.5 to 7% Na_2O+K_2O.

13) The Pleistocene-Holocene stage (Q) is represented by volcanics from the last 2–2.5 Ma (see Fig. 83). The youngest volcanic activity is known from ancient Chinese documents. The volcanics of this stage mainly form low terraces of the 'valley' generation. The surfaces of the lava flows are quite fresh, in many places preserving their vitreous upper crusts. In addition, well-preserved slag-bomb cones and isolated shield volcanoes are also common.

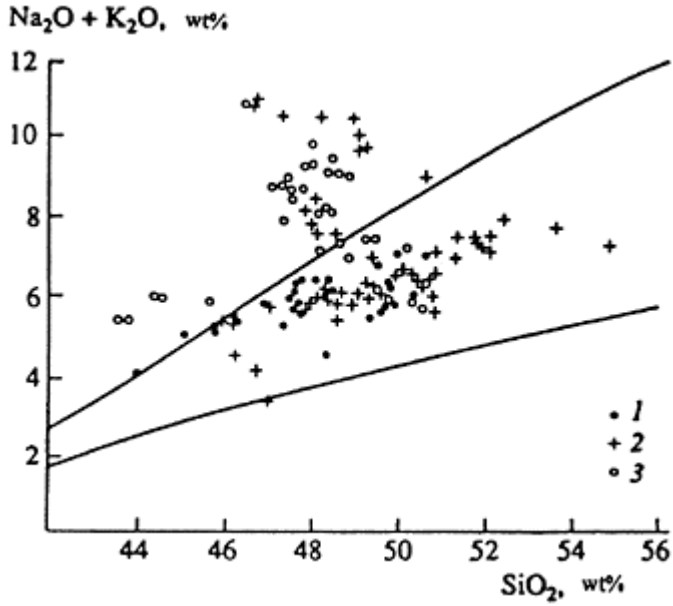

Figure 91 Compositions of the Pliocene (1), Pleistocene (2), and Holocene (3) volcanics, plotted on a classification diagram.

The volcanic activity of this stage tended to recur, giving similar structures, therefore it is not always possible to distinguish separate volcanic episodes in the field. The volcanic products consist of subalkaline and alkali basalts, in many places containing various deep-seated inclusions. Kepezhinskas (1979) distinguished limburgites, basanites, tephrites, potassic hawaiites, and olivine-basalts. As a whole, they show variations in their SiO_2 contents from 45 to 53% and $Na_2O + K_2O$ contents from 4 to 11% (see Fig. 91).

On the Nature of Upper Mesozoic-Cainozoic Volcanicism

As shown above, the products of Upper Mesozoic-Cainozoic volcanicism occur throughout vast areas of Central and South Mongolia. The volcanics from the various different stages of volcanism have many features in common, including the order of their sequences.

Firstly, it should be noted that the separate stages were separated by very short time intervals. This is suggested by the way in which dates from the rocks of successive stages generally overlap.

The spatial distribution of volcanics of different ages can be correlated with the order of migration of the volcanic foci. Therefore the volcanics of the successive stages form volcanic areas mostly overlapping each other. The morphology of the areas varies from linear to more or less compact. However, the linear areas also usually surround a central subcircular region, characterized by greater thickness of the rocks in the cross-section and the concentration of most of the volcanic rocks within this area. Here the volcanic areas, formed during successive volcanic episodes, tended to intersect.

Lastly, there is a marked similarity in compositional parameters of the volcanic rocks throughout almost the entire period of formation of the volcanic region. The various volcanic associations are dominated by basic rocks (Table 33), accounting for no less than 95% of the total volume of the volcanic rocks. They are represented by subalkaline olivine-basalts and alkali basaltoids. The compositions of the rocks are consistent with so-called intraplate associations, and suggest that their primary melts were derived from the mantle. This is also suggested by the sporadic appearance of inclusions of mantle Iherzolites in volcanics from the early Cretaceous onwards, but particularly widely distributed within Cainozoic rocks. The age given above, and the topographic and compositional features of the volcanic rocks of the region suggest an affinity and a relationship with a persistent sublithospheric source of volcanism.

Data on the quantitative parameters of volcanic activity at different stages of formation of the volcanic region are brought together and presented in Table 34. This table shows the volume of volcanics and the areas where they were distributed. Figure 92 is a composite diagram showing the distribution of volcanic areas

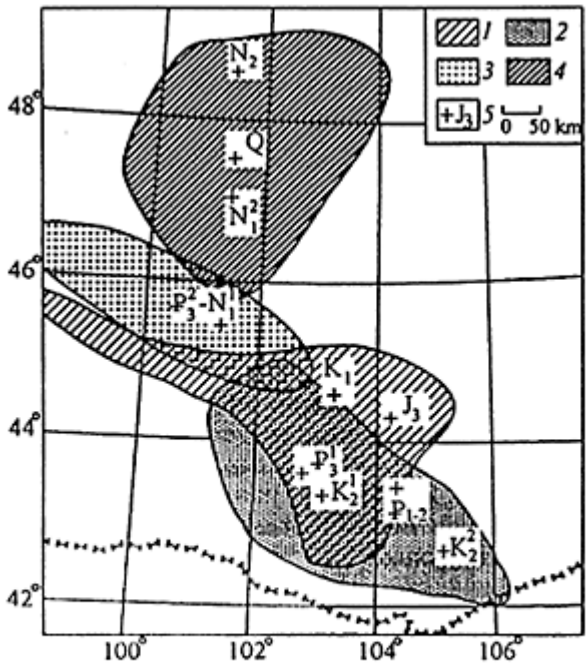

Key: 1–4—Areas of volcanic rocks: 1—Upper Jurassic-Lower Cretaceous, 2—Upper Cretaceous-Early Cenozoic (up to the Late Oligocene), 3—Late Oligocene–Lower Miocene, 4—Middle Miocene–Holocene, 5—centres of distribution areas for rocks of individual stages of volcanism, identified by age indices.

Figure 92 Map of the distribution of areas of different ages for intraplate volcanic rocks.

Table 33 Average chemical compositions, reduced to 100%, of the late Mesozoic-Cainozoic basic volcanics of Central and South Mongolia (after Yarmolyuk *et al.*, 1994).

I	II	III	SiO_2	TiO_2	Al_2O_3	Fe_2O_3	FeO	MnO	MgO	CaO	Na_2O	K_2O	P_2O_5
1	a	8	46.84	1.39	15.20	4.86	4.19	0.16	6.88	10.80	4.64	3.48	1.55
2	Ws	3	51.45	2.12	15.91	6.14	4.44	0.14	4.92	7.44	3.53	2.74	1.17
	Cs	37	53.16	2.18	16.17	5.64	3.98	0.11	3.81	7.00	4.00	2.87	1.07
	Es	7	53.18	2.97	15.84	5.50	4.58	0.10	3.32	6.21	3.57	2.98	1.75
4	Ws	14	54.20	1.60	16.82	4.27	4.99	0.14	4.62	6.96	4.16	1.69	0.54

	Cs	22	54.04	1.86	16.71	4.21	5.13	0.13	3.97	7.01	4.21	1.93	0.79
	Es	1	53.57	1.40	17.45	5.47	4.16	0.10	4.42	7.54	4.33	1.15	0.40
5	a	22	52.19	1.78	17.07	3.60	5.49	0.15	5.21	7.51	4.20	2.20	0.60
6	N	28	50.00	2.33	15.57	5.20	5.85	0.14	5.76	8.34	4.01	2.19	0.61
	S	6	44.51	2.12	14.41	5.79	6.82	0.22	7.74	10.58	4.90	1.97	0.94
7	a	7	49.84	2.25	15.83	5.28	5.64	0.14	5.58	8.70	4.12	2.13	0.47
8	a	6	51.44	2.41	15.15	4.87	5.06	0.12	5.54	7.17	4.20	3.26	0.79
9	a	40	47.87	2.51	14.35	4.49	6.60	0.15	7.62	9.27	3.79	2.42	0.86
10	a	52	49.60	2.56	14.45	4.03	6.32	0.14	7.11	8.18	4.18	2.54	0.87
11	CKh	13	49.27	2.19	15.51	3.35	7.18	0.15	7.80	8.03	3.81	2.08	0.62
	Or	6	51.77	2.77	14.18	3.91	6.44	0.12	5.74	6.88	3.98	3.35	0.86
12	a	67	51.00	2.47	15.33	2.59	7.38	0.13	6.41	7.66	4.10	2.31	0.62
13	CKh	31	50.11	2.04	15.58	2.37	7.96	0.13	7.24	7.68	4.14	2.31	0.14
	Or	79	51.21	2.44	15.31	2.81	6.95	0.13	6.23	7.20	4.47	2.56	0.69

Note: I—volcanic epoch; II—volcanic regions: a—the volcanic area as a whole; Ws—the western segment of the Gobi-Altai rift zone; Cs—central segment; Es—eastern segment; N—northern and central parts of the Upper Cretaceous volcanic area; S—southern part of the same volcanic area; CKh—Central Khangai including the Verkhnechulutin and Verkhneorkhon volcanic fields; Or—the middle Orkhon River basin including Tariat and Khanui regions; III—number of samples.

Table 34 Quantatitive characteristics of volcanicism in late Mesozoic-Cainozoic times in Central and South Mongolia.

Stage of volcanicism	Duration (from radiometric dating) in Ma	Areas affected by volcanism (1,000 km ^{2})	Volume of erupted products, (km ^{2})	Intensity of volcanicism, (km/Ma)
1. Late Jurassic	10	7	160	16
2. Early early Cretaceous	15	50	5,000	330
3. Middle early Cretaceous	5	25	30	6
4. Late early Cretaceous	11	35	500	45
5. Early late Cretaceous	15	30	>20	1.3
6. Late late Cretaceous	5	40	>25	5
7. Paleocene-Eocene	15	15	>10	1

8. Early Oligocene	9	25	>50	4.5
9. Late Oligocene	6	30	>250	40
10. Early Miocene	5	25	25	5
11. Middle-late Miocene	6	35	900	150
12. Pliocene	3	15	60	20
13. PleistoceneHolocene	2	60	300	150

of differing ages. Each area shown is isolated, suggesting that the volcanic products are localized. Also, each area can be described by a specific centre, corresponding with the action of a point source of volcanic activity on the lithosphere, and the boundaries of the areas describe the projection of the size and outline of the source. The above evidence suggests that the source was roughly circular in form, although at some stages it changed to become linearly elongated, and was then accompanied by intensive graben emplacement.

From this discussion we can infer that throughout the late Mesozoic and the Cainozoic, Central and South areas of Mongolia were affected by a local sublithospheric source of magmatism, varying slightly in its lateral dimensions. The position of the source at the Earth's surface varied regularly with time and did not suddenly change position, as would have been the case if the magmatic source changed. This magmatic source was probably related to a mantle plume, which was also recognized as the South Khangai mantle hot-spot. In accordance with hypotheses regarding the fixed position of mantle plumes within the sublithospheric mantle, and the movement of the projection of the centre of the hot-spot on the Earth's surface, both reflect the movements of the Eurasian plate in late Mesozoic-Cainozoic times. However, by and large these motions were insignificant.

Thus the long-term development of the hot-spot provided a unique means of studying the long-term evolution of the composition of intraplate magma sources. With this as the primary objective, the isotopic Sr and Nd compositions were studied in basic rocks of all ages (Yarmolyuk *et al.*, 1995d). The results of these studies are given in Table 35 and Figure 93 (Table 36 gives the composition of the researched rocks). They indicate substantial variations in the isotopic composition of the rocks. The role of crustal contamination in these variations was probably minimal. This is suggested by: the lack of correlation between the isotopic Sr and Nd composition and their content in the rocks; the high Sr content; and the low Rb/Sr ratios. Also, rocks from practically all stratigraphic levels contain mantle xenoliths, indicating that the melts rose rapidly to the surface, thus precluding their interaction with crustal rocks. Therefore, the variations recorded in the isotopic composition of the rocks probably indicate that the mantle melt sources were isotopically heterogeneous. Their parameters can be estimated from Figure 93, which shows two groups of points. One group represents the late Jurassic-Cretaceous volcanics and forms a linear trend from early rocks (150–120 Ma),

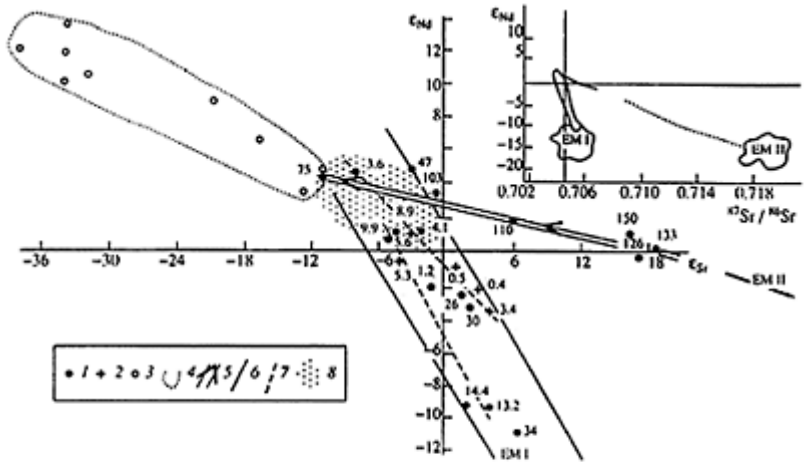

Key: 1—data from Table 35 (age in Ma), 2—data from Kononova *et al.*, (1993); 3—composition of mantle xenoliths from volcanics in the Khangai Highland (after Kovalenko *et al.*, 1990); 4—compositional field of depleted mantle, as determined from xenoliths; 5—trend of the evolution of rock composition for the late Mesozoic stages of volcanism; 6—compositional field for the Cainozoic stages of volcanism; 7—plots of variation in rock composition in a single age group; 8—weakly depleted lithospheric mantle: a source of igneous melts. The inset map shows the trends in the variation in isotopic compositions for volcanics of the South Khangai mantle hot-spot relative to the enriched mantle of EM I and EM II type (after Zindler and Hart, 1986).

Figure 93 Strontium and Nd isotopic compositions of basic volcanics of the South Khangai hot-spot.

Table 35 Isotopic composition of Sr and Nd in basic volcanics of the South Khangai mantle hot-spot (after Yarmolyuk et al., 1995d).

Sample no. and composition	Volcanic stage and age (Ma)	Rb	Sr	$^{87}Rb/^{86}Sr$	$^{87}Sr/^{86}Sr$	ε^{T}_{Sr}	Nd	Sm	$^{147}Sm/^{144}Nd$	$^{143}Nd/^{144}Nd$	ε^{T}_{Nd}
4140/11, melanephelinite	1,150	108.9	6970	0.0452+3	0.7055±44	+16.5	281.7	36.74	0.07885	0.512582	+1.2
4147/5, basalt	II, 133	80.1	2323	0.0998+5	0.705835±39	+18.5	106.1	16.04	0.09151	0.512569	+1.4
1/5, basalt	126	57.3	592.3	0.1762+9	0.705894±45	+17.4	45.3	8.8	0.1175	0.512569	−0.1
4070/9, basalt	111, 110	18.8	604.5	0.0900+8	0.704914±31	+5.7	19.4	4.53	0.1412	0.512695	+1.9
4902/2, basalt	IV, 103	20.3	753	0.0780+8	0.704427±18	−0.9	23.73	5.327	0.1358	0.512781	+3.6
1741, basanite	V, 75	15.5	1400	0.0320+3	0.703632±17	−11.6	65.78	11.64	0.107	0.512844	+4.6
1743, basalt	VI, 47	23.7	548	0.1251+13	0.704302 ± 21	−3.2	21.84	5.108	0.1411	0.512856	+4.8
1720–1, basalt	VII, 34	51	1,031	0.1431+6	0.704977±16	+6.4	38.1	7.73	0.1227	0.512073	−10.7
3/21, basanite	VIII, 30	19.7	840	0.0678+7	0.704620±15	+1.8	36.51	7.508	0.1244	0.512466	−3.1

3/39, tephrite	26	39.4	927	0.1230+8	0.704601±14	+1.3	40.98	8.3	0.1226	0.512491	−2.6
3/37, basalt	X, 14.4	36	1,018	0.1023+8	0.704614±13	+1.6	39.38	4.722	0.07256	0.512157	−9.2
5/2, basalt	13.2	37.2	1,044	0.1031+7	0.704787±19	+4	42.15	8.348	0.1198	0.512162	−9.2
6/1, tephrite	XI, 9.9	35.6	942	0.1095+7	0.704127±17	−5.3	40.79	11.64	0.1727	0.512671	+0.7
6/3, basalt	8.9	28.6	834	0.0994+8	0.704154±19	−4.9	33.52	7.08	0.1278	0.512696	+1.2
8/1, basalt	XII, 4.1	36.4	1,000	0.1052+7	0.704301±17	−2.8	42.26	6.101	0.08735	0.512695	+1.2
21/6, basalt	3.6	21.4	740	0.0836+8	0.703936±14	−8	29.61	6.928	0.1416	0.512885	+4.8
2564/11, tephrite	XIII, 1.2	28.2	683	0.1195+10	0.704386±21	−1.6	29.33	6.516	0.1344	0.512531	−2.1

Note: Isotopic analyses of Nd and Sr were performed using an MAT-262 mass spectrometer. The accuracy of the ratios was 0.2 and 0.5% for $^{147}Sm/^{144}Nd$ and $^{87}Rb/^{86}Sr$, respectively. The following parameters of the undifferentiated mantle were used to calculate ε_{Nd} and ε_{Sr}: $^{143}Nd/^{144}Nd=0.512638$, $^{147}Sm/^{144}Nd=0.1987$ (CHUR) and $^{87}Sr/86Sr=0.7045$, 87Rb/86Sr=0.0825 (UR).

Table 36 Chemical composition of representative rocks of the South Khangai mantle hot-spot.

Sample	**474 0/11**	**414 7/5**	**1/500**	**40 70/9**	**49 02/2**	**1741**	**1743**	**17 20/1**	**3/21**	**3/39**	**3/37**	**5/20**	**6/10**	**6/30**	**8/10**	**21/6**	**25 64/ 11**
SiO_2	45.29	54.04	51.05	53.77	51.80	45.00	49.68	52.78	46.67	48.49	53.17	52.24	47.69	48.54	49.91	51.21	49.09
TiO_2	1.18	1.98	1.78	1.57	2.25	2.01	2.27	2.24	2.21	2.50	1.93	2.00	2.26	2.21	2.44	2.44	2.04
Al_2O_3	14.35	14.60	16.19	17.26	16.35	14.17	15.49	14.74	13.73	14.44	15.29	15.69	15.20	15.09	15.29	15.51	15.28
Fe_2O_3	5.97	6.79	5.96	5.11	4.63	4.28	3.49	5.10	5.06	4.34	3.80	2.58	2.93	2.87	1.65	1.36	3.05
FeO	3.89	1.76	4.49	3.77	5.34	8.04	6.90	4.94	6.54	6.76	6.06	6.79	7.73	7.74	8.32	8.40	7.74
MnO	0.17	0.12	0.12	0.07	0.13	0.22	0.13	0.12	0.14	0.15	0.10	0.12	0.16	0.15	0.13	0.12	0.14
MgO	6.39	4.32	6.64	3.99	4.99	8.40	4.84	5.44	9.29	7.39	4.77	5.04	8.81	8.67	6.40	6.42	8.47
CaO	11.52	7.02	7.99	8.66	7.46	10.49	10.39	6.08	9.69	9.27	6.13	6.06	8.64	8.95	7.58	7.26	8.12
Na_2O	5.68	3.89	3.34	4.53	4.32	5.20	4.06	4.01	3.77	3.13	4.26	4.62	3.58	3.21	4.38	4.18	3.58
K_2O	3.92	4.08	1.69	0.97	2.22	1.31	2.28	3.82	2.07	2.75	3.74	4.03	2.28	1.97	2.94	2.44	2.01
P_2O_5	1.63	1.41	0.75	0.29	0.51	0.88	0.46	0.73	0.82	0.78	0.74	0.82	0.72	0.61	0.96	0.65	0.47
Total	100.00	100.00	100.00	100.00	100.00	100.00	100.00	100.00	100	100.00	100.00	100	100	100.00	100.00	100.00	100.00
Pb	25	34	21	13	11	10	2	5	3	3	2	2	6	6	4	1	3
Sn	3.4	3.19	3.11	4.20	3.17	2.55	1.85	4.21	4.55	4.32	4.70	2.76	5.65	5.59	5.52	2.92	2.93
Rb	81	88	27	17	17	12	32	48	21	35	33	31	35	26	35	22	28
Cs	4.61	10.28	6.95	0.63	4.49	0.51	0.72	0.72	1.86	0.62	0.41	0.51	0.51	0.61	1.02	0.00	0.40
Ba	4273	2262	695	483	772	812	478	704	931	1233	716	624	719	610	716	473	556
Sr	3596	1851	612	630	707	1263	616	942	869	1027	1105	1044	1120	844	1114	695	707

Li	55.33	38.04	14.53	15.75	14.09	14.77	6.68	13.25	12.42	12.33	9.20	12.28	7.19	6.10	7.16	7.76	8.08
Ta	0.92	1.23	0.83	0.52	1.74	5.50	1.85	1.95	2.38	2.77	2.35	2.56	2.98	2.24	2.66	2.01	1.62
Nb	14.3	13.4	35.3	9.4	26.6	63.2	26.7	31.8	47.6	72.6	35.2	53.2	44.2	43.7	27.0	33.2	38.4
Hf	6.25	7.92	5.91	3.15	3.78	8.66	4.72	4.31	4.45	4.62	4.81	5.32	5.55	4.37	5.52	4.84	3.84
Zr	410	225	259	126	173	263	158	197	259	303	235	215	344	341	143	166	263
Y	37	29	34	20	23	28	25	21	18	18	14	17	18	18	19	16	16
Th	15.88	9.56	3.32	0.73	2.14	9.48	2.47	1.64	3.10	4.11	2.86	2.76	4.11	3.05	3.07	2.01	3.03
U	1.33	2.78	0.52	0.31	1.33	3.46	1.34	0.92	1.66	1.34	1.74	0.82	2.06	1.52	1.74	1.61	2.22
La	282.79	126.45	44.41	15.54	19.81	78.76	18.49	27.53	37.47	39.97	33.65	39.49	43.88	32.94	45.39	23.27	27.98
Ce	447.75	202.53	85.49	31.49	39.12	128.27	38.31	58.45	73.38	74.39	68.42	77.66	81.70	64.35	86.18	49.36	56.77
Nd	191.60	87.08	45.24	17.74	21.45	56.55	22.08	34.51	39.64	38.01	38.56	42.15	41.72	34.16	45.08	29.21	32.32
Sm	39.96	18.30	11.21	4.62	5.41	12.12	5.85	9.35	9.94	9.14	10.02	10.64	10.07	8.64	11.04	7.86	8.28
Eu	9.12	4.52	2.59	1.68	1.94	3.46	1.85	2.57	2.43	2.54	2.45	2.56	2.53	2.03	2.76	2.21	2.12
Gd	18.55	8.22	9.13	4.80	5.72	9.88	5.55	5.75	5.90	6.88	6.55	7.26	7.40	5.29	7.77	5.64	6.67
Tb	2.35	1.15	1.44	0.70	0.87	1.41	0.84	0.81	0.83	0.82	0.82	0.82	1.03	0.81	1.02	0.81	0.91
Yb	2.28	1.63	2.79	1.67	1.71	2.14	1.69	1.20	1.28	1.45	1.05	0.92	1.40	1.33	1.46	1.11	1.35
Lu	0.27	0.21	0.37	0.20	0.22	0.28	0.23	0.15	0.21	0.18	0.12	0.10	0.21	0.20	0.18	0.19	0.17

Note: numbers of the specimens correspond to numbers of table 35.

rich in radiogenic Sr, to late varieties (75 Ma), which are low in Sr, and show a slight increase in ε_{Nd}. The second group represents Cainozoic volcanics. It exhibits more marked variations in isotopic Nd composition and therefore shows a steeper trend as compared with that of the first group.

The aggregate distribution of representative points on a diagram suggests three possible sources for the melts, whose mixing could have caused the observed variations in isotopic composition. The two successions recognized above had a common source, whose parameters correspond with the area of their convergence on the diagram (see the dotted area on Fig. 93). Taking into account the relationship between this source and composition of mantle xenoliths studied in Central Mongolia (Kovalenko *et al.,* 1990), we can state that this source is consistent with the least-depleted fragments of the lithospheric mantle. The other two sources represent a generalized mantle composition. Judging by trends in their compositional variations: one of them is rich in radiogenic Sr and resembles EM II-type mantle. The other source can be correlated with EM I-type Nd-rich mantle (Zindler and Hart, 1986).

The data show a specific relationship between the compositions and geodynamic environment of volcanicism. For example, the rocks from the volcanic stages where volcanic activity was only localized (late Cretaceous, early Cainozoic, and some other stages) are more-or-less similar in their isotopic compositions, which is consistent with a slightly depleted lithospheric mantle. The products of volcanic phases characterized by large-scale eruptions, show a major contribution from undepleted mantle of various types. These include the early Cretaceous, late Oligocene, middle Miocene and Pleistocene-Holocene volcanic complexes, which are the result of plateau eruptions of hundreds and thousands of cubic kilometres of melt. The contribution of EM II-type mantle was very substantial in late Jurassic and earlier early Cretaceous times, but after this it was much reduced and has now ceased. In late Cretaceous-Eocene times, lithospheric mantle provided the main source for the melts. Starting in the Oligocene, an

EM I-type source was involved; its products could have mixed in various proportions with the melting products of the lithospheric mantle, even within one magmatic stage (see Fig. 93). The change in the sources of the melts of the South Khangai 'hot-spot' with time probably reflects the evolution of mantleplume material in the area where it supplies various igneous centres, as well as the thermal and/or material interaction of the plume with the lithospheric mantle.

Other Regions of Upper Mesozoic-Cainozoic Magmatism of Mongolia

The Dariganga hot-spot is believed to be responsible for the formation of the Eastern Mongolian volcanic belt and the Dariganga lava plateau (see Fig. 82). Traditionally they have been dated as early Cretaceous and late Cainozoic, respectively (Luchitsky, 1983). In East Mongolia, where the products of both volcanic areas occur together, volcanics from other age levels, particularly the late Jurassic and late Cretaceous rocks, have been found recently (Samoilov *et al.*, 1988a). Currently, the following succession of magmatic events has been confirmed in the region:

1) The late Jurassic is represented by lithium-fluoric granites and trachytetrachydacite volcanic complexes in association with syenites and carbonatite-like bodies. They were discovered on the fringe of the Dariganga Plateau: lithiumfluoric granites with isochron Rb-Sr and U-PB (sphen) ages of 155 Ma were found at the north-eastern edge of the plateau in the Yugodzyr area, and the volcanic complex on the south-western fringe of the plateau near Bayan-Munkh-Khuduk Well. The K-Ar ages of the trachytes fall in the range 136–146 Ma.

2) The earlier early Cretaceous was a time of large-scale eruptions of plateau basalts of the Tsagantsab Suite, which were associated with the emplacement of a linear system of grabens and horsts of the East Mongolian volcanic belt. Basalts rest disconformity on Upper Jurassic trachyte; their ages fall in the range 138–125 Ma (Frikh-Khar and Luchitskaya, 1978; Samoilov *et al.*, 1988a). Usually they form lava plateaux with sections reaching a few hundred metres in thickness.

3) The middle early Cretaceous is represented by trachyrhyolites, ongorhyolites and trachydacites, generally forming discrete lava terrains, but also occurring as sills, laccoliths, dykes, and stocks, intruding lower Lower Cretaceous basic rocks within the East Mongolian belt. The thickness of the acid volcanics is 100–200 m. They are coeval with a few small intrusions of leucogranites, including rare-metal lithium-fluoric granites. They occur within the volcanic belt and in its vicinity. The K-Ar ages of the acid volcanics are in the range 122–130 Ma (Samoilov *et al.*, 1988a); the lithium-fluoric granites were Rb-Sr dated as 125 Ma (Kovalenko et al., 1996).

4) The later early Cretaceous was characterized by plateau eruptions of the subalkaline basalts of the Dzunbai Suite, which are interbedded in many places with Aptian-Albian sedimentary rocks (Leonov, 1983). They were erupted in the same grabens of the East Mongolian belt as those in which the lower and middle Lower Cretaceous sequences were formed. However, the eruptions were smallscale and the true terrains are generally discrete and thin (a few tens of metres thick).

5) The Upper Cretaceous volcanicism is still poorly understood; however, small flows and stocks of olivine-basalts were found near the Bayan-Munkh-Khuduk Well (on the

Western fringe of the Dariganga Plateau). The stocks intrude Cenomanian deposits; the K-Ar ages of the basalts are in the range 87–105 Ma (Samoilov *et al.,* 1988a).

6) The late Cainozoic volcanicism of the region is represented by the Dariganga lava plateau (Yarmolyuk *et al.,* 1995a). The plateau started forming no later than the early Miocene (23 Ma). A further volcanic episode took place in the middle Miocene (14 Ma ago), and most of the basalts were formed in the Pliocene (5–3 Ma) when the lava plateau, which occupied an area of more than 14,000 km^2, was formed. Intensive volcanic activity also continued into the Pleistocene-Holocene. The volcanics are represented by subalkaline olivine-basalts, basanites, tephrites, mugearites, and hawaiites (Saltykovsky and Genshaft, 1985).

It is evident from the above, brief, review that the magmatic evolution of East Mongolia can be roughly correlated with that of the South Khangai hot-spot. In East Mongolia, as in the area of the South Khangai hot-spot, magmatism started with localized trachyte volcanism and also the appearance of lithium-fluoric granites. The early Cretaceous was also characterized by its: large-scale eruptions and their association with graben emplacement as well as the tripartite structure of the volcanic sections, which show a phase of acid magmatism occurring in the middle of an early Cretaceous. A successive reduction in the scale of volcanic activity has been noted for the whole of the early Cretaceous, and here the late Cretaceous was localized as in the South Khangai volcanic region. As yet, no evidence has been found of magmatic activity in the early Cainozoic. However, in its phases of evolution, late Cainozoic volcanicism is similar to that of volcanic episodes on the central and southern parts of the Khangai Ridge. It should also be noted that the Dariganga Plateau and its nearest periphery is an area where a number of igneous episodes of different ages were concentrated. Based on all the above data and the way in which the volcanic regions of Eastern Mongolia occur spatially separated from the South Khangai hot-spot region, we can infer that the late Mesozoic-Cainozoic magmatism of East Mongolia was controlled by the Dariganga hot-spot.

Volcanic terrains of the Lake Khubsugul area

These terrains (see Fig. 82) belong to a fragment of the Upper Cainozoic South Baikal volcanic region, the main terrains of which occur in the adjacent areas of Russia. The development of this region is related to the activity of the mantle hotspot of the same name, over a time interval from the end of the early Cainozoic to the late Cainozoic (Yarmolyuk *et al.,* 1990a). The region first developed in Oligocene times (>30 Ma). Outbursts of activity have also been noted for the early (20–15 Ma) and middle-late Miocene (12–8 Ma), Pliocene, Pleistocene, and Holocene. The volcanic products are purely basic in composition, and are determined by the development of subalkaline olivine-basalts, tephrites, nephelinites, and mugearites (Kiselev *et al.,* 1979).

Composition of the Upper Mesozoic-Cainozoic Igneous Associations of Mongolia

The Upper Mesozoic-Cainozoic igneous associations are made up of various rock types, all showing increased and high alkalinity. Compositionally, they can be classified as basic, alkali-salic, and acid rocks.

The bulk of the Upper Mesozoic-Cainozoic associations are basic rocks, accounting for about 90% of the rock volume. They are dominated by subalkaline olivine- and pyroxene-plagioclase basalts; other rocks include tephrites, nephe-linites, and basanites, etc. The rocks show high alkali contents (>5.5%), TiO_2 (as a rule >2%), moderate (<17.5%) and low (up to 13%) alumina, with increased concentrations of rare elements (Sr, Ba, Zr, Nb, and REE).

The alkali-salic rocks are typical of the earlier stages of development of the province; they were formed mainly in the late Jurassic and, to a lesser degree, in the early Cretaceous. This is exemplified by the Upper Jurassic volcanoplutonic associations of the South Khangai Region. The alkali-salic rocks are most common in the structure of the above-mentioned Mushugai-Khuduk volcanic region.

The acid rocks that make up the Upper Mesozoic-Cainozoic associations were formed at the early Cretaceous stage of development, following plateau-basalt eruptions at the beginning of the early Cretaceous. As noted above, they are represented by trachyrhyolites and ongonites (topaz thyolites) in volcanic suites, as well as rarer intrusions of granitoids, including lithium-fluoric rare-metal granites. The rocks are of particular interest because of the presence of rare-metal (Sn, W, Be, Li, and Ta) mineralization.

The plutonic rocks form small intrusions, which are widely spaced and tend to be localized within the fractures that bound the volcanic areas, or within horst uplifts. Compositionally, they vary from granites to leucogranites and lithiumfluoric granites (Table 37), whose contained rare-metal mineralization is of particular interest. The Rb-Sr isochron ages of the formation of these granites fall in the range 130–120 Ma. Texturally and structurally they resemble the Lower Mesozoic lithium-fluoric granites, and therefore they will not be considered in detail here.

General Trends in the Development of Upper Mesozoic-Cainozoic Magmatism

When comparing trends in the development of Mongolian late Mesozoic-Cainozoic magmatism, the independent development of individual igneous regions should be emphasized. This development is characterized by its lack of structural control on the distribution of the regions, and their spatial isolation. The latter suggests that the magmatic regions are related to discrete sources feeding their igneous activity. The uninterrupted record of eruptions indicates that the magma sources were stable for very long time intervals (160 Ma for the South Khangai and, presumably, the Dariganga regions), suggesting that these sources were related to the activity of isolated mantle plumes (mantle hot-spots). Outside the confines of the Mongolian part of Central Asia, there were also some hot-spots active in late Mesozoic-Cainozoic times (Yarmolyuk *et al.*, 1995a). The activity of all these hot-spots provides an explanation for the synchronous nature of the largest-scale phases of volcanicism. For instance, the earlier early Cretaceous phase of plateau-basalt formation and the following phase of acid magmatism—as well as the middle Miocene outburst of plateau-basalt eruptions—were all recorded from different volcanic regions of Central Asia. This correlation of events can be explained (Yarmolyuk *et al.*, 1995a) from the viewpoint of a relationship between the Late Mesozoic-Cainozoic hot-spots and the mantle ‘hot

Table 37 Compositions of the late Mesozoic leucogranites of the East Mongolian volcanic belt.

n/n	**1**	**2**	**3**	**4**	**5**	**6**	**7**	**8**	**9**	**10**	**11**
SiO_2	71.10	70.70	74.90	72.63	74.20	75.00	74.90	70.90	72.50	72.00	76.25
TiO_2	0.28	0.43	0.14	0.17	0.01	0.05	0.81	0.02	0.02	0.02	0.02
Al_2O_3	14.25	14.43	12.30	12.80	12.92	13.02	11.68	17.14	16.81	15.59	13.92
Fe_2O_3	0.53	1.40	1.18	0.89	1.06	0.15	1.83	n.d.	n.d.	1.37	0.16
FeO	2.00	1.40	1.49	2.35	0.71	1.36	1.01	0.62	0.73	0.53	0.53
MnO	0.05	0.04	0.04	0.05	0.04	0.08	0.07	0.16	0.15	0.06	0.09
MgO	0.29	0.47	0.12	0.22	0.10	0.04	0.38	0.02	0.01	0.01	0.01
CaO	1.86	1.40	0.69	1.04	0.71	0.41	0.99	0.89	0.14	0.18	0.20
Na_2O	3.93	3.85	3.63	3.37	3.82	4.68	3.59	6.07	5.44	6.05	5.38
K_2O	5.22	4.71	4.80	4.81	4.52	4.54	3.89	3.55	3.44	3.85	2.95
P_2O_5	0.19	0.09	0.13	0.06	0.12	0.03	0.08	0.06	0.04	0.01	0.01
H_2O	0.08	0.91	0.66	1.11	1.30	0.31	0.32	0.15	0.21	0.17	0.39
Total	99.78	99.83	100.08	99.56	99.56	99.66	99.55	99.58	99.48	99.83	99.91
Cr	4	5	4	11	4	2	3	2	3	7	1
Co	2	3	2	4	2	n.d.	2	1	1	n.d.	1
Sc	3.4	5.6	1.5	2.8	2.5	2.2	5	11	10	2	3
Cu	n.d.	n.d.	n.d.	20	8	n.d.	n.d.	n.d.	n.d.	n.d.	n.d.
Pb	n.d.	n.d.	n.d.	30	50	n.d.	n.d.	n.d.	n.d.	n.d.	n.d.
Zn	n.d.	n.d.	n.d.	140	40	n.d.	n.d.	n.d.	n.d.	n.d.	n.d.
Sn	n.d.	n.d.	n.d.	n.d.	n.d.	n.d.	n.d.	n.d.	n.d.	n.d.	n.d.
Rb	194	300	404	391	539	414	168	1730	1606	1089	719
Cs	25	10	10	17	22	33	3.3	86	63	14	12

Ba	589	534	127	305	281	100	263	100	100	100	100
Sr	302	162	52	83	66	36	104	20	19	35	36
Ta	2.6	2.5	4	4.5	8	5	5	42	49	42	43
Nb	15	22	47	40	49	62	47	111	110	90	70
Hf	6.1	6	6.5	8	5.6	7	11	11	9.4	12	15
Zr	174	227	182	235	125	118	297	17	25	50	62
Y	40	35	95	71	129	89	52	418	376	224	126
Th	40.6	32	65	50	35	23	56	11.5	11.7	10	12.5
U	7.2	7.8	25	11.1	5.3	2	15.9	4.5	3.7	7.2	5.6
La	57.8	39.8	55.1	69.5	27.1	23.3	106	8.1	7.25	5.6	7.8
Ce	93.6	72.6	97.7	108.9	50.9	55.1	197	23.2	20.9	13	19
Nd	41	36.3	47.4	45.9	26.2	36.6	85	19.1	17.3	8.4	13
Sm	8.7	8.6	10.9	9.5	6.4	10.9	17.5	6.7	6.2	2.5	4
Eu	0.9	1.01	0.37	0.65	0.37	0.17	1.6	0.02	0.02	0.04	0.06
Gd	4.2	4.67	7.3	5	5.6	9.2	11.5	5.77	4.50	1.6	2.1
Tb	0.7	0.83	1.29	0.9	1.06	1.47	1.8	0.97	0.74	0.31	0.43
Yb	2.19	3.1	4.56	3.35	5.35	3.56	4	2.93	2.05	1.6	2.8
Lu	0.32	0.46	0.67	0.5	0.84	0.49	0.54	0.42	0.29	0.25	0.4
F	900	1300	1500	n.d.	2000	2300	1100	11100	9000	2300	1600

Note: 1–7—leucogranite, 8–11—lithium-fluorine granite; n.d.-not determined.

field' which was common to all of them and which dictated their activity. Analysis of the volcanic events in Central Asia showed that three stages can be recognized in the development of the hot field. The early (late Jurassic-early Cretaceous) stage is noted for its intensive igneous and tectonic activity, resulting in the emplacement of numerous rift systems (including the Gobi-Altai and East Mongolian systems), infilled with essentially basic volcanic rocks with a ubiquitous phase of acid magmatism. The middle (late Cretaceous-early Cainozoic) stage saw a drastic reduction in activity, resulting in the formation of small, isolated scattered lava terrains. The late (late Cainozoic) stage, associated with the renewed activity of deep-seated mantle sources, was responsible for the formation of many lava plateaux, which can be found scattered throughout Central Asia.

8
ORE DEPOSITS AND METALLOGENY OF MONGOLIA

V.I.Kovalenko and V.V.Yarmolyuk

Mongolia is rich in mineral deposits, including iron ore, copper, polymetals, precious metals, and rare and rare-earth (RE) elements. The copper-molybdenum, RE and rare metals (Sn and W) have the greatest commercial value. This chapter describes the most economically viable deposits and presents a general overview of the metallogeny of Mongolia, including a wide range of endogenic ore deposits.

8.1 Copper-Molybdenum Deposits

The copper-molybdenum mineralization of Mongolia was developed over a long time interval (Middle and Late Palaeozoic, and early and late Mesozoic). It was mostly associated with subalkaline granitoids: monzonites, granosyenites, and leucogranites (Sotnikov *et al.,* 1985). The late Palaeozoic saw the most extensive mineralization. As discussed in previous chapters, at that time, the area of presentday Mongolia was developing as an active Andean-type continental margin, with widespread occurrences of copper-molybdenum mineralization. Three roughly parallel volcanic belts: the South, Central and North Mongolian belts were formed, at that time, along the continental margin. Numerous copper-molybdenum ore shows and deposits, including two of the largest ones—Erdenettwin-Obo and Tsagan-Suburga—are associated with the igneous rocks of these belts (Sotnikov *et al., 1985*).

The Erdenettuin-Obo deposit is located within an ore node of the same name, within the late Palaeozoic North Mongolian Volcanic Belt (Figs. 63 and 66). The ore node (Sotnikov *et al.,* 1985) is confined to the centre of the Orkhon-Selengin Trough, which is infilled by Permian volcanic beds of the differentiated and bimodal complex. These volcanic beds are intruded by granitoids of a Selengin Complex, which are dated as late Permian and early Triassic. The largest is the Erdenetsky Massif, which covers an area of about 1,500 km^2. It is made up of gabbro-diorites, diorites, and quartz-diorites, and by predominant equigranular and porphyritic granodiorites and plagiogranites. In a regional sense, the rocks of the massif can be regarded as the components of a gabbro-syenitic, granite-granosyenitic association (Matrenitsky, 1981).

The morphologically different porphyritic bodies: granodiorite- and plagiogranite-porphyries, quartz-dioritic porphyries, and the less-frequent granite- and granosyenite-porphyries, which at their endocontacts grade into dacitic and rhyolite-dacitic units, probably represent a separate group of intrusions. These bodies, which intrude the rocks

of the Erdenetsky Complex, are associated with mineralization. Pre-ore, intra-ore and post-ore porphyries of similar composition are distinguished according to their geological relationships. The porphyritic bodies decrease in volume, and the stocks give way to dykes here. As a whole, the porphyries show a high alkalinity, with a consistently high sodium content. The more recent post-ore porphyritic intrusions have been K-Ar dated at between 210 and 240 Ma (Sotnikov *et al.,* 1985).

The porphyritic rocks have been directly affected by hydrothermal alteration at the Erdenettwin-Obo deposit. The pre-ore porphyries were the most affected. The intra-ore porphyries are the best preserved. Post-ore porphyritic dykes are generally much more fresh.

The primary mineralization of the deposit is streaky-disseminated. It is concentrated mostly in stocks of porphyritic rocks, and in their nearest exocontact zones, forming an ore stockwork. Streaky-disseminated mineralization grades into streaky mineralization towards the periphery of the stockwork. Quartz streaks of irregular sinuous shape condense to form breccia ores in the central parts of the ore body, especially in the outer contact zone of the porphyritic stock. These ores occur at the sites of pre-ore explosive breccias (including the porphyries involved in the formation of the stock), and in the zones that show the most fracturing. The ore-bearing zone as a whole can be considered as a zone of intense pre-ore brecciation and fracturing, which is a suitable site for ore-metasomatic processes and concentrated ore deposition.

The deposit as a whole is characterized by irregular but continuous primary mineralization. The distribution of molybdenum is particularly heterogeneous. The concentrations of copper and molybdenum vary from 0.3 to 0.7% and from 0.008 to 0.026%, respectively; gold and silver occur associated with these metals; arsenic, bismuth, lead and zinc are ubiquitous (Khasin *et al.*, 1977). Copper and molybdenum do not always occur together. The concentrations of copper are observed to gradually decrease from the centre (0.4–0.5%) to the periphery (0.2–0.3% and even up to 0.07%) of the stockwork. Copper shows an insignificant vertical zonal distribution. In the centre of the deposit, primary ores with concentrations of copper of 0.4–0.5% persist down to a depth of 500 m. Molybdenum shows a reverse zonal distribution relative to copper: mineralization is richer (up to 0.02%) towards the margins and poorer (0.012%) towards the centre of the ore body. The average copper/molybdenum ratio is 20:1 in the primary ores.

Pyrite, chalcopyrite, and molybdenite dominate in the primary ores. The most widespread pyrite is almost always observed as disseminations in hydrothermally altered rocks and within the quartz streaks. Chalcopyrite forms thin disseminations, granular aggregates and small streak-like formations in the quartz and quartz-sericitic streaks and in altered rocks. The molybdenite usually occurs within the quartz streaks. Grey ore (containing silver, sphalerite, and galena) typical of the late polymetal mineral association occasionally occurs in these coppermolybdenum ores.

A characteristic feature of the deposit is a prominent zone of secondary sulphide concentration, up to 300 m and 60–90 m thick, in the centre and at the margins, respectively. This zone contains 86% of the ore reserves (Khasin *et al.,* 1977). Its upper boundary mirrors the present-day topography, and the lower boundary is highly dependent upon the degree of local tectonic activity. The zone may occur at depth along some zones of increased fracturing. Chalcosite and covellite are the main secondary

sulphide ore minerals. Bornite is much less frequent. The primary minerals: pyrite, chalcopyrite, and especially the more stable molybdenite are ubiquitous. The concentrations of copper and molybdenum in the secondary ores vary from 0.3 to 7.6% and 0.001 to 0.76%, respectively (Khasin *et al.*, 1971).

Along with the Erdenetsky ore body a number of additional ore-bearing areas have been discovered within the northern Mongolian volcanic belt (Sotnikov *et al.,* 1985). These areas are characterized by sites where hydrothermally altered rocks are developed, and by copper-bearing ore mineralization. However, they remain poorly studied, both geologically and commercially.

The Tsagan-Suburga deposit is located within the South Mongolian Volcanic Belt (Fig. 56) where numerous, and as yet poorly studied copper ore shows are also known (Sotnikov *et al.,* 1985). The Tsagan-Suburga deposit, which follows the intracontinental margin of the volcanic belt, is located within a block made up of Carboniferous volcanic-sedimentary beds and major intrusions. The rocks of the Tsagan-Suburgin Massif form the main part of the block. The massif is subcircular in plan view and occupies an area of about 90 km^2. It has been K-Ar dated as middle-late Carboniferous (Sotnikov *et al.,* 1985).

The massif is made up of syenite-diorites, adamellites, granosyenites, and granodiorites (Sotnikov *et al.,* 1985). All the rock units have similar mineral compositions, and contain mainly plagioclase (albite-oligoclase), orthoclase or nonperthitic microcline, hornblende, quartz, and scarce biotite.

Minor intrusive bodies are widely distributed within the deposit. Two types have been distinguished: is represented by pre-ore (or partly intra-ore) bodies of fine-grained leucocratic granites, granite- and granosyenite-porphyries, and aplites, associated with the ore-bearing igneous complex (Sotnikov *et al.,* 1985). These bodies are distributed mostly within the ore-bearing areas, where they form stocklike bodies, mainly subcircular in plan view and up to 0.1 km^2 in area, and also dykes ranging from several centimetres to up to 3–5 m thick and up to 120–150 m long. Most of these intrusions have been affected by explosive brecciation and post-magmatic processes (orthoclasization and silicification). These rocks cover a narrow age interval, ranging from 265±2 up to 270±4 Ma. The K-feldspar's metasomatites are of the same age (Sotnikov *et al.,* 1985).

Numerous dyke-like bodies of albitophyres, keratophyres, and syeniteporphyries, which are obviously later than the ores, form the other group of minor intrusions. These rocks are dated by the K-Ar age method as the Upper Permian (Sotnikov *et al.,* 1985).

The Tsagan-Suburga deposit (Fig. 94) is located at the north-western endocontact of the massif. The ore stockwork represents a combination of sites where

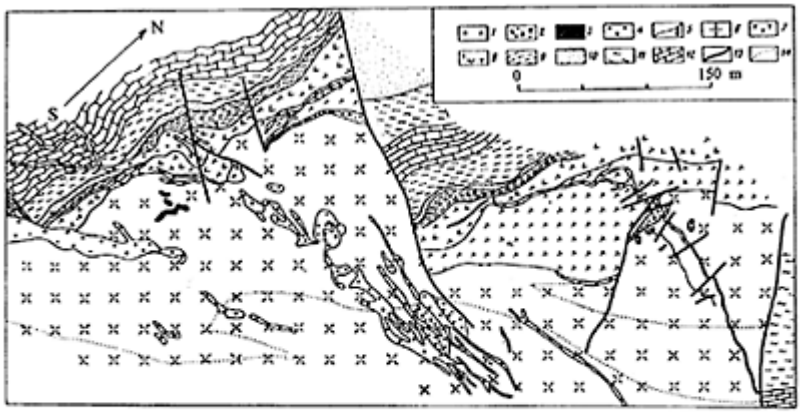

Key: 1—trachyte-porphyry, syenite-porphyry and keratophyre (P); 2—explosion breccia; 3—quartz bodies of irregular shape; 4—leucocratic granite, granosyenite, granosyenite-porphyry (metalliferous intrusive complex); 5 and 6—Tsagansuburgin intrusive complex: 5—diorite porphyry and gabbro-porphyry dikes, 6—syenite–diorite, granosyenite, and granodiorite; 7–12—volcanosedimentary formations (C_1): 7—tuff and sandstone, 8—vitroclastic andesite-porphyry tuff, 9—tuff, tuffstone, and tuffite, 10—sandstone, 11—siltstone, marl, and marl slate, 12—limestone; 13—faulting; 14—boundary of copper–molybdenum mineralization terrain.

Figure 94 Geologic structure of the Tsagan-Suburga deposit (XIII on Fig. 56).

quartz-sulphidic and quartz-sericite-sulphidic streaks of the striking NE-SW and NW-SE respectively. An ore-bearing zone, 1,600 m long and from 60 to ≤400 m wide generally follows the contact between the Tsagan-Suburgin granitoids and the Carboniferous volcanic-sedimentary rocks. The ore bodies that occur mainly in the upper parts of the ore-bearing zone are gradually replaced by poorly mineralized rocks at depths from 20 m down to 400 m. The streaky-disseminated mineralization gives way to disseminated mineralization, following the same trend.

Ore formation within the deposit was accompanied by orthoclasization, sericitization and mostly streaky silicification of the enclosing rocks. Sericitization and silicification zones are directly associated with the orebodies and are most typical of the inner parts of the ore-bearing zones. At greater depths, there are fewer quartz-sericitic streaks, and the mineralization becomes poorer and grades into the streaky-disseminated type, which occurs within variably orthoclasized granitoids.

The primary ores, containing 0.3–1.5% copper and 0.001–0.1% molybdenum, are most typical of the deposit. The most common ore minerals are chalcopyrite and pyrite, which occur as small, nest-like and streak-like formations in quartz, quartz-sericitic streaks, within sericitization zones, and as trace disseminations within orthoclasized rocks.

Commonly, thin-flaky molybdenite is concentrated in quartz veins and quartzsericitic streaks, where it is associated with chalcopyrite, and forms thin molybdenitic seams within the sericitized rocks. The disseminations of molybdenite are less frequent.

Galena, sphalerite and tennantite intergrown with chalcopyrite are occasionally encountered as secondary minerals within the primary ores. Rare late disseminations of galena and sphalerite, occasionally associated with cinnabar, are also found in the explosive breccias.

The main ore mineralization involves two distinct mineral associations: a quartz-molybdenitic association containing pyrite and a small amount of chalcopyrite (orthoclase and sericite have also been recorded) and a quartz-sericitepyrite-bornite-chalcopyritic association containing molybdenite (chlorite and carbonate) are met. The proportions of these minerals may differ at the various sites, but molybdenum within the former and copper within the latter association predominate. Insignificant amounts of chalcopyrite are recorded from the late quartz-pyritic, quartz-sericite-pyritic and sulphide-rich streaks, and galena and sphalerite also occur rarely as disseminations.

The other ore components are less typical of the deposit. The concentrations of zinc occasionally increase slightly towards the periphery of the deposit and within some of the ore shows. Generally, the combination of rare elements in the ores of the deposit is comparable with that of other copper-molybdenum deposits formed under similar geological conditions and with similar copper/molybdenum ratios (Sotnikov *et al.,* 1985).

8.2 Tin-Tungsten Mineralization in Mongolia

Endogenic tungsten and tin mineralization is the most typical type of mineralization in Mongolia and has been the best studied. It has also given rise to extensive placer shows. Most of the known tin-tungsten deposits and ore shows in Mongolia are described in: Khasin and Marinov (1977); Shcherbakov (1986); Sotnikov (1986); Obolensky (1986); and Kovalenko (1986).

Endogenic tin-tungsten mineralization is clearly associated with igneous rocks. This association controls the spatial and temporal distribution of mineralization throughout Mongolia. Most of the known, and all the commercial, shows of this mineralization were formed during two periods of igneous activity, in the Early Mesozoic and the Late Mesozoic. As has been mentioned above, igneous rocks occur mainly in East Mongolia, and it is there that nearly all of the Mongolian tintungsten mineralization is concentrated.

The tin-tungsten mineralization of Mongolia is very diverse, and includes hydrothermal and pegmatitic shows as well as skarns (Kovalenko and Yarmolyuk, 1995). The most commercially viable are hydrothermal deposits containing wolframite and quartz and cassiterite, wolframite and quartz. These ore types tend to grade into ore another. Tungsten predominates over tin, and the proportion of tungsten is higher in the first type of ore: the wolframite-quartz type. In both instances, the mineralization is associated with the granite-leucogranitic association and with lithium-fluoric granites. Therefore, the distribution pattern of this type of mineralization was mainly controlled by the outer zone of aurele of the Khentei batholith (zone of diffuse magmatism) in the early Mesozoic and by block faulting in the East Mongolian Volcanic Belt in the late Mesozoic.

The Modotin ore deposit is confined to the Modotin granitic massif, located near the western margin of the Khentei batholith (ⓐ on Fig. 76). A group of placer and primary deposits with combined tin-tungsten mineralization has been discovered within a

relatively small area (Khasin and Marinov, 1977). Its primary shows are concentrated within two sites: the Modotin site itself and also at Khuchzhikhan, 16 km away.

The Modotin Massif tapers in a north-westerly direction, and cuts across the strike of the surrounding Palaeozoic structures. Its area is about 500 km^2. The northern contact of the massif is steeply dipping and rectilinear. The southern contact dips more gently and is sinuous. The massif cuts across Upper Proterozoic metamorphic beds, Lower- and Upper Palaeozoic granitoids and Upper Permian marine deposits. The massif has been dated, using the K-Ar method as between 175 and 199 Ma (Upper Triassic-Lower Jurassic (Zaitsev (1971))).

The rocks of two intrusive phases are involved in the structure of the massif. The major phase is presented by medium- and coarse-grained, rarely porphyritic granites, which occupy more than 95% of the area of the massif. These granites show increasing amounts of biotite and scarce hornblendes at the endocontacts of the massif. Granites with a gneissoid structures have been observed within the north-western contact zone.

The granites of the major intrusive phase are cross-cut by dykes of finegrained, often pegmatoid, second-phase granites (the second phase is also known as the phase of extra intrusions): Zaitsev (1971). Biotite-bearing, two-mica and muscovitic granite units predominate among these intrusions. Dykes of second-phase granites are observed within both the massif and the enclosing rocks. They vary in thickness from tens of centimetres $\leq$ 10 m+, while their length along the strike is up to a few hundred metres.

Zones of greisenization make up the later formations of the Modotin Massif. Greisenization occurs within the coarse-grained granites of the main phase of intrusion and also in the fine-grained and pegmatoid granites of the second phase. The greisenized rocks form long, thin zones, striking in a similar direction to the granite dykes. These zones vary in thickness from several centimetres up to several metres thick, while their length is up to tens and even hundreds of metres.

The greisen bodies have a zonal structure, with the following pattern from the periphery to the centre:

1) granite;
2) two-mica or muscovitic granites;
3) greisenized granites;
4) quartz-muscovitic greisens;
5) quartz rocks (veins).

The rocks of all of these zones are cross-cut by very thin muscovitic streaks. Thin bodies of lamprophyres, which cross-cut the greisens, are very scarce within the massif.

The Modoto deposit is confined to the margin of the massif, characterized by widespread ore-bearing greisens and quartz veins. The latter are commonly accompanied by greisenization adjacent to the vein. Wolframite, cassiterite, arsenopyrite, chalcopyrite, galena, and sphalerite are developed within the greisens and quartz veins.

Wolframite, with a $MnWO_4$ content varying from 32 to 42%, forms thickcolumnar or thin-tabular crystals. Clusters of these crystals form nest-like accumulations (Khasin and Marinov, 1977). They are concentrated in both the centres and on the edges of the veins. In the thicker veins, wolframite occurs in much higher concentrations than cassiterite. Cassiterite is represented by euhedral crystals, from 0.1 mm to $\leq$1–2 cm in size. The cassiterite tends to occur on the edges of the quartz veins and streaks, and less frequently forms trace disseminations on the edges and in the centres of the veins. Generally,

cassiterite and wolframite do not occur adjacent to each other, but when they do occur together, their ratios indicate that they formed simultaneously.

At Bine-Mod, located west of the Modoto deposit, there is an unusual type of ore-bearing vein. The mineralization occurs as thin streaks of quartz and topaz, containing abundant disseminated cassiterite and occasionally fluorite and feldspar. The streaks vary in thickness from fractions of a millimetre up to 10 cm. They occur within both the granites and their roof rocks, and occasionally saturate them (this is a stockwork type of mineralization).

The *Baga-Gazryn deposit*, which is confined to the granitic massif of the same name, is represented by primary and placer ore shows.

The Baga-Gazryn granitic massif is located at the south-western end of the Khentei uplift, in the eastern part of the transition zone between the Khentei and Khangai mountain chains (ⓑ on Fig. 76). It occurs within Permian and probably Triassic basic and acid lavas and their tuffs inside sedimentary rocks. The massif was formed in the early Mesozoic. Potassium-argon dating gave an age of between 200 and 236 Ma (Zaitsev, 1971).

In plan, the massif is oval (Fig. 95) and has an E–W strike. The outcrop is about 120 km^2 in area. Judging from the strike of the contact surface, the massif is nearly dome shaped. The contact surface of the massif slopes gently from the north, west and south towards the country rocks, roughly concordant with their strike. The eastern contact of the massif is discordant relative to the country rocks.

The structure of the massif involves rocks of two intrusive phases. The central part of the massif (Fig. 95) is made up of coarse-grained, biotite-bearing Li-F granites, which belong to the main phase of intrusion.

The rocks of the second phase of intrusion form veined bodies confined to the gently dipping main-phase granite. These tend to occur within the endocontact zone of the massif, and also around the margins of the main-phase granites to the west, south, and east, and are represented by fine-grained Li-F granites containing biotite and topaz.

All these rocks are cross-cut by zwitters (biotite-bearing greisens containing topaz). These bodies have a distinct zonal structure involving:

1) biotite-bearing granites;
2) microcline granite;
3) biotite-bearing zwitter;
4) topaz zwitter;
5) quartz.

The zwitters are characterized by later streaks of lithium biotite or zinnwaldite, topaz, or occasionally by a mixture of topaz and mica. The late streaks, which contain mica, are common within the zone of biotite-bearing zwitters, and those without mica can also be found within the zone of quartz-topaz-bearing rocks. The streaks often contain rich cassiteritic mineralization.

The tin mineralization of the deposit is associated with thick (1 to 20 m) quartz-topaz-bearing zwitters, both veins and stocks, located within the endocontact zone of the granitic massif. Numerous quartz-topaz streaks are also recorded from within the sandstones/shales of the exocontact zone. The ore bodies consist mostly of quartz and topaz. Fluorite, beryl, cassiterite, wolframite, and molybdenite, are present in smaller

amounts. The exocontact zones where the streaks occur are richer in cassiterite compared with the veins and thus are of major interest to prospectors.

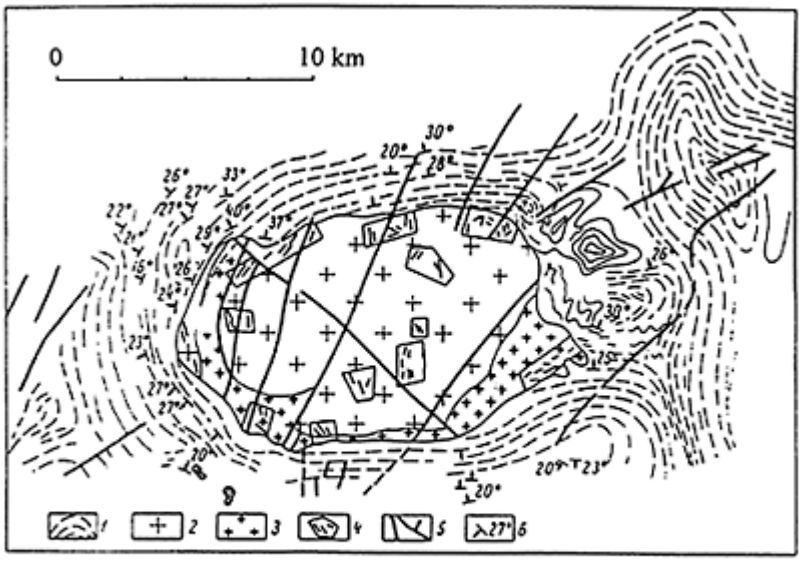

Key: 1—sandy–shale sequence interbedded with Permian effusive rocks; 2—coarse-grained topaz-bearing granites of the first main phase with a porphyry endocontact facies; 3—fine-grained topaz-bearing granites of the second, supplementary intrusion phase; 4—localities where biotite and quartz–topaz zwitters are found; 5—brecciation zone and fault; 6—dip.

Figure 95 Schematic geological map of the Baga-Gazryn Massif (ⓑ on Fig. 76).

The *Ikh-Khairkhan deposit* is located in central Mongolia (ⓐ on Fig. 82), within a structural zone of the western boundary of the Khentei Uplift. The deposit is associated with the granitic massif of the same name (Zaitsev, 1971). This oval-shaped massif is about 100 km^2 in area. The massif occurs within Upper Permian-Lower Triassic beds and is made up mainly of medium- and coarse-grained biotite-bearing leucogranites. They are cross-cut by veined bodies of fine-grained leucocratic biotite-bearing granites, represented by pegmatoid units. The massif is dated by the Rb-Sr age method as 121 Ma old (from unpublished data).

The Ikh-Khairkhan deposit contains mainly tungsten-type mineralization (Khasin and Marinov, 1977). Ore-bearing quartz veins were formed at the hydrothermal stage, preceded by a stage of granite greisenization.

The ore-bearing quartz veins are confined to the contact zone between the granites and the enclosing andesitic porphyries. As the quartz veins pass into the granites, the veins decrease markedly in thickness. The quartz veins infill fractures that roughly parallel the main fault zones and have north-westerly 300–340° and north-easterly 40–70° strikes.

The veins are steeply dipping, and average 0.65–3.25 m thick and 60–260 m long. The ore-bearing veins were recorded by prospecting boreholes down to a depth of 200 m. The wolframite is thought to be distributed as ore chute in the quartz veins as a whole.

The veins are made up mainly of an aggregate of quartz and wolframite. Orthoclase, muscovite, fluorite, sulphides (pyrite, chalcopyrite, and bismuthine) and very scarce cassiterite, beryl, and scheelite have also been recorded from the veins. The secondary minerals are hydrous ferric oxides, malachite, azurite, tungstite, and basobismuthine. The muscovite usually forms thin streaks within the quartz veins and the enclosing rocks.

The *Ongon-Khairkhan deposit* is located some 60 km north-west of the Ikh-Khairkhan deposit (ⓑ on Fig. 82), and as a whole shows similar characteristics.

The Ongon-Khairkhan Massif forms the geological setting for the deposit. Its area is about 200 km^2. The massif is made up of main-phase, medium-grained biotitic granites, fine-grained, second-phase granites, and the pegmatoid granites and pegmatites cross-cutting them (Figs. 96 and 98). This massif is similar in composition to the Ikh-Khairkhan Massif, and is probably similar in age.

The Ongon-Khairkhan deposit contains quartz veins with wolframite, which are concentrated near the eastern margin of the massif. The mineralization is cross-cut by dykes of topaz-bearing rhyolites (ongonites*) (Zaitsev and Tauson, 1971). They have been Rb-Sr dated as 121 Ma. Therefore the geological relationships observed within the Ongon-Khairkhan deposit indicate that magmatism and mineralization processes are coeval here. It should also be noted that the ongonites are cross-cut by thin quartz-mica-topaz streaks with wolframite, which form a stockwork within the enclosing Palaeozoic sedimentary rocks. The presence of minerals such as lithium mica, topaz and cassiterite

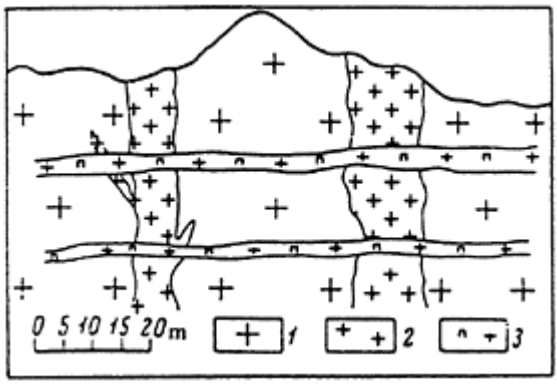

Figure 96 Relationship between the granites of the main intrusive phase (1) and the second, supplementary, phase of granite intrusion (2) and pegmatites and pegmatoid granites (3) in the Ongon-Khairkhan Massif.

distinguishes this type of mineralization from the pre-ongonitic type. In these terms, the mineralization of the

* Ongonites were first found in the Ongon-Khairkhan deposit and bear its name.

Ongon-Khairkhan deposit is believed to consist of two stages (Zaitsev and Tauson, 1971). The first is a quartz-wolframitic veined stage. It is associated with leucocratic granites, and is identical to the mineralization of the Ikh-Khairkhan deposit. The stockwork mineralization, which is combined wolframite-cassiteritic, with Li and Ta minerals was formed during the second phase of ore formation. We can draw a parallel between this type of mineralization and the stockwork, (mainly Sn) mineralization of the Baga-Gazryn deposit.

As evidenced by the above examples, most of the commercial tin and tungsten deposits of Mongolia contain a combination of these elements. Tungsten commonly predominates over tin in the ores; however, the concentrations of tin did increase during particular stages in the process of ore formation.

8.3 Rare-Earth Mineralization of Mongolia

The discovery of a number of large-scale deposits of rare-earth elements (REE) is one of the main achievements in practical geology of Mongolia over the last two decades. These deposits are associated with alkaline rocks of differing compositions which were formed during the continental rifting that sometimes occurred during Mongolia's geological history. The nature of the rifting phases, including their structural styles and igneous associations, has been described in detail above. Here we will draw attention to the fact that rare-earth deposits have been recorded in association with alkaline rocks from the middle Palaeozoic, late Palaeozoic and late Mesozoic rift zones.

In the Middle Palaeozoic, alkaline igneous associations, rich in rare-earth elements, appeared in north-western Mongolia, within a system of grabens bounding the Ozernaya (Lake) Zone of Caledonides. These associations consist of raremetal peralkaline granites, pantellerites, comendites, and albitic nepheline syenites (mariupolites), which occur over a huge area (Kovalenko and Yarmolyuk, 1995). They are characterized by increased concentrations of REE (up to 1%), plus Zr, Nb, Y, Be and Sn. However, these associations remain poorly studied in most cases—Khaldzan-Buregtey deposit being an exception (Kovalenko *et al.*, 1995).

The Khaldzan-Buregtey deposit is associated with a massif of peralkaline granitoids of the same name, which occurs within the Tsagan-Shibetin graben system. The geological structure of the massif involves the products of more than eight intrusive phases: nordmarkites, peralkaline granites, pantellerites, gabbroids, and leucitic basaltoids. The massif has already been described in this book (see Chapter 4). Here we would like to note that the rare-metal peralkaline granites of the fifth and seventh intrusive phases also contain ores (Table 38). They form domeshaped stocks about 0.85 km^2 in total area. The granites contain K-Na feldspar, quartz, albite, arfvedsonite, aegirine, fluorite, and rare-metal minerals, which make up to 25% of the volume of the rock. The Zr minerals are: elpidite, gittinsite, and zircon; Pyrochlore (which concentrates Nb); REE F-carbonates

and monazite all of which rare-earth elements; and polylithionite, which concentrates Li have all been identified. The concentrations of ore elements are (in mass %): up ≤5.3 Zr; ≤0.8 Nb; ≤0.4 REE; and ≤0.3 Y. The rocks are also enriched in Be, Sn, Rb, Li, Pb, Zn, Hf, and Ta. Data obtained on the volume of ore-bearing rocks and those of ore elements in the latter allow us to estimate the reserves of the deposit (Kovalenko *et al.,* 1995). They make 0.4×10^6 t, 1.2×10^6 t and 8×10^6 t for Nb, REE, and Zr, respectively.

The geological relationships between the rare-metal granites and the rocks of the other intrusive phases show that the former are igneous in nature. This is also evidenced by data obtained from the study of melt-inclusions in the quartz of raremetal granitoids, which indicate high concentrations of rare-metals and rare-earth elements in the melts that provided the source for these ore-bearing granites (Kovalenko *et al.,* 1995).

In the late Palaeozoic, alkali-granitic and comendite-pantelleritic associations were extremely widespread throughout Mongolia, due to the formation of the Late Palaeozoic Central Asian rift system (see Chapter 6). The rocks of these associations frequently show high concentrations of REE, Zr, and Nb, of possible economic value. Large-scale rare-metal mineralization has recently been established within the Khan-Bogdin peralkaline granite massif, which is the largest massif of its type in Mongolia (>1,000 km^2).

As has been mentioned above, *the Khan-Bogdin Massif is* made up mainly of massive, medium-grained one-feldspar arfvedsonite-aegirine granites. The massifs internal and external zones are separated by a ring structure, with its crest being associated with roof sag structures in the country rocks. The diverse ekerites, grorudites, peralkaline granite-porphyry, and pantellerite dykes and peralkaline granite pegmatites often contain rare-metal mineralization and are spatially associated with the crest of this ring structure (Kovalenko *et al.,* 1977). These rocks show relatively high concentrations of REE (up to 3–4.5%) (Table 39), niobium (≤0.3%), thorium (≤0.07%), zirconium (≤6.7%), and also increased concentrations of tantalum, hafnium, and lithium. Rare-earth elements are concentrated in REE F-carbonate, monazite, rare-earth sphene, a hydrous Mn-Fe rare-earth

Table 38 Compositions of rare-metal granites of the Khaldzan—Buregtey (main component in mass%; rare elements in ppm).

Sample	**4535/11**	**4538/1**	**4766/3**	**4322**	**4357**	**4321**	**4535/2**	**4535/9**	**4631/19**	**4631/21**	**4323**
n	**1**	**2**	**3**	**4**	**5**	**6**	**7**	**8**	**9**	**10**	**11**
SiO_2	71.97	70.30	68.60	71.10	70.00	74.30	63.48	69.47	68.00	72.80	72.00
TiO_2	0.29	0.39	0.34	0.34	0.17	0.45	0.24	0.31	0.35	0.45	0.23
Al_2O_3	10.40	9.36	10.26	10.20	10.98	10.40	5.54	9.80	11.07	10.60	11.40
Fe_2O_3	3.63	2.64	3.00	4.62	2.44	1.58	3.77	0.68	3.45	4.00	2.68
FeO	0.72	1.36	0.86	0.61	1.67	0.28	1.44	2.01	0.81	0.18	1.28
MnO	0.14	0.06	0.02	0.12	0.20	0.04	0.19	0.16	0.19	0.14	0.12
MgO	0.02	0.015	0.03	0.02	0.08	0.04	0.03	0.06	0.02	0.02	0.02
CaO	1.38	3.48	3.86	0.32	2.23	0.44	9.30	5.37	3.47	0.59	0.31
Na_2O	4.90	3.58	3.31	5.36	4.73	2.19	1.91	4.21	5.29	3.57	5.08
K_2O	4.28	3.78	3.95	4.19	4.16	5.63	4.93	3.61	4.29	4.27	4.76

P_2O_5	0.07	0.01	n.d.	n.d.	0.04	0.03	n.d.	0.03	n.d.	0.05	n.d.
F	0.75	2.08	1.99	0.28	0.58	0.92	3.54	2.38	1.43	0.39	0.19
H_2O^+	n.d.	0.01	0.63	0.47	0.54	0.30	0.12	n.d.	0.24	0.76	0.32
H_2O-	n.d.	0.56	0.63	0.66	0.48	1.02	0.33	n.d.	0.27	0.13	0.44
LOI	1.02	—	—	—	—	—	—	2.64	—	—	—
CO_2	0.01	n.d.	n.d.	n.d.	n.d.	n.d.	n.d.	0.65	n.d.	n.d.	n.d.
Total	99.58	97.625	97.48	98.29	98.30	97.62	94.82	101.38	98.88	97.95	98.83
Li	65	6.5	3	423	33	3158	29	42	6	6	130
Rb	402	446	379	314	274	593	416	264	346	459	348
Cs	1	0.6	0.7	2.4	0.3	1.4	1.2	n.d.	0.5	0.5	1.4
Zr	12,622	16,506	23,908	10,732	9,326	15,396	45,152	16,366	8,290	12,657	7,180
Nb	1,262	1,070	1,398	1,258	839	1,118	1,200	854	1,887	2,166	769
Y	1,093	1,207	1,612	1,392	1,022	793	233	339	1,562	1,317	929
REE	3,367	3,605	1,825	3,134	3,647	3,268	2,428	2,622	2,807	2,889	1,855

Note: 1–6—phase 5, 7–11—phase 7.

Table 39 REE content in rocks of the Khanbogdin Massif (after Kovalenko, 1977).

	1	2	3	4	5	6
La	64	657	2,400	9,400	487	2,900
Ce	138	1,280	4,450	1,300	577	3,700
Pr	12	203	953	1,900	53	560
Nd	58	687	1,933	5,700	303	1,700
Sm	19	203	308	1,000	80	370
Gd	15	177	230	5,200	109	240
Dy	17	237	148	450	131	210
Ho	2	47	26	79	33	33
Er	10	53	54	170	64	77
Yb	21	267	73	195	150	93
Y	63	733	918	2,500	593	1,200
(TR+Y)%	0.04	0.45	1.1	2.8	0.26	1.1
La/Yb	3	2.5	32.9	48.2	3.2	31.2

Note: 1—main-phase granites, 2–5—elpidite ekerites and pegmatites, 6—elpidite-armstrongiteic ekerite.

silicate, a hydrous REE-zirconium silicate, and a rare-earth silicophosphate (Vladykin *et al.*, 1981). The main Zr minerals are elpidite, zircon, and armstrongite, hydrous rare-earth-zirconium silicate and less-common secondary spherulites of zircon that developed within these minerals. Niobium is found in mongolite, pyrochlore, sphene, and in some silicates of as-yet unknown composition.

In the late Mesozoic riftogenic complexes, rare-metal alkali rocks were involved in near-surface volcanic-plutonic associations with rare-metal magnetite-apatite rocks and carbonatites (Samoilov and Kovalenko, 1983).

The *Mushugaikhuduk deposit* is the most conspicuous and has been the most studied. It is associated with Upper Jurassic alkali rocks that belong to the early evolutionary stage of the Gobi-Altai rift zone in the structure of the Upper Mesozoic-Cainozoic South Khangai volcanic area (hot-spot).

The volcanic rocks within the deposit were erupted in the following order: melanephelinites, melaleucitites, subalkali trachytes, trachydacites, trachyrhyodacites, and lastly trachyte-latites. The shonkinite porphyries that form the small stocks and dykes are the oldest of these intrusive rocks. The syenites and syeniteporphyries (including nepheline-and quartz-bearing types) are rather younger, and often contain subalkaline units (the geochemical analogues of the extrusive leucotrachytes). The Ore-bearing rocks were formed later than the syenites but before the cessation of igneous activity (Samoilov and Kovalenko, 1983; Samoilov *et al.*, 1988). The ores are represented by:

1) mineralized breccias;

2) rocks of the carbonatite series;

3) rocks rich in apatite (magnetite-apatite, phlogopite-apatite, and feldsparapatite).

The mineralized breccias, which are confined to zones of alkali-rock brecciation, including zones of eruptive breccias, and which form steeply dipping zones up to 1 km long and up to 300 m wide, are relatively widespread. Syenites and syenite-porphyries predominate in these breccias; the cement consists of carbonates, fluorite and silica. The mineralized breccia zones are commonly associated with occurrences of carbonatite-series rocks, characterized by vein-like bodies ≤1.5 m thick and ≤100 m long, which frequently form stockwork zones ≤80× 200 m in size. These rocks are represented by carbonatites (mostly calcitic) and rocks composed of variable compositions of fluorites, carbonates and silica minerals (Samoilov and Kovalenko, 1983).

Veins of magnetite-apatite rocks ≤3 m thick and ≤35 m long are also spatially associated with zones of mineralized breccias. The late-stage veins of the magnetite-fluorite-celestite-apatite rocks are locally observed as vein-like or lensshaped bodies up to 30×80 m in size.

Two of the main types of rare-earth ores have been found within the deposit: 1) carbonatitoid and 2) rare-metal-phosphatic ores. The ore types differ markedly in their compositions, their concentrations of economically valuable minerals and their paragenesis.

The carbonatitoid-type ores are represented by two closely related varieties, formed during a single process. These varieties are mineralized breccias and veined rocks of the carbonatite series, with the former being predominant. The breccias are cemented mostly by carbonate (up to 40–50%); significant amounts of fluorite (up to 20%); quartz and chalcedony (up to 25%); and frequently by baryte (up to 15%) and celestine (up to 10%). Bastnäsite (up to 10–15%), galena and anglesite can also form part of the cement. Variations in the composition of the cement are also responsible for the variable concentrations of commercial components, which make up 0.17–7.6 REE, 0.08–9.2 SrO, 0.01–8.6 BaO, and 0.01–1.1 PbO (mass %). This type of ore contains, on average, 1.1% REE_2O_3 with a peak in the concentration of light lanthanoids (Ce/Yb=31.2). The rare earths are concentrated in the bastnäsite, but also occur dispersed in the carbonates and fluorites.

The rocks of the carbonatite series are similar in mineral composition to the cement of the mineralized breccias. The rare earths contained in the rocks are found dispersed

mainly in the REE F-carbonate and fluorite. Their concentrations are commonly less than 1% REE_2O_3 (Samoilov *et al.*, 1988b).

Rare-earth-phosphatic ores can be divided into the following groups: magnetite-apatite, magnetite-fluorite-celestine-apatite (these usually tend to occur at localities where mineralized breccias are developed), and also apatite- and phlogopiteapatite, and feldspar-apatite (these show no association with the breccias).

These ores are on the average richer in REE, with concentrations varying between 2.3 and 13.9%. Apatite is the main concentrator of REE. Somewhat lower concentrations of light lanthanoids (Ce/Yb=23) are typical of these ores (Samoilov *et al.*, 1988b).

The examples presented demonstrate that the rare-earth mineralization associated with the alkali rocks of the continental rifts in Mongolia was formed over a wide age range. There are grounds for believing that this mineralization is quite widespread throughout the rift structures. This supposition is supported by the discovery of numerous shows of alkali rocks with high concentrations of REE and other incompatible elements (Kovalenko *et al.*, 1990b). However, special studies are needed to estimate their practical value. It should also be noted that, although we have considered these deposits to be REE-type, actually they are combined (REE-rare-metal) in all cases. Along with the REE, significant concentrations of Zr and Nb also occur in the alkali granites, and Sr, Ba, Pb and phosphorus occur in the alkali associations, with the carbonatites.

The examples of different types of mineralization considered here do not give a complete picture of the wide diversity of commercial mineral deposits in Mongolia; they simply describe the deposits of primary commercial interest. More information on the endogenic mineralization of Mongolia and its pattern of distribution is presented below in a review of the endogenic metallogeny in Mongolian continental structures. This is because most of the endogenic ore shows and deposits so far discovered are associated with these continental structures.

8.4 Metallogenic Zoning and Metallogenic Provinces at the Continental Stage of Crust Evolution

Data on the distribution of continental endogenic mineralization within Mongolia are summarized in the maps: *Metallogeny of the Mongolian People's Republic* and their attached explanatory notes (Kovalenko, 1986; Obolensky, 1986; Shcherbakov, 1986; Sotnikov, 1986) The associations between mineralization and certain types of igneous activity have been established from these maps, which have revealed the metallogenic belts and zones where the most important type of mineralization is concentrated. These metallogenic structures are shown on Figure 97.

All of the types of commercial minerals are grouped in Fig. 97 in the order of their most common metal(s). These groups include: 1) copper-molybdenum, 2) polymetallic, 3) rare-metal-REE, 4) fluoritic. The groups are arranged in the plot in order of their ages, in order to determine the metallogenic profiles of particular geological epochs. The following metallogenic epochs and their respective regions are as follows: Middle Palaeozoic, Late Palaeozoic, Early Mesozoic, and Late Mesozoic.

The Middle Palaeozoic metallogenic region consists of two belts: copperpolymetal and rare-metal-REE belts. The copper-polymetal belt coincides with a belt of cal-alkaline

and subalkaline rocks in the Mongolian Altai, and therefore is known as the Mongol-Altai belt. The polymetals are associated with both the subalkaline rocks and with rocks of normal alkalinity. Copper mineralization tends to occur in areas of subalkaline rocks.

Rare-metal-REE mineralization is associated with a zone of alkaline rocks within the inner part of the Devonian igneous region. The Khaldzan-Buregteg rare-metal-REE deposit considered above is located there. Tantalum, Nb, Zr, and

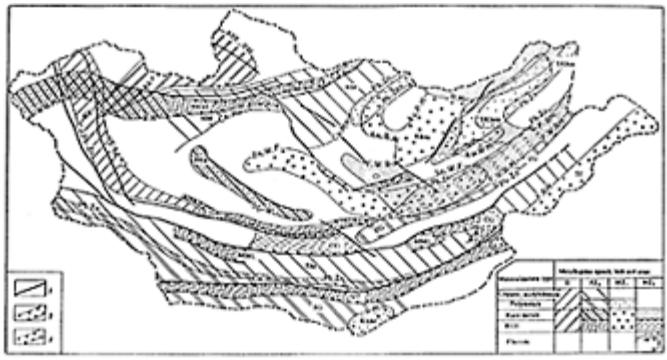

Key: 1—major structural boundaries: 2—Upper Palaeozoic rift zones; 3—Upper Mesozoic rift zones. Symbols on the boundaries of the metallogenic belts and zones indicate the important ores (RM—rare metals); Metallogenic zones and belts: Devonian (MA—Mongol-Altai copper-polymetallic, Kh-P—Khan-Khukhei-Prikhubsugul REE-rare metallic); Upper Palaeozoic (copper-molybdenum SM—South Mongolia, NM—North Mongolian; polymetallic—South Gobi, EG—East Gobi; rare-metal-REE—Gobi-Tien Shan, MML—Main Mongolian lineament, GA—Gobi-Altai, NG—North Gobi, NKhS—North Khangai-Selengin, BKh—Bayan-Khongor); Early Mesozoic (rare-metal—Khen-Khentei gold-rare-metal, P—Peripheral, SE—South-eastern, KhM—Khara-Moritin district, polymetallic—NKhen—North Khentei, SKhen—South Khentei); Upper Mesozoic (RM—rare-metal, I—Internal tin-tungsten; Cl—Closing tungsten; CG—Central Gobi rare-metal-REE).

Figure 97 Metallogenic zonation of structural complexes of the continental stage of evolution of Mongolia.

Li mineralization is known in the Prikhubsugulye area, where it occurs in association with the massifs of alkali nephelinic syenites. The alkaline rocks of the Khan-Khukhei Ridge contain potential rare-metal mineralization. Therefore this belt has been christened the Khan-Khukhei-Prikhubsugulian belt, from the main areas where the mineralization is located.

The Late Palaeozoic is the largest metallogenic region in Mongolia, and covers the whole of the country. The related metallogenic epoch was characterized by shows of copper-molybdenum and polymetal ores and also by rare-metal and REE mineralization.

Polymetal shows known from different areas of Mongolia primarily tend to occur in areas where cal-alkaline rocks are located. Two metallogenic belts, dominated by polymetal mineralization are prominent: the South Gobi and East Gobi belts. The South Gobi belt encompasses polymetal shows in the southern, Upper Paleozoic South Mongolian volcanic area, while the East Gobi belt represents a band of concentrated polymetal mineralization along the Central Mongolian volcanic area. In both instances the areas of mineralization coincide with those in which the alkaline rocks do not occur.

Unlike the polymetal type, copper-molybdenum mineralization tends to occur where subalkaline rocks are located. These rocks dominate the structure of the northern Mongolian volcanic area and are widely distributed in the northern part of the Southern

Mongolian volcanic area. Numerous shows of copper and molybdenum and some major deposits have been observed, associated with occurrences of these rock types in North and South Mongolia. South Mongolian and North Mongolian copper-molybdenum metallogenic belts have been distinguished on this basis. Areas of distribution of subalkaline rocks in the Central Mongolian volcanic area, for example those that are found directly north of the East Gobi polymetal belt are of particular interest for mineral exploration. However, we have no data on the copper-molybdenum metallogenic zone in this area.

As has been noted in Chapter 6, the Upper Palaeozoic igneous region was formed under complex geodynamic conditions, at a California-type active plate margin. Therefore, large rift-related zones, showing bimodal and alkali magmatism, are typical of this region. The largest of these are the Gobi-Tian Shan Zone, the Major Mongolian Lineament Zone, and the Gobi-Altai and North Gobi zones. REE-rare-metal mineralization is associated with the igneous rocks of these rift zones. Large ore shows have been confirmed in the Gobi-Tian Shan Zone (Khan-Bogdo, Lugin-Gol, and Khar-Khad), and in the Gobi-Altai Zone (Dzarta-Khuduk). The mineralization is associated with highly differentiated alkali granites and their extrusive analogues: the pantellerites and comendites. These rocks are widely distributed within all of the Upper Palaeozoic rift zones. Therefore the rift zones are shown in the plot as metallogenic belts with potential rare-metal-REE mineralization.

From the geological analysis, tungsten mineralization occurs at the extension of the rift zones, where they cut across rigid Precambrian structures. For example, Late Palaeozoic lithium-fluorine granites containing rare-metal (Ta, Li, Be, Sn, W) mineralization appear within the Ulan-Ul block of Precambrian basement, within the eastern extension of the Gobi-Tian Shan Zone, near Yugodzyr. In a similar way, tungsten mineralization is concentrated in NW Mongolia (Songino area), where the Precambrian block is cut by the North Mongolian rift zone. However, the type of magmatism responsible for the mineralization in this area remains unknown. Another area of Upper Palaeozoic tungsten mineralization, confined to the northern Mongolian Altai, has been observed in the same part of Mongolia. Within this area, ore shows are concentrated in a band striking ENE, cutting across the structural complexes of the Mongolian Altai. This band can be traced towards the western end of the North Mongolian rift zone, and appears to merge with the latter. On this basis, and since tungsten mineralization and potentially ore-bearing granitoids of standard and lithium-fluorine types are present at other localities within the North Mongolian rare-metal belt, we can assume that the tungsten shows of the northern Mongolian Altai belong to this belt.

Another area of distribution of Upper Palaeozoic rare-metal mineralization is associated with the SW boundary of the Bayan-Khongor Zone. Scattered shows of tungsten and tin have been recorded there. This metallogenic belt is probably similar in structure to other Late Palaeozoic rare-metal riftogenic belts. A narrow Late Palaeozoic marine trough, containing bimodal magmatism, which was formed during rifting, affected the whole of Mongolia in the late Palaeozoic, can be traced along the southern margin of the Bayan-Khongor Zone. Graniteleucogranite massifs containing rare-metal mineralization tend to occur within this trough. The position of this rift zone within the Pre-Riphean Bayan-Khongor block resembles that of the Gobi-Tian Shan Zone within the Ulan-Ul block. The rare-metal-tin-tungsten mineralization there is also similar. It should

also be noted that ore shows of Hg, Au, Ag, Sn, Be, U, and fluorite are fairly common within the zones of rare-metal-REE mineralization. They are associated with the acid igneous rocks of the rifts and therefore are representative of this type of zone.

The Lower Mesozoic metallogenic region clearly reflects the zonal structure of the magmatic region of the same age. Its core consists of the almost barren central zone of the Khentei batholith. The batholith's margins are saturated with numerous shows of gold, tungsten, and tin, with associated tantalum, beryllium and molybdenum mineralization. This mineralization is associated with leucogranites and lithium-fluorine granites. This area of ore shows is known as the Khentei goldrare-metal belt, and has a U-shaped structure.

The shows of polymetallic ores can be observed along the northern and southern margins of the Khentei belt. They are partly involved in the area of goldrare-metal mineralization and were controlled by igneous activity of similar composition. Areas of polymetallic mineralization may be divided into the external metallogenic zones (North and South Khentei) of the Khentei metallogenic belt.

The Khentei belt is bounded by the Peripheral metallogenic belt, which merges with a zone of highly alkaline granitoids and volcanics, which represents the margin of the Early Mesozoic igneous region. Some specific features of the Peripheral belt related to the increasing alkalinity of the magmatism are the increasing role of wolframite-quartz mineralization, the development of tantalum-bearing granites and shows of phenacite-fluorite-bertranditic mineralization and the formation of rare-metal-polymetallic skarns.

The South-eastern metallogenic belt, which coincides with a zone of isolated granite-leucogranitic massifs involving lithium-fluorine granites, is especially well developed in the Lower Mesozoic metallogenic region. These granites are associated with commercial tungsten mineralization, shows of tantalum-bearing granites, Sn-bearing zwitters, rare-metal skarns, and cassiterite-sulphide mineralization.

The Upper Mesozoic metallogenic region coincides spatially with the Upper Mesozoic igneous region. It is characterized by a predominance of tungsten over tin, its more widespread subvolcanic and rare-metal formations, including raremetal-REE, carbonatitic and fluoritic ones. Inner tin-tungsten, 'Peripheral', tungsten-fluoritic and Central Gobi rare-metal-REE belts can be distinguished within this metallogenic region.

The Inner tin-tungsten belt corresponds with a zone of 'diffuse' magmatism, most of which is located within the Transbaikalie area. Tin-tungsten mineralization is concentrated within this zone. The predominant ore-bearing rock type is leucocratic granite, and less frequently granodiorite-granitic intrusions and Li-F-type granitoids.

The Peripheral tungsten-fluorine belt is confined to the external periphery of the Upper Mesozoic eastern Mongolian volcanic belt, and its structural position is similar to the peripheral belt of the Lower Mesozoic metallogenic region. In detail their mineral deposits are also similar. In these belts, leucocratic granites, which are often associated with lithium-fluoric granites and ongonites, and bimodal volcanic associations, are also ore bearing. Tungsten and fluorine mineralization are the major types. Tantalum-bearing granites and ongonites are of particular interest.

The Central Gobi rare-metal-REE ore belt coincides with a zone of rift-related igneous associations (potassic alkaline lavas with carbonatites, bimodal associations with ongorhyolites etc.) which is confined to a fault zone of the Main Mongolian Lineament. Newly discovered rare-metal ore formations are concentrated within this ore belt. They

include: ongonitic volcanics, beryllium-bearing tuffs, rare-earth alkaline volcanic-plutonic rocks, including the Mushugai deposit, and the ore shows of Khotagor, Bayan-Khoshu, and Teg-Ula, etc.

Some typical patterns in the distribution of different types of mineralization, which are responsible for the distribution of metallogenic belts and zones within Mongolia and are thus important in assessing mineral reserves, can be inferred from the information presented:

1) The type of metallogenic zoning and the specific metals occurring in the belts and zones, are controlled primarily by the geodynamic conditions that led to the igneous activity (active Andean-type and California-type continental margins, continent-continent destructive margins).

2) The specific metallogenic conditions found in Andean-type active margins of Mongolia were controlled primarily by polymetallic and copper-molybdenum mineralization. Polymetallic mineralization within the igneous regions commonly occurred in zones where calcalkaline rocks were developed; copper-molybdenum shows are associated with subalkaline igneous rocks.

3) Rare-metal-rare-earth mineralization is associated with alkaline rocks, whose structural position was controlled by continental rift zones. These occurred under all of the types of condition that prevailed during the continental evolutionary stage of Mongolia. The rifts occur within inner zones of the igneous regions (Andean-type margin conditions), throughout the igneous regions, being concentrated along the margins of large dome-shaped uplifts such as the Khangai High (formed under complex, California-type conditions), and on the margins of the igneous regions (continental collision conditions). The metallogeny of the riftrelated magmatism remains poorly studied, but major ore shows have been found in association with alkaline igneous rocks from every metallogenic epoch. Therefore the rift zones thus distinguished may be considered as diagnostic for the rare-metal-REE belts.

4) The specific type of metallogeny associated with the continental-collision zones is mostly controlled by the rare-metal profile of the mineralization. Ore mineralization tends to follow the structural-facies boundaries within particular metallogenic regions. It is probable that the position of the relatively barren interior of the metallogenic region is influenced by the geometry of the large palingenic granitoid batholiths. The nearest boundaries of the batholiths, represented by belts of scattered, relatively small massifs, are characterized by mineralization of various types. As well as shows of rare metals, shows of gold and polymetals are also present. Peripheral metallogenic belts, merging with the contours of the igneous regions, are an important element of collision zones. It is precisely these belts where major shows of rare-metal and fluorite mineralization are recorded.

8.5 The Major Metallogenic Provinces of Mongolia

Metallogenic provinces are considered here as a combination of metallogenic belts of different ages and zones containing similar types of mineralization. It is necessary to map these provinces in order to study the main patterns of distribution of the mineralization, without taking into account its age. For example, polymetallic, copper-molybdenum,

rare-metal, REE and other metallogenic provinces were formed during the continental evolutionary stage of Mongolia (Fig. 98).

The Polymetallic Province brings together the polymetallic ore belts of the middle and late Palaeozoic, and is associated with geodynamic conditions active Andean-type continental margins. The province is limited by calcalkaline igneous rocks of normal alkalinity, which occur scattered within the marginal igneous belts. Polymetallic shows of Early Mesozoic North and South Khentei polymetallic zones, where mineralization is associated with igneous rocks of normal alkalinity, also appear to belong to this province. However, these zones also show combined polymetallic-rare-metal mineralization. Therefore these ore belts may also be included in the Rare-Metal Province (Fig. 98).

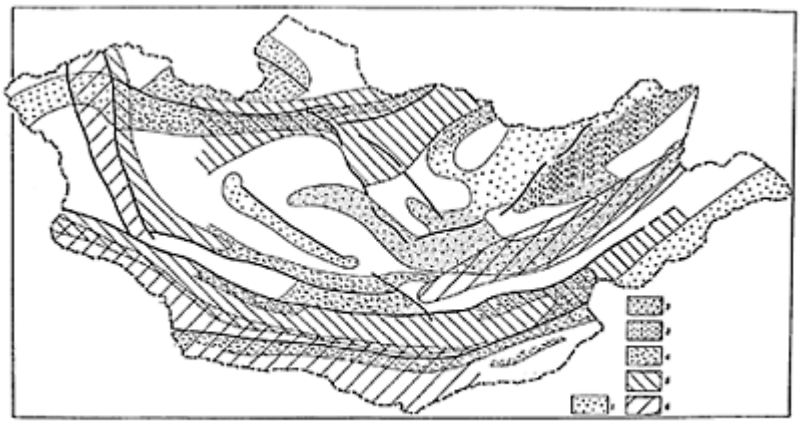

Key: 1–3—rare-metal (2—with fluorite, 3—with polymetallic mineralization); 4—REE; 5—copper–molybdenum; 6—polymetallic.

Figure 98 Metallogenic provinces of Mongolia.

The Copper-Molybdenum Province is associated with igneous complexes of active continental margins of the Middle and Late Palaeozoic. Mineralization is most common within areas of subalkaline igneous rocks. Within the zonal structures of the igneous regions within Andean-type active margins, copper-molybdenum belts and zones are displaced deep into the palaeocontinents relative to the poly-metallic belts and zones. However, there is no distinct boundary between these belts and zones, and the zones tend to mutually penetrate each other.

The Rare-Metal and Rare-Earth provinces show very similar ranges of commercially valuable minerals. The differences between them are caused mainly by the presence or absence of REE mineralization associated with the alkali magmatism of the rift zones.

Most of the Rare-Metal (Mo, Sn, W, Ta, Be, and Li, etc.) Province is located within the axial structure of the large-scale metallogenic region of Mongolia (Fig. 97). The location of the province is defined by its restriction to the periphery of the Mesozoic granitoid batholiths and the margin of the Late Palaeozoic metallogenic province (the zone of ‘dispersed’ magmatism).

The Rare-Earth Province overlies the Rare-Metal Province to the north and south. It is structurally associated with the major fault systems of Mongolia, which were active at virtually every evolutionary stage. At the continental stage, geological processes were often riftogenic and were accompanied by intense alkali magmatism, associated with REE mineralization.

In areas where rigid Precambrian cratons are cross-cut by rift zones, alkali magmatism gave way to granitoid magmatism, including lithium-fluorine granitoids, and rare metals were generated. From this description, a single rare-metal-REE province may be distinguished. The response of the superficial tectonic structures to sublithospheric activity influenced the type of mineralization and magmatism. Fragmentation and riftogenesis, with the intrusion of deep-seated magmas and their differentiation products occurred more easily within the fragile structural zones corresponding with the ancient lithospheric plate boundaries.

The Precambrian continental crust was probably thicker than the younger crust of the riftogenic structures. Therefore, in zones of Precambrian crust, melting penetrated the sialic crust under the same geothermal gradient, which resulted in intense granitoid magmatism, together with tin, tungsten, molybdenum, and rare-metal mineralization.

CONCLUSION: TECTONIC DEVELOPMENT AND GEODYNAMICS OF CENTRAL ASIA

S.V.Ruzhentsev, V.I.Kovalenko, A.B.Dergunov, and V.V.Yarmolyuk

As has been mentioned before, the Central Asiatic orogenic belt, including Mongolia, formed at the site of the palaeo-Asiatic ocean and oceanic basins of the Tethyan type. The ocean structures there are Late Riphean, Vendian-early Cambrian, late Cambrian-Early Ordovician, Ordovician, and Carboniferous in age. (Fig. 99). They are represented by rocks of ocean basins, island arcs, back-arc and interarc basins. Around the periphery of the Siberian continent and microcontinents of the Gondwana series, we can find fragments of complexes of continental margins of corresponding age. Palaeomagnetic and structural-geological reconstructions (Didenko *et al.,* 1994; Ruzhentsev and Mossakovsky, 1995) show that in the late Riphean, the palaeo-Asiatic ocean opened northwards. Being part of the palaeo-pacific, it was 3,000 to 4,000 km wide and was located between east Gondwanaland and Siberia (Fig. 100). Proto-Tethyan structures located between west Gondwanaland and Baltia (the Baltic Sea area) apparently joined the structure in the east (within present-day Central Asia).

The analysis of sections of microcontinents such as the Tuva-Mongolian, Dzabkhan, Central Mongolian, South Gobi, Sino-Korean, and Tarimian continents enables us to conclude that they formed part of east Gondwanaland and only became structurally separated after the Vendian. Therefore, for example, breakup of the Dzabkhan and South Gobi microcontinents took place in the Vendian, due to the formation of a system of rift troughs. The rocks that infill them are represented by volcanics (intraplate alkali basalts, rhyolites and terrigenous rocks, differing in composition and thickness. The above rock complex is transgressively overlain by terrigenous-carbonate deposits ($V–Є_1$) marking the passive margins of the massifs. Thus, the late Vendian was the time of opening of the Khantaishir palaeo-ocean (rift-drift transition) as reflected in the deposition of a synchronous ophiolite association. The Neimongol (Ondersum ophiolite suture), the Sibadzhi (Beinshan) and probably the Karatau-Baikonur (Kazakhstan) basins (Fig. 101) are ranked as similar structures. The authors relate the formation of the Vendian-Cambrian rift basins to the wedging of the proto-Tethyan (Riphean) structures into East Gondwanaland.

The palaeo-Asiatic ocean was also involved in the Vendian process of continental breakup. Its structure changed, as reflected in the emplacement of a complex microplate system. It was at that time that the West Sayan, Dzhidin, and Ozernya (Lake) basins were formed.

Thus, in Central Asia (including Mongolia) the joining of the paleo-Asiatic (Pacific) and Tethyan structures took place. Palaeomagnetic data (Didenko *et al.,*

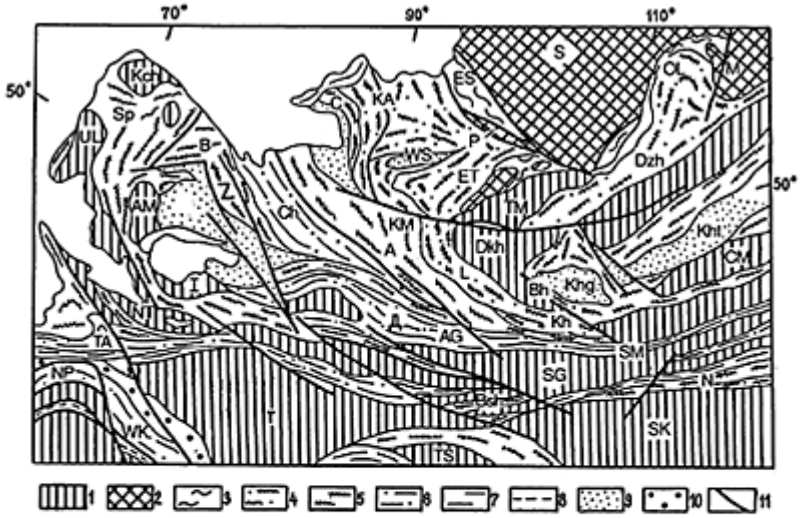

Key: 1—continental masses of Gondwanan (Katasian) type (AM—Aktau-Mountain, Dkh—Dzabkhan, I—Ili, Kch—Kokchetav, SK—Sino-Korean, NT—North Tien Shan, T—Tarim, TM—Tuva-Mongolian, Ul—Ulutau, Ts—Tsaidam, CM—Central Mongolian, SG—South Gobi); 2—Siberian-type continental massifs (M—Muya, P—Protero-Sayan, S—Siberian); 3–8—orogenic zone: 3—Baikal (ES—East Sayan, OL—Olokit), 4—Salair (Bh—Bayankhongor, ET—East Tuva; Dzh—Dzhidin, KA—Kuznetsk Alatau, L—lake (Ozernaya), Kh—Khantaishir), 5—Caledonian (A—Altai, B—Boshchekul, Bsh—Beishan, WS—West Sayan, N—Nejmongolian, Sp—Stepnyak, Ch—Chingiz), 6—Variscan (D—Dzungar, Z—Ob-Zaisan, WK—West Kunlun, NP—North Pamir, TA—Turkestan-Alai, SM—South Mongolian), 7—Indo-Sinian, 8—Kimmerian; 9—relic trough (P—Pribalkhash, Khg—Khangai, Kht—Khentei); 10—Predkunlun foredeep; 11—fault (AG—Altai-Gobi, Kh—Khankhukhei).

Figure 99 Tectonic map of the Central Asian orogenic belt (after Ruzhentsev and Mossakovsky, 1995).

1994) suggest that each age level was marked by an unusual, complex structural pattern, changing with time. For example, during the late Vendian-early Cambrian a system of basins formed at equatorial latitudes. Their north-eastern, northwestern, E-W and N-S orientation is of particular interest. Some basins (Khantaishir, Neimongol, and Karatau-Baikonur) opened south-westward to join the proto-Tethys, the others (Bayan-Khongor and Dzhidin) opened to the north and north-east, as paleo-Pacific structures. The structures were superimposed on each other, forming an orthogonal system of structural directions. In the author's opinion, their interference patterns gave rise to the mosaic structure of the region; this structure existed up to and including the Ordovician and is recorded in the Salairides and Caledonides of Central Asia.

Island-arc complexes are very common in the Salair and Caledonian zones of Central Asia. They form most of the accretionary edifices of the Siberian continent. These include the Ripheides of the Yenesei Range, Tuva, North and Central Mongolia, and the Caledonides of the West Sayan, Altai and Kazakhstan. Hence

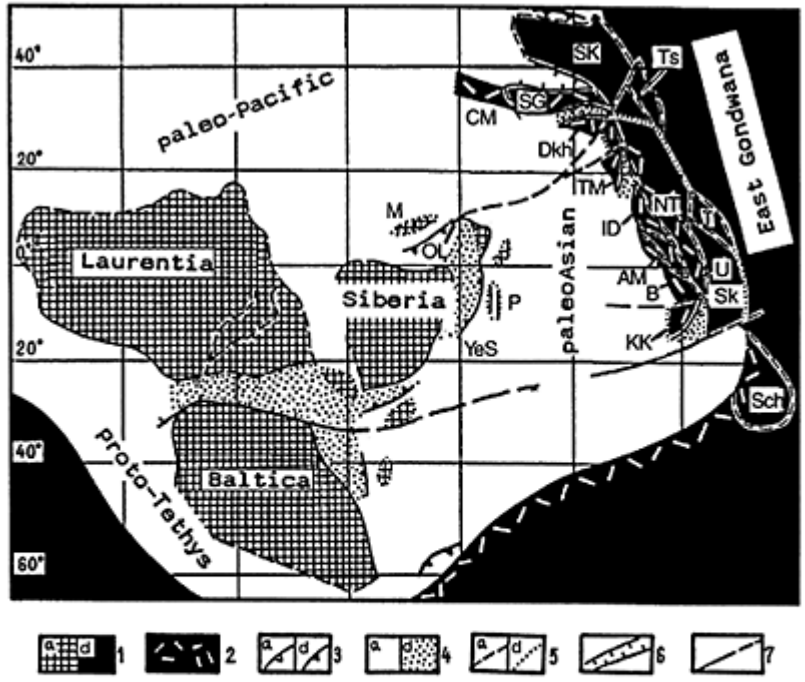

Key: 1—Riphean continents of the northern (a) and southern (b) series; 2—peri-Gondwana volcanic belt; 3—island arc: active (a), extinct (b); 4—basins underlain by oceanic crust (a) and transitional-type crust (b); 5—boundaries of blocks within young complexes (a) the same for inferred boundaries; 6—riftogenic trough; 7—transform fault and wrench fault; Symbols on the diagram: microcontinent: (AM—Aktau-Mountain, B—Boshchekul, Dkh—Dzabkhan, ID—Ilii-Dzhungar, KK—Kulundin-Kokchedav, M—Muya, P—protero-Sayan, Sk—Syr Darya-Karakum, SK—Sino-Korean, NT—northern Tien Shan, T—Tarim, TM—Tuva-Mongolian, Ts—Tibet-Tsaidam, U—Ulutau, CM—Central Mongolian, SG—South Gobi, SCh—South Chinese island arc (YeS—Yenesei-Sayan, Ol—Olokit).

Figure 100 Palaeotectonic reconstruction of Central Asia for the late Riphean (after Didenko *et al.*, 1994).

spatial-temporal groups of island arcs can be recognized. The former contains numerous Salairide island arcs. In Mongolia, these are the Khantaishir, Ulanshandin, Khan-Khukhei, and other arcs. Their formation goes back as far as the Vendian/Cambrian boundary or to the Early Cambrian, and they had disappeared by the middle Cambrian (10–20 Ma). The Salair system contained the maximum number of microcontinents, which led to the wedging out of the subduction zones and the rapid cessation of subduction. On the other hand, the second group, which is similar to the former in its time of emplacement, developed until the late Ordovician and even the Silurian. In Caledonian times, accretion took place over a period of 100–140 Ma and was associated with the inner part of the palaeo-ocean, which contained no microcontinents.

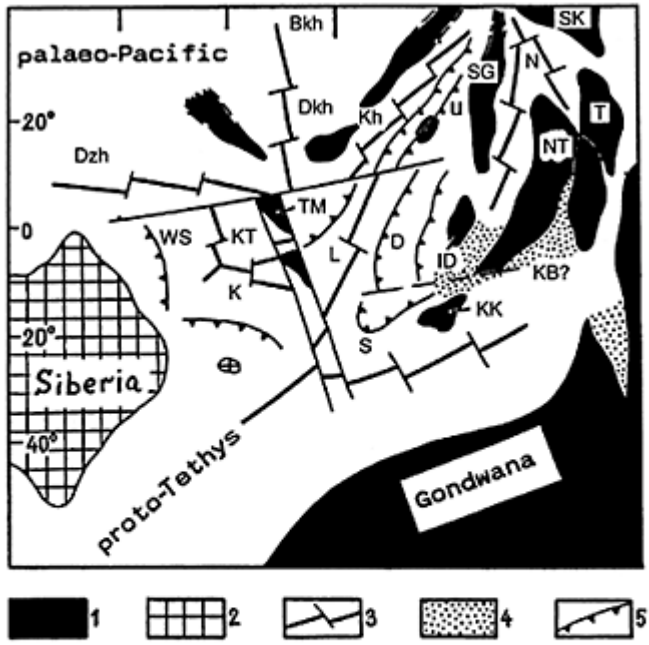

Key: 1 and 2—continent (1—Gondwana and 2—Siberian-type); 3—inferred spreading zone, 4—destructive basin underlain by transitional crust, 5—island arc; Symbols on the schematic diagram: microcontinent (Dkh—Dzabkhan, KK—Kulundin-Karakum, SK—Sino-Korean, NT—North Tien Shan, T—Tarim, TM—Tuva-Mongolian, SG—South Gobi); Palaeo-ocean basin (Bkh—Bayankhongor, Dzh—Dzhidin, KB—Karatau-Baikonur, KT—Kurtushubin, N—Neimongol, L—Lake (Ozernaya), Kh—Khantaishir; island arc DKh—Daribi-Kharkhirin, WS—West Sayan, K—Kurai, S—Seletin U—Ulanshandin).

Figure 101 Palaeotectonic reconstruction of Central Asia for the late Vendian-early Cambrian (after Ruzhentsev and Mossakovsky, 1995).

The destruction of the palaeo-Asiatic ocean took place in the late Ordovician. An extensive Caledonian accretionary structure, including relict basins underlain by suboceanic crust (West Sayan, Pribalkhash, and Khangai-Khantei) formed there. During the Silurian a thin carbonate-terrigenous cover began to form on the Caledonian basement.

The late Ordovician was not only the time of closure of the palaeo-Asiatic ocean, but also the time of the appearance of the first new generation of destructive basins. In Mongolia, they can be equated with the Late Caledonides of the Gobi-Altai (D_1–C_1), and the Indo-Sinides of Inner Mongolia (C_1–T_1). The tectonic development of these structures fits in with the normal Wilson cycle, and their formation is associated with the breakup of the Siberian Caledonian continent and Katasia. The Variscan basins of Dzungaria and South Mongolia, and the Turkestan Basin of Central Asia (located farther west) are

identified by the authors as a single system of palaeo-oceanic basins, or palaeo-Tethys I, and, respectively, the Indosinian palaeo-ocean of Inner Mongolia, which belong to a system of basins of palaeo-Tethys II.

The pattern of development of the structures discussed here is fairly conventional. Rifting of the Caledonian continent gave way to ocean opening. In South Mongolia, since the late early Devonian, and in Inner Mongolia since the middle Carboniferous, ensimatic island-arc and back-arc complexes have been formed. Concurrently, an ensialic volcanic belt (an active continental margin of Andean type) formed around the periphery of the continental masses bounding the basins. The superimposition of the process of continental collision slightly complicated the pattern. Convergence and the emergence of continental blocks resulted in the appearance of a basin on structurally complex accretionary basement. This basin was infilled with greywackes. A transzonal cover was also deposited. Tectonically, it is a neoautochthon, reflecting the contact of the opposite continental margin with an accretionary prism and the disappearance of the ocean basin. The late stage of continental collision is marked by the closure of the greywacke basin, accompanied by the emplacement of a nappe-fold structure.

All of the above-mentioned basins had an asymmetric structure. Active and passive continental margins can be recognized along their northern and southern parts, respectively (according to present-day co-ordinates), reflecting the absolute plate displacement towards the Siberian continent. Integration of Gondwanaland and its Katasian massifs took place, as well as separation of a series of microcontinents, their drift and accretion at the expense of Siberia, and, since the late Palaeozoic, at the expense of Eurasia. The opening of each southern basin was accompanied by the closure of the contiguous northern basin. Such a pattern is in good agreement with the mode of development of the Iapetus, and Lizherian palaeo-oceans. In a broad sense it can also be applied to the Kimmerian (Yanshim) and Alpine basins of the meso- and neo-Tethys.

The emplacement of large masses of continental crust was another important event occurring at the Silurian-Devonian boundary; it resulted in the appearance of the Kazakhstan and Katasia Devonian continents and an increase in the size of the Siberian continent. The formation of a new generation of palaeo-oceans and new large continental masses are related phenomena: the rapid development of the first tectonic deformations, the sudden activation of metamorphic processes, and the emplacement of granites. All of these gave rise to the accretion of a granite-metamorphic layer, its homogenization, and also to synchronous intracontinental igneous activity.

The process of continental-crust formation within Mongolia is quite specific, and therefore it will be discussed in detail.

One of the principal hypotheses elaborated upon in this book is not just confined to the multistage formation of continental crust in this area, but also deals with the various modes of formation or processes of transformation of basic mantle material into sialic continental crust; the involvement of synchronous compression and tension in the processes responsible for the formation of continental crust and the tectonic reworking of existing crust. The area of the Mongol Popular Republic was used as an example to construct a specific Mongol—Okhotsk collision model of the formation and reworking of the continental crust, similar to the present-day geodynamic environment of California.

One should distinguish between the continental crust in the pre-Riphean blocks and that in the Palaeozoic fold systems of Mongolia. The continental crust as a sialic product

in the pre-Riphean crystalline-basement blocks of Mongolia was emplaced no later than the Late Archaean. If we use just a few isotopic dates for the Precambrian rocks of Mongolia we can suggest that at 2 Ga (late Early Proterozoic) the continental crust in these Precambrian blocks was fairly mature. Based on the data of F.P.Mitrofanov *et al.*, the maturity of this crust can be inferred not only from the extensive development of normal calcalkaline granitoids, but also from the replacement of relatively plastic, apparently warmed, ancient crust, by more rigid, thicker and colder crust prior to its breakup in the Riphean. According to Mitrofanov *et al.*, starting at approximately 2 Ga, the destruction of continental crust becomes of greater importance, as evidenced by belts of basic dykes. The emplacement of anorthosite massifs of *c.*1.7 Ga in age may also indicate the maturity of the continental crust at that time. The above-mentioned dyke belts might very well indicate the presence of embryonic greenstone belts, which are very common in the more rigid shield structures.

The generation of continental crust, in fact the whole of northern Mongolia (the Northern megablock), separated from the Southern megablock by the Main Mongolian lineament, took place at the Silurian/Devonian boundary. For most of the Southern megablock, this process had ceased by the earlier late Palaeozoic, and, for the Solonker Zone, in the late Permian or in the early Triassic.

Magmatism of the transitional stage in the Ozernaya Zone during the early Palaeozoic is very similar to that of a mature island-arc environment and continental margins containing belts of batholith-like granitoids. The characteristic early Palaeozoic igneous associations mark a complete cessation of tensional processes within the former basins at the site of ophiolites, even within the marginal seas, and their replacement by compressional environments. At the Silurian/Devonian boundary, the continental stage, with its characteristic features, was initiated over the entire area of the Northern megablock. In terms of magmatism, the initial stage was marked by the intrusion of huge masses of granites and granodiorites. This was apparently the termination of the first complete cycle of continentalcrust formation in the area of Mongolia which led to the accretion of the Northern megablock to the Siberian palaeocontinent. It should be noted that destruction of continental crust took place at that time in the northern part of the Devonian volcanoplutonic belt. This process was accompanied by the development of alkali basic and sialic bimodal magmatism. The crustal destruction was caused by sublithospheric intraplate processes. The regular back-arc position of the destructive margin (continental rifting) within the Devonian volcanoplutonic belt implies that the processes responsible for the formation and destruction of the mature continental crust operated together, as in the case of active Andean-type continental margins at the present day.

The second (Hercynian) cycle resulted in the destruction of almost the entire Southern megablock. However, there is no evidence for the formation of continental crust during the Precambrian and Caledonian cycles, at least in the area of the southern megablock. The involvement of extensive areas where folding had ceased, in the tectonomagmatic activity (different researchers consider it as either an orogenic or an activation process) led to the formation of zoned tectonomagmatic areas, whose zones were at different stages of crustal evolution.

Unlike earlier epochs, the late Palaeozoic was characterized by a system of zones of continental-crust destruction in the Northern megablock, as reflected in the development

of a series of linear zones of continental rifting and bimodal magmatism. These processes took place on an active Californian-type continental margin, when the spreading zone of the Hercynian palaeo-ocean (palaeo-Tethys I) was overlapped by the Asian plate. Concurrently, typical granitoid batholiths (Khangai), equivalent to American batholiths, were formed nearby. The formation of the complex Mongol-Okhotsk collision belt took place concomitantly.

The continuing movement of the continental plates led to the closure of the late Palaeozoic palaeo-Tethys I and finally resulted in the assembly of the continental blocks. The closure of palaeo-Tethys I took place by the subduction of the oceanic plate under the Asian continent. The spreading system of palaeo-Tethys I was also involved in the subduction zone. The formation of a collision belt started with the collision of the spreading system with an active continental margin (Californiatype environment). The collision of the continental plates is the second important integral part of the Mongol-Okhotsk type of environment. The joint action of these two processes determined the specific geodynamic environment of the Mongol-Okhotsk belt.

Thus the California-type environment led to the splitting of a continental plate along zones of weakness in areas that had not yet entered the continental collision environment. Splitting was in fact a large-scale separation, followed by the formation of a marine trough (of Gulf of California type) within the Mongol-Okhotsk lineament zone, as early as in the later late Palaeozoic.

The ongoing convergence of the continents led to subsequent closure of the marine trough. Igneous activity was most prevalent where the continental blocks were brought close together, thus creating the joint effect of subduction, collision (especially in connection with the closure of intracontinental marine troughs), and spreading processes in a relatively small part of the continental lithosphere. This joint action of differently oriented forces could explain the appearance of a large number of microplates showing the features of spreading and subduction magmatism in collision zones.

The formation of continental crust within the late Hercynian Solonker Zone encompassed the whole of the third cycle. The magmatism of the oceanic and transitional stages occurred within the zone itself. The synchronous magmatism of the Northern megablock was typically continental and was characterized by marginal igneous belts, arched uplifts, and intense granitoid magmatism. Other indicators of the continental stage include the bimodal basalt-comendite-alkali-granite magmatism of the continental rift structures, which was very common in the late Palaeozoic and which in time replaced the calcalkaline series of the marginal igneous belts. This cycle terminated continental-crust formation in Mongolia. Tectonomagmatic reworking of this crust took place during the Mesozoic, and was caused by collision processes of Mongol-Okhotsk type, which have occurred in the early Mesozoic since the later late Palaeozoic, together with intense intraplate hot-spot magmatism. As it is similar to late Palaeozoic collision magmatism, it exhibits features transitional with late Mesozoic intraplate environments. The early Mesozoic intraplate magmatism was recorded in the western part of the country, in the form of isolated volcanic fields, small granitoid massifs, and belts of dikes.

During the late Mesozoic-Cainozoic, intraplate magmatism predominated throughout Mongolia, and developed mainly under a continental regime. The late Cretaceous-Palaeogene was characterized by the platform stage, interrupted in areas of hot-spot activity and in zones where microplates were formed by the collision of Asia with India.

The most extensive collision belt of Central Asia had been formed by that time (at about 30–35 Ma ago). The high ridges of the Altai, the arched uplifts of the Khangai, the numerous seismically active faults, and rift grabens, all appeared in the eastern part of the belt. In this area, mainly basalt, or locally ongorhyolite and rhyolite hot-spot magmatism was concentrated. The latter controlled the formation of many microplates within Mongolia. In particular, the N-S band of Cainozoic grabens and basalt lava fields, extending from Lake Khubsugul southwards was controlled by the South Baikal and Khangai hotspots, where triple junctions were formed; the hot-spots were separated by the active boundary of the largest Amur microplate—a seismically active zone. There is also another, the Darigan, hot-spot within Mongolia.

The hot-spots of Mongolia form part of a giant geothermal field tapping into the lower mantle of Central Asia, which thus is responsible for the relatively synchronous activity of the individual hot-spots.

On the whole, within Mongolia a distinct geodynamic trend can be detected although some of the geodynamic environments are superimposed on each other. However, the importance of the intraplate environments has increased during the Mesozoic and especially in the Cainozoic.

Thus, two trends: Pacific and Tethyan, can be recognized in the tectonic development of Mongolia. The combination of the two led to its extremely complex Phanerozoic geodynamics. The following stages of the process can be recognized:

1) Riphean—the existence of a single extensive palaeo-Asiatic ocean (southern palaeo-Pacific) and the formation of the proto-Tethys

2) Vendian-early Cambrian—the powerful destruction, and penetration of the Tethyan structures into East Gondwanaland and into the paleo-Asiatic ocean, and the formation of a mosaic-like structural framework that reflected the interference pattern of Pacific and Tethyan trends.

3) Cambrian-Ordovician—the formation of accretionary systems around the periphery of the Siberian continent (the Pacific trend was the predominant process). There are two sets of this type of structure: the Siberian (the Ripheides, Salairides, and Caledonides), and Kazakhstanian (Caledonides). The accretionary structures of Mongolia make up the southern part of the former.

4) Late Ordovician-Triassic. The Tethyan trend was dominant. The Caledonian accretionary structures had mainly formed by that time. Since the late Ordovician (actually mainly since the early Devonian) an extensive system of short-lived (up to 80 Ma) rift basins (Dzungar-South Mongolian, and Inner Mongolian) was formed, whose closure resulted in the formation of the collision belts that make up the Siberian continent. During the late Palaeozoic, the Dzargalantuin Trough was emplaced in the Khentei area. Intense reworking of the old and newly formed crust, followed by the formation of powerful and extensive zones of continental rifting and conjugate collision zones was caused by tectonic movements within the basins and lasted over the entire time interval.

5) Mesozoic-Cainozoic. The entire area developed under continental conditions. The superposition of collisional and interplate geodynamic environments was also characteristic of the Mesozoic and the Cainozoic. The participation of hot-spots in the formation of microplates is an ongoing process.

6) The most important types of mineralization in Mongolia (copper-molybdenum, rare metals, REE, polymetals, and fluorite) are genetically related to the continental stage of development in the area, starting from the Middle Palaeozoic. The specific metallogeny of the area is determined by a combination of geodynamic environments of differing ages and their distinctive magmatism.

Concluding our data, we would like to note that the geological study of Mongolia is still in progress. Let us recall the most important results obtained by the team of the Joint Russian—Mongolian Geological Expedition and included in this monograph.

The comprehensive geochronological and isotopic geochemical study of magmatic and metamorphic rocks led us to the very important conclusions. The ophiolite complexes of the Ozernaya and Dzhida zones were dated by Sm-Nd method at 522–527 Ma (Kovalenko *et al.,* 1996b). The source of ophiolites was confined to depleted mantle (εNd~8)

The new basic data were obtained on the Precambrian evolution of the geologic structures of Mongolia. We demonstrated that the Early Precambrian rocks are low abundant in the region. The Archean (2.6–3.3 Ga) and Early Proterozoic (1.8–2.5 Ga) rocks are revealed only in the Baidarik Block (Kozakov *et al.,* 1997). The most of the Precambrian microcontinents are generally composed of metamorphic complexes with the Cambrian age of metamorphic transformations. For example, the metamorphic events in the rocks of the Tuva-Mongolia microcontinent were dated by U-Pb method on zircon at 507–536 Ma (Kozakov *et al.,* 1999). Meanwhile, the age of the detrital zircon from metaterrigenous rocks varies from 750 to 900 Ma and traces the earliest sedimentation events.

Based on the systematics of Nd isotope compositions and isotopic model ages of Nd in the crustal protoliths of granitoids, we estimated the age of the crustgenerating processes in various structural zones of Mongolia (Kovalenko *et al.,* 1996a, 1999). The following isotopic provinces with distinct model ages of crustal sources of granitoids are distinguished: Caledonian (700–950 Ma), Hercynian (550–700 Ma), and Mesozoic (300–360 Ma). These provinces structurally coincide with corresponding foldbelts. The isotopic model ages of Nd of granitic protoliths from the Precambrian microcontinents vary within the interval of 1100–1600 Ma (Yarmolyuk *et al.,* 1999b) and indicate an absence of pre-Riphean protoliths in the structure of these microcontinents. In view of geological data (Kozakov *et al.,* 1999), we concluded that the Riphean epoch of crust-generating processes was very important in formation of the geologic structure of Mongolia (Yarmolyuk *et al.,* 1999b).

Our new data also demonstrated the multiple occurrence of the within-plate magmatic processes in the Phanerozoic evolution of Mongolia (Kovalenko *et al.,* 1999, Yarmolyuk *et al.,* 1996, 1999a, 2000). We concluded that the magmatic events of different ages (including those related to subduction at the plate boundaries) were preceded, associated with, and terminated by the within-plate (alkaline, bimodal, and alkaline basaltic) magmatism. We believe that this specific feature in the magmatic evolution of the region is caused by the following scenario. After the separation of Rodinia, the Siberian continent drifted north and underwent the influence of the North Asian hot superplume (Kovalenko *et al.,* 1999, Yarmolyuk *et al.,* 2000). The subsequent Phanerozoic evolution of the continent, particularly along its Central Asian active margin (including Mongolia)

proceeded under the continuous effect of the superplume periodically initiating magmatic activity.

This work was carried out with the financial aid of the Russian Foundation for Basic Researches under projects 99-05-65645, 99-05-65647 and 00-15-985600 and Russian State Programs ‘Global Change of Environment and Climate’ (project 2) and Russian scientific schools support.

REFERENCES

Alekseeva, R.E. (1993) *Biostratigrafiya Devona Mongolii (Biostratigraphy of Devonian of Mongolia)* , 132 pp., Moscow: Nauka (in Russian).

Amantov, V.A. (1963) *Osnovnye cherty stratigrafii i usloviya obrazovaniya Kembriiskikh otlozlienii Severo-Zapodnoi Mongolii* (The essential features of stratigraphy of the Cambrian depositions of North-West Mongolia) *Procerdings on Geology of MPR. 1963* , pp. 15–28, Moscow: Gostopotekhizdat (in Russian).

Amantov, V.A. and Matrosov P.S. (1961) *Osnovnye cherty geotectonicheskogo razvitiya i razmesheniya structur Mongolii* (The essential features of geotectonical development and position of the structures of Mongolia) *Transaction VSEGEJNS* **58 ,** 183–205, Leningrad: Nauka (in Russian).

Baikova, V.S. and Amelin, Yu.V. (1994) *Doklady AN SSSR* , **334**(3), 343–5 (in Russian).

Baikova, V.S., Kazakov, I.K. and Krylov, I.N. (1992) *Izvestiya RAN, Ser. Geol.* , **4 ,** 42–51 (in Russian).

Belichenko, V.G. and Boos, R.G. (1990) *Geologiya i Geofizika* , **11 ,** 3–9 (in Russian).

Belichenko, V.G., Sklyarov, E.N., Dobretsov, N.L. and Tomurtogoo, O. (1994) *Geologiya i Geofizika* , **7–8 ,** p. 29 (in Russian).

Berzin, N.A. (1995) Tectonics of South Siberia and horizontal movements of continental crust. *ScD Thesis* , OIGGIM, Siberian Branch, Russian Academy of Sciences, Russian (in Russian).

Berzin, N.A., Kolman, R.G., Dobretsov, N.L., Zonenshain, L.P., Syao Syuchan, and Chang, E.Z. (1994) *Geologiya i Geofizika* , **7–8 ,** 8–28 (in Russian).

Bezzubtsev V.V. (1963) O stratigrafii kembriya u dokembriya MNR. (About stratigrapy of Cambrian and Precambrian MPR) *Proceedings on Geology MPR* . Moscow: Nedra, pp. 29–42 (in Russian).

Bibikova, E.V., Grachyeva, T.V. and Kozakov, I.K. *et al.* (1989) *Geologiya i Geokhronologiya Sibirskoi Platformy (Geology and Geochronology of the Siberian Platform)* , pp. 94–7, Leningrad: Nauka (in Russian).

Bibikova, E.V., Baikova, V.S., Gorokhovsky, B.M., Grachyeva, T.V., Kirnozova, T.I., Kozakov, I.K., Kotov, A.B., Neimark, L.A., Ovchinnikova, G.V., Somin, L.M. and Shuleshko, I.K. (1990) *Izvestiya AN SSSR, Ser. Geol* , **7 ,** 57–62 (in Russian).

Bibikova, E.V., Kirnozova, T.I., Kozakov, I.K., Kotov, A.B., Neimark, L.A., Gorokhovsky, B.M. and Shuleshko, I.K. (1992) *Izvestiya RAN. Ser Geol* , **2 ,** 104–12 (in Russian).

Blagonravov V.A. (1970) O srednedevonskich otlozheniyach khrebta Bolnay (Stratigraphy and Tectonics of the Mongolian People's Republic), pp. 102–105, Moscow: Nauka (in Russian).

Blagonravov, V.A., Filippova, I.B., Blagonravova, L.A., Suprunov, E.A., Dobrolyubov, V.A., Levintov, M.E. and Fomenko, A.E. (1990) *Geologiya i Poleznye Iskopaemye Mongolskoi Narodnoi Respubliki (Geology and Mineral Resources of the Mongolian People's Republic)* , pp. 14–44 (in Russian).

Bogatikov, O.A., Bogdanova, S.V. and Borsuk, A.M. *et al.* (1987) *Magmaticheskie Gornye Porody (Igneous Rocks)* **6 ,** 440 pp., Moscow: Nauka (in Russian).

Boishenko, A.F. (1977) *Sovetskaya Geologiya* , **12 ,** 136–141 (in Russian).

Boishenko, A.F. (1978) *Izvestiya AN SSSR. Ser. Geol* , **1 ,** 48–55 (in Russian).

Boishenko, A.F. (1987) *Izvestiya Vysshei Shkoly. Geologiya i Razvedka* , pp. 2–36, Moscow (in Russian).

Borzakovsky, Yu.A. and Suetenko, O.D. (1970) *Geotektonika* , **5 ,** 12–25 (in Russian).

Burashnikov, V.V. and Ruzhentsev, S.V. (1993) *Doklady AN SSSR* , **322**(1), 54–7 (in Russian).
Dergunov, A.B. (1967) *Structury Zony Sochleneniya Gornogo Altaya i Zapadnogo Sayana (Structures of the Mountainous Altai/West Sayan junction zone)* , 216 pp., Moscow: Nauka (in Russian).
Dergunov, A.B. (1974) *Tektonika Mongolskoi Narodnoi Respubliki (Tectonics of the Mongolian People's Republic)* , pp. 107–110, Moscow: Nauka (in Russian).
Dergunov, A.B. (1988) *Geotektonika* , **3 ,** 63–75 (in Russian).
Dergunov, A.B. (1989) *Kaledonides Tsentralnoi Azii (Caledonides of Central Asia)* , 192 pp., Moscow: Nauka (in Russian).
Dergunov, A.B. and Kheraskova, T.N. (1981) *Byulleten MOIP. Otd. Geol* , **56(5) ,** 35–53 (in Russian).
Dergunov, A.B. and Kheraskov, N.N. (1985) *Geologiya i Geofizika* , **6 ,** 13–20, (in Russian)
Dergunov, A.B. and Luvsandanzan, B. (1984) *Geotektonika* , **3 ,** 40–52 (in Russian).
Dergunov, A.B. and Kovalenko, V.I. (Eds) (1995) *Geologicheskie Formatsii Mongolii (Geological Formations of Mongolia)* , 179 pp., Moscow: Shag (in Russian).
Dergunov, A.B., Zaitsev, N.S., Mossakovsky, A.A. and Perfiliev, A.S. (1971) *Problemy Teoreticheskoi i Regionalnoi Tektoniki (Problems of Theoretical and Regional Tectonics)* , pp. 87–103; Moscow: Nauka (in Russian).
Dergunov, A.B., Luvsandanzan, B. and Pavlenko, V.S. (1980) *Geologiya Zapadnoi Mongolii (Geology of West Mongolia)* , 196 pp., Moscow: Nauka (in Russian).
Dergunov, A.B., Ryazantsev, A.V., Luneva, O.I. and Richter, A.V. (1997) *Geotektonika* 2, 53–62 (in Russian).
Deruelle, B. (1982) *J. Volcanol Geotherm. Res.* , **14(1/2) ,** 63–81.
Devyatkin, E.V. (1981) *Kainozoi Vnutrennei Azii (Cainozoic of Inner Asia)* , 195 pp., Moscow: Nauka (in Russian).
Didenko, A.N., Mossakovsky, A.A., Pechersky, D.M., Ruzhentsev, S.V., Samygyn, S. Y. and Kheraskova, T.N. (1994) *Geology and Geophysics* , **10 ,** pp. 59–75.
Durante, M.V. (1976) *Paleobotanicheskoe Obosnovanie Stratigrafii Karbona i Permi Mongolii (Paleobotanical Rationale of the Stratigraphy of the Carboniferous and Permian of Mongolia)* , 280 pp., Moscow: Nauka (in Russian).
Fedorova, M.E. (1977) *Geologicheskoe Polozhenie i Petrologiya Granitoidov Khangaiskogo Nagoriya (Geological Position and Petrology of Granitoids of the Khangai Upland)* , 167 pp., Moscow: Nauka (in Russian).
Flozensov, N.A. (Ed.) (1963) *Gobi-Altai earthquakes* , 391 pp., Moscow, Nauka (in Russian).
Flozensov, N.A. and Khilko, S.D. (1979) *Geology and Magmatism of Mongolia* , pp. 46–60, Moscow: Nauka (in Russian).
Frikh-Khar, D.N. and Luchitskaya, A.I. (1978) *Pozdnemezozoiskie Vulkanity i Svyazannye s Nimi Gipabissalnye Intrusivy Mongolii (Late Mesozoic Volcanic Rocks and Associated Hypabyssal Intrusions of Mongolia)* , 166 pp., Moscow: Nauka (in Russian).
Frikh-Khar, D.N., Sinitsa, S.M., Ivanov, V.G., Samoilov, V.S. and Yarmolyuk, V.V. (1982) *Doklady AN SSSR* , **264**(2), 425–8 (in Russian).
Gonikberg, V.E. (1995) Geological structure and tectonic nature of the early Caledonian margin of the Sangilen Mountains, Tuva. *ScD Thesis* , Institute of the Lithosphere, RAN, Moscow, Russia (in Russian).
Gordienko, I.V. (1984) *Geologiya i Geofizika* , 19–31 (in Russian).
Gordienko, I.V. (1987) *Paleozoisky Magmatizm i Geodinamika Tsentralno-Aziatskogo Skladchatogo Poyasa (Paleozoic Magmatism and Geodynamics of the Central Asiatic Fold Belt)* , 238 pp., Moscow: Nauka (in Russian).
Hu, Baoquan and Zhu, Shiqian (1991) *IGCP Project* , **283 ,** Rep. 2, pp. 35–39.
Ilyin, A.V. (1973) *Khubsugulsky Fosforitonosnyi Bassein (The Khubsugul Phosphatebearing Basin)* , 167 pp., Moscow: Nauka (in Russian).

Ilyin, A.V. (1982) *Geologicheskoe Razvitie Yuzhnoi Sibiri v Pozdnem Dokembrii-Kembrii (Geological Development of Southern Siberia in the Late Precambrian-Cambrian)* , 116 pp., Moscow: Nauka (in Russian).

Ilyin, A.V. (1990) *Drevnie Fosfatonosnye Basseiny (Ancient Phosphate-bearing Basins)* , 176 pp., Moscow: Nauka (in Russian).

Jzokh A.E., Polyakov G.V., Krivenko A.P. Bognibov V.J. and Bayarbileg L. (1990) *Gabbroidnye formathii Zapadnoi Mongolii* (The Gabbroid Formations of the West Mongolia) 269 pp., Novoribirsk; Nauka sib. branch (in Russian).

Kazmin, V.G. and Kudanov, V.V. (1966) *Izvestiya Vuzov. Geologiya i Razvedka* , **9 ,** 11–17 (in Russian).

Kepezhinskas, P.K., Kepezhinskas K.B. and Pukhtel J.S. (1991) *Doklady AN SSSR* , **316**(3), 718–21 (in Russian).

Kepezhinskas, K.B., Kepezhinskas, V.V. and Zaitsev, N.S. (1987) *Evolyutsiya Zemnoi Kory Mongolii v Dokembrii-Kembrii (Evolution of the Earth's Crust of Mongolia in the Precambrian-Cambrian)* , 165 pp., Moscow: Nauka (in Russian).

Kepezhinskas, V.V. (1979) *Kainozoiskie Shchelochnye Bazaltoidy Mongolii i ikh Glubinnye Vklyucheniya (Cainozoic Alkalic Basaltoids of Mongolia and their Deep-seated Inclusions)* , 230 pp., Moscow: Nauka (in Russian).

Kepezhinskas, V.V. and Luchitsky, I.V. (1974) *Kontinentalnye Vulkanicheskie. Assotsiatsii Tsentralnoi Mongolii (Continental Volcanic Rock Associations of Central Mongolia)* , 72 pp., Moscow: Nauka (in Russian).

Khasin, R.A. and Marinov, N.A. (Eds) (1977) *Geologiya Mongolskoi Narodnoi Respubliki, Tom 3. Poleznye Iskopaemye (Geology of the Mongolian People's Republic, Vol. 3. Mineral Resources)* , 703 pp., Moscow: Nedra (in Russian).

Khasin, R.A., Marinov, N.A., Khurts, Ch. and Yakimov, L.I. (1977) *Geologiya Rudnykh Mestorozhdenii* , **6 ,** 3–15 (in Russian).

Khasin R.A., Suetenko O.D. and Filippova J.B. (1980) *Geologia i poleznye iskopaemye Mongolskoi Narodnoi Respubliki, Vypusk 1* (Geology and Mineral Resources of the Mongolian People's, Republic, Vol. 1) 20–34. Moscow: Nedra (in Russian).

Kheraskova, T.N. (1986) *Vend-Kembriiskie Formatsii Kaledonid Azii. Trudy Geologicheskogo Instituta AN SSSR (Vendian-Cambrian Formations of the Caledonides of Asia. Transactions of the Geological Institute, Academy of Sciences, SSSR)* , vyp. **386 ,** 247 pp., Moscow: Nauka (in Russian).

Kheraskova, T.N. and Voznesenskaya, T.A. (1995) *Geologicheskie Formatsii Mongolii (Geological Formations of Mongolia)* , p. 27, Moscow: Shag (in Russian).

Kheraskova, T.N., Dergunov, A.B. and Luvsandanzan, B. (1983) *Vend-Nizhne-kembriiskie Formatsii Zapadnoi Mongolii (Vendian-Lower Cambrian Formations of Western Mongolia)* , pp. 32–6, Ulan-Bator (in Russian).

Kheraskova, T.N., Tomurtogoo, O. and Khain, E.V. (1985) *Izvestiya AN SSSR. Ser. Geol.* , 6, 25–51 (in Russian).

Kheraskova, T.N., Ilyinskaya, M.N., Luvsandanzan, B. and Dashdava, Z. (1987) *Rannegeosinklinalnye Formatsii i Struktury (Early Geosynclinal Formations and Structures)* , pp. 67–100, Moscow: Nauka (in Russian).

Kheraskova, T.N., Samygin, S.G., Ruzhentsev, S.V. and Mossakovsky, A.A. (1995) *Doklady RAN* , **342** (5), 661–4 (in Russian).

Kiselev, A.I., Medvedev, M.E. and Golovko, G.A. (1979) *Vulkanizm Baikalskoi Riftovoi Zony (Volcanicism of the Baikal Rift Zone)* , 195 pp., Novosibirsk: Nauka (in Russian).

Kolman, R.G. (1979) *Ofiolity (Ophiolites)* , 262 pp., Moscow: Mir (in Russian).

Kononova, V.A., Pervov, V.A., Kovalenko, V.I. and Laputina, I.P. (1981) *Izvestiya AN SSSR, Ser. Geol.* , **5 ,** 20–37 (in Russian).

Kononova, V.A., Zhuravlev, D.Z., Yashina, R.M. and Pervov, V.A. (1993) Doklady AN USSR, **331** (2), 224–227 (in Russian).

Kopteva, V.V., Kuzmin, M.G. and Tomurtogoo, O. (1984) *Geotektonika* , **6 ,** 39–54 (in Russian).
Koval, P.V., Yakimov, V.M. and Kovalenko, V.I. (1980) *Izvestiya AN SSSR, Ser. Geol.* , **8 ,** 21–34 (in Russian).
Koval, P.V., Yakimov, V.M., Naigebauer, V.A. and Goreglyad, A.V. (1982) *Regionalnaya Petrokhimiya Mezozoiskikh Intruzy Mongolii (Regional Petrochemistry of Mesozoic Intrusions of Mongolia)* , 107 pp., Moscow: Nauka (in Russian).
Kovalenko, V.I. (1977) *Petrologiya i Geokhimiya Redkometalnykh Granitoidov (Petrology and Geochemistry of Rare-Metal Granitoids)* , 250 pp., Novosibirsk: Nauka (in Russian).
Kovalenko, V.I. (Ed.) (1986) *Metallogeniya Mongolii (Volfram, Olovo, Redkie i Redkozemelnye Elementy), Metallogeny of Mongolia (Tungsten, Tin, Rare and Rare-earth Elements))* , 51 pp., Novosibirsk: IGiG, Siberian Branch, Academy of Sciences, USSR (in Russian).
Kovalenko, V.I. (Ed.) (1991) *Vulkano-plutonicheskie Assotsiatsii Tsentralnoi Mongolii (Volcano-plutonic Associations of Central Mongolia)* , 230 pp., Moscow: Nauka (in Russian).
Kovalenko, V.I. and Kovalenko, N.I. (1976) *Ongonity (Ongonites)* , 125 pp., Moscow: Nauka (in Russian).
Kovalenko, V.I. and Yarmolyuk, V.V. (1990) *Evolyutsiya Geologicheskikh Protsessov i Metallogeniya Mongolii (Evolution of Geological Processes and Metallogeny of Mon-golia)* , pp. 23–54, Moscow: Nauka (in Russian).
Kovalenko, V.I., Vladykin, N.V. and Goreglyad, A.V. (1977) *Osnovnye Problemy Geologii Mongolii (Basic Problems of the Geology of Mongolia)* , pp. 189–206, Moscow: Nauka (in Růssian).
Kovalenko, V.I., Goreglyad, A.V. and Samoilov, V.S. (1979) *Doklady AN SSSR* , **246** (3), 682–6 (in Russian).
Kovalenko, V.I., Mossakovsky, A.A. and Yarmolyuk, V.V. (1983) *Geotektonika* , **6 ,** 13–29 (in Russian).
Kovalenko, V.I., Tsaryeva, G.M., Goreglyad, A.V., Yarmolyuk, V.V. and Arakelyants, M.M. (1989) *Izvestiya AN SSSR. Ser. Geol.* , **9 ,** 25–35 (in Russian).
Kovalenko, V.I., Zaitsev, N.S. and Yarmolyuk, V.V. *et al.* (1984a) *Endogennye Rudnye Formatsii Mongolii (Endogenic Ore Formations of Mongolia)* , pp. 3–40, Moscow: Nauka (in Russian).
Kovalenko, V.I., Nagibina, M.S. and Dobrov, G.M. *et al.* (1984b) *Izvestiya Akademii Nauk SSSR; Ser. Geol.* , **4 ,** 75–89 (in Russian).
Kovalenko, V.I., Yarmolyuk, V.V., Ionov, D.A., Yagutts, D. and Stosh, Kh. (1990a) *Geotektonika* , **4 ,** 3–16 (in Russian).
Kovalenko, V.I., Yarmolyuk, V.V. and Bogatikov, O.A. (1995a) *Magmatism, Geodynamics and Metallogeny of Central Asia* , 270 pp., Moscow: MIKO.
Kovalenko, V.I., Yarmolyuk, V.V., Samoilov, V.S. and Koval, P.V. *et al.* (1990b) *Evolyutsiya Geologicheskikh Protsessov i Metallogeniya Mongolii (Evolution of Geological Processes and Metallogeny of Mongolia)* , pp. 187–213, Moscow: Nauka (in Russian).
Kovalenko, V.I., Tsaryeva, G.M., Goreglyad, A.V., Yarmolyuk, V.V., Troitsky, V.A., Hervig, R.L. and Farmer, G.L. (1995b) *Economic Geology* , **90 ,** 530–47.
Kovalenko, V.I., Yarmolyuk, V.V., Kovach, V.P., Kotov, A.B., Kozakov, I.K. and Salnikova, E.B. (1996) *Geokhimiya* **8 ,** pp. 399–712 (in Russian).
Kovalenko, V.I., Yarmolyuk, V.V., Kovach, V.P., *et al.* (1999) Magmatism as Factor of Crust Evolution in the Central Asian Foldbelt: Sm-Nd Isotopic Data. *Geotectonika* , **3 ,** 21–40 (in Russian).
Kovalenko, V.I., Yarmolyuk, V.V., Kovach, V.P. *et al.* (1996) Sources of Phanerozoic Granitoids in Central Asia: Sm-Nd isotope Data. *Geochim. Intern.* , **34**(8), 628–640.
Kovalenko, V.I., Yarmolyuk, V.V., Pukhtel, I.S. *et al.* (1996) Igneous Rocks and Magma Sources of the Ozernaya Zone Ophiolites, Mongolia. *Petrology* , **4**(5), 420–459.
Kozakov, I.K. (1986) *Dokembriiskie Infrastrukturnye Kompleksy Paleozoid Mongolii (Precambrian Infrastructural Complexes of the Paleozoic of Mongolia)* , 144 pp., Leningrad: Nauka (in Russian).

Kozakov, I.K. (1993) *Rannii Dokembrii Tsentralnoaziatskogo Skladchatogo Poyasa (The Early Precambrian of the Central Asiatic Fold Belt)* , pp. 158–9, St Petersburg: Nauka (in Russian).

Kozakov, I.K., Bibikova, E.V., Neimark., L.A. and Kirnozova, T.I. (1993) *Rannii Dokembrii Tsentralnoaziatskogo Skladchatogo Poyasa (The Early Precambrian of the Central Asiatic Fold Belt)* , pp. 115–37, St Petersburg: Nauka (in Russian).

Kozakov, I.K., Kotov, A.B., Kovach, V.P., Sal'nikova, E.B. (1997) Crustal Growth in the Geologic Evolution of the Baidaric Block, Central Mongolia: Evidence from Sm-Nd Isotopic Systematics. *Petrology* , **5**(3), 201–207.

Kozakov, I.K., Sal'nikova, E.B., Bibikova, E.V. *et al.* (1999) Polichronous Evolution of the Paleozoic Granitoid Magmatism in the Tuva-Mongolia Massif: U-Pb Geochronological Data. *Petrology* , **7**(6), 592–601.

Leonov, Yu. G. (Ed.) (1983) *Mezozoiskaya Tektonika i Magmatizm Vostochnoi Azii (Mesozoic Tectonics and Magmatism of Eastern Asia)* , 232 pp., Moscow: Nauka (in Russian).

Lisitsyn, A.P. (1983) *Litologiya i Poleznye Iskopaemye* , **6 ,** 3–27 (in Russian).

Luchitsky, I.V. (Ed.) (1975) *Granitoidnye i Schelochnye Formatsii v Strukturakh Zapadnoi i Severnoi Mongolii (Granitoid and Alkaline Formations in Structures of Western and Northern Mongolia)* , 288 pp., Moscow: Nauka (in Russian).

Luchitsky, I.V. (Ed.) (1983) *Kontinentalny Vulkanizm Mongolii (Continental Volcanicism of Mongolia)* , 190 pp., Moscow: Nauka (in Russian).

Lutz B.G. (1980) *Geokhimiya okeanicheskogo i kontinentalnogo magmatirma* (Geochemistry of the oceanic and continental magmatism) 248 pp. Moscow: Nedra (in Russian).

Luvsandanzan, B. (1970) *Stratigrafiya i Tektonika Mongolskoi Narodnoi Respubliki (Stratigraphy and Tectonics of the Mongolian People's Republic)* , pp. 105–13, Moscow: Nauka (in Russian).

Luvsandanzan, B. and Tomurtogoo, O. (1982) *Problemy Geologii Mongolii (Problems of the Geology of Mongolia)* , pp. 3–12, Ulan-Bator Makary chev 1985 (in Russian).

Makarychev, G.I. (1993) *Byulleten MOIP. Otd. Geol.* , **68**(5), 36–48 (in Russian).

Marinov, N.A. (Ed.) (1973) *Geologiya Mongolskoi Narodnoi Respubliki, Tom 2. Magmatizm, Metamorfizm, Tektonika (Geology of the Mongolian People 's Republic, Vol. 2. Magmatism, Metamorphism, and Tectonics)* , 752 pp., Moscow: Nedra (in Russian).

Markova, N.G. (1975) *Stratigrafiya Nizhnego i Srednego Paleozoya Zapadnoi Mongolii (Stratigraphy of the Lower and Middle Palaeozoic of Western Mongolia)* 119 pp., Moscow: Nauka (in Russian).

Markova, N.G. and Fedorova, M.E. (1971) *Problemy Teoreticheskoi i Regionalnoi Tektoniki (Problems of Theoretical and Regional Tectonics)* , pp. 94–103, Moscow: Nauka (in Russian).

Matrenitsky, A.T. (1981) *Petrologiya i Rudonosnost Indikatornykh Magmaticheskikh Formatsii (Petrology and Ore Potential of Indicator Rock Associations)* , pp. 353–73, Moscow: Nauka (in Russian).

Mitrofanov, F.N., Bibikova, E.S. and Grachyeva, T.V. *et al.* (1985) *Doklady AN SSSR* , **284**(3), 670–74 (in Russian).

Mitrofanov, F.N., Kozakov, I.K. and Palei, I.P. (1981) *Dokembrii Zapadnoi Chasti Mongolii i Yuzhnoi Tuvy (The Precambrian of the Western Part of Mongolia and Southern Tuva)* , 156 pp., Leningrad: Nauka (in Russian).

Mitrofanov, F.N., Bibikova, E.S. and Grachyeva, T.V. *et al.* (1985) *Doklady AN SSSR* , **284**(3), 670–74 (in Russian).

Molnar, P. and Tapponier, P. (1975) *Science* , **189**(4), 419–26.

Mossakovsky, A.A. (1975) *Orogennye Struktury i Vulkanizm Evrazii i ikh Mesto v Protsesse Formirovaniya Kontinentalnoi Zemnoi Kory (Orogenic Structures and Volcanicsm of Eurasia and their Place in the Process of Formation of the Earth's Continental Crust)* , 318 pp., Moscow: Nauka (in Russian).

Mossakovsky, A.A. and Tomurtogoo, O. (1976) *Verkhnii Paleozoi Mongolii (The Upper Paleozoic of Mongolia)* , 125 pp., Moscow: Nauka (in Russian).

Mossakovsky, A.A., Saltykovsky, A.Ya. and Tomurtogoo, O. (1973) *Assotsiatsii Vulkanogennykh Porod Mongolii, ikh Sostav i Stratigraficheskoe Polozhenie (Volcanic Rock Associations of Mongolia, their Composition and Stratigraphic Position)* , pp. 94–106, Moscow: Nauka (in Russian).

Mossakovsky, A.A., Ruzhentsev, S.V., Samygin, S.G. and Kheraskova, T.N. (1993) *Geotektonika* , **6 ,** 3–32 (in Russian).

Mueller, J.F., Rogers, J.J.W., Jin, Yugan, Wang, Huayu, Li, Wenguo and Chronic, J. (1991) *J. Geology* , **99**(2), 251–64.

Neymark., L.A. (1993) *Rannii Dokembrii Tsentralnoaziatskogo Skladchatogo Poyasa (The Early Precambrian of the Central Asiatic Fold Belt)* , pp. 13–19, St Petersburg: Nauka (in Russian).

Neymark, L.A. *et al.* (1993) *Rannii Dokembrii Tsentralnoaziatskogo Skladchatogo Poyasa (The Early Precambrian of the Central Asiatic Fold Belt)* , pp. 194–206, St Petersburg: Nauka (in Russian).

Obolenskaya, R.V. (1971) *Chuisky Kompleks Shchelochnykh Bazaltoidov Gornogo Altaya (The Chu Complex of Alkali Basaltoids of the Gorny Altai)* , 150 pp., Novosibirsk: Nauka (in Russian).

Obolensky, A.A. (Ed.) (1986) *Metallogeniya Mongolii (Rtut, Epitermalnoe Orudenenie) (Metallogeny of Mongolia (Mercury, Epithermal Mineralization))* , 47 pp., Novosibirsk: IGiG, Siberian Branch, Academy of Sciences, USSR (in Russian).

Palei, I.P. (1979) *Geotektonika* , **4 ,** 11–19 (in Russian).

Palei, I.P. and Zhuravleva, Z.A. (1978) *Byulleten MOIP* , **53**(3), 38–41 (in Russian).

Peive, A.V. (1980) *Tektonicheskaya Rassloennost Litosfery: Vvedenie (Tectonic Stratification of the Lithosphere: Introduction)* , Moscow: Nauka (in Russian).

Perfiliev, A.S. and Kheraskov, N.N. (1980) *Tektonicheskaya Rassloennost Litosfery (Tectonic Stratification of the Lithosphere)* , pp. 64–104, Moscow: Nauka (in Russian).

Philippova J.B. (1976) *Geologiya i Geopizika* . **6 ,** 42–58 (in Russian).

Pinus, G.V., Agafonov, A.V., Kuznetsov, P.P. and Lesnov, F.P. (1981) *Voprosy Geneticheskoi Petrologii (Problems of Genetic Petrology)* , pp. 180–94, Novosibirsk: Nauka (in Russian).

Rozman, Kh. S. and Minzhin, Ch. (1981) *Atlas Fauny Ordovika Mongolii (Atlas of Ordovician Fauna of Mongolia)* , pp. 26–63, Moscow: Nauka (in Russian).

Ruzhentsev, S.V. (1985) *Izvestiya Vysshei Shkoly. Geologiya i Razvedka* , **6 ,** 12–19 (in Russian).

Ruzhentsev, S.V. and Mossakovski A.A. (1995) *Geotektonika* , **4 ,** 29–47 (in Russian).

Ruzhentsev, S.V. and Burashnikov, V.V. (1995) *Geotektonika* , **5 ,** 25–40 (in Russian).

Ruzhentsev, S.V. and Pospelov, I.I. (1992) *Geotektonika* , **5 ,** 78–95 (in Russian).

Ruzhentsev, S.V., Badarch, G. and Voznesenskaya, T.A. (1985) *Geotektonika* , **4 ,** 28–40 (in Russian).

Ruzhentsev, S.V., Badarch, G., Voznesenskaya, T.A. and Sharkova, T.T. (1987) *Rannegeosinklinalnye Formatsii i Struktury (Early Geosynclinal Formations Structures)* , pp. 101–37, Moscow: Nauka (in Russian).

Ruzhentsev, S.V., Pospelov, I.I. and Badarch, G. (1989) *Geotektonika* , **6 ,** 13–27 (in Russian).

Ruzhentsev, S.V., Samygin, S.G. and Pospelov, I.I. (1990a) *Doklady AN SSSR* , **315**(2), 456–61 (in Russian).

Ruzhentsev, S.V., Badarch, G., Voznesenskaya, T.A., Markova, N.G. (1990b) *Evolyutsiya Geologicheskikh Protsessov i Metallogeniya Mongolii (Evolution of Geological Processes and Metallogeny of Mongolia)* , pp. 111–16, Moscow: Nauka (in Russian).

Ruzhentsev, S.V., Pospelov, I.I. and Badarch, G. (1992a) *Geotektonika* , **1 ,** 94–110 (in Russian).

Ruzhentsev, S.V., Pospelov, I.I. and Badarch, G. (1992b) *Doklady AN SSSR* , **322** (5), 953–8 (in Russian).

Saltykowsky, A.Ja. and Genshaft, Ju.S. (1985) *Cenozoic geodynamics of volcanism of South-East Mongolia* , 135 pp., Moscow: Nauka (in Russian).

Samoilov, V.S. (1989) *Geologiya i Geofizika* , **9 ,** 12–21 (in Russian).

Samoilov, V.S. and Kovalenko, V.I. (1983) *Kompleksy Shchelochnykh Porod i Karbonatitov Mongolii (Complexes of Alkali Rocks and Carbonatites of Mongolia)* , 170 pp., Moscow: Nauka (in Russian).

Samoilov, V.S., Ivanov, V.G., Smirnov, V.N. (1988a) *Geologiya i Geofizika* , **10 ,** 13–21 (in Russian).

Samoilov, V.S., Kovalenko, V.I. and Sangee, D. (1988b) *Geologiya Rudnykh Mestorozhdenii* , **30**(2), 62–74 (in Russian).

Serri G. (1981) The petrochemistry of ophiolitic gabbroic complex: a key for the classification of ophiolites into low-Ti and high-Ti types, Earth Planet. *Sci. Lett* . **52 ,** 203–212..

Sharkova, T.T. (1981) *Siluriiskie i Devonskie Tabulyaty Mongolii (Silurian Devonian Tabulates of Mongolia)* , 104 pp., Moscow: Nauka (in Russian).

Shcherbakov, Yu.G. (Ed.) (1986) *Metallogeniya Mongolii (Zoloto)(Metallogeny of Mongolia (Gold))* , 40 pp., Novosobirsk: IGiG, Siberian Branch, Academy Sciences, USSR (in Russian).

Shustova, L.E. (1993) *Rannii Dokembrii Tsentralnoaziatskogo Skladchatogo Poyasa (The Early Precambrian of the Central Asiatic Fold Belt)* , pp. 207–13, St Petersburg: Nauka (in Russian).

Shuvalov, V.F. (1988) *Mezozoiskie Ozyernye Basseiny Mongolii (Mesozoic Lake Basins of Mongolia)* , pp. 18–81, Leningrad: Nauka (in Russian).

Shuvalov, V.F. and Nikolaeva, T.V. (1985) *Vestnik LGU* , **14 ,** 52–9 (in Russian).

Sinitsin, V.M. (1956) *Zaaltaiskaya Gobi (The Transaltai Gobi)* , 176 pp., Moscow: Izd-vo AN SSSR (in Russian).

Sotnikov, V.I. (Ed.) (1986) *Metallogeniya Mongolii (Med, Molibden)(Metallogeny of Mongolia (Copper, Molybdenum))* , 40 pp., Novosibirsk: IGiG, Siberian Branch, Academy of Sciences, USSR (in Russian).

Sotnikov, V.I., Berzina, A.P. and Zhamsran, M. (1985) *Mednorudnye Formatsii Mongolii (Copper Ore Deposits of Mongolia)* , 220 pp., Novosibirsk: Nauka (in Russian).

Suetenko, O.D. (1973) *Geotektonika* , **3 ,** 102–15 (in Russian).

Tang Kedong (1990) *Tectonics* , **9**(2), 249–60.

Tauson, L.V. (Ed.) (1982) *Regionalnaya Petrokhimiya Mezozoiskikh Intruzii Mongolii (Regional Petrochemistry of Mesozoic Intrusions of Mongolia)* , 207 pp., Moscow: Nauka (in Russian).

Tomurtogoo, O. (1972) Tectonics and history of developments of the Orkhon-Selenga Trough (Mongolia). *ScD Thesis (Cand. Sc.)* , GIN AN SSSR, Moscow, USSR (in Russian).

Tomurtogoo, O. (1989) Ophiolites and formation of fold regions of Mongolia. *ScD Thesis (D.Sc.),* GIN AN SSSR, Moscow, USSR (in Russian).

Ulitina, L.M., Bolshakova, L.N. and Kopaevich, G.V. (1976) *Paleontologiya i Biostrati-grafiya Mongolii (Palaeontology and Biostratigraphy of Mongolia)* , **3 ,** pp. 327–40, Moscow: Nauka (in Russian).

Vladykin, N.V., Kovalenko, V.I. and Dorfman, M.D. (1981) *Mineralogicheskie i Geokhimicheskie Osobennosti Khan-Bogdinskogo Massiva Shchelochnykh Granitov (Mineralogical and Geochemical Features of the Khan-Bogdin Intrusion of peralkaline Granites)* , 135 pp., Moscow: Nauka (in Russian).

Volochkovich, K.L. and Leontiev, A.N. (1964) *Talitsko-Mongolo-Altaiskaya Metallogen-icheskaya Zona (The Talitsa-Mongolia-Altai Metallogenic Zone)* , 184 pp., Moscow: Nauka (in Russian).

Volochkovich, K.L. and Leontiev, A.N. (1990) *Evolyutsiya Geologicheskikh Protsessov i Metallogeniya Mongolii (Evolution of Geological Processes and Metallogeny of Mon-golia)* , pp. 122–38, Moscow: Nauka (in Russian).

Voronin, Yu. I. and Drozdova, N.A. (1976) *Paleontologiya i Stratigrafiya Mongolii (Paleontology and Stratigraphy of Mongolia)* , pp. 279–91, Moscow: Nauka (in Russian).

Vorontsov, A.A. (1994) *Geology and Geochemistry of Early-Middle Devonian Igneous Rock Associations with Alkali Rocks of North-West Mongolia* . ScD Thesis, Institute of Geochemistry, Siberian Branch, Russian Academy of Sciences, Irkutsk, Russia (in Russian).

Voznesenskaya T.A. and Dergunov A.B. (1982) *Byulleten MOJP. Otd. Geol* t. **57**. vyp. 4. 79–94 (in Russian).

Voznesenskaya, T.A. (1993) *Litologiya i Poleznye Iskopaemye*, **6 ,** 69–83 (in Russian).
Voznesenskaya, T.A. (1995) *Litologiya i Poleznye Iskopaemye* , **5 ,** 537–47 (in Russian).
Voznesenskaya, T.A., Dergunov, A.B. and Dashdavaa, Z. (1992) *Izvestiya AN SSSR. Ser. Geol.* , 3, 34–9 (in Russian).
Wang, Shiguang and Han, Baofu (1994) *Scientia Geologica Sinica* , **29**(4), 373–83.
Windley, B.F., Tszinkhuei, Li Ini and Chzhan, Chi (1994) *Geologiya i Geofizika* , **7–8 ,** 116–17 (in Russian).
Yanshin, A.L. (Ed.) (1978) Tectonic Map of the Mongolian People's Republic, scale 1:1 500,000, Moscow: GUGK (in Russian).
Yanshin, A.L. (Ed.) (1975) *Mezozoiskaya i Kainozoiskaya Tektonika i Magmatizm Mongolii (Mesozoic and Cainozoic Tectonics and Magmatism of Mongolia)* , 308 pp., Moscow: Nauka (in Russian).
Yanshin, A.L. (Ed.) (1989) *Map of Geological Formations of the Mongolian People's Republic, scale 1:1 500,000* , Novosibirsk: GT sGK SSSR (in Russian).
Yarmolyuk, V.V. (1978) *Verkhnepaleozoiskie Vulkanogennye Assotsiatsii l Strukturnopetrologicheskie Osobennosti ikh Razvitiya (Upper Palaeozoic Volcanic Associations and Structural-Petrological Features of their Evolution)* 150 pp., Moscow: Nauka (in Russian).
Yarmolyuk, V.V. (1983) *Pozdnepaleozoisky Vulkanizm Kontinentalnykh Riftogennykh Struktur Tsentralnoi Azii (Late Paleozoic Volcanicity of Continental Rift-originated Structures of Central Asia)* , 198 pp., Moscow: Nauka (in Russian).
Yarmolyuk, V.V. (1986) *Geologya i Geofizika* , **9 ,** pp. 3–16 (in Russian).
Yarmolyuk, V.V. and Kovalenko, V.I. (1980) *Doklady AN SSSR* , **252** (1), 232–5 (in Russian).
Yarmolyuk, V.V. and Kovalenko, V.I. (1991) *Riftogenny Magmatizm Aktivnykh Kontinentalnykh Okrain i ego Rudonosnost (Rift-originated Magmatism of Active Continental Margins and its Ore Potential)* , 263 pp., Moscow: Nauka (in Russian).
Yarmolyuk, V.V. and Vorontsov, A.A. (1993) *Geotektonika* , **4 ,** 76–86 (in Russian).
Yarmolyuk, V.V., Kovalenko, V.I. and Goreglyad, A.V. (1981) *Doklady AN SSSR* , **258** (2), 452–86 (in Russian).
Yarmolyuk, V.V., Gordienko, I.V., Durante, M.V. and Bold, D. (1987) *Geotektonika* , **3 ,** 22–36 (in Russian).
Yarmolyuk, V.V., Kovalenko, V.I. and Bogatikov, O.A. (1990a) *Doklady AN SSSR* , **312** (1), 187–91(in Russian).
Yarmolyuk, V.V., Kovalenko, V.I. and Oldone, M. *et al.* (1990b) *Izvestiya AN SSSR, Ser. Geol.* , **5 ,** 2–23 (in Russian).
Yarmolyuk, V.V., Kovalenko, V.I. and Samoilov, V.S. (1991) *Geotektonika* , **1 ,** 69–83 (in Russian).
Yarmolyuk, V.V., Ivanov, V.G., Kovalenko, V.I. and Samoilov, V.S. (1994) *Geotektonika* , **5 ,** 28–45 (in Russian).
Yarmolyuk, V.V., Kovalenko, V.I. and Ivanov, B.G. (1995a) *Geotektonika* , **5 ,** 41–68 (in Russian).
Yarmolyuk, V.V., Ivanov, V.G., Samoilov, V.S. and Arakelyants, M.M. (1995b) *Doklady RAN* , **344**(5), 673–6 (in Russian).
Yarmolyuk, V.V., Vorontsov, A.A., Sandimirova, G.P. and Pokolchenko, Yu. A. (1995c) *Geologiya i Geofizika* , **36**(5), 38–47 (in Russian).
Yarmolyuk, V.V., Zhuravlev, D.Z., Ivanov, V.G. and Kovalenko, V.I. (1995d) *Doklady RAN* , **3**(2), 230–4 (in Russian).
Yarmolyuk, V.V., Kovalenko, V.I., Ivanov, V.G. (1996) The Interplate late Mesozoic-Cenozoic Volcanic Province in Central Asia as a Proection of the Mantle Hot-Field. *Geotectonics* , **29**(5), 395–421.
Yarmolyuk, V.V., Vorontsov, A.A., Kovalenko, V.I. and Zhuravlev, D.Z. (1997) *Geologiya i Geofizika* , **38**(6), pp. 1142–1147 (in Russian).

Yarmolyuk, V.V., Samoilov, V.S., Ivanov, V.G., *et al.* (1999a) Composition and Sources of Basalts in the late Paleozoic Rift System of Central Asia: Geochemical and Isotopic Data. *Geochim. Intern.* , **37**(10), 921–935.

Yarmolyuk, V.V., Kovalenko, V.I., Kovach, V.P. *et al.* (1999b) Nd-Isotopic Systematics of West Transbaikalian Crustal Protoliths: Implication to Riphean Crust Formation in Central Asia. *Geotectonika* , N4, pp. 3–20 (in Russian).

Yarmolyuk, V.V., Kovalenko, V.I., Kuzmin, M.I. (2000) North-Asian Superplume in Phanerozoic: Magmatism and Geodynamics. *Geotectonika* , N4, pp. 3–28 (in Russian).

Yashina, R.M. (1982) *Shchelochnoi Magmatizm Skladchato-glybovykh Oblastei (na Primere Yuzhnogo Obramleniya Sibirskoi Platformy) (Alkaline Magmatism of Fold-Block Regions) (with Reference to the Southern Fringe of the Siberian Platform)* , 276 pp., Moscow: Nauka (in Russian).

Zaitsev, N.S. and Tauson, L.V. (Eds) (1971) *Redkometalnye Granitoidy Mongolii (Rare Metal Granitoids of Mongolia)* , 207 pp., Moscow: Nauka (in Russian).

Zindler, A. and Hart, S. (1986) *Ann. Rev. Earth Planet. Sci.* , **14 ,** 493–571.

Zonenshain, L.P. and Philippova, I.B. (1974) *Tektonika Mongolskoi Narodnoi Respubliki (Tectonics of the Mongolian People's Republic)* , pp. 98–107, Moscow: Nauka (in Russian).

Zonenshain, L.P. and Kuzmin, M.I. (1978) *Geotektonika* , **1 ,** 19–42 (in Russian).

Zonenshain, L.P., Kuzmin M.I., Moralev, V.M. (1976) *Global tectonics, magmatism and metallogency* , 231 p., Moscow: Nedra (in Russian).

Zonenshain, L.P. and Savostin, L.A. (1979) *Vvedenie v Geodinamiku (Introduction to Geodynamics)* , 310 pp., Moscow: Nedra (in Russian).

Zonenshain, L.P. and Tomurtogoo, O. (1979) *Geologiya i Magmatizm Mongolii (Geology and Magmatism of Mongolia)* , pp. 135–44, Moscow: Nauka (in Russian).

Zonenshain, L.P. Suetenko, O.D., Zhamyan Damba, L. and Eenzhin, G. (1975) *Geotektonika* , **4 ,** 28–44 (in Russian).

INDEX